2012

The Arabidopsis CRINKLY4 receptor-like kinase and homologs: Regulation of kinase activity through intra- and intermolecular interactions

Matthew Richard Meyer
Iowa State University

The *Arabidopsis* CRINKLY4 receptor-like kinase and homologs: Regulation of kinase activity through intra- and intermolecular interactions

by

Matthew Richard Meyer

A dissertation submitted to the graduate faculty

in partial fulfillment of the requirements for the degree of

DOCTOR OF PHILOSOPHY

Major: Biochemistry

Program of Study Committee:
A. Gururaj Rao, Major Professor
Robert Thornburg
Alan DiSpirito
Philip Becraft
Anumantha Kanthasamy

Iowa State University

Ames, Iowa

2012

TABLE OF CONTENTS

ACKNOWLEDGMENTS

I would like to thank my major professor and mentor Dr. A. Gururaj Rao for his tremendous knowledge and guidance during my formative years as a graduate student. He has exhibited great wisdom and patience in providing the skill and expertise I will require as a future researcher. He has been a true inspiration for learning and succeeding during my graduate career at Iowa State University.

I want to thank my Program of Study committee members, Dr. Robert Thornburg, Dr. Alan DiSpirito, Dr. Philip Becraft, and Dr. Anumantha Kanthasamy. Their advice and guidance has aided me in my path towards my degree.

I would like to extend warm gratitude towards my coworkers who have provided their time and knowledge in the laboratory. Thank you, Dr. Kevin Stokes, Dr. Shweta Shah, and Dr. Yasufumi Yamamoto for your help and guidance. Your insight and friendship has proven valuable to my education, both at the lab bench and in your homes.

Over my years as a graduate student, my family has provided me the immense love and support during this time. Thank you Mom and Dad, Victoria and Clarence, your unrestrained encouragement and understanding of my aspirations have kept me motivated to keep striving to be great. Thank you to my sisters, Jody and Amy, you two have always driven me to push my personal frontiers more and more every day. And thank you Kathy and Tim Eibes, for your immense love and help along the way.

Lastly, I want to extend immeasurable gratitude to by fiancée, Amanda Eibes, your love, time, and encouragement have inspired me to learn and better myself each day. I am deeply grateful for your support and devotion. Thank you, Peach.

ABSTRACT

Arabidopsis CRINKLY4 (ACR4) is a receptor-like kinase (RLK) that is required for the global development of the plant. In aerial tissues ACR4 promotes the differentiation of the outer, epidermal layer in the leaves and reproductive tissues. Loss of ACR4 function results in malformed, 'crinkled' leaves due to graft-like fusions of vegetative tissues. Underground, ACR4 is responsible for stem cell differentiation in the root tip and for the initiation of lateral roots. *Acr4* mutant plants show increased proliferation of stem cells and increase lateral root initiation sites. ACR4 has architectural features analogous to receptor tyrosine kinases (RTK). It includes an extracellular ligand binding domain, a transmembrane helix, and an intracellular kinase domain. The intracellular domain contains two subdomains, the juxtamembrane domain (JMD) and the C-terminal domain (CTD) which flank the core kinase domain (KD). The *Arabidopsis* genome also encodes four homologs of ACR4, referred to as *Arabidopsis* CRINKLY4 Related (AtCRR) proteins, that contain equivalent architectural domains to ACR4 and have high sequence similarity. Genetic and cell biology studies have suggested potential communication between members of the ACR4 gene family. However, a biochemical basis for receptor hetero-oligomerization among these family members has not been established. An additional RLK, ABNORMAL LEAF SHAPE 2 (ALE2), is involved in proper epidermal layer formation. ALE2 is also known to synergistically enhance ACR4 kinase activity *in vitro*. Furthermore, the spatial expression of a transcription factor, WOX5, has been demonstrated to be regulated by ACR4 signaling. However, the precise signaling pathway(s) modulated by these RLKs and the molecular basis of their biological function remain to be determined.

Although significant advancements have been made in understanding the biological relevance of ACR4, little is known about the biochemical aspects of ACR4 signaling. In this dissertation, we provide a fundamental biochemical analysis of the activation of the ACR4 intracellular kinase domain. We have expressed and purified the intracellular domains of ACR4, the AtCRRs, and ALE2 as C-terminal fusions to the yeast SUMO protein. We provide evidence for an intramolecular interaction mechanism between the ACR4 JMD and the amino-terminal region of the KD and demonstrate its potential role in the regulation of kinase activity. Additionally, we provide evidence for an intermolecular interaction mechanism between ACR4 and the AtCRRs, and potential regulation of this interaction by the ACR4 JMD. Lastly, we demonstrate that ACR4 can bind to the WOX5 transcription factor and phosphorylate it *in vitro* at four sites.

CHAPTER 1. GENERAL INTRODUCTION

Introduction

Higher organisms must maintain controlled equilibrium between cell proliferation and differentiation throughout development. Failure to retain this balance results in developmental problems which lead to increased disease states and decreased survival. Utilization of cell-surface receptors to perceive external or internal signals is a widespread characteristic of all organisms. Mammalian systems have acquired signal transduction mechanisms via the use of receptor tyrosine kinases (RTK) to regulate cellular processes such as proliferation, migration, differentiation, and cell-cycle control (1). The use of RTKs allows the cell to perceive proper signaling cues and communicate their message intracellularly. RTKs consist of an extracellular ligand binding domain, a single transmembrane helix, and an intracellular tyrosine kinase domain. The general paradigm of RTK activation entails ligand binding to the extracellular domain of the receptor, followed by receptor oligomerization, and activation of the kinase domains by *trans* phosphorylation (2, 3). Activation of the intracellular kinase domain of the receptor initiates a coordinated signal transduction cascade involving cytoplasmic components that ultimately lead to regulation of gene transcription in the nucleus (1, 4).

Dissimilar to animals, plants are inherently sessile organisms i.e. they are not free-moving. Their immobility prohibits them from escaping predation, mobilizing towards favorable conditions, or moving from hostile surroundings. Therefore, plants have acquired the ability to recognize various stimuli and coordinate an appropriate response to their prevailing conditions. In order to perceive and respond to both external and internal cues,

plants have developed extensive signaling mechanisms to help adapt to changing environments. Similar to animals, plants make use of receptor-like kinases (RLK) in order perceive extracellular signals and transport the signal across the plasma membrane to regulate transcriptional activation in the nucleus. Signal transduction via RLKs ultimately guides a host of cellular responses such as cell growth, proliferation, differentiation. Thus, the ability for a plant to respond according to its environment, both internally and externally, drives the proper growth and development of the organism to ensure its survival.

Dissertation Organization

This dissertation is organized into six chapters. Chapter 1 provides a literature review of the past and current knowledge of CRINKLY4 biology and signaling in plants. Chapter 2 has been published in the ACS journal, *Biochemistry* (5). This article represents the *in vitro* biochemical characterization of the intracellular kinase domain of *Arabidopsis* CRINLY4 (ACR4) and the identification of multiple autophosphorylation sites. A manuscript describing the expression and purification of the intracellular domains of ACR4, the ACR4 homologs, and ALE2 receptor-like kinases as C-terminal fusions to the yeast SUMO protein is outlined in Chapter 3. This includes characterization of their autophosphorylation activity, oligomerization, and intrinsic fluorescence properties. Additionally, the effect of Ala point mutations of the ACR4 autophosphorylation sites is examined. Chapter 4 is a manuscript describing the autoregulatory role of the ACR4 juxtamembrane domain (JMD) on kinase autophosphorylation. A potential intramolecular mechanism involving the JMD and the N-lobe of the kinase domain has been established. A manuscript outlined in Chapter 5 examines and provides evidence for intermolecular interactions between the intracellular

domains of ACR4 and its homologs, the AtCRRs, and a transcription factor involved in stem cell differentiation. Furthermore, evidence for an intermolecular mechanism in which the JMD of ACR4 modulates intermolecular contacts between the homologs is illustrated. Lastly, Chapter 6 is a general conclusion that draws together the work described in the previous chapters and outlines ideas for future research in the elucidation of the ACR4 signaling pathway. The references cited in each chapter are listed at the end of their respective chapter.

Literature Review

RLKs in plant development

The *Arabidopsis* genome encodes over 600 RLKs with a large variety of putative extracellular ligand binding domains. The RLK family is one of the largest and represents 2.5% of the known coding sequences in *Arabidopsis* (6). Furthermore, this family accounts for 60% of the total number of kinases encoded in *Arabidopsis* (7). The architectural features of the majority of RLKs consist of an extracellular ligand binding domain, a transmembrane spanning helix, and an intracellular kinase domain, similar to mammalian receptors. The sequence diversity of the extracellular domains of the RLK family allows them to be further subdivided into 15 groups which share similar domain features common among animal RTKs. The leucine-rich repeat (LRR) RLKs are the largest group within the family, containing more than 200 members (6). The diversity of extracellular domains suggests plants are able to distinguish between a broad array of signaling molecules including hormones, peptides, pathogen recognition motifs, steroids, and small molecules (8-16). However, examples exist in which receptors lack an extracellular or intracellular region

which define their overall functionality at the cell surface (6, 17, 18). RLKs are reasoned to act in a similar fashion to RTKs but, in contrast to the the RTKs, the kinase activity of the RLKs is predominantly via phosphorylation of serine/threonine residues, although evidence of tyrosine phosphorylation has emerged in more recent studies (19, 20). A key way to regulate kinase activity is through activation loop phosphorylation. Structural analyses comparing Ser/Thr and Tyr kinases has revealed differing mechanisms of activation loop stabilization via phosphorylated residue contacts with the N-lobe of the kinase. The mode of contact differentiates the two classes of enzymes. The phosphorylated residue(s) in Ser/Thr kinases make use of electrostatic contacts with basic residues in the N-lobe, whereas Tyr kinases primarily use cation-π interactions between a conserved Phe residue just C-terminal to the activation loop and the kinase N-lobe (21). Nevertheless, there is remarkable structural conservation of kinase domains across the Ser/Thr and Tyr kinase families even though the activation loop regions are highly divergent in both conformation and sequence (Fig. 4). This exemplifies the evolutionary differences arising from kinase-specific activation and functionality (22).

Insofar as very few of the RLKs have been characterized in detail at the molecular level, the biological functions of several RLKs involved in plant-pathogen interactions, defense and stress responses as well as in plant growth and development have emerged in recent times (6, 16, 23-25). These studies suggest that activation of the kinase domain elicits an amplification of the extracellular signal via recruitment of cytoplasmic downstream protein targets and their subsequent phosphorylation. The phosphorylated effector proteins can then act to modulate transcriptional activity in the nucleus.

Plant embryo development begins when sperm cells from the pollen fertilize the cells of the female gametophyte (26). During the early stages of embryogenesis two polar stem cell niches form to create the apical meristems of the developing shoot and root. All new tissues and organs originate from these meristems to give rise to the aerial and underground portions of the plant (27, 28). In the shoot apical meristem (SAM) a small population of pluripotent cells has the ability to differentiate into leaf and stem structures, but can be reprogrammed to form reproductive tissues. In the root apical meristem (RAM), the pluripotent stem cell niche has the ability to form all tissues of the roots (27). A small number of RLKs that modulate plant development have been studied extensively, namely the *Brassinosteroid insensitive 1* (BRI1) and *CLAVATA1* (CLV), and have shed light on receptor complex formation, ligand identification, and downstream signaling components. They have provided valuable insight into the mechanistic aspects of the signal transduction events that regulate the proper growth of the plant.

BRI1 is a LRR RLK that binds to a steroid hormone, brassinosteroid (BR), in the extracellular domain (29). BRs are growth promoting hormones that influence cell division and elongation in the plant and can be regulated by environmental conditions such as light and temperature (30). Loss of BRI1 function leads to a variety of plant defects ranging from dwarfism, to delayed senescence, to aberrant skotomorphogenesis when plants are grown in the dark (30-32). BRI1 is constitutively expressed in all parts of the plant ranging from the root meristem to the apical meristem. Although BRI1 is globally expressed in the plant, temporal regulation of the receptor occurs and is more actively expressed in younger tissues than mature tissues (33).

At the cell surface, BRI1 can form homo- or heterodimeric receptor complexes. Studies have shown that BRI1 has the capacity to form inactive homodimers in the absence of BR stimulation and that homodimerization is a mechanism of autoregulation (34, 35). The formation of the homodimeric complex and the binding of kinase inhibitor BRI1 KINASE INHIBITOR 1 (BKI) (36) ensures BRI1 signaling is maintained in the inactive state. *In vivo* demonstration in both yeast cells and *Arabidopsis* has provided confirmation that BRI1 forms an active heterodimer with another LRR RLK, BRI1-Associated Receptor Kinase1 (BAK1) (34, 37, 38). Direct binding of BR (39) to the extracellular domain leads to activation and transphosphorylation of the intracellular kinase domains within the BRI-BAK1 receptor complex (40) and levels of phosphorylation are directly associated with BR binding (41). BR binding and establishment of the active BRI1-BAK1 receptor complex initiates an intracellular signaling cascade involving recruitment and activation of membrane-localized kinases BSK1 and 2 (24), a protein phosphatase BSU1 (25, 42), the cytoplasmic kinase BIN2 (43), and transcription factors BZR1 and 2 (44-46). Thus, like mammalian systems, plants use receptor mediated signaling cascades to moderate their own growth.

A challenge in the developmental biology of all multicellular organisms is striking a balance between cell proliferation, specification, and differentiation. In higher plants, new tissues and organs are produced post-embryonically from stem cell populations in the SAM and the RAM. A meristem is defined as a formative region of cells that divide and differentiate into a number of tissues that eventually comprise the entire plant. The boundaries of the meristem are classified by genetic, cellular, and molecular constraints as well as the ability of this zone to produce primordia which eventually give rise to the organs of the plant (47). The SAM can be divided into three cell layers. The L1 layer is the outer,

single-cell layer that gives rise to epidermal tissues by anticlinal cell division. The L2 layer produces cells of the mesophyll and the L3 layer produces cell the make up the inner tissues of the stems and leaves (48). Furthermore, the SAM can be divided into three radial sectors: the central zone (CZ), the peripheral zone (PZ), and the rib zone (RZ). Cell division in the CZ is slow, whereas in the PZ it is rapid in order to produce all cells necessary for organ development (49). The RZ harbors the Organizing Center (OC) which is the pool of pluripotent stem cells in the SAM (27). These layers work in concert to maintain SAM homeostasis during the lifetime of the plant. Thus, all aerial organs are formed from differentiation of cells at the summit of the SAM.

Multiple factors control cell proliferation and specification in the SAM. Studies in *Arabidopsis* indicate that the balance between the antagonistic processes of stem cell renewal and organogenesis is maintained by a signal transduction process involving the *CLV* genes *CLV1*, *CLV2*, and *CLV3* which are expressed in adjacent regions of the SAM and function in the same genetic pathway (50-54). *clv1*, *clv2*, and *clv3* loss-of-function mutants display abnormal phenotypes of shoot fasciation, enlarged meristems, and increased number of floral organs (48). CLV1 is an LRR RLK that is expressed only in the central L3 layer of the SAM and CLV2 is an LRR RLK that is similar to CLV1 but lacking the kinase domain (55). The *CLV3* gene encodes a 78-amino acid precursor protein that is expressed only in the L1 and L2 layers. Proteolytic processing of CLV3 releases the active 12-amino acid peptide ligand containing two post-translationally modified hydroxyproline residues (56, 57) that binds directly to the CLV1 ectodomain (58). CLV1 and CLV2 have been shown to form an inactive disulfide linked heterodimeric complex in the absence of CLV3. The CLV1/CLV2 heterodimer can form a larger complex which includes a kinase associated protein

phosphatase (KAPP) and an ROP-GTPase which is dependent on CLV3 ligand binding directly to the CLV1 extracellular domain (58, 59). CLV3 binding activates the intracellular kinase domain of CLV1 and initiates downstream signaling events ultimately leading to repression of the WUSCHEL (WUS) transcription factor. WUS is expressed in the underlying OC of the meristem and functions to prevent stem cell differentiation. Activation of the CLV signaling pathway leads to suppression of the WUS expression domain, thus inhibiting the WUS signal. Inhibition of the WUS signal now promotes the differentiation of stem cells. Thus, a feedback loop is generated in the SAM between opposing CLV3 and WUS signals to regulate stem cell proliferation and differentiation (60, 61).

The CRINKLY4 gene and its role in plant development

The maize CRINKLY4 (CR4) gene was first identified by transposon tagging as a putative receptor-like kinase encoding gene involved in the proper differentiation of epidermal tissues in the aerial organs of the plant. It was observed that the loss of epidermal cell identity led to improper formation of the cuticle on the leaf surface and fusions between leaf tissues, causing the leaves to be "crinkled" (62). Genetic analyses confirmed the role of this gene in regulating epidermal cell specification and morphology primarily in the leaves and the kernel. Leaf epidermal cells of *cr4* mutants showed irregular cell patterning, enlargement, and irregular shape compared to wild-type. In some instances, cell proliferation was affected in mutant *cr4* epidermal cell lines, leading to wart-like structures (62, 63). This gave rise to the notion that CR4 was involved in a growth factor like signaling event within the plant. Further studies have shown that CR4 behaves in a cell autonomous fashion. Genetic mosaic analysis revealed that the *cr4* mutant phenotype could not be rescued by neighboring wild-type cells (64, 65). This suggested that signaling cues from wild-type cells

could not be perceived or that *cr4* mutant cells were unable to activate intracellular signaling networks to effect proper differentiation.

Orthologs of CR4 have been identified in rice (OsCR4) and *Arabidopsis* (ACR4) (66, 67). In addition, both rice and *Arabidopsis* contain homologous RLKs. In *Arabidopsis,* there are four Crinkly4 related proteins (CRRs) designated as AtCRR1, AtCRR2, AtCRR3 and AtCRK1, that share similar structural features with ACR4 (67), suggesting functional redundancy in dicot plants (67-69). The ACR4 receptor-like kinase is primarily expressed in the outer cell layers of the developing plant. *In situ* hybridization studies have shown ACR4 transcripts to be localized to the protoderm in the early stages of embryo formation (66). In later stages of embryogenesis, transcripts were located predominantly in the L1 layer at the tips of the cotyledons and in meristematic tissues in both the shoot and root apices. Post germination, high transcript levels were found primarily in the epidermal tissues of the shoot, shoot apical meristem (SAM), and outer layers of flower and leaf primordia, and in the root tip (66, 68). ACR4 protein expression patterns mirror RNA transcript localization. In aerial organs, ACR4 is found in the L1 layer of the SAM, ovule integuments, and epidermal layer of the leaves (67-69). In the roots, ACR4 expression is found in the quiescent center (QC), underlying columella cells, and flanking cells of the lateral root cap (68, 70, 71). The global expression of ACR4 throughout the plant implicates its importance to the overall development of the plant.

ACR4 has been described to have similar phenotypic effects as maize CR4. In the leaves, alterations in epidermal cells could be observed as outgrowths of cells at the leaf tip and the lack of cuticle formation. Loss of cuticle was observed by the presence of hydrophilic toluidine blue staining of underlying dermal tissues, indicating a deficiency in

epidermal cell establishment (69). The reproductive organs of the plant displayed similar characteristics. In the absence of ACR4, mutant plants have abnormalities in the organization of the L1 layer of ovule integuments and in the sepal margins. Gross morphological characteristics could be distinguished when compared to wild-type tissues. Mutant plants showed irregular seed coat formation with unusual outgrowths and fusions to adjacent seeds. Furthermore, affected seeds showed increased abortion rates most likely due to the morphological abnormalities derived from loss of functional ACR4 (68, 69).

In the root apical meristem (RAM), all cells are derived from a population of undifferentiated initial cells surrounding a small pool of rarely dividing cells, designated the quiescent center (QC) (72). Short-range signals from the QC maintain strict control of the stem cell population in the undifferentiated state. Stem cell division gives rise to daughter cells that are distal to the quiescent center and the surrounding mature, differentiated cells then cue the daughter cell to differentiate into its appropriate cell type (73, 74). ACR4 has been connected to two developmental processes within the RAM. First, at the primary root tip, the gravity sensing, starch granule containing columella cells (CC) are born from a defined set of columella stem cells (CSC) situated just below the quiescent center. CSC differentiation leads to a daughter cell that eventually differentiates into a CC given the proper signal by the underlying CCs (71, 73, 75, 76). In the absence of functional ACR4, CSCs fail to differentiate into CCs, leading to a proliferation of CSCs and disorganization of CCs in the root tip (70, 71).

A feedback loop has been proposed involving the CLE40 peptide, ACR4, and the WOX5 transcription factor in which ACR4 acts to perceive the CLE40 peptide and controls the expression pattern of WOX5, similar to the CLAVATA signaling mechanism in the SAM

(71). CLE40 belongs to the CLAVATA3/ENDOSPERM SURROUNDING REGION (70) family of peptide hormones in plants. The gene encodes an 80 amino acid precursor protein and contains the 14 amino acid CLE box sequence common to members of the CLE family (77, 78). Exogenous application of the active, 14-amino acid CLE40 peptide to *Arabidopsis* roots is able to promote meristem consumption by promoting differentiation of CSCs into CCs (71, 79). The WUSCHEL RELATED HOMEOBOX 5 (WOX5) belongs to the 14 member WOX gene family of transcription factors in *Arabidopsis* and is solely expressed in the QC of the RAM (74, 80). WOX5 contains a homeobox DNA binding domain and a stretch of sequence C-terminal of the homeodomain, termed the WUS box. This sequence, in WUS, is required for stem cell maintenance and floral patterning (81, 82). Interestingly, WOX5 and WUS can functionally replace each other in their respective meristems of the SAM or RAM, suggesting that these two transcription factors operate similarly in stem cell maintenance regardless of their location (74). WOX5 functions antagonistically to CLE40 in that it promotes stem cell maintenance, whereas CLE40 encourages stem cell differentiation (71, 74). Spatial expression of WOX5 is shifted toward the apical side of the QC when CLE40 peptide is exogenously applied to *Arabidopsis* roots. Restriction of WOX5 expression to this domain is presumably through ACR4 activation since application of the CLE40 peptide in the *acr4* mutant background fails to differentiate CSCs to CCs in the root tip (71). Thus, a postulated feedback mechanism has been proposed where CLE40 binds to ACR4 in the extracellular domain, activates the receptor, which in turn regulates WOX5 influence inside the cell.

In addition to stem cell maintenance in the RAM, ACR4 has been implicated in the initiation of lateral roots. Coordinated signaling events within the root are needed to

commence lateral root formation. During the initiation event, longitudinal pericycle cells develop characteristics of founder cells and undergo anticlinal, asymmetric cell division to produce daughter initial cells. These initial cells then undergo another round of anticlinal, asymmetric division to produce two central cells. In a final step, the latter divide periclinally to produce the site where the lateral root emerges from the primary root (70, 83). ACR4 is required for the proper regulation of cell division during this process. Loss of ACR4 results in increased division in the pericycle, fusion of lateral initials, and an increase in opposing lateral root initiation sites (70). Additionally, double and triple mutants in which combinations of ACR4 and the ACR4 homologs have been knocked out displayed increased lateral root meristems. Functional redundancy has been suggested in Arabidopsis due to ACR4 having four homologs with similar structural features (67, 70).

The 901amino acid maize CR4 protein (Fig. 1) has a putative extracellular ligand binding domain, a single transmembrane helix, and an intracellular kinase domain, all architectural features similar to mammalian RTKs (62). Orthologs in rice, OsCR4, and *Arabidopsis* ACR4, share the same features (66, 67). The extracellular domain of CR4, a putative ligand binding domain, contains seven repeat regions approximately 39 amino acids in length, followed by three cysteine-rich regions similar to the tumor necrosis factor receptor ligand binding domain. However, a ligand has yet to be identified. A single alpha helix spanning the membrane connects the extracellular domain to the intracellular, active serine/threonine kinase domain (62, 63, 67). Studies utilizing truncation mutants lacking single/multiple domains of ACR4 in transgenic plants demonstrated that the extracellular domain is required for receptor function and turnover (84). However, opinions differ on

whether or not the intracellular kinase domain is absolutely necessary for receptor function (69, 84).

Fundamental functional analysis by biological and biochemical methods of the varying domains within ACR4 has provided some insight into the importance of these regions on receptor function. The extracellular crinkly repeat domain is thought to fold into a β-propeller like structure that may be involved in protein-protein interactions (67, 84). The structure of the crinkly repeat domain of ACR4 was determined by homology modeling to two crystal structures of 7-bladed propeller proteins, the β-Lactamase inhibitor protein-II (85) and the Regulator of Chromosome Condensation protein (86). The model showed conserved, regularly spaced Cysteine residues in the repeats were likely to contribute to structural stability in the oxidizing environment of the extracellular space (84). In RTKs, evidence indicates that TM domains function in a dynamic fashion and have the intrinsic capacity to drive receptor dimerization (87, 88). Thus, the propensity of the transmembrane (TM) helices of the CR4, ACR4, and ACR4 homologs (AtCRRs) to dimerize has been studied by a modified TOXCAT assay. The TM domains of the receptors vary in their ability to homodimerize with AtCRR1 possessing the highest propensity to dimerize, whereas the ACR4 TM showed the lowest potential (89). Further mutagenesis studies also demonstrated the important role of specific amino acids within the TM helix of CR4 and ACR4 that profoundly affected dimer formation (90). The intracellular domain of ACR4 has been demonstrated to possess intrinsic kinase activity (67-69). More recently, the biochemical properties of the ACR4 kinase domain have been extensively characterized *in vitro* with regard to autophosphorylation and its mechanism, preference for divalent metal ions, conformational and oligomerization properties (5). This description also constitutes a major

chapter in this dissertation along with other significant descriptions on sub-domain regulation of kinase activity and protein-protein interactions among ACR4 and ACR4 homologs.

Kinase domain structure and regulation

Reversible phosphorylation is one of the primary post-translational modifications utilized by metazoans to communicate between cellular components in order to regulate cell growth, proliferation, and differentiation. Uncontrolled phosphorylation events can lead to increased disease states of an organism and ultimately death if left unchecked. Protein phosphorylation can alter protein conformation, modulate protein-protein interactions, control catalytic activity, and regulate subcellular localization of proteins (91). Communication using phosphorylation is regulated by protein kinases and phosphatases in order to preserve cellular homeostasis.

A kinase is an enzyme that catalyzes the transfer of a phosphate group to a specified substrate. For the majority of kinases, the γ-phosphate donor is a molecule of adenosine triphosphate (ATP) and phosphotransfer occurs on the hydroxyl groups of serine, threonine, and tyrosine residues (92). The kinase catalytic domain comprises approximately 250-300 amino acids and, based on numerous structural and biochemical studies, can be separated into 11 distinct subdomains that house roughly 10 highly conserved residues and/or motifs that contribute to the activity and stability of the molecule (93). These subdomains and residues are depicted in Fig. 2 for the ACR4 kinase domain. The kinase domain folds into a highly conserved structure with an N-terminal lobe that is comprised predominantly of β-sheets and a C-terminal lobe that is mostly α-helical, as seen in the first crystal structures solved using the cyclic AMP-dependent kinase (94-96). Fig. 3a shows the homology model for the ACR4 kinase domain. The tertiary structure produced at the interface of the N and C-

terminal domains creates a pocket that serves as the active site of the enzyme. Conserved features (Fig. 2 and 4) include the Gly rich motif (P-loop) between β-strands 1 and 2 of the N-lobe which function to help bind and stabilize the α and β phosphates of the bound ATP molecule. The essential Lys residue in β-strand 3 of the N lobe also helps to stabilize the α and β phosphates of ATP and forms a salt bridge with the invariant Glu residue in helix-C. The C-lobe of the kinases harbors a conserved HRD motif, termed the catalytic loop, in which the aspartic acid serves as the catalytic base during the phosphotransfer reaction and chelates a Mg^{2+} ion that bridges the α and γ phosphates. Loss of this amino acid results in complete inactivity of the kinase. The activation loop of kinases is slightly downstream of the catalytic loop and located between two conserved DFG and APE motifs (DPE in ACR4) that serve as hinge points for activation loop movement. The Asp in the DFG motif functions to chelate a Mg^{2+} ion that stabilizes the β and γ phosphates of ATP. The APE motif serves a structural role in stabilizing the C-lobe (22, 93, 96). These conserved features work to coordinate the efficient transfer of phosphate from ATP to the appropriate target.

Phosphotransfer from ATP to the substrate occurs at the active site. A molecule of ATP binds to the kinase domain in an orientation that stages the γ-phosphate for transfer to the substrate (Fig. 3b). The adenine ring of ATP is buried in the hydrophobic cleft of the active site and the γ-phosphate is presented outwards toward the target molecule. The reaction mechanism of phosphotransfer can occur by two possible extremes, an *associative* mechanism or a *dissociative* mechanism. The associative mechanism, comparable to a S_n2 reaction, implies that the hydroxyl group on the substrate undergoes nucleophilic attack on the γ-phosphate moiety, formation of a transition intermediate, followed by release of adenosine diphosphate (ADP) and the phosphorylated protein. Whereas, the dissociative

mechanism, similar to a S_n1 reaction, involves expulsion of the γ-phosphate as a monomeric metaphosphate ion, followed by nucleophilic attack by the substrate hydroxyl group (97). It is likely that the associative mechanism occurs during phosphotransfer of di- and triesters, while the dissociative mechanism takes place in phosphotransfer of monoesters (97, 98). Structural studies of protein kinases have revealed how the enzyme facilitates phosphotransfer using conserved residues lining the active site. These residues help coordinate the ATP molecule and assist in stabilizing the transition state during the phosphotransfer reaction (99).

Regulation of phosphorylation events is crucial to cellular signaling networks. Unfettered kinase activity can lead to different disease types including a multitude of cancers. These cancers arise from mutations within the kinase domains of many RTKs causing constitutive activation that drives uncontrolled signaling in the cell (100-102). There are several mechanisms exploited by kinases to maintain tight regulation of their activity. The activation loop of the kinase, ~20-35 residues, is a key regulatory element. Most kinases are activated by one or more phosphorylations within the activation loop. A subsequent conformational change occurs to remove inhibitory constraints imposed on the kinase. Once phosphorylated, the activation loop can also serve as a docking site for kinase substrates (103). The intracellular kinase domains of cell-surface receptor kinases are flanked by N and C-terminal regions that assist in modulating kinase activity. The juxtamembrane domain (JMD) is the region between the inner membrane and the kinase domain and the C-terminal domain (CTD) is located downstream of the kinase domain. In the absence of ligand, the JMD and CTD adopt a conformation that preserves the kinase in an inactive state (104). For instance, the JMD of the KIT RTK binds directly to the N-terminal lobe of the kinase causing

inhibition as demonstrated by exogenous application of JMD peptides to KIT proteins in a kinase assay *in vitro*. Furthermore, overexpression of the KIT JMD caused a reduction of KIT activity *in vivo* (105). Evidence exists in the Eph receptor family in which the JMD adopts a conformation that binds to the N-lobe of the kinase and distorts a crucial salt bridge required for activity therefore inhibiting kinase activity. Phosphorylation of two tyrosine residues in the JMD forces the domain into an alternate conformation, relieving its inhibitory effect (106, 107). During receptor activation, residues within the JMD and CTD are phosphorylated, which drives a conformational change that opens up the molecule and relieves inhibition of kinase activity and allows for substrate binding (104). Lastly, intermolecular interactions can take place between kinases and proteins that act as inhibitors. In the case of the TGFβ receptor (TβR-I), the kinase domain is kept in the inhibited state by the FKBP12 protein. The JMD region of TβR-I contains a TTSGSGSG motif (GS motif) that binds the FKBP12 in the unphosphorylated state and represses kinase activity. Phosphorylation of multiple Ser and Thr residues in the GS motif is required for full kinase activity (108) and causes structural changes in the JMD that releases FKBP12 binding (109, 110).

Other components in epidermal cell fate

The epidermal layer in plants helps regulate gas and nutrient exchange, maintain water, and provides a barrier against insect/pathogen attack. The proper formation of the epidermis on multiple organs is necessary for the overall growth and development of the plant. The protoderm originates at embryogenesis and it is still unclear how these cells are cued to differentiate into their final cell type (111). A multitude of candidate genes have

been identified that engage in a variety of mechanisms to promote, specify, and maintain epidermal cell type.

Maize DEK1 is a member of the calcium-dependent calpain proteinase superfamily and shares the highly conserved cysteine proteinase domain common among the family. DEK1 is a membrane bound protein that differs from mammalian calpains in the fact that it contains a large N-terminal domain. This region contains 21 transmembrane passes and a 300 amino acid extracellular loop, raising the possibility that this region plays a role in perceiving an extracellular signal and causes autolytic cleavage of the intracellular calpain domain to release from the membrane to transducer a signal inside the cell (112, 113). The intracellular calpain domain contains a conserved catalytic triad common to cysteine proteinases (112, 114). Enzymatic activity of the calpain domain is enhanced in the presence of Ca^{2+}, however, Ca2+ is not a requirement for catalytic activity as seen with mammalian calpains, indicating that DEK1 may be regulated in some other manner (114). DEK1 is mandatory for the maintenance of aleurone cell identity in the kernel during endosperm development. However, DEK1 is not required for specification of aleurone cell fate and it is thought that CR4 perceives positional cues to prompt aleurone differentiation. Loss of DEK1 results in a reversion of aleurone cells to starchy endosperm, indicating DEK1 works separately from, but overlaps with CR4 to maintain aleurone identity (64, 112).

A putative class E vacuolar sorting protein named SUPERNUMERARY LAYER1 (SAL1) is another protein involved in epidermal differentiation and maintenance. SAL1 is a negative regulator of epidermal cell differentiation, where loss of SAL1 function leads to multiple aleurone layers in the maize kernel and weak epidermal defects in vegetative tissues (115). Sequence alignment of SAL1 shows similarity to the human CHMP1 gene which is

involved in vesicle trafficking of proteins targeted for proteasomal degradation, suggesting SAL1 may be involved in membrane protein turnover. Interestingly, SAL1 has been shown to co-localize with DEK1 in cellular vesicles in maize, signifying its possible role in protein turnover (116).

In *Arabidopsis,* a putative subtilisin-like protease, ABNORMAL LEAF SHAPE 1 (ALE1), and a LRR RLK, ALE2, have also been implicated in epidermal development. During embryo and seedling development *ale1* mutants show seedling lethality, loss of cuticle formation in the leaves, and the adherence of adjacent leaf tissues (117). ALE1 contains a N-terminal signal sequence for secretion into the extracellular space and may function to provide a peptide ligand for a cell-surface receptor such as ACR4. Genetic analysis of *ale1/acr4* double mutants showed a stronger mutant than either single mutant, suggesting that ALE1 and ACR4 act in separate but overlapping pathways (69). The ALE2 gene encodes a LRR RLK that has an active, intracellular kinase domain. Both ACR4 and ALE2 have been shown to synergistically enhance phosphorylation *in vitro* (118). *ale2/acr4* double mutants are phenotypically similar to the *ale2* single mutant (118). The epidermal phenotype analysis along with the phosphorylation enhancement suggests these two receptors may function in the same pathway.

Overall, multiple modulators of epidermal specification and differentiation have been identified. Individual components have been determined to be involved at various stages of communication in order to properly form and maintain epidermal cell type. However, the exact molecular mechanisms of how these components function and their ability to communicate with each other remains largely unknown.

Conclusions

Cellular signaling via cell-surface receptors is a highly regulated process across all organisms. Loss of control in phosphorylation events can lead to a multitude of defects and diseases in an organism. Receptor kinases are emerging as key components of growth and development in plants, as seen with the BRI1 and CLAVATA signaling pathways. In recent years the ACR4 RLK has also emerged as an important player since it appears to be involved in the entire development of the plant as evidenced by its global role in the differentiation of both aerial and underground tissues. A plethora of biological data has been amassed about the functional significance of the ACR4 RLK. However, little information is known acknowledging the molecular mechanisms of how the receptor functions in putative ligand perception and receptor activation, the regulatory aspects of kinase activity, and the downstream components involved in ACR4 signaling. Therefore, this dissertation begins to address the fundamental biochemical properties of ACR4 including its kinase activity, the role of the juxtamembrane domain on kinase activity, the recombinant expression of some of the homologs and other proteins implicated in epidermal cell fate specification and provides evidence for potential intermolecular interactions that could further impact downstream signaling events.

References

1. Lemmon, M.A. and J. Schlessinger, *Cell signaling by receptor tyrosine kinases.* Cell, 2010. **141**(7): p. 1117-34.
2. Ullrich, A. and J. Schlessinger, *Signal Transduction by Receptors with Tyrosine Kinase-Activity.* Cell, 1990. **61**(2): p. 203-212.
3. Schlessinger, J., *Cell signaling by receptor tyrosine kinases.* Cell, 2000. **103**(2): p. 211-25.
4. Scott, J.D. and T. Pawson, *Cell signaling in space and time: where proteins come together and when they're apart.* Science, 2009. **326**(5957): p. 1220-4.

5. Meyer, M.R., C.F. Lichti, R.R. Townsend, and A.G. Rao, *Identification of in vitro autophosphorylation sites and effects of phosphorylation on the Arabidopsis CRINKLY4 (ACR4) receptor-like kinase intracellular domain: insights into conformation, oligomerization, and activity.* Biochemistry, 2011. **50**(12): p. 2170-86.
6. Shiu, S.H. and A.B. Bleecker, *Plant receptor-like kinase gene family: diversity, function, and signaling.* Sci STKE, 2001. **2001**(113): p. re22.
7. Shiu, S.H. and A.B. Bleecker, *Expansion of the receptor-like kinase/Pelle gene family and receptor-like proteins in Arabidopsis.* Plant Physiol, 2003. **132**(2): p. 530-43.
8. McGurl, B., G. Pearce, M. Orozco-Cardenas, and C.A. Ryan, *Structure, expression, and antisense inhibition of the systemin precursor gene.* Science, 1992. **255**(5051): p. 1570-3.
9. Pearce, G., D.S. Moura, J. Stratmann, and C.A. Ryan, Jr., *RALF, a 5-kDa ubiquitous polypeptide in plants, arrests root growth and development.* Proc Natl Acad Sci U S A, 2001. **98**(22): p. 12843-7.
10. Matsubayashi, Y., M. Ogawa, A. Morita, and Y. Sakagami, *An LRR receptor kinase involved in perception of a peptide plant hormone, phytosulfokine.* Science, 2002. **296**(5572): p. 1470-2.
11. Scheer, J.M., G. Pearce, and C.A. Ryan, *Generation of systemin signaling in tobacco by transformation with the tomato systemin receptor kinase gene.* Proc Natl Acad Sci U S A, 2003. **100**(17): p. 10114-7.
12. Torii, K.U., *Leucine-rich repeat receptor kinases in plants: Structure, function, and signal transduction pathways.* International Review of Cytology - a Survey of Cell Biology, Vol. 234, 2004. **234**: p. 1-+.
13. Chow, B. and P. McCourt, *Plant hormone receptors: perception is everything.* Genes Dev, 2006. **20**(15): p. 1998-2008.
14. Matsubayashi, Y. and Y. Sakagami, *Peptide hormones in plants.* Annu Rev Plant Biol, 2006. **57**: p. 649-74.
15. Shinohara, H., M. Ogawa, Y. Sakagami, and Y. Matsubayashi, *Identification of ligand binding site of phytosulfokine receptor by on-column photoaffinity labeling.* J Biol Chem, 2007. **282**(1): p. 124-31.
16. Afzal, A.J., A.J. Wood, and D.A. Lightfoot, *Plant receptor-like serine threonine kinases: roles in signaling and plant defense.* Mol Plant Microbe Interact, 2008. **21**(5): p. 507-17.
17. Muller, R., A. Bleckmann, and R. Simon, *The receptor kinase CORYNE of Arabidopsis transmits the stem cell-limiting signal CLAVATA3 independently of CLAVATA1.* Plant Cell, 2008. **20**(4): p. 934-46.
18. Guo, Y., L. Han, M. Hymes, R. Denver, and S.E. Clark, *CLAVATA2 forms a distinct CLE-binding receptor complex regulating Arabidopsis stem cell specification.* Plant Journal, 2010. **63**(6): p. 889-900.
19. Oh, M.H., X. Wang, U. Kota, M.B. Goshe, S.D. Clouse, and S.C. Huber, *Tyrosine phosphorylation of the BRI1 receptor kinase emerges as a component of brassinosteroid signaling in Arabidopsis.* Proc Natl Acad Sci U S A, 2009. **106**(2): p. 658-63.
20. Oh, M.H., X. Wu, S.D. Clouse, and S.C. Huber, *Functional importance of BAK1 tyrosine phosphorylation in vivo.* Plant Signal Behav, 2011. **6**(3): p. 400-5.

21. Krupa, A., G. Preethi, and N. Srinivasan, *Structural modes of stabilization of permissive phosphorylation sites in protein kinases: distinct strategies in Ser/Thr and Tyr kinases.* J Mol Biol, 2004. **339**(5): p. 1025-39.
22. Nolen, B., S. Taylor, and G. Ghosh, *Regulation of protein kinases: Controlling activity through activation segment conformation.* Molecular Cell, 2004. **15**(5): p. 661-675.
23. Haffani, Y.Z., N.F. Silva, and D.R. Goring, *Receptor kinase signalling in plants.* Canadian Journal of Botany-Revue Canadienne De Botanique, 2004. **82**(1): p. 1-15.
24. Tang, W.Q., T.W. Kim, J.A. Oses-Prieto, Y. Sun, Z.P. Deng, S.W. Zhu, R.J. Wang, A.L. Burlingame, and Z.Y. Wang, *BSKs mediate signal transduction from the receptor kinase BRI1 in Arabidopsis.* Science, 2008. **321**(5888): p. 557-560.
25. Kim, T.W., S. Guan, Y. Sun, Z. Deng, W. Tang, J.X. Shang, A.L. Burlingame, and Z.Y. Wang, *Brassinosteroid signal transduction from cell-surface receptor kinases to nuclear transcription factors.* Nat Cell Biol, 2009. **11**(10): p. 1254-60.
26. Ma, H. and V. Sundaresan, *Development of flowering plant gametophytes.* Curr Top Dev Biol, 2010. **91**: p. 379-412.
27. Scheres, B., *Stem-cell niches: nursery rhymes across kingdoms.* Nat Rev Mol Cell Biol, 2007. **8**(5): p. 345-54.
28. De Smet, I., U. Voss, G. Jurgens, and T. Beeckman, *Receptor-like kinases shape the plant.* Nature Cell Biology, 2009. **11**(10): p. 1166-1173.
29. He, Z., Z.Y. Wang, J. Li, Q. Zhu, C. Lamb, P. Ronald, and J. Chory, *Perception of brassinosteroids by the extracellular domain of the receptor kinase BRI1.* Science, 2000. **288**(5475): p. 2360-3.
30. Clouse, S.D., M. Langford, and T.C. McMorris, *A brassinosteroid-insensitive mutant in Arabidopsis thaliana exhibits multiple defects in growth and development.* Plant Physiol, 1996. **111**(3): p. 671-8.
31. Li, J. and J. Chory, *A putative leucine-rich repeat receptor kinase involved in brassinosteroid signal transduction.* Cell, 1997. **90**(5): p. 929-38.
32. Noguchi, T., S. Fujioka, S. Choe, S. Takatsuto, S. Yoshida, H. Yuan, K.A. Feldmann, and F.E. Tax, *Brassinosteroid-insensitive dwarf mutants of Arabidopsis accumulate brassinosteroids.* Plant Physiol, 1999. **121**(3): p. 743-52.
33. Friedrichsen, D.M., C.A.P. Joazeiro, J.M. Li, T. Hunter, and J. Chory, *Brassinosteroid-insensitive-1 is a ubiquitously expressed leucine-rich repeat receptor serine/threonine kinase.* Plant Physiology, 2000. **123**(4): p. 1247-1255.
34. Russinova, E., J.W. Borst, M. Kwaaitaal, A. Cano-Delgado, Y. Yin, J. Chory, and S.C. de Vries, *Heterodimerization and endocytosis of Arabidopsis brassinosteroid receptors BRI1 and AtSERK3 (BAK1).* Plant Cell, 2004. **16**(12): p. 3216-29.
35. Wang, X., X. Li, J. Meisenhelder, T. Hunter, S. Yoshida, T. Asami, and J. Chory, *Autoregulation and homodimerization are involved in the activation of the plant steroid receptor BRI1.* Dev Cell, 2005. **8**(6): p. 855-65.
36. Wang, X. and J. Chory, *Brassinosteroids regulate dissociation of BKI1, a negative regulator of BRI1 signaling, from the plasma membrane.* Science, 2006. **313**(5790): p. 1118-22.
37. Nam, K.H. and J. Li, *BRI1/BAK1, a receptor kinase pair mediating brassinosteroid signaling.* Cell, 2002. **110**(2): p. 203-12.

38. Li, J., J. Wen, K.A. Lease, J.T. Doke, F.E. Tax, and J.C. Walker, *BAK1, an Arabidopsis LRR receptor-like protein kinase, interacts with BRI1 and modulates brassinosteroid signaling.* Cell, 2002. **110**(2): p. 213-22.
39. Kinoshita, T., A. Cano-Delgado, H. Seto, S. Hiranuma, S. Fujioka, S. Yoshida, and J. Chory, *Binding of brassinosteroids to the extracellular domain of plant receptor kinase BRI1.* Nature, 2005. **433**(7022): p. 167-71.
40. Wang, X., U. Kota, K. He, K. Blackburn, J. Li, M.B. Goshe, S.C. Huber, and S.D. Clouse, *Sequential transphosphorylation of the BRI1/BAK1 receptor kinase complex impacts early events in brassinosteroid signaling.* Dev Cell, 2008. **15**(2): p. 220-35.
41. Wang, X., M.B. Goshe, E.J. Soderblom, B.S. Phinney, J.A. Kuchar, J. Li, T. Asami, S. Yoshida, S.C. Huber, and S.D. Clouse, *Identification and functional analysis of in vivo phosphorylation sites of the Arabidopsis BRASSINOSTEROID-INSENSITIVE1 receptor kinase.* Plant Cell, 2005. **17**(6): p. 1685-703.
42. Mora-Garcia, S., G. Vert, Y. Yin, A. Cano-Delgado, H. Cheong, and J. Chory, *Nuclear protein phosphatases with Kelch-repeat domains modulate the response to brassinosteroids in Arabidopsis.* Genes Dev, 2004. **18**(4): p. 448-60.
43. Li, J. and K.H. Nam, *Regulation of brassinosteroid signaling by a GSK3/SHAGGY-like kinase.* Science, 2002. **295**(5558): p. 1299-301.
44. He, J.X., J.M. Gendron, Y. Sun, S.S.L. Gampala, N. Gendron, C.Q. Sun, and Z.Y. Wang, *BZR1 is a transcriptional repressor with dual roles in brassinosteroid homeostasis and growth responses.* Science, 2005. **307**(5715): p. 1634-1638.
45. Yin, Y.H., D. Vafeados, Y. Tao, S. Yoshida, T. Asami, and J. Chory, *A new class of transcription factors mediates brassinosteroid-regulated gene expression in Arabidopsis.* Cell, 2005. **120**(2): p. 249-259.
46. Vert, G. and J. Chory, *Downstream nuclear events in brassinosteroid signalling.* Nature, 2006. **441**(7089): p. 96-100.
47. Scofield, S. and J.A. Murray, *The evolving concept of the meristem.* Plant Mol Biol, 2006. **60**(6): p. V-VII.
48. Miwa, H., A. Kinoshita, H. Fukuda, and S. Sawa, *Plant meristems: CLAVATA3/ESR-related signaling in the shoot apical meristem and the root apical meristem.* J Plant Res, 2009. **122**(1): p. 31-9.
49. Kwiatkowska, D., *Flowering and apical meristem growth dynamics.* J Exp Bot, 2008. **59**(2): p. 187-201.
50. Fletcher, J.C., *Shoot and floral meristem maintenance in arabidopsis.* Annu Rev Plant Biol, 2002. **53**: p. 45-66.
51. Clark, S.E., M.P. Running, and E.M. Meyerowitz, *CLAVATA1, a regulator of meristem and flower development in Arabidopsis.* Development, 1993. **119**(2): p. 397-418.
52. Clark, S.E., M.P. Running, and E.M. Meyerowitz, *Clavata3 Is a Specific Regulator of Shoot and Floral Meristem Development Affecting the Same Processes as Clavata1.* Development, 1995. **121**(7): p. 2057-2067.
53. Clark, S.E., R.W. Williams, and E.M. Meyerowitz, *The CLAVATA1 gene encodes a putative receptor kinase that controls shoot and floral meristem size in Arabidopsis.* Cell, 1997. **89**(4): p. 575-585.

54. Kayes, J.M. and S.E. Clark, *CLAVATA2, a regulator of meristem and organ development in Arabidopsis.* Development, 1998. **125**(19): p. 3843-3851.
55. Jeong, S., A.E. Trotochaud, and S.E. Clark, *The Arabidopsis CLAVATA2 gene encodes a receptor-like protein required for the stability of the CLAVATA1 receptor-like kinase.* Plant Cell, 1999. **11**(10): p. 1925-34.
56. Fletcher, J.C., U. Brand, M.P. Running, R. Simon, and E.M. Meyerowitz, *Signaling of cell fate decisions by CLAVATA3 in Arabidopsis shoot meristems.* Science, 1999. **283**(5409): p. 1911-4.
57. Kondo, T., S. Sawa, A. Kinoshita, S. Mizuno, T. Kakimoto, H. Fukuda, and Y. Sakagami, *A plant peptide encoded by CLV3 identified by in situ MALDI-TOF MS analysis.* Science, 2006. **313**(5788): p. 845-8.
58. Ogawa, M., H. Shinohara, Y. Sakagami, and Y. Matsubayashi, *Arabidopsis CLV3 peptide directly binds CLV1 ectodomain.* Science, 2008. **319**(5861): p. 294.
59. Trotochaud, A.E., T. Hao, G. Wu, Z.B. Yang, and S.E. Clark, *The CLAVATA1 receptor-like kinase requires CLAVATA3 for its assembly into a signaling complex that includes KAPP and a Rho-related protein.* Plant Cell, 1999. **11**(3): p. 393-405.
60. Brand, U., J.C. Fletcher, M. Hobe, E.M. Meyerowitz, and R. Simon, *Dependence of stem cell fate in Arabidopsis on a feedback loop regulated by CLV3 activity.* Science, 2000. **289**(5479): p. 617-9.
61. Schoof, H., M. Lenhard, A. Haecker, K.F. Mayer, G. Jurgens, and T. Laux, *The stem cell population of Arabidopsis shoot meristems in maintained by a regulatory loop between the CLAVATA and WUSCHEL genes.* Cell, 2000. **100**(6): p. 635-44.
62. Becraft, P.W., P.S. Stinard, and D.R. McCarty, *CRINKLY4: A TNFR-like receptor kinase involved in maize epidermal differentiation.* Science, 1996. **273**(5280): p. 1406-9.
63. Jin, P., T. Guo, and P.W. Becraft, *The maize CR4 receptor-like kinase mediates a growth factor-like differentiation response.* Genesis, 2000. **27**(3): p. 104-16.
64. Becraft, P.W. and Y. Asuncion-Crabb, *Positional cues specify and maintain aleurone cell fate in maize endosperm development.* Development, 2000. **127**(18): p. 4039-48.
65. Becraft, P.W., S.H. Kang, and S.G. Suh, *The maize CRINKLY4 receptor kinase controls a cell-autonomous differentiation response.* Plant Physiol, 2001. **127**(2): p. 486-96.
66. Tanaka, H., M. Watanabe, D. Watanabe, T. Tanaka, C. Machida, and Y. Machida, *ACR4, a putative receptor kinase gene of Arabidopsis thaliana, that is expressed in the outer cell layers of embryos and plants, is involved in proper embryogenesis.* Plant and Cell Physiology, 2002. **43**(4): p. 419-428.
67. Cao, X., K. Li, S.G. Suh, T. Guo, and P.W. Becraft, *Molecular analysis of the CRINKLY4 gene family in Arabidopsis thaliana.* Planta, 2005. **220**(5): p. 645-57.
68. Gifford, M.L., S. Dean, and G.C. Ingram, *The Arabidopsis ACR4 gene plays a role in cell layer organisation during ovule integument and sepal margin development.* Development, 2003. **130**(18): p. 4249-58.
69. Watanabe, M., H. Tanaka, D. Watanabe, C. Machida, and Y. Machida, *The ACR4 receptor-like kinase is required for surface formation of epidermis-related tissues in Arabidopsis thaliana.* Plant Journal, 2004. **39**(3): p. 298-308.

70. De Smet, I., V. Vassileva, B. De Rybel, M.P. Levesque, W. Grunewald, D. Van Damme, G. Van Noorden, M. Naudts, G. Van Isterdael, R. De Clercq, J.Y. Wang, N. Meuli, S. Vanneste, J. Friml, P. Hilson, G. Jurgens, G.C. Ingram, D. Inze, P.N. Benfey, and T. Beeckman, *Receptor-like kinase ACR4 restricts formative cell divisions in the Arabidopsis root.* Science, 2008. **322**(5901): p. 594-7.
71. Stahl, Y., R.H. Wink, G.C. Ingram, and R. Simon, *A signaling module controlling the stem cell niche in Arabidopsis root meristems.* Curr Biol, 2009. **19**(11): p. 909-14.
72. Dinneny, J.R. and P.N. Benfey, *Plant stem cell niches: standing the test of time.* Cell, 2008. **132**(4): p. 553-7.
73. van den Berg, C., V. Willemsen, G. Hendriks, P. Weisbeek, and B. Scheres, *Short-range control of cell differentiation in the Arabidopsis root meristem.* Nature, 1997. **390**(6657): p. 287-9.
74. Sarkar, A.K., M. Luijten, S. Miyashima, M. Lenhard, T. Hashimoto, K. Nakajima, B. Scheres, R. Heidstra, and T. Laux, *Conserved factors regulate signalling in Arabidopsis thaliana shoot and root stem cell organizers.* Nature, 2007. **446**(7137): p. 811-4.
75. Blancaflor, E.B. and P.H. Masson, *Plant gravitropism. Unraveling the ups and downs of a complex process.* Plant Physiol, 2003. **133**(4): p. 1677-90.
76. Perrin, R.M., L.S. Young, U.M.N. Murthy, B.R. Harrison, Y. Wang, J.L. Will, and P.H. Masson, *Gravity signal transduction in primary roots.* Ann Bot, 2005. **96**(5): p. 737-43.
77. Fiers, M., K.L. Ku, and C.M. Liu, *CLE peptide ligands and their roles in establishing meristems.* Current Opinion in Plant Biology, 2007. **10**(1): p. 39-43.
78. Wang, G. and M. Fiers, *CLE peptide signaling during plant development.* Protoplasma, 2010. **240**(1-4): p. 33-43.
79. Fiers, M., E. Golemiec, J. Xu, L. van der Geest, R. Heidstra, W. Stiekema, and C.M. Liu, *The 14-amino acid CLV3, CLE19, and CLE40 peptides trigger consumption of the root meristem in Arabidopsis through a CLAVATA2-dependent pathway.* Plant Cell, 2005. **17**(9): p. 2542-53.
80. Haecker, A., R. Gross-Hardt, B. Geiges, A. Sarkar, H. Breuninger, M. Herrmann, and T. Laux, *Expression dynamics of WOX genes mark cell fate decisions during early embryonic patterning in Arabidopsis thaliana.* Development, 2004. **131**(3): p. 657-68.
81. van der Graaff, E., T. Laux, and S.A. Rensing, *The WUS homeobox-containing (WOX) protein family.* Genome Biol, 2009. **10**(12): p. 248.
82. Ikeda, M., N. Mitsuda, and M. Ohme-Takagi, *Arabidopsis WUSCHEL Is a Bifunctional Transcription Factor That Acts as a Repressor in Stem Cell Regulation and as an Activator in Floral Patterning.* Plant Cell, 2009. **21**(11): p. 3493-3505.
83. Benkova, E. and A. Bielach, *Lateral root organogenesis - from cell to organ.* Curr Opin Plant Biol, 2010. **13**(6): p. 677-83.
84. Gifford, M.L., F.C. Robertson, D.C. Soares, and G.C. Ingram, *ARABIDOPSIS CRINKLY4 function, internalization, and turnover are dependent on the extracellular crinkly repeat domain.* Plant Cell, 2005. **17**(4): p. 1154-66.
85. Lim, D., H.U. Park, L. De Castro, S.G. Kang, H.S. Lee, S. Jensen, K.J. Lee, and N.C. Strynadka, *Crystal structure and kinetic analysis of beta-lactamase inhibitor protein-II in complex with TEM-1 beta-lactamase.* Nat Struct Biol, 2001. **8**(10): p. 848-52.

86. Renault, L., N. Nassar, I. Vetter, J. Becker, C. Klebe, M. Roth, and A. Wittinghofer, *The 1.7 angstrom crystal structure of the regulator of chromosome condensation (RCC1) reveals a seven-bladed propeller.* Nature, 1998. **392**(6671): p. 97-101.
87. Tanner, K.G. and J. Kyte, *Dimerization of the extracellular domain of the receptor for epidermal growth factor containing the membrane-spanning segment in response to treatment with epidermal growth factor.* J Biol Chem, 1999. **274**(50): p. 35985-90.
88. Li, E., M. You, and K. Hristova, *Sodium dodecyl sulfate - Polyacrylamide gel electrophoresis and Forster resonance energy transfer suggest weak interactions between fibroblast growth factor receptor 3 (FGFR3) transmembrane domains in the absence of extracellular domains and ligands.* Biochemistry, 2005. **44**(1): p. 352-360.
89. Stokes, K.D. and A. Gururaj Rao, *Dimerization properties of the transmembrane domains of Arabidopsis CRINKLY4 receptor-like kinase and homologs.* Arch Biochem Biophys, 2008. **477**(2): p. 219-26.
90. Stokes, K.D. and A.G. Rao, *The role of individual amino acids in the dimerization of CR4 and ACR4 transmembrane domains.* Arch Biochem Biophys, 2010. **502**(2): p. 104-11.
91. Kersten, B., G.K. Agrawal, P. Durek, J. Neigenfind, W. Schulze, D. Walther, and R. Rakwal, *Plant phosphoproteomics: An update.* Proteomics, 2009. **9**(4): p. 964-988.
92. Lieser, S.A., B.E. Aubol, L. Wong, P.A. Jennings, and J.A. Adams, *Coupling phosphoryl transfer and substrate interactions in protein kinases.* Biochim Biophys Acta, 2005. **1754**(1-2): p. 191-9.
93. Hanks, S.K. and T. Hunter, *Protein kinases 6. The eukaryotic protein kinase superfamily: kinase (catalytic) domain structure and classification.* FASEB J, 1995. **9**(8): p. 576-96.
94. Knighton, D.R., J.H. Zheng, L.F. Ten Eyck, V.A. Ashford, N.H. Xuong, S.S. Taylor, and J.M. Sowadski, *Crystal structure of the catalytic subunit of cyclic adenosine monophosphate-dependent protein kinase.* Science, 1991. **253**(5018): p. 407-14.
95. Knighton, D.R., J.H. Zheng, L.F. Ten Eyck, N.H. Xuong, S.S. Taylor, and J.M. Sowadski, *Structure of a peptide inhibitor bound to the catalytic subunit of cyclic adenosine monophosphate-dependent protein kinase.* Science, 1991. **253**(5018): p. 414-20.
96. Zheng, J.H., D.R. Knighton, L.F. Teneyck, R. Karlsson, N.H. Xuong, S.S. Taylor, and J.M. Sowadski, *Crystal-Structure of the Catalytic Subunit of Camp-Dependent Protein-Kinase Complexed with Mgatp and Peptide Inhibitor.* Biochemistry, 1993. **32**(9): p. 2154-2161.
97. Aqvist, J., K. Kolmodin, J. Florian, and A. Warshel, *Mechanistic alternatives in phosphate monoester hydrolysis: what conclusions can be drawn from available experimental data?* Chem Biol, 1999. **6**(3): p. R71-80.
98. Williams, N.H., *Models for biological phosphoryl transfer.* Biochimica Et Biophysica Acta-Proteins and Proteomics, 2004. **1697**(1-2): p. 279-287.
99. Madhusudan, E.A. Trafny, N.H. Xuong, J.A. Adams, L.F. Teneyck, S.S. Taylor, and J.M. Sowadski, *Camp-Dependent Protein-Kinase - Crystallographic Insights into Substrate Recognition and Phosphotransfer.* Protein Science, 1994. **3**(2): p. 176-187.

100. Holbro, T. and N.E. Hynes, *ErbB receptors: Directing key signaling networks throughout life.* Annual Review of Pharmacology and Toxicology, 2004. **44**: p. 195-217.
101. Wieduwilt, M.J. and M.M. Moasser, *The epidermal growth factor receptor family: biology driving targeted therapeutics.* Cell Mol Life Sci, 2008. **65**(10): p. 1566-84.
102. Acevedo, V.D., M. Ittmann, and D.M. Spencer, *Paths of FGFR-driven tumorigenesis.* Cell Cycle, 2009. **8**(4): p. 580-8.
103. Huse, M. and J. Kuriyan, *The conformational plasticity of protein kinases.* Cell, 2002. **109**(3): p. 275-82.
104. Hubbard, S.R., *Protein tyrosine kinases: autoregulation and small-molecule inhibition.* Curr Opin Struct Biol, 2002. **12**(6): p. 735-41.
105. Chan, P.M., S. Ilangumaran, J. La Rose, A. Chakrabartty, and R. Rottapel, *Autoinhibition of the kit receptor tyrosine kinase by the cytosolic juxtamembrane region.* Mol Cell Biol, 2003. **23**(9): p. 3067-78.
106. Binns, K.L., P.P. Taylor, F. Sicheri, T. Pawson, and S.J. Holland, *Phosphorylation of tyrosine residues in the kinase domain and juxtamembrane region regulates the biological and catalytic activities of Eph receptors.* Mol Cell Biol, 2000. **20**(13): p. 4791-805.
107. Davis, T.L., J.R. Walker, P. Loppnau, C. Butler-Cole, A. Allali-Hassani, and S. Dhe-Paganon, *Autoregulation by the juxtamembrane region of the human ephrin receptor tyrosine kinase A3 (EphA3).* Structure, 2008. **16**(6): p. 873-884.
108. Wieser, R., J.L. Wrana, and J. Massague, *Gs Domain Mutations That Constitutively Activate T-Beta-R-I, the Downstream Signaling Component in the Tgf-Beta Receptor Complex.* Embo Journal, 1995. **14**(10): p. 2199-2208.
109. Huse, M., Y.G. Chen, J. Massague, and J. Kuriyan, *Crystal structure of the cytoplasmic domain of the type I TGF beta receptor in complex with FKBP12.* Cell, 1999. **96**(3): p. 425-36.
110. Huse, M., T.W. Muir, L. Xu, Y.G. Chen, J. Kuriyan, and J. Massague, *The TGF beta receptor activation process: an inhibitor- to substrate-binding switch.* Mol Cell, 2001. **8**(3): p. 671-82.
111. Javelle, M., V. Vernoud, P.M. Rogowsky, and G.C. Ingram, *Epidermis: the formation and functions of a fundamental plant tissue.* New Phytol, 2011. **189**(1): p. 17-39.
112. Lid, S.E., D. Gruis, R. Jung, J.A. Lorentzen, E. Ananiev, M. Chamberlin, X. Niu, R. Meeley, S. Nichols, and O.A. Olsen, *The defective kernel 1 (dek1) gene required for aleurone cell development in the endosperm of maize grains encodes a membrane protein of the calpain gene superfamily.* Proc Natl Acad Sci U S A, 2002. **99**(8): p. 5460-5.
113. Johnson, K.L., C. Faulkner, C.E. Jeffree, and G.C. Ingram, *The Phytocalpain Defective Kernel 1 Is a Novel Arabidopsis Growth Regulator Whose Activity Is Regulated by Proteolytic Processing.* Plant Cell, 2008. **20**(10): p. 2619-2630.
114. Wang, C.X., J.K. Barry, Z. Min, G. Tordsen, A.G. Rao, and O.A. Olsen, *The calpain domain of the maize DEK1 protein contains the conserved catalytic triad and functions as a cysteine proteinase.* Journal of Biological Chemistry, 2003. **278**(36): p. 34467-34474.

115. Shen, B., C. Li, Z. Min, R.B. Meeley, M.C. Tarczynski, and O.A. Olsen, *sal1 determines the number of aleurone cell layers in maize endosperm and encodes a class E vacuolar sorting protein.* Proc Natl Acad Sci U S A, 2003. **100**(11): p. 6552-7.
116. Tian, Q., L. Olsen, B. Sun, S.E. Lid, R.C. Brown, B.E. Lemmon, K. Fosnes, D.F. Gruis, H.G. Opsahl-Sorteberg, M.S. Otegui, and O.A. Olsen, *Subcellular localization and functional domain studies of DEFECTIVE KERNEL1 in maize and Arabidopsis suggest a model for aleurone cell fate specification involving CRINKLY4 and SUPERNUMERARY ALEURONE LAYER1.* Plant Cell, 2007. **19**(10): p. 3127-3145.
117. Tanaka, H., H. Onouchi, M. Kondo, I. Hara-Nishimura, M. Nishimura, C. Machida, and Y. Machida, *A subtilisin-like serine protease is required for epidermal surface formation in Arabidopsis embryos and juvenile plants.* Development, 2001. **128**(23): p. 4681-4689.
118. Tanaka, H., M. Watanabe, M. Sasabe, T. Hiroe, T. Tanaka, H. Tsukaya, M. Ikezaki, C. Machida, and Y. Machida, *Novel receptor-like kinase ALE2 controls shoot development by specifying epidermis in Arabidopsis.* Development, 2007. **134**(9): p. 1643-1652.

Figures

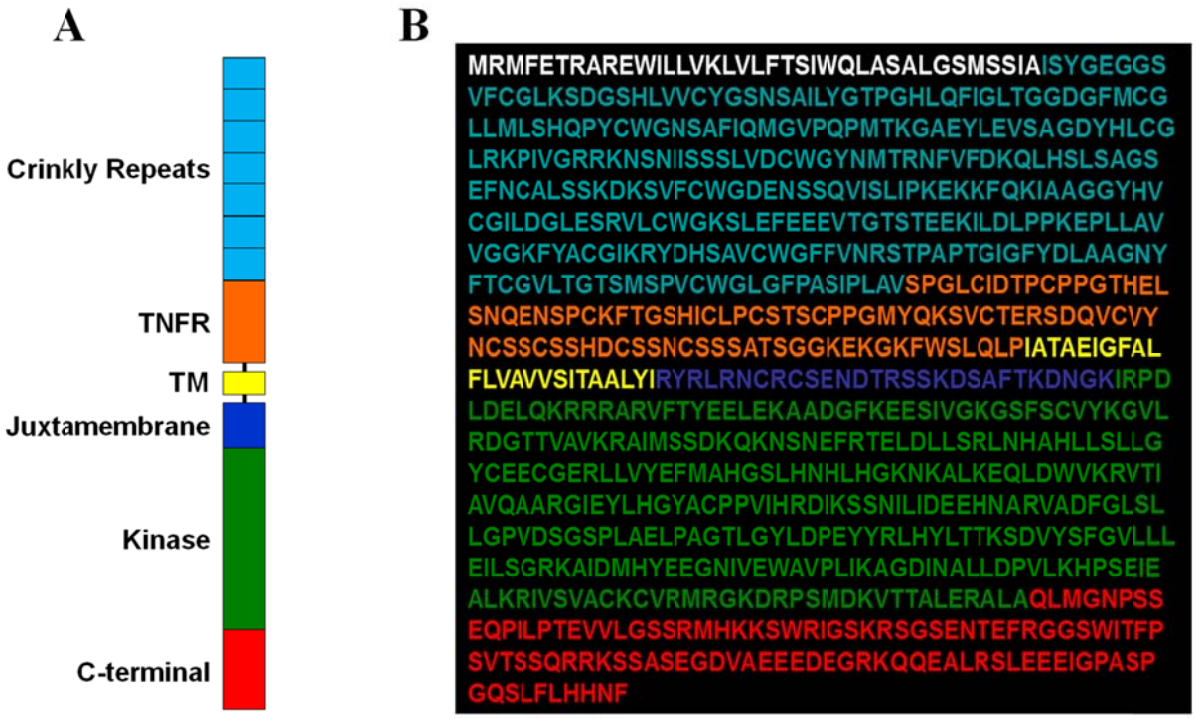

Figure 1. Diagram of the ACR4 receptor architecture. (A) Cartoon of the subdomains of the ACR4 protein. In the extracellular region, the 'Crinkly' repeats (light blue) and TNFR-like domain (orange). In the intracellular region, the juxtamembrane domain (blue), kinase domain (green), and C-terminal domain (red). A transmembrane helix (yellow) connects the extracellular and intracellular portions of the protein. (B) The 895-amino acid sequence of ACR4. The sequences is color coded as in A. The signal sequence for membrane targeting is highlighted (white).

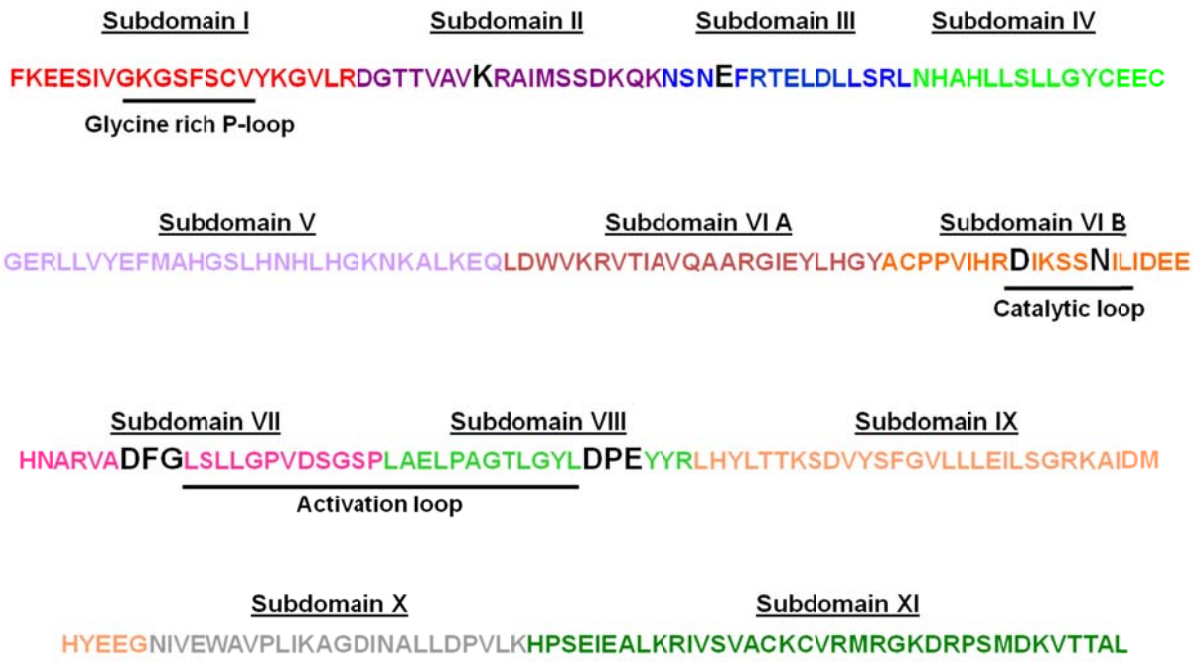

Figure 2. The subdomain architecture of the ACR4 kinase domain. The 11 subdomains of the ACR4 kinase domain are highlighted in varying colors. Residues essential to catalytic activity are depicted (black, bold). Regions involved in kinase activation and catalysis are underlined.

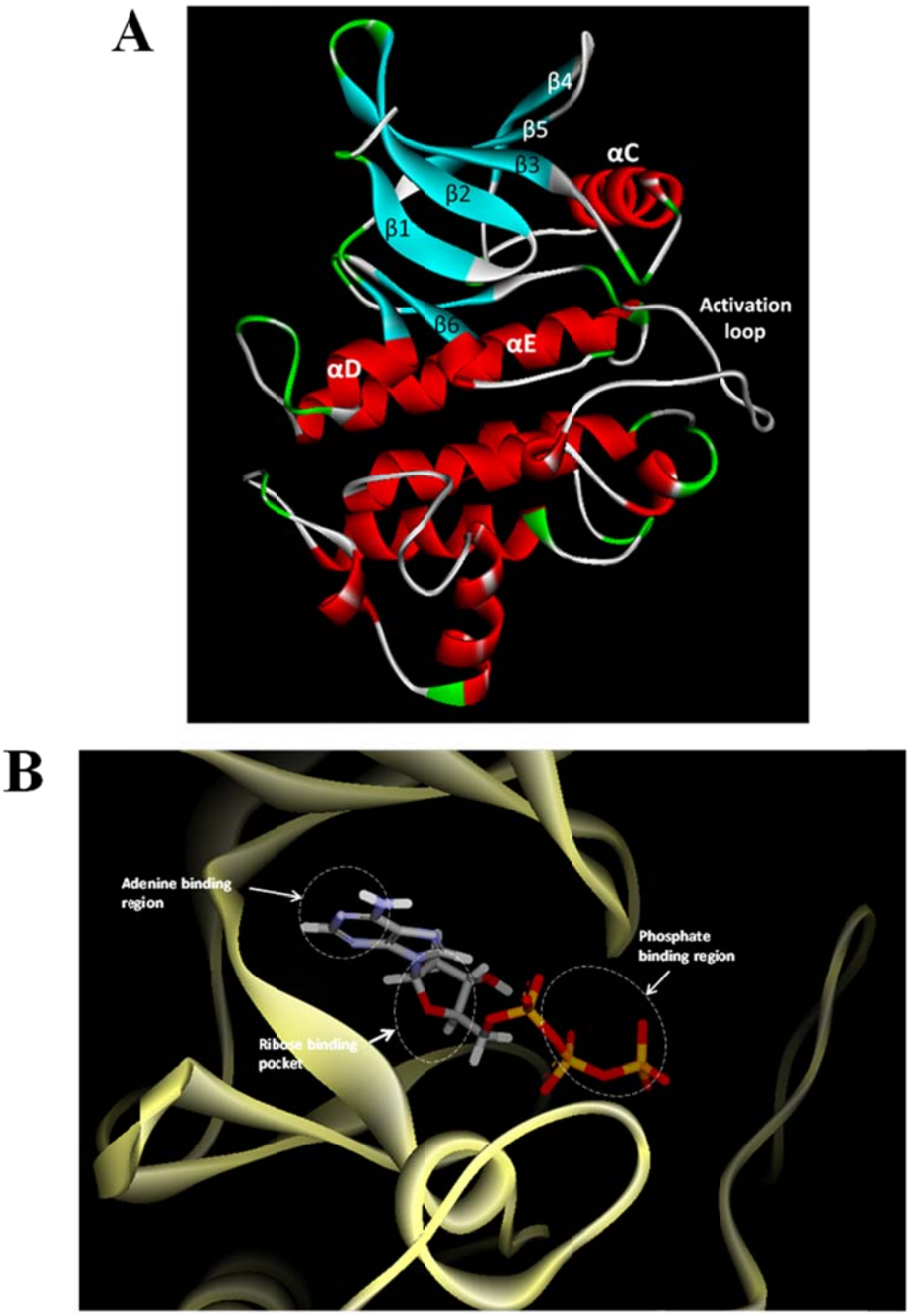

Figure 3. (A) General structure of a kinase domain. The kinase domain forms a bilobal structure with an N-lobe (blue) and a C-lobe (red). The N-lobe is primarily comprised of β-sheets, whereas the C-lobe is predominantly α-helical. Secondary structures surrounding the active site are labeled. (B) Close-up showing the bound ATP.

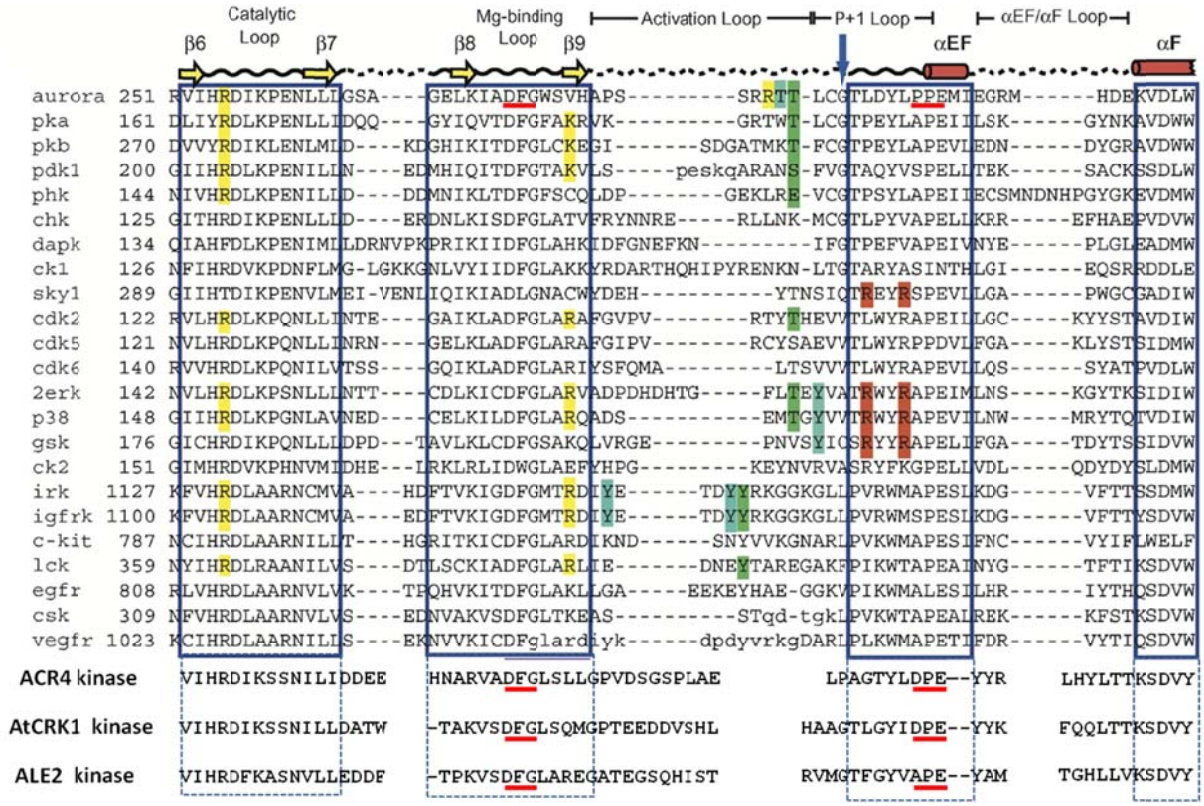

Figure 4. Alignment of the activation segments of ACR4, AtCRK1, and ALE2 receptor-like kinases with the structure-based alignment of kinases with known structures (adapted from Nolen et al., 2004). The alignment highlights structural features that are conserved among most kinases. However, the activation loop is divergent among species, indicating evolutional diversity.

CHAPTER 2. IDENTIFICATION OF *IN VITRO* AUTOPHOSPHORYLATION SITES AND THE EFFECTS OF PHOSPHORYLATION ON THE *ARABIDOPSIS* CRINKLY4 (ACR4) RECEPTOR-LIKE KINASE INTRACELLULAR DOMAIN: INSIGHTS INTO CONFORMATION, OLIGOMERIZATION AND ACTIVITY

A paper published in the journal

***Biochemistry*[1]**

Matthew R. Meyer[2], Cheryl F. Lichti[3], R. Reid Townsend[3,4,†] and A. Gururaj Rao[2]

Abstract

Arabidopsis CRINKLY4 (ACR4) is a receptor-like kinase (RLK) that consists of an extracellular domain and an intracellular domain (ICD) with serine/threonine kinase activity. While genetic and cell biology experiments have demonstrated that ACR4 is important in cell fate specification and overall development of the plant, little is known about the biochemical properties of the kinase domain and the mechanisms that underlie the overall function of the receptor. To complement *in planta* studies on the function of ACR4, we have expressed the ICD in *Escherichia coli* as a soluble C-terminal fusion to the N-utilization substance A (NusA) protein, purified the recombinant protein and characterized the enzymatic and conformational

---

Reprinted from Biochemistry (2011, 50 [12], pp 2170–2186) with permission from American Chemical Society.
Department of Biochemistry, Biophysics and Molecular Biology, Iowa State University, Ames, Iowa 50011
[b] Department of Medicine, Washington University School of Medicine, 660 S. Euclid Ave, St. Louis, MO 63130
[b,c] Departments of Medicine, Cell Biology and Physiology, Washington University School of Medicine, 660 S. Euclid Ave, St. Louis, MO 63130

properties. The protein autophosphorylates via an intramolecular mechanism, prefers Mn^{2+} over Mg^{2+} as the divalent cation and displays typical Michaelis-Menten kinetics with respect to ATP with an apparent K_m of 6.68 ± 1.62 μM and V_{max} of 193.8 ± 15.14 pmole/min/mg. Autophosphorylation is accompanied by a conformational change as demonstrated by circular dichroism, fluorescence spectroscopy and limited proteolysis with trypsin. Analysis by nano-liquid chromatography mass spectrometry (nano-LC-MS) revealed 16 confirmed sites of phosphorylation at Ser and Thr residues. Sedimentation velocity and gel-filtration experiments indicate that the ICD has a propensity to oligomerize and that this property is lost upon autophosphorylation.

Abbreviations

ACR4, *Arabidopsis* CRINKLY4; ALE2, ABNORMAL LEAF SHAPE 2; ATP, adenosine triphosphate; BRI1, Brassinosteroid insensitive 1; CR4, maize CRINKLY4; CD, circular dichroism; AtCRR, *Arabidopsis* CRINKLY4 related; CTD, carboxy-terminal domain; DTT, dithiothreitol; EGFR, epidermal growth factor receptor; ICD, intracellular domain; JKC, juxtamembrane + kinase + carboxy terminal domain; pJKC, phosphorylated JKC; JM, juxtamembrane; KD, kinase domain; MyBP, myelin basic protein; NusA, N-utilization substance A; PDGF, platelet derived growth factor; RLK, receptor-like kinase; RTK, receptor tyrosine kinase; SERK, somatic embryogenesis receptor-like kinase; SYMRK, symbiosis receptor kinase; TCEP, Tris (2-carboxyethyl) phosphine hydrochloride; UV, ultraviolet.

Introduction

A fundamental challenge in the developmental biology of higher organisms is striking a balance between cell proliferation, differentiation, and specification in order to undergo proper organogenesis and development. In mammalian systems, receptor tyrosine kinases (RTKs), such as the members of epidermal growth factor (EGF) receptor family, represent a class of proteins which perceive and regulate inter- and intracellular processes pertaining to stem cell proliferation and differentiation (*1, 2*). The architecture of RTKs consists of an extracellular ligand binding domain, a transmembrane helix, and an intracellular kinase domain. In the classic example, members of the EGF receptor family undergo ligand induced homo- or heterodimerization, followed by intracellular kinase activation via *trans* phosphorylation (*3, 4*). Homo- or heterodimerization regulates which downstream signaling pathways are activated through phosphorylation of specific tyrosine residues and recruitment of specific intracellular substrates in response to differential ligand binding (*3, 5, 6*). Mounting evidence, as in the case of the well characterized Brassinosteroid pathway and the *CLAVATA* (*CLV*) pathway, supports the occurrence of ligand induced, receptor mediated signaling involved in plant development similar to RTK signaling in mammalian systems (*7, 8*). Although >400 putative receptor-like kinases (RLKs) have been identified in the *Arabidopsis* genome, only a few have been characterized in detail (*9, 10*).

First described as a growth factor like receptor in maize, CRINKLY4 (CR4) is a RLK involved in the proper formation of the epidermal layer in the leaves and the aleurone monolayer in the kernel (*11, 12*). The protein consists of an extracellular domain with seven repeating regions (each of 39 amino acids), three cysteine-rich regions which are similar to the extracellular motifs of the tumor necrosis factor receptor, a single transmembrane

spanning region, and an active intracellular serine/threonine kinase domain (*11, 13, 14*). An ortholog in *Arabidopsis*, ACR4, contains all the architectural features of maize CR4 and functions in a similar manner. ACR4 primarily affects epidermal cell morphology in the ovules and sepal margins of the plant, is required for proper morphogenesis of developing embryos, and is necessary for the proper formation of the epidermal layer in leaves. Seeds from *acr4* plants show defects in seed coat development and loss of epidermal and cuticle formation, leading to fusion of tissues (*14-17*). Recently, ACR4 has been described as a regulator of columella stem cell differentiation in the root apical meristem and lateral root formation in the developing root (*18, 19*). Loss of ACR4 function results in the proliferation of columella stem cells and a module involving interactions between the CLE40 peptide, ACR4 and a homeobox transcription factor, WOX5, has been proposed as a signaling mechanism that is similar to the CLV signaling pathway that mediates stem cell proliferation and differentiation in the apical meristem (*19*).

Thus, ACR4 is a RLK whose functions are critical to the development of virtually the entire plant (*15-19*). Importantly, while genetic and cell biology studies have made it apparent that the RLK is important in cell fate specification, there is little or no knowledge of the biochemical basis of its function and its involvement in regulatory networks. *In vitro* biochemical and biophysical studies of recombinant proteins can often provide valuable clues towards an understanding of *in vivo* physiological functions. Indeed, detailed structural and mechanistic studies on a number of recombinantly expressed receptor kinase domains in both animal and plant systems have not only facilitated the development of useful biochemical models to validate *in vivo* functions but also fostered the development of various protein probes for the dissection of signaling pathways and isolation of interacting proteins.

However, such studies require adequate amounts of soluble protein. To this end, we have successfully expressed milligram quantities of the intracellular domain (ICD) of ACR4 in fusion with the NusA protein in an *E. coli* system. We have characterized the autophosphorylation activity, mapped the autophosphorylation sites by mass spectrometry and demonstrate that the RLK is a member of the RD family of kinases.

Materials and Methods

Construction of ACR4 Intracellular Domain (ICD) Expression Plasmid.

The ACR4 intracellular domain, termed JKC (residues 456-895), was cloned into the pET-44b(+) (Novagen) which encodes an N-terminal NusA fusion tag, two 6X His tags, a Thrombin cleavage site, and an Enterokinase cleavage site. The ACR4 JKC was PCR amplified with primer 1 and primer 2 (Table I), cloned between the BamHI and Sal1 restriction sites, and verified by DNA sequencing. The plasmid, termed pNusA:JKC, was used for subsequent protein expression.

Preparation of the kinase inactive mutant plasmid was completed using the QuickChange Multi Site-Directed Mutagenesis Kit (Stratagene) by introducing point mutations into pNusA:JKC plasmid at codons encoding residues required for kinase activity. Mutagenic primer 3 mutated lysine 540 to alanine (K540A) and primer 4 mutated the catalytic aspartate 641 to alanine (D641A). The plasmid, termed pNusA:JKC2m, was subsequently used for expression of the kinase inactive form of the ACR4 ICD, JKC2m. Activation loop mutations were similarly made using mutagenic primers 5 through 16 described in Table I.

Protein Expression and Purification of NusA fused ACR4 JKC Proteins.

The ACR4 JKC was expressed as a C-terminal fusion to the NusA solubility tag. Plasmids were transformed into chemically competent BL21 (DE3) pLysS (Promega) *E. coli* cells. A 500 ml culture was supplemented with ampicillin (100 μg/ml) and grown at 37 °C, with shaking, to an OD_{600}=0.6-0.8. The temperature was then reduced to 20 °C and protein expression induced with isopropyl-1-thio-β-D-galactopyranoside (IPTG) to a final concentration of 1 mM. After 6h of incubation, the cells were harvested by centrifugation and the cell pellet was used immediately. The pellet was resuspended in 10 ml of Lysis Buffer (1X TBS pH 7.5, 50 mM imidazole, 1% TritonX-100, 1 mM DTT) and supplemented with AEBSF (1 mM final concentration). The cell suspension was sonicated to release soluble fusion protein and the resulting lysate was centrifuged in a microcentrifuge at max speed for 25 min at 4 °C. The lysate was then incubated for 1h at 4 °C in batch mode with 0.5 ml bed volume of Ni^{2+} IMAC Sepharose High Performance resin (GE Healthcare) equilibrated with Lysis Buffer. After incubation, the lysate/resin mixture was added to a 10 ml disposable chromatography column and the unbound material was allowed to flow through. The resin was then washed with 10 ml of Wash Buffer (1X TBS pH 7.5, 50 mM imidazole, 0.1% TritonX-100, 1 mM DTT) and bound protein was successively eluted with 2ml of Elution Buffer (50 mm Tris-HCl pH 8.0, 150 mM NaCl, 150 mM imidazole, 1 mM DTT). The final concentration of metal-affinity purified protein at this stage is typically greater than 6 mg/ml.

A secondary gel filtration step was used to purify the NusA fusion proteins using an ÄKTA FPLC system (Amersham). The metal affinity enriched fusion proteins were passed

through a Superdex G200 Global 10/30 column (GE Healthcare) equilibrated with column buffer (50 mM Tris-HCl pH 8.0, 150 mM NaCl, and 1 mM DTT). Peak fractions corresponding to the fusion protein were collected, pooled, and concentrated. The resulting purified proteins were used in further experiments.

Purification of JKC Proteins without tags.

The affinity enriched protein sample (as described above) was treated with 1 U/3.5 mg of Restriction Grade Thrombin (Novagen) for 20 min at room temperature. The cleavage reaction was then loaded onto a MonoQ Global 10/50 column (GE Healthcare) equilibrated with Anion Exchange Buffer (50 mM Tris-HCl pH 8.0, 1 mM DTT). Cleaved ACR4 JKC was eluted off the column by gradient elution with Anion Elution Buffer (50 mM Tris pH 8.0, 1 M NaCl, 1 mM DTT). According to the ExPASy Proteomics Server, the calculated pI of the NusA tag is 4.83 and that of the JKC is 6.47. Peak fractions corresponding to the ACR4 JKC were collected, pooled, and concentrated. The resulting purified proteins were used in subsequent experiments. Note, after cleavage the ACR4 JKC recombinant protein contains 20 extraneous amino acids encoded by the pET-44b(+) vector at the N-terminus.

Antibodies.

Polyclonal antibodies to the JKC protein were raised at the Hybridoma Facility at Iowa State University by repeated immunizations of rabbits with the highly purified antigen and purified IgG was prepared from whole serum by affinity chromatography. Monoclonal antibody to the NusA tag was purchased from Novagen (EMD Chemicals, Gibbstown). This antibody specifically detects fusion proteins containing the NusA tag sequence expressed with the pET-44 vector series.

Circular Dichroism (CD) measurements.

JKC purified from *E. coli* (naïve JKC) autophosphorylated JKC (pJKC), and JKC2m were dialyzed overnight at 4 °C in 10 mM Tris-HCl, pH 7.4 and 0.1 mM TCEP and concentrated to an A_{280} value of approximately 1.0. Far-UV spectrums of each protein were obtained on a Jasco J-710 spectropolarimeter, in a 0.1cm path-length cuvette with excitation wavelengths ranging from 190 nm-260 nm.

Fluorescence Measurements.

Naïve JKC, JKC2m, and pJKC were dialyzed in 10 mM Tris-HCl, pH 7.4 and 0.1 mM TCEP and brought to a concentration of A_{280}=0.1 prior to fluorescence scans. Measurements were made in a 1 cm cuvette at room temperature with a Cary Eclipse spectrofluorimeter (Varian). Scans were executed at an excitation wavelength of 280 nm and a band width of 5 nm and a scan speed of 120 nm/min.

Kinase Activity Assays.

The optimal buffer condition for kinase activity was determined to be 20 mM BIS-TRIS pH 7.2, 25 mM NaCl, 5 mM $MnCl_2$, 1 mM DTT, 25 μM ATP and a temperature of 30 ˚C. This was established by performing individual reactions with 2 μg of NusA:JKC protein incubated in varying buffer conditions containing Mn^{2+} (0.05-50 mM), ATP (1-50 μM), DTT (0-10 mM) and NaCl (0-300 mM), in the pH range 5.8-8.8. All reactions were carried out in a 20 μl volume in the presence of 5 μCi of [γ^{32P}]ATP (6000 Ci/mmol, Perkin-Elmer) and incubated for 1 hr at room temperature. Reactions were terminated by adding 6 μl 4X Laemmli buffer and boiled for 5 min. Proteins were resolved by 10% SDS-PAGE, gels

stained with Coomassie Brilliant Blue R-250, and then analyzed by exposure to an autoradiograph film or a phosphorimaging screen.

Assays to determine the autophosphorylation mechanism were performed using the NusA:JKC and JKC proteins. A series of reactions was carried out containing increasing concentrations of NusA:JKC in the range 0.2-3.4 μM (or up to ~2.4 μM in the case of JKC). The protein was incubated in 20 μl reactions of optimized kinase buffer containing 2.5 μCi of [γ-^{32}P]ATP. Reactions were initiated with the addition of the enzyme and incubated for 15 min at room temperature. They were then terminated and treated as above. Protein bands were excised from the gel and radioactivity was determined by scintillation counting. Phosphate incorporation for each sample was calculated based on the radioactive counts and the use of a [γ-^{32}P]ATP standard curve. The data was then used to generate a van't Hoff plot (log of enzyme activity vs log of enzyme concentration) and the intramolecular nature of the mechanism inferred from the slope of this plot. Kinetic data were fit using the Sigma Plot 11.2 (Systat Software Inc., San Jose, CA) Enzyme Kinetics module (version 1.3) to determine Michaelis-Menten constants by non-linear regression analysis.

In a parallel experiment, autophosphorylation assays were also performed independently with naïve NusA:JKC, JKC2m, or with both proteins incubated together. Incubations of the NusA tag alone or with either protein were used as controls for the assay. Each reaction was carried out with 2 μg of protein in optimized kinase buffer containing 5 μCi of [γ-^{32}P]ATP. Reactions were allowed to proceed for 1h at room temperature and processed as above. To determine if the kinase could phosphorylate other exogenous

substrates, naïve NusA:JKC was incubated with 2 μg of Myelin Basic protein (MyBP) and the phosphorylation reaction carried out as described above.

Analysis of Phosphorylation status.

Two techniques were utilized to determine the phosphorylation status of JKC2m, naïve JKC and pJKC. One approach utilized the phosphoprotein stain, Pro-Q Diamond (Invitrogen). Approximately 1 μg of each protein was separated by 12% SDS-PAGE. The gel was first fixed for 2x 30 min with solution containing 50% methanol and 10% acetic acid then washed three times with deionized water. It was then stained with Pro Q diamond stain for 90 min in the dark and then destained using 50 mM sodium acetate buffer pH 4.0 containing 20% acetonitrile. Images of the stained gel were acquired on a Molecular Dynamics Typhoon scanner (Amersham Biosciences) with an excitation source of 532 nm laser and a 580 nm bandpass emission filter.

In the second approach, phosphorylation was assessed by western blot analysis using a polyclonal, anti-phosphothreonine antibody (Cell Signaling Technology, #3981). Briefly, ~1 μg of each protein was separated by 12% SDS-PAGE followed by blotting to a PVDF membrane. The membrane was blocked, probed with the primary antibody (1:1000), washed, and then probed with a secondary anti-rabbit IgG antibody (1:30,000) conjugated to alkaline phosphatase (Sigma). Protein detection was completed using an AP Conjugate Substrate kit (Bio-Rad).

Sample Preparation for LC-MS/MS Analysis.

To prepare peptides, the proteins were concentrated by TCA precipitation and resuspended in 4 M urea in 50 mM NH_4HCO_3, pH 7.8. Proteins were reduced with 10 mM TCEP for 30 min at 50 °C followed by alkylation with 20 mM iodoacetamide for 30 min at

room temperature in the dark. 50 mM NH_4CO_3, pH 7.8 was added to the sample to dilute urea to less than 1 M. The protein was then digested with 1:50 (w/w, enzyme to substrate) Sequencing Grade Modified Trypsin (Promega) overnight at 37 °C. The resulting peptides were desalted on a SOURCE 15 RPC column (GE Healthcare) and eluted in 90% acetonitrile, 0.1% TFA. The eluted peptides were then dried down in a vacuum centrifuge. Phosphopeptides were enriched using the PHOS-Select Ga^{3+} Silica Spin Column kit (Supelco) according to the kit instructions.

Peptides were eluted into autosampler vials with 60% acetonitrile in 1% formic acid. The quality of the peptide digests was assessed using MALDI-TOF mass spectrometry. The remaining sample was dried, dissolved in 25 µL of aqueous acetonitrile/formic acid (1%/1%), and analyzed by high resolution nano-LC-MS.

High Resolution Mass Spectrometry.

The complex peptide mixtures were analyzed using high-resolution nano-LC-MS on a hybrid mass spectrometer consisting of a linear quadrupole ion-trap and an Orbitrap (LTQ-Orbitrap XL, Thermo Fisher Scientific). Chromatographic separations were performed using a NanoLC-1D™ Plus (Eksigent) for gradient delivery and a cHiPLC-nanoflex (Eksigent) containing a 15 cm x 75 µm C18 column (ChromXP C18-CL, 3 µm, 120 Å, Eksigent). The liquid chromatograph was interfaced to the mass spectrometer with a nanospray source (PicoView PV550; New Objective). The mobile phases were 1% formic acid in water (solvent A) and 1% formic acid in acetonitrile (solvent B). After equilibrating the column in 98% solvent A and 2% of solvent B, the samples (5 µL) were injected from vials using the LC-system autosampler at a flow rate of 500 nL/min. The peptides were eluted at 250 nL/min with the following gradient: isocratic at 2% B, 0-3 min; 2% B to 50% B, 3-73 min; 50% to

80%, 73-83 min; isocratic at 80%, 83-86 min; 80% to 2%, 86-87; and isocratic at 2% B, 87-102 min. The total run time, including column equilibration, sample loading, and analysis was 128 min. The survey scans (*m/z* 350-2000) (MS1) were acquired at high resolution (60,000 at *m/z* = 400) in the Orbitrap and the MS/MS spectra (MS2) were acquired in the linear ion trap at low resolution, both in profile mode. The maximum injection times for the MS1 scan in the Orbitrap and the LTQ were 50 ms and 100 ms, respectively. The automatic gain control targets for the Orbitrap and the LTQ were 5×10^5 and 3×10^4, respectively. The MS1 scans were followed by six MS2 events in the linear ion trap with collision activation in the ion trap (parent threshold = 1000; isolation width = 2.0 Da; normalized collision energy = 30%; activation Q = 0.250; activation time = 30 ms). Dynamic exclusion was used to remove selected precursor ions (-0.20/+1.0 Da) for 90 s after MS2 acquisition. A repeat count of 1, a repeat duration of 45 s, and a maximum exclusion list size of 500 was used. The following ion source parameters were used: capillary temperature 200 ºC, source voltage 3.5 kV, source current 100 μA, capillary voltage 33 V, and the tube lens at 120 V. The data were acquired using *X*calibur, version 2.0.7 (Thermo Fisher). For high resolution targeted analysis, the parent ions from an inclusion *m/z* list within a retention time window were selected for acquisition of peptide fragmentation spectra at 7500 resolution. MS/MS spectral acquisition was triggered with an isolation width of 4 Da when the signal for the ion of interest exceeded 10,000 counts. The maximum injection times for the MS1 scan in the Orbitrap and the LTQ were both 500 ms, and the maximum injection times for the MSn scan in the Orbitrap and the LTQ were 750 ms and 1000 ms, respectively. The automatic gain control targets for the Orbitrap and the LTQ were 2×10^5 and 3×10^4, respectively for the MS1 scans and 1×10^5 and 1×10^4, respectively for the MSn scans. The MS1 scan was followed by one MS2 event

with collision activation in the ion trap (parent threshold = 10000; isolation width = 4.0 Da; normalized collision energy = 30%; activation Q = 0.250; activation time = 30 ms). The following ion source parameters were used: capillary temperature 200 ºC, source voltage 3.3 kV, source current 100 μA, capillary voltage 34 V, and the tube lens at 125 V.

Data Analysis.

The MS2 spectra were analyzed by searching against the ACR4 sequence and expert manual interpretation. The exact masses of the phosphopeptide and fragmentation ions were calculated using the MS-Product utility within Protein Prospector (http://prospector.ucsf.edu). For database searches, the LC-MS files were processed using MASCOT Distiller (Matrix Science, version 2.3.0.0) with the settings previously described (20). The resulting MS2 centroided files were used for database searching with MASCOT, version 2.1.6, against a custom, in-house database containing the ACR4 using the following parameters: enzyme, trypsin; MS tolerance = 15 ppm, MS/MS tolerance = 0.8 Da with a fixed carbamidomethylation of Cys residues and the following variable modifications: oxidation (Met) and phosphorylation (Ser, Thr, and Tyr); Maximum Missed Cleavages = 9; and 1+, 2+ and 3+ charge states. For analysis of the tandem spectra from spectral acquisitions in the Orbitrap (MS2), the raw files were processed using MASCOT Distiller (Matrix Science, Oxford, UK) with the following settings: 1) MS processing: 200 data points per Da; sum aggregation method; maximum charge state, 3+; minimum number of peaks, 1; 2) MS/MS processing: 200 data points per Da; time domain aggregation method; minimum number of peaks, 10; use precursor charge as maximum; precursor charge and *m*/*z*, "try to re-determine charge from the parent scan (tolerance, 1.2 Da)"; charge defaults, 1; maximum charge state, 3) time domain parameters: minimum precursor mass, 300; maximum precursor

mass, 16,000; precursor *m*/*z* tolerance for grouping, 0.01; maximum number of intermediate scans, 0; minimum number of scans in a group, 1; 4) peak picking: maximum iterations, 500; correlation threshold, 0.60; minimum signal to noise, 2; minimum peak *m*/*z*, 50; maximum peak *m*/*z*, 100,000; minimum peak width, 0.002; maximum peak width, 0.2; expected peak width, 0.02. The resulting files were used for database searching with a fragment tolerance of 100 mmu; all other search parameters are identical to those described above.

Analytical Ultracentrifugation.

Sedimentation velocity analysis of NusA:JKC, naïve and phosphorylated, was performed on an XL-A analytical ultracentrifuge (Beckman Coulter). The purified protein was dialyzed overnight at 4 °C in 10 mM Tris-HCl pH7.4, 50 mM NaCl, and 0.1 mM TCEP. The protein sample was concentrated to an Abs_{280} = 0.6. 300 µl of the sample was loaded into a preassembled Flow-Through Assembly housing an Epon, 2-channel centerpiece and quartz windows. The rotor and sample cell temperatures were allowed to equilibrate to 20 °C for 2 h. The sample was spun at 40,000 rpm, at 20 °C for a total of 400 scans with a scan rate of 1 scan/min. Boundaries were monitored by recording the absorbance at 280nm. Scan analysis was performed using van Holde - Weischet analysis (*21*) as implemented in the program Ultrascan 6. Sedimentation coefficients ($S_{20,w}$) were corrected for 20 ˚C and water.

Limited Proteolysis.

Conformational difference between naïve JKC and pJKC proteins was probed by limited proteolysis using trypsin. The naïve protein was purified as described above and 125 µg of the protein was diluted into 200 µl volume containing 50 mM Tris-HCl pH 8.0, 1 mM $CaCl_2$, 1 mM DTT. Trypsin (Promega) was added at a 1:1000 w/w, protease:substrate and

incubated at room temperature. 25 μl aliquots were removed at predetermined time points and the reaction stopped by the addition of 6 μl of 4X SDS sample buffer and boiling for 5 min. For pJKC, 125 μg of the protein was first incubated in a 200 μl reaction containing 1X kinase buffer and 100 μM ATP for 90 min. Subsequently, 5 μl of 2 M Tris-HCl pH 8.0 was added to adjust the pH to 8.0 followed by 1 μl of 0.2 M $CaCl_2$ to a final concentration of 1 mM. The digestion reaction was then carried out as described above. Protein samples (~0.5 μg/lane) were separated by 7% SDS-PAGE and gels were silver stained using the SilverSNAP stain kit from Pierce (Rockford,Ill).

Results

Expression, Purification and Characterization of JKC.

The intracellular domain (ICD) of ACR4 (residues 456-895) may be subdivided into the juxtamembrane domain (JM), kinase domain (KD) and the carboxy-terminal domain (CTD). Using the NusA protein as the fusion partner we have expressed and purified milligram quantities of the ICD for biochemical characterization. Fig. 1A shows the SDS-PAGE analysis of protein fractions during various steps in the purification of the NusA:JKC (lane 3) and JKC (lane 5) from *E. coli* cells (as described in Materials & Methods). Approximately 6 mg of soluble NusA:JKC and <0.25 mg of JKC protein were obtained from a 500 ml culture. Similar yield was obtained for the inactive mutant (JKC2m). The identities of the proteins were confirmed by western blots probed with rabbit polyclonal antibodies raised against the JKC (Fig. 1B) and antibody to the NusA tag (Fig. 1C). These blots validate the homogeneity of the protein preparation and demonstrate the absence of co-purification of

non-full length NusA-tagged proteins. The identity of the purified JKC protein was also confirmed by MALDI-MS analysis of tryptic peptides of the excised protein band (data not shown).

The far-UV CD spectrum of the JKC (Fig. 2A) is similar to that reported for other examples of recombinantly expressed kinase domains of receptor tyrosine kinases (*22, 23*). The three-dimensional structures of several kinase domains show a number of helices and the observed CD spectrum for naïve JKC (combined with the robust catalytic activity described below) strongly supports the preservation of an ordered structure. Typical α-helical structures display negative bands at 208 nm and 222 nm. The more negative molar ellipticity value at 208 nm could be attributed to contributions from the juxtamembrane and carboxy-terminal regions of the molecule as well as the 20 extraneous amino acids at the N-terminus encoded by the pET-44b(+) vector (see Materials & Methods). Fluorescence spectroscopy (Fig. 2B) shows almost identical profiles for both the mutant and naïve proteins with an emission maximum at 342 nm, consistent with the tryptophan residues being located in similar environments.

Preliminary evidence for the ability of the ICD to oligomerize was obtained during the purification of the metal-affinity enriched NusA:JKC protein by size exclusion chromatography. Typically, at the affinity-enrichment step, the protein concentration is > 6 mg/ml and is subsequently diluted to ~ 2 mg/ml (~18 μM) for batch-wise purification by gel filtration on a Superdex G200 column. As shown in Fig. 3, in addition to eluting as a monomer (peak at ~12.5 ml volume), a small proportion of the protein elutes as an aggregate in the void volume. Analysis of these fractions by SDS-PAGE (inset A) indicates that the void volume fraction consists entirely of aggregates of the monomer. An

autophosphorylation assay of the aggregate fraction indicated that no kinase activity could be detected in comparison with that of the monomer fraction (inset B). It is also worth noting that the propensity for oligomerization may be concentration dependent since little or no aggregate is observed in gel filtration experiments at protein concentrations below ~1.5 μM (data not shown).

The self-association of naïve NusA:JKC was also monitored by sedimentation velocity experiments. During sedimentation velocity, homogeneous non-interacting molecules will sediment with discrete sedimentation coefficient (S) values whereas interacting molecules that lead to higher order oligomers will show a broad distribution of sedimenting species. Fig. 4A shows the percent distribution of species (plotted as diffusion corrected sedimentation coefficients) along the sedimentation boundary in velocity sedimentation experiment for naïve NusA:JKC. Approximately 60% of the protein sedimented with an $S_{20,w}$ value of 4 with the remaining 40% showing a considerably wider range of much higher S values, commensurate with association to heterogeneous polymeric species. We also analyzed the data by the Van Holde-Weischet method (*21*) (Fig. 4B). In this analysis, the sedimenting boundary is first divided into a number of segments and the data fit by linear least square analysis to the apparent sedimentation coefficient of each boundary segment. Extrapolation to the y-axis then yields the diffusion-corrected sedimentation coefficient for that boundary segment. Typically, a homogeneous sample would be expected to have the same sedimentation coefficient as a function of time in all parts of the boundary and the extrapolated lines for the various segments should converge to a single value at the y-axis (*24*). It is also clear by this method of analysis that the naïve protein shows a distinct propensity to aggregate to species with S values >4. The NusA protein is not known to

dimerize (*25-28*) and we also did not see any evidence of dimerization with the recombinantly expressed NusA protein (data not shown). In contrast, after autophosphorylation the protein does not aggregate and shows a predominantly homogeneous monomeric species sedimenting with an $S_{20,w}$ value of ~4 (Fig. 4 C, D). We were unable to perform sedimentation velocity experiments with the protein minus the NusA tag owing to inadequate recovery of soluble protein.

Kinase activity of NusA:JKC.

Interestingly, as observed for some of the other RLK's characterized so far (*29-31*) the recombinantly expressed ACR4 ICD as a NusA fusion protein prefers Mn^{2+} over Mg^{2+} as the metal ion for autophosphorylation, although the precise physiological significance of this is not obvious. A linear increase in phosphorylation activity is seen with Mn^{2+} concentrations ranging from 0.1 to 5 mM, with maximal activity occurring at 5 mM and quenching at higher concentrations of the metal ion (Fig. 5A). A similar linear relationship is seen with Mg^{2+} but much higher concentrations of Mg^{2+} are required to achieve activity comparable with Mn^{2+} as the divalent cation i.e., 1 mM Mn^{2+} versus 50 mM Mg^{2+} (Fig. 5A). This is further illustrated in Fig. 5B that shows an autoradiogram of the kinase activity in the presence of 10 mM concentrations of Mg^{2+}, Mn^{2+} and Ca^{2+}. No activity is observed with Ca^{2+} and the activity with Mg^{2+} is significantly less. In the presence of Mn^{2+} the reaction is completed in 60 min (for JKC as well) (Fig. 5C) at 30 ˚C at an optimal pH of 7.2 in 20 mM BIS-TRIS buffer containing 1 mM DTT and 25 mM NaCl (Fig. 5D). The enzyme displays typical Michaelis-Menten kinetics with respect to ATP (Fig. 5E) and analysis of the ATP dependence for autophosphorylation by fitting the data to the Michaelis-Menten equation (using the Enzyme Kinetics Module on SigmaPlot 11.2) revealed the K_m and V_{max} for ATP

to be 6.68 ± 1.62 μM and 193.8 ± 15.14 pmole/min/mg, respectively. The apparent K_m for ATP is also comparable with that observed for other RLKs (*29, 30*). Since the native substrate for ACR4 kinase is yet to be determined, we used Myelin Basic Protein (MyBP) as a model substrate in an assay to assess the ability of the kinase to phosphorylate exogenous proteins. As indicated in Fig. 5F (lane 2), MyBP is phosphorylated by NusA:JKC.

Autophosphorylation occurs through an intramolecular mechanism.

Autophosphorylation reactions of kinases can proceed either through an intramolecular mechanism (first order with respect to enzyme concentration) or an intermolecular mechanism (second order with respect to enzyme concentration). We used two approaches to ascertain the mechanism of activity of NusA:JKC. First, we conducted a series of kinase reactions using increasing concentrations of NusA:JKC in the range 0.1-3.4 μM. As shown in Fig. 6A, the rate of autophosphorylation was linear with respect to enzyme concentration and the amount of phosphate incorporation per molecule remained fairly constant over two-orders of magnitude difference in protein concentration (Fig. 6B). The van't Hoff analysis (plot of logarithm of phosphorylation rate versus logarithm of enzyme concentration, with the value of the slope indicating the order of the reaction) gave a slope of 1.05 ± 0.05 and a correlation coefficient of 0.97 for the linear regression (Fig. 6C), suggesting an intramolecular mechanism. Similar results were obtained in assays performed with the JKC minus the NusA tag (Fig. 6D-F) and the van't Hoff plot yielded a slope of ~1.2 (Fig. 6F). Importantly, the lower specific activity of JKC in the concentration range employed (Fig. 6E) and the decreased solubility of the protein at higher concentrations, attests to the stabilizing influence of the NusA tag on the activity of the enzyme. For further confirmation of the intramolecular mechanism, we performed kinase assays by incubating the

active NusA:JKC with the inactive mutant JKC2m to determine if the latter could be phosphorylated. As shown in Fig. 7, panel A, the NusA:JKC could undergo autophosphorylation (lane 1) and also phosphorylate the NusA tag (lane 4) but ***could not*** phosphorylate the inactive mutant (lane 3). The reduced activity of NusA:JKC in lane 3 may potentially be attributed to the formation of a less active heterodimer between the wild-type and mutant protein. Taken together with the kinetic data, this strongly suggests that the dominant mechanism of autophosphorylation is intramolecular.

Mapping of autophosphorylation sites.

The data-dependent tandem mass spectrometric analysis of the tryptic peptides and searching against ACR4 protein sequence revealed several phosphopeptides. The identified phosphopeptides encompassed all the subdomains of the ICD (Fig. 8A). Determination of the exact site of phosphorylation within the phosphopeptides was performed by inspection of their fragmentation pattern for specific diagnostic site-determining y_n and b_n ions (*32*). As an example, the collisionally induced tandem mass spectrum for the phosphopeptide ^{533}DG(pT)TVAVK^{540} is shown in Fig. 8B. The most prominent ion is the doubly charged $[M+2H-98]^{2+}$ species at a *m/z* of 386.71. This is characteristic of a neutral loss of phosphoric acid by which phosphorylation sites are identified. An unambiguous confirmation of Thr^{535} as the phosphorylated residue was afforded by the presence of the phosphorylated b_3 (theoretical *m/z* 354.1; observed 354.1) and y_6 (theoretical *m/z* 698.3; observed 698.2) ions, along with non-phosphorylated b_2 (theoretical *m/z* 173.1; observed 173.1) and y_5 (theoretical *m/z* 517.3; observed 517.3) ions. Table II summarizes the site-determining ions for 16 peptides with confirmed phosphorylation at amino acid residues Ser^{475}, Thr^{478}, Thr^{501}, Ser^{516*}, Ser^{522*}, Thr^{535}, Thr^{536}, Ser^{552}, Thr^{557}, Ser^{563*}, Ser^{644}, Ser^{645}, Thr^{831}, Ser^{837*}, Ser^{875} and

Ser^{888*} (Fig. 8A). Five of these confirmed residues, indicated with an asterisk, are also found in the naïve JKC and represent the basal phosphorylation state of the protein expressed in *E. coli*. One additional phosphorylation site in the naïve protein, is located at either Ser^{811*} or Ser^{812*} in the peptide ^{788}ALAQLMGNPSSEQPILPTEVVLGSSR^{813} (theoretical mass including phosphate group, 2789.34; observed $[M+3H]^{3+}$, *m/z* 930.79). Specific y-series ions were obtained showing phosphorylation at the C-terminal end of the peptide but no site-determining ions were obtained in the fragmentation spectrum to distinguish between the two serine residues.

In addition to these 16 confirmed sites, we identified parent ions with *m/z* values corresponding to 2 other peptides, each supporting one phosphorylation site. The peptide, ^{852}SSASEGDVAEEEDEGR^{867} (theoretical mass including phosphate group, 1745.63; observed $[M+2H]^{2+}$, *m/z* 873.82) could potentially be phosphorylated at any one of the three serine residues, Ser^{852}, Ser^{853} or Ser^{855}. However, an exact assignment of the site was not possible since the fragmentation pattern did not reveal the characteristic b and y series of ions. Similarly, the mass spectrum of the 35-residue tryptic peptide, ^{657}VADFGLSLLGPVDSGSPLAELPAGTLGYLDPEYYR^{691} (Fig. 8C) (theoretical mass including phosphate group, 3731.81; observed $[M+3H]^{3+}$, *m/z* 1244.94), while supporting the presence of one phosphorylated residue among the multiple phosphorylation sites (Ser^{663}, Ser^{670}, Ser^{672}, Thr^{681}, Tyr^{684}, Tyr^{689}, Tyr^{690}) did not yield the expected set of diagnostic ions in the fragmentation spectrum and hindered a precise localization of the phosphorylated residue. Nevertheless, we were able to narrow down the location to either Ser^{670} or Ser^{672} on the basis of a series of y and b ions without a phosphate group. Thus, Thr^{681}, Tyr^{684}, Tyr^{689}and Tyr^{690} can be eliminated as potential sites based on the [M+H] y ions y_5 (*m/z*

727.341), y_6 (*m/z* 842.367), y_8 (*m/z* 1118.513), y_9 (*m/z* 1175.533) and y_{14} (*m/z* 1614.782). The m/z values clearly indicate the absence of a phosphate group. Similarly, the b ions, b_9 (*m/z* 916.510) and b_{10} (*m/z* 973.530) do not support Ser^{663} as a phosphorylation site (Fig. 8C).

We also assessed the phosphorylation levels of the mutant, naïve and phosphorylated JKC proteins by staining with Pro-Q Diamond, a phosphospecific stain, and western blot analysis using anti-phosphothreonine antibody. Commensurate with data from phosphorylation analysis by mass spectrometry that showed many more phosphorylated residues for the pJKC protein compared with the naïve protein, staining with ProQ Diamond showed a very intense band for the autophosphorylated protein (pJKC) and a much weaker intensity band for the naïve JKC (Fig. 9A). Only a faint band could be seen for the mutant, as would be expected from an inactive protein undergoing little or no phosphorylation. In the western blot analysis with anti-phosphothreonine antibody, pJKC showed a band of high intensity and the naïve protein barely registered a band (Fig. 9B). This correlates well with the observation that all observed phosphorylated sites in the naïve protein are located exclusively on serine residues (Ser^{516*}, Ser^{522*}, Ser^{563*}, Ser $^{811* \text{ or } 812*}$, Ser^{837*} and Ser^{888*}) whereas pJKC has at least six confirmed phosphorylated threonine residues (Thr^{478}, Thr^{501}, Thr^{535}, Thr^{536}, Thr^{557}, Thr^{831}).

ACR4 RLK belongs to the RD family of kinases.

Significantly, the large tryptic peptide ^{657}VADFGLSLLGPVDSGSPLAELPAGTLGYLDPEYYR^{691} also includes the activation loop sequence (the double-underlined residues in between residues DFG and DPE respectively in Fig. 8A). It is known that autophosphorylation of specific residue(s) within the activation segment is a critically important regulatory element, and necessary for kinase

activity, in many kinases belonging to the Ser/Thr family subgroup (that includes plant kinases and plant RLKs), and the Tyr kinase family subgroup (*33-37*). This is a characteristic feature of kinases belonging to the RD family, which contain an Arg residue preceding the invariant catalytic Asp (Fig. 10). Crystal structures of RD kinases indicate that phosphorylation in the activation segment promotes a conformational change driven by electrostatic interactions between the negatively charged phosphorylated residue and a cluster of conserved basic residues, including the Arg residue in the RD motif. This conformational change reorients the catalytic and substrate binding residues and presents an optimal spatial environment for substrate binding and catalysis. The presence of the RD motif in the ACR4 kinase domain and evidence of phosphorylation of a Ser residue in the activation segment strongly suggest that ACR4 RLK is an RD kinase. To further correlate phosphorylation of the activation loop and kinase activity, we conducted autophosphorylation assays with site-directed mutants in which each of the residues Ser^{663}, Ser^{670}, Ser^{672}, Thr^{681} and Tyr^{684} was replaced separately with either an alanine, which cannot be phosphorylated (Fig. 11A), or an aspartic acid (Fig. 11B), which mimics phosphorylation. The kinase activity of the S663A mutant was indistinguishable from that of the wild type protein but the S663D mutation abolished all activity, suggesting that a negatively charged amino acid was unacceptable at this position but also simultaneously discounting the likely role of Ser^{663} as a substrate. With regard to Ser^{672}, the fact that neither mutation, S672A nor S672D, changes the kinase activity makes it quite unlikely that it is a favored phosphorylation site. In contrast, the activity of the S670A mutant is significantly knocked down but vigorously restored in the S670D mutant, even though aspartic acid itself is not a substrate for the kinase. This suggests that a negative charge at position 670 is necessary for kinase activity and that this requirement is

fulfilled by phosphorylation of Ser^{670}, the most likely candidate residue for phosphorylation. Interestingly, complete loss of autophosphorylation activity is observed when Thr^{681} is mutated to either an alanine or an aspartic acid indicating that the loss of activity is not linked to the property of the introduced amino acid but is directly attributable to the removal of Thr residue. Importantly, the fact that even the introduction of a negative charge via an aspartate as a phosphomimetic does not restore kinase activity implicates Thr^{681} as a structurally important residue (*38*), in keeping with the tight conservation of this amino acid across a number of RLKs (Fig. 10). However, the conserved threonine, Thr^{760}, in the Symbiosis Receptor Kinase, SYMRK, (*39*) and Thr^{468} in the *Arabidopsis thaliana* somatic embryogenesis receptor-like kinase, *At*SERK1, (*40*) have also been shown to undergo phosphorylation *in vitro*. The complete loss of activity seen when Tyr^{684} is replaced with Phe, Asp, Ser or Thr, attests to the importance of non-phosphoamino acid interactions in maintaining the spatial orientations of the activation and catalytic loops in the kinase domain (*38*).

Autophosphorylation induces a conformational change.

The "conformational plasticity" and structural modifications of kinases in response to phosphorylation and dephosphorylation is well-documented in the literature (*41-43*). We have addressed structural perturbations propagated through phosphorylation of the JKC using spectroscopy and limited proteolysis, all techniques that are particularly sensitive to conformational changes in proteins (*44, 45*). Thus, the CD spectrum of pJKC (16 confirmed phosphorylated residues) in the far-UV region (Fig. 3A) is indicative of an alteration in the secondary structure of the protein towards a less compact state in comparison with the naïve form (5 confirmed phosphorylated Ser residues) and the mutant protein that is unlikely to

contain any phosphorylated residues based on the Pro-Q Diamond staining described earlier. In addition, numerous studies have demonstrated that tryptophan fluorescence in proteins is a sensitive probe of folding and tertiary structure and quite revealing of changes in the microenvironment of aromatic residues (*46, 47*). In comparison with the fluorescence spectra of naïve JKC and JKC2m mutant (Fig. 3B), the intensity of the intrinsic tryptophan fluorescence of the pJKC was observed to decrease significantly, accompanied by a blue-shift in the λ_{max} of emission (from 342 nm to 338 nm) and the appearance of a shoulder at 310 nm, attributable to tyrosine fluorescence. Limited proteolysis is also a well-established technique for probing protein conformation and dynamics and relies on the fact that proteolysis occurs at sites with enhanced local flexibility (*48-50*). Well-folded regions within proteins usually resist protease digestion and, therefore, the protected fragments remaining after trypsin digestion represent stably folded domains. The digestion patterns of naïve JKC and pJKC with trypsin as a function of time (Fig. 12) provide additional evidence of phosphorylation induced conformational change. Whereas with naïve JKC, undigested protein could be detected through the first 10 minutes of incubation with trypsin (Fig. 12A), there was little evidence of undigested protein in the case of pJKC after the first 2.5 to 5 minutes (Fig. 12B) and there was significantly faster accumulation of the ~37 kDa protein, presumably the kinase domain, as indicated by western blot analysis (data not shown).

Discussion

In this study we have demonstrated that the ACR4 intracellular domain encodes a functional kinase that undergoes autophosphorylation on 16 confirmed sites, 2 of which occur in the juxtamembrane domain, 10 in the kinase domain and 4 in the carboxy-terminal

domain. However, as noted earlier, there is evidence for three other unconfirmed phosphorylation sites. Owing to sub-stoichiometric representation of phosphopeptides, it is quite likely that additional phosphorylated residues may have gone undetected in our LC-MS/MS analysis. Regulation of kinase activity and recruitment of downstream interacting proteins via multiple sites of phosphorylation is a common feature of animal RTKs, as exemplified by EGFR (*5, 6, 51*). Their occurrence in many plant RLKs (*52*) suggests a conserved mechanism of control of signal transduction processes across the two kingdoms. In the RTKs, for example, phosphorylated residues in the juxtamembrane and carboxy-terminal regions not only serve a regulatory role (*41, 53*) but act as docking sites for specific signaling molecules such as those containing Src homology 2 (SH2) domains or phosphotyrosine-binding (PTB) domains (*54-56*). Phosphorylation of Ser/Thr residues also creates binding surfaces for diverse phosphoamino acid binding modules such as the 14-3-3, WW and Forkhead-associated (FHA) (*57, 58*). The 14-3-3 modules are well represented in the *Arabidopsis* genome (*59-61*). An example of the FHA containing module in *Arabidopsis* is the kinase-associated protein phosphatase (KAPP). KAPP binds to phosphorylated Ser/Thr residues of several plant RLKs such as CLAVATA 1 (CLV1), SERK1, HAESA and FLS2 and acts as a negative regulator of receptor signaling (*62-65*). The phosphorylated Ser and Thr residues in the ACR4 juxtamembrane and carboxy-terminal domains of ACR4 could very well serve as docking sites for similar interacting proteins.

Many protein kinases also achieve maximal enzymatic activity only after phosphorylation of specific residues in the activation loop sequence that occurs between subdomains VII and VIII of the kinase domain (*66*). In some RD kinases among plant RLKs, activation loop phosphorylation is essential for both autophosphorylation and substrate

phosphorylation. Thus, in BRI1, the mutation T1049A abolishes autophosphorylation and substrate phosphorylation in *vitro* and the mutant is also unable to rescue the weak *bri1-5* Brassinolide insensitive mutant in planta (*37*). In the activation segment sequence alignment the correspondingly conserved residue in SYMRK (Thr^{760}) is phosphorylated *in vitro* and the Ala mutant has little or no autophosphorylation or substrate phosphorylation activity (*39*). Similarly, the conserved Thr^{468} in AtSERK1 is important for both autophosphorylation and phosphorylation of artificial substrates *in vitro* (*36*). The strict conservation of Thr at this position in the activation segment of RD-type RLKs (Fig. 10) suggests that it may be an important *in vivo* phosphorylation site. In ACR4, the equivalent residue Thr^{681} does not appear to be phosphorylated by LC-MS/MS analysis but our mutagenesis experiments clearly demonstrate that it is required for *in vitro* kinase activity. This result, however, does not preclude the possibility of Thr^{681} being phosphorylated *in vivo*. Importantly, as in the case of BRI1, SYMRK and AtSERK1, additional phosphorylation sites within the activation segment of RD-type RLKs that are not conserved in the sequence alignment appear to be required for activation and function. Presumably, multiple phosphorylations induce conformational changes that regulate binding sites for ATP and other substrates (*67*). Intriguingly, in addition to regulating kinase activity, phosphorylations in the activation segment can also facilitate recruitment of downstream partners, as in the case of the interaction between the SH2 domain of the adaptor protein APS and the phosphotyrosines in the activation loop of the insulin receptor kinase (*68, 69*). In another interesting example, in the extracellular signal-regulated kinase (ERK), phosphorylation-dependent conformational changes in the activation loop affect the subcellular localization of the protein (*70*)

It appears likely that autophosphorylation induced conformational changes also affect the gross structure of the intracellular domain. Thus, molecular interactions within the JKC, involving both the juxtamembrane and the carboxy-terminal domains, could hold the molecule in a 'closed' conformation and the release of these interactions upon phosphorylation, results in a more 'open' conformation. Some support for this comes from the limited proteolysis experiment that shows a relatively faster accumulation of the 37 kDa kinase domain after phosphorylation. Indeed, in the case of BRI1, the carboxy-terminal region negatively regulates BRI1 function and deletion of this region enhances kinase activity (*71*). Even in RTKs, proximal regions to the catalytic domain are known to play vital roles in kinase activation mechanisms. In several receptors such as the ephrin binding receptor (EpH) family, platelet-derived growth factor (PDGF) receptor family and epidermal growth factor receptor (EGFR) family, the juxtamembrane domain is a major regulatory domain (*72-75*). Similarly, the domain on the carboxyl side of the kinase domain can be autoinhibitory as has been demonstrated for EGFR and the receptor TIE2, an RTK that is activated by angiopoietin-1 (*76, 77*).

The classical paradigm of receptor kinase function invokes ligand binding, followed by dimerization of the receptor, concomitant conformational change and activation of the kinase domain by *cis*- (intramolecular) or *trans*- (intermolecular) autophosphorylation (*1, 2*). The ligand for ACR4 is as yet unknown, but here we report that the autophosphorylation of NusA:JKC occurs through an intramolecular mechanism, a property associated with similar domains from RLKs such as the XA21 involved in rice disease resistance (*78*), BRI1 (Brassinosteroid Insensitive 1) an essential receptor controlling plant development (*31*), and CrRLK1 from the plant *Cantharanthus roseus* (*30*). This would suggest that ligand mediated

dimerization may not be essential for activation of kinase activity. However, *in vivo*, alternative modes of activation remain distinctly viable. It is conceivable that ligand binding to the extracellular domain of ACR4 induces a conformational change in its intracellular domain that enables subsequent interaction with a second kinase (membrane bound or soluble) that is capable of *trans*-phosphorylating at a specific site on the ACR4 intracellular domain and 'activating' an intramolecular autophosphorylation event. In *Arabidopsis*, candidate proteins that could be involved in such interactions include the CRINKLY4-related (CRR) proteins (*13*) and the receptor like kinase, ABNORMAL LEAF SHAPE 2 (ALE2) (*79*). The four CRR proteins found in *Arabidopsis*, AtCRR1, AtCRR2, AtCRR3 and AtCRK1 share similar structural features with ACR4 but only AtCRK1 encodes a kinase domain with phosphorylation activity in an *in vitro* assay (*13*). It is possible that receptor activation and autophosphorylation of ACR4 kinase could be stimulated by heteromeric interactions with the AtCRR proteins. Evidence for the involvement of ACR4 and the AtCRRs in a common signal transduction pathway, perhaps mediated by heterodimerization, comes from the observation that, *in vitro*, the ACR4 kinase domain can phosphorylate the inactive kinase domain of AtCRR2 (*13*). Similarly, genetic studies indicate that pathways involving ALE2 and ACR4 might act positively to regulate the specification of the protoderm and/or protoderm specific genes in the formation of leafy organs (*79*). Intriguingly, in *in vitro* experiments, the kinase domains of ACR4 and ALE2 can also phosphorylate each other (*79*).

Our experiments suggest that the intracellular domain of ACR4 possesses an intrinsic propensity to form higher order oligomers, although the precise contributions of the JM region and the CTD remain to be ascertained in future experiments. The fact that the NusA

protein itself does not dimerize, rules out the possibility of any influence of the NusA tag on the oligomerization of the JKC. The significance of this observation in the context of ACR4 function remains to be established in more detailed molecular studies both *in vitro* and *in vivo*. In animals, in addition to ligand-induced dimerization, RTKs such as NGFR, EGFR and the erythropoietin receptor can exist as preformed dimers *even in the absence of ligand (80-84*). Furthermore, in the case of EGFR, the juxtamembrane domain *is required* for dimerization of the cytoplasmic domain (*85*). Among RLK's, BRI1 (*86-88*) and the S-locus receptor kinase (*89*) have been shown to exist as ligand-independent dimers but structural features contributing to the dimerization process are unknown. The precise mechanism of productive oligomer formation and activation among plant RLKs is not completely understood and could vary among the receptor subclasses. However, in the case of BRI1, biochemical and genetic evidence has been provided for a model in which ligand binding activates a pre-exisiting BRI1 dimer which then associates with the co-receptor BAK1 and transphosphorylates key residues in the kinase domain, followed by reciprocal transphosphorylation of BRI1 by the activated BAK1 (*90*).

The sedimentation velocity experiments also demonstrate that autophosphorylation of NusA:JKC prevents oligomerization, perhaps attributable to electrostatic repulsions between negatively charged phosphorylated residues on the protein. However, the large size of the NusA tag, and the fact that it also is phosphorylated, precludes an unambiguous interpretation of the precise effect of autophosphorylation on the association-dissociation properties of the intracellular domain.

In conclusion, in this study we describe for the first time the biochemical properties of the intracellular domain of ACR4 and provide key insights into its phosphorylation kinetics.

Ongoing and future experiments in our laboratory will address more detailed molecular analyses to delineate the role of the subdomains in ACR4 structure and function, interactions with putative partners, and mutational analysis of phosphorylation sites. Mutating different phosphorylation sites within ACR4 could have strikingly different effects including changes in receptor function, changes in receptor stability/turnover and changes in subcellular localization. Clearly, the identification of the physiological substrates of the kinase and *in vivo* phosphorylation sites are essential to understanding the signaling pathway mediated by ACR4. Our *in vitro* studies will complement genetic approaches and contribute to an overall understanding of ACR4 function in plants.

Acknowledgements

We thank Prof. Alan DiSpirito and Dr. Raji Joseph of the Dept. of BBMB and Dr. Suman Kundu (Department of Biochemistry, University of Delhi) for their critical reading of the manuscript. The mass spectrometry at Washington University was supported by NIH grants P41RR00954 and UL 1 RR024992 from the National Center for Research Resources. The expert technical assistance of Petra Erdmann-Gilmore and Alan E. Davis is gratefully acknowledged.

References

1. Jiang G, Hunter T (1999) Receptor activation: When a dimer is not enough, *Curr. Biol*. *9***,** R568-R571.
2. Schlessinger, J. (2000) Cell signaling by receptor tyrosine kinases, *Cell 103,* 211-225.
3. Olayiye, M., Neve, R.M., Lane, H.A., Hynes, N.E. (2000) The ErbB signaling network: Receptor heterodimerization in development and cancer, *EMBO J. 19,* 3159-3167

4. Schlessinger, J. (2002) Ligand-induced, receptor-mediated dimerization and activation of EGF receptor, *Cell 110*, 669-672.
5. Schulze, W.X., Deng, L., Mann, M. (2005) Phosphotyrosine interactome of the ErbB-receptor kinase family, *Mol.Sys.Biol. 2005.0008,* doi:10.1038/msb410001.
6. Jones, R.B., Gordus, A., Krall, J.A., MacBeath, G. (2006) A quantitative protein interaction network for the ErbB receptors using protein microarrays, *Nature 439* 168-174.
7. Holbro, T., Hynes, N.E. (2004) ErbB receptors: directing key signaling networks throughout life, *Annu. Rev. Pharmacol. Toxicol. 44,* 195-217.
8. Wieduwilt, M.J., Moasser, M.M. (2008) The epidermal growth factor receptor family: biology driving targeted therapeutics, *Cell. Mol. Life Sci. 65*, 1566-1584.
9. Shiu, S-H, Bleecker, A.B. (2001) Plant receptor-like kinase gene family: Diversity, Function and Signaling, *Science STKE.*
10. Heffani, Y.Z., Silva, N.F., and Goring DR (2004) Receptor kinase signaling in plants, *Can.J.Bot. 82*, 1-15.
11. Becraft, P.W., Stinard, P.S., and McCarty, D.R. (1996) CRINKLY4: A TNFR-like receptor kinase involved in maize epidermal differentiation, *Science 273*, 1406-1409.
12. Jin, P., Guo, T., and Becraft, P.W. (2000) The maize CR4 receptor-like kinase mediates a growth factor-like differentiation response, *Genesis 27*, 104-116.
13. Cao, X., Li, K., Suh, S-G., Guo, T., and Becraft, P.W. (2005) Molecular analysis of the CRINKLY4 gene family in *Arabidopsis thaliana*, *Planta 220*, 645-657.
14. Gifford, M.L., Robertson, F.C., Soares, D.C., Ingram, G.C. (2005) *Arabidopsis* CRINKLY4 function, internalization and turnover are dependent on the extracellular crinkly repeat domain, *The Plant Cell 17*, 1154-1166.
15. Tanaka, H., Watanabe, M., Watanabe, D., Tanaka, T., Machida, C., and Machida Y (2002) ACR4, a putative receptor kinase gene of *Arabidopsis thaliana*, that is expressed in the outer cell layers of embryos and plants, is involved in proper embryogenesis, *Plant Cell Physiol. 43*, 419-428.
16. Gifford, M.L., Dean, S., Ingram, G.C. (2003) The *Arabidopsis* ACR4 gene plays a role in cell layer organization during ovule integument and sepal margin development, *Development 130,* 4249-4258.
17. Watanabe, M., Tanaka, H., Watanabe, D., Machida, C., and Machida, Y (2004) The ACR4 receptor-like kinase is required for surface formation of epidermis-related tissues in *Arabidopsis thaliana*, *The Plant Journal 39*, 298-308.
18. De Smet, I., Vassileva, V., De Rybel, B., Levesque, M.P., Grunewald, W., Van Damme, D., Van Noorden, G., Naudts, M., Van Isterdael, G., De Clercq, R., Wang, J.Y., Meuli, N., Vanneste, S., Friml, J., Hilson, P., Jürgens, G., Ingram, G.C., Inzé, D., Benfey, and P.N., Beeckman, T. (2008) Receptor-like kinase ACR4 restricts formative cell divisions in the *Arabidopsis* root, *Science 322*,594-597.
19. Stahl, Y., Wink, R.H., Ingram, G.C., and Simon, R. (2009) A signaling module controlling the stem cell niche in *Arabidopsis* root meristems, *Curr. Biol.* doi:10.1016/j.cub.2009.03.060.
20. Nittis, T., Guittat, L., LeDuc, R.D., Dao, B., Duxin, J.P., Rohrs, H., Townsend, R.R., and Stewart, S.A. (2010) Revealing novel telomere proteins using in vivo cross-

linking, tandem affinity purification, and label-free quantitative LC-FTICR-MS, *Mol.Cell.Proteomics 9,* 1144-1156.

21. Van Holde, K.E., Weischet, W.O. (1978) Boundary analysis of sedimentation velocity experiments with monodisperse and paucidisperse solutes, *Biopolymers 17*, 1387-1403.
22. Wente, S.R., Villalba, M., Schramm, V., and Rosen, O.M. (1990) $Mn^{2(+)}$-binding properties of a recombinant protein-tyrosine kinase derived from the human insulin receptor, *Proc. Natl. Acad. Sci. USA 87*, 2805-2809.
23. Sierke, S.L., Cheng, K., Kim, H.H, and Koland, J.G. (1997) Biochemical characterization of the protein tyrosine kinase homology domain of the ErbB3 (HER3) receptor protein, *Biochem. J. 322*, 757-763.
24. Hansen, J.C., Lebowitz, J., and Demeler, B. (1994) Analytical ultracentrifugation of complex macromolecular systems, *Biochemistry 33*, 13155-13163.
25. Gill, S.C., Weitzel, S.E., and von Hippel, P.H. (1991) *Escherichia coli* sigma 70 and NusA proteins. I. Binding interactions with core RNA polymerase in solution and within the transcription complex, *J. Mol. Biol. 220*, 307-324.
26. Gill, S.C., Weitzel, S.E., and von Hippel, P.H. (1991) *Escherichia coli* sigma 70 and NusA proteins. II. Physical properties and self-association states, *J. Mol. Biol. 220*, 325-333.
27. Shin, D.H., Nguyen, H.H., Jancarik, J., Yokota, H., Kim, R., and Kim, S-H. (2003) Crystal Structure of NusA from *Thermotoga Maritima* and Functional Implication of the N-Terminal Domain, *Biochemistry 42*, 13429-13437.
28. Gopal, B.**,** Haire, L.F., Gamblin, S.J., Dodson, E.J., Lane, A.N., Papavinasasundaram, K.G., Colston, M.J., and Dodson, G. (2001) Crystal structure of the transcription elongation/anti-termination factor NusA from Mycobacterium tuberculosis at 1.7 A resolution, *J. Mol. Biol. 314,* 1087-1095.
29. Horn, M.A., and Walker, J.C. (1994) Biochemical properties of the autophosphorylation of RLK5, a receptor-like protein kinase from Arabidopsis thaliana. *Biochim. Biophys. Acta 1208***,** 65–74.
30. Schulze-Muth, P., Irmler, S., Schroder, G., and Schroder, J. (1996) Novel type of receptor-like protein kinase from a higher plant (*Catharanthus roseus*). cDNA, gene, intramolecular autophosphorylation, and identification of a threonine important for auto- and substrate phosphorylation, *J. Biol.Chem. 271***,** 26684–26689.
31. Oh, M.H., Ray, W.K., Huber, S.C., Asara, J.M., Gage, D.A., Clouse, S. D. (2000) Recombinant brassinosteroid insensitive 1 receptor-like kinase autophosphorylates on serine and threonine residues and phosphorylates a conserved peptide motif *in vitro*, *Plant Physiol. 124*, 751–766.
32. Beausoleil, S.A., Villen, J., Gerber, S.A., Rush, J., and Gygi, S.P. (2006) A probability based approach for high-throughput protein phosphorylation analysis and site localization, *Nat. Biotech. 24,* 1485-
33. Johnson, L.N., Noble, M.E.M and Owen, D.J. (1996). Active and inactive protein kinases: Structural basis for regulation, *Cell 85,* 149-158.
34. Johnson, L.N., and Lewis, R.J. (2001) Structural basis for control by phosphorylation, *Chem. Rev. 101,* 2209-2242.

35. Burza, A.M., Pekala, I., Sikora, J., Siedlecki, P., Malagocki, P., Bucholc, M., Koper, L., Zielenkiewicz, P., Dadlez, M., and Dobrowolska, G. (2006) *Nicotiana tobaccum* osmotic stress-activated kinase is regulated by phosphorylation on Ser-154 and Ser-158 in the kinase activation loop, *J. Biol.Chem. 281,* 34299-34311.
36. Shah, K., Vervoort, J., and de Vries, S.C. (2001) Role of threonines in the Arabidopsis *thaliana* somatic embryogenesis receptor kinase 1 activation loop in phosphorylation, *J. Biol.Chem. 276,* 41263-41269.
37. Wang, X., Goshe, M.B., Soderblom, E.J., Phinney, B.S., Kushar, J.A., Li, J., Asami, T., Yoshida, S., Huber, S.C., and Clouse, S.D. (2005) Identification and functional analysis of in vivo phosphorylation sites of the *Arabidopsis* BRASSINOSTEROID-INSENSITIVE 1 receptor kinase, *The Plant Cell 17,* 1685-1703.
38. Krupa, A., Preethi, G., and Srinivasan, N. (2004) Structural modes of stabilization of permissive phoshphorylation sites in protein kinases: Distinct strategies in Ser/Thr and Tyr kinases, *J. Mol. Biol. 339,* 1025-1039.
39. Yoshida, S., and Parniske, M. (2005) Regulation of plant symbiosis receptor kinase through Serine and Threonine phosphorylation, *J. Biol.Chem. 280,* 9203-9209.
40. Karlova, R., Boeren, S., van Dongen, W., Kwaaitaal, M., Aker, J., Vervoort, J., and de Vries, S. (2009) Identification of in vitro phosphorylation sites in the Arabidopsis thaliana somatic embryogenesis receptor-like kinases, *Proteomics 9,* 368-379.
41. Huse, M., and Kuriyan J. (2002) The conformational plasticity of protein kinases, *Cell 109*, 275-282.
42. Nolan, B.**,** Taylor, S., and Ghosh, G. (2004) Regulation of protein kinases: Controlling activity through activation segment conformation, *Mol. Cell 15*, 661-675.
43. Groban, E.S., Narayanan, A., Jacobson, M.P. (2006) Conformational changes in protein loops and helices induced by post-translational phosphorylation, *PLoS Comput Biol*. *2(4):e32*. Epub 2006 Apr 21.
44. Roesler, K.R., and Rao, A.G. (1999) Conformation and stability of barley chymotrypsin inhibitor-2 (CI-2) mutants containing multiple lysine substitutions, *Protein Eng. 12*, 967-973.
45. Roesler, K.R., and Rao, A.G. (2000) A single disulfide bond restores thermodynamic and proteolytic stability to an extensively mutated protein, *Protein Science 9*, 1642-1650.
46. Laskowicz, J.R. (1983) in *Principles of Fluorescence Spectroscopy*, Plenum Press, New York.
47. Barry, J.K.**,** Selinger, D.A., Wang, C., Olsen, O-A., and Rao, A.G. (2006) Biochemical characterization of a truncated penta-EF-hand Ca2+ binding protein from maize. *Biochim.Biophys. Acta 1764*, 239-245.
48. Fontana, A.**,** Fassina, G., Vita, C., Dalzoppo, D., Zamai, M., and Zambonin, M. (1986) Correlation between sites of limited proteolysis and segmental mobility in thermolysin, *Biochemistry 25,* 1847-1851.
49. Polverino, P.**,** Frare, E., Gottardo, R., Dael, V.H., and Fontana, A. (2002) Partly folded states of members of the lysozyme/lactalbumin superfamily: A comparative study by circular dichrosim spectroscopy and limited proteolysis, *Protein Science 11*, 2932-2946.

50. Kamath, N., Karwowska-Desaulniers, P., Pflum, M.K.H. (2006) Limited proteolysis of human histone deacetylase 1. *BMC Biochemistry 7*, 22-36.
51. Lemmon, M.A., and Schlessinger, J. (2010) Cell signaling by receptor tyrosine kinases, *Cell 141,* 1117-1134.
52. Nuhse, T.S., Stensballe, A., Jensen, O.N., and Peck, S.C. (2004). Phosphoproteomics of the Arabidopsis plasma membrane and a new phosphorylation site database, *Plant Cell 16,* 2394-2405.
53. Adams, J.A. (2003) Activation loop phosphorylation and catalysis in protein kinases: is there functional evidence for the autoinhibitor model? *Biochemistry 42,* 601-607.
54. Yarden, Y., and Sliwkowski, M.X. (2001) Untangling the ErbB signaling network, *Nat, Rev. Mol. Cell. Biol. 2,* 127-137.
55. Pawson, T., and Nash, P. (2000). Protein-protein interactions define specificity in signal transduction, *Genes Develop. 14,* 1027-1047.
56. Herbst, R., and Burden, S.J. (2000) The juxtamembrane region of MuSK has a critical role in agrin-mediated signaling, *EMBO J* 19, 67-77.
57. Yaffe, M.B., and Elia, A.E. (2001). Phosphoserine/threonine-binding domains, *Curr. Opin. Cell Biol. 13,* 131–138.
58. Li, J., Lee, G-I., Van Doren, S.R. and Walker, J.C. (2000) The FHA domain mediates phosphoprotein interactions, *J. Cell Science 113,* 4143-4149.
59. DeLille, J., Sehnke, P.C., and Ferl, R.J. (2001) The Arabidopsis thaliana 14-3-3 family of signaling regulators, *Plant Physiol. 126,* 35-38.
60. Rosenquist, M., Alsterfjord, M., Larsson, C., and Sommarin, M. (2001). Data mining the *Arabidopsis* genome reveals fifteen 14-3-3 genes. Expression is demonstrated for two out of five novel genes, *Plant Phys. 127,* 142-149.
61. Sehnke, P.C., DeLille, J.M., and Ferl, R.J. (2002). Consummating signal transduction: The role of 14-3-3 proteins in the completion of signal-induced transitions in protein activity, *The Plant Cell, S339-S354.*
62. Williams, R.W., Wilson, J.M., and Meyerowitz, E.M. (1997) A possible role for kinase-associated protein phosphatase in the *Arabidopsis* CLAVATA1 signaling pathway, *Proc. Natl. Acad. Sci. USA 94,* 10467-10472.
63. Shah, K., Russinova, E., Gadella, T.W., Jr., Willemse, J., and De Vries, S.C. (2002) The *Arabidopsis* kinase- associated protein phosphatase controls internalization of the somatic embryogenesis receptor kinase 1, *Genes Dev. 16,* 1707-1720.
64. Stone, J.M., Colinge, M.A>, Smith, R.D., Horn, M.A., and Walker, J.C. (1994) Interaction of a protein phosphatase with an Arabidopsis serine-threonine receptor kinase, *Science 266,* 793-795.
65. Gomez-Gomez, L., Bauer, Z., and Boller, T. (2001) Both the extracellular leucine-rich repeat domain and the kinase activity of FLS2 are required for flagellin binding and signaling in *Arabidopsis*, *The Plant Cell 13,* 1155-1163.
66. Hanks, S.K., and Hunter, T. (1995) Protein kinases 6. The eukaryotic protein kinase superfamily: kinase (catalytic) domain structure and classification, *FASEB J. 9,* 576-596.
67. Hubbard, S.R. (1997) Crystal structure of the activated insulin receptor tyrosine kinase in complex with peptide substrate and ATP analog, *EMBO J 16,* 5572-5581.

68. Moodie, S.A., Alleman-Sposeto, J., and Gustafson, T.A. (1999). Identification of the APS protein as a novel insulin receptor substrate, *J. Biol. Chem. 274,* 11186-11193.
69. Hu, J., Liu, J., Ghirlando, R., Saltiel, A.R., and Hubbard, S.R. (2003). Structural basis for recruitment of the adaptor protein APS to the activated insulin receptor, *Molec. Cell 12,* 1379-1389.
70. Wolf, I., Rubenfeld, H., Yoon, S., Marmor, G., Hanoch, T., and Seger, R. (2001) Involvement of the activation loop of ERK in the detachment from cytosolic anchoring, *J. Biol. Chem. 276*, 24490-24497.
71. Wang, X., Li, X., Meisenhelder, J., Junter, T., Yoshida, S., Asami, T., and Chory, J. (2005) Autoregulation and homodimerization are involved in the activation of the plant steroid receptor BRI1, *Developmental Cell 8*, 855-865.
72. Wybenga-Groot, L.E.**,** Baskin, B., Ong, S.H., Tong, J., Pawson, T., and Sicheri, F. (2001) Structural basis for autoinhibition of the EphB2 receptor tyrosine kinase by the naive juxtamembrane region, *Cell 106*, 745-757.
73. Griffith, J., Black, J., Faermon, C., Swenson, L., Wynn, M., Lu, F., Lipke, J., and Saxena, K. (2004) The structural basis for autoinhibition of FLT3 by the juxtamembrane domain, *Mol.Cell 13*, 169-178.
74. Thiel, K.W.**,** and Carpenter, G. (2007) Epidermal growth factor receptor juxtamembrane region regulates allosteric tyrosine kinase activation, *Proc. Natl. Acad. Sci USA 104***,** 19238-19243.
75. Hubbard, S.R. (2004) Juxtamembrane autoinhibition in receptor tyrosine kinases. *Nat. Rev. Mol.Cell. Biol. 5*, 464-470.
76. Lee, N.Y., and Koland, J.G. (2005) Conformational changes accompany phosphorylation of the epidermal growth factor receptor C-terminal domain, *Protein Science 14*, 2793-2803
77. Niu, X.L., Peters, K.G., and Kontos, C.D. (2002) Deletion of the carboxy terminus of Tie2 enhances kinase activity, signaling and function: evidence for an autoinhibitory mechanism, *J. Biol.Chem. 277*, 31768-31773.
78. Liu, G-Z., Pi, L-Y, Walker, J.C., Ronald, P.C., and Song, W-Y. (2002) Biochemical characterization of the kinase domain of the rice disease resistance receptor-like kinase XA21. *J. Biol. Chem. 277*, 20264-20269.
79. Tanaka, H., Watanabe, M., Sasabe, M., Hiroe, T., Tanaka, T., Tsukuya, H., Ikezaki, M., Machida, C., and Machida, Y. (2007) Novel receptor-like kinase ALE2 controls shoot development by specifying epidermis in *Arabidopsis*, *Development 134*, 1643-1652.
80. Gadella, T.W.J.,Jr, and Jovin, T.M (1995) Oligomerization of epidermal growth factor receptors on A431 cells studied by time-resolved fluorescence imaging microscopy. A stereochemical model for tyrosine kinase receptor activation, *J. Cell. Biol. 129*, 1543-1558.
81. Livnah, O., Stura, F.A., Middleton, S.A., Johnson, D.L., Jolliffe, I.K., and Wilson, I.A. (1999) Crystallographic evidence for preformed dimers of erythropoietin receptor before ligand activation, *Science 283*, 987-990.
82. Moriki, T., Maruyama, H., Maruyama, I.N. (2001) Activation of preformed EGF receptor dimers by ligand induced rotation of the transmembrane domain, *J. Mol. Biol. 311*, 1011-1026.

83. Mischel, P.S., Umbach, J.A., Eskandari, S., Smith, S.G., Gunderson, C.B., Zamphigi, G.A. (2002) Nerve growth factor signals via preexisting TrkA receptor oligomers, *Biophys. J. 83*, 968-976.
84. Ferguson, K.M., Berger, M.B., Mendrola, J.M., Cho, H.S., Leahy, D.J., Lemmon, M.A. (2003) EGF activates its receptor by removing interactions that autoinhibit ectodomain dimerization, *Mol.Cell 11*, 507-517.

85. Aifa, S., Aydin, J., Nordvall, G., Lundtrom, I., Svensson, S.P.S., Hermanson, O. (2005) A basic peptide within the juxtamembrane region is required for EGF receptor dimerization, *Exp. Cell Res. 302*, 108-114.
86. Russinova, E.**,** Borst, J-W., Kwaaitaal, M., Cano-Delgado, A., Yin, Y., Chory, J., de Vries, S.C. (2004) Heterodimerization and endocytosis of *Arabidopsis* brassinosteroid receptors BRI1 and AtSERK3 (BAK1), *The Plant Cell 16*, 3216-3229.
87. Wang, X., Goshe, M.B., Soderblom, E.J., Phinney, B.S., Kuchar, J.A., Li, J., Asami, T., Yoshida, S., Huber, S.C., Clouse, S.D. (2005) Identification and functional analysis of *in vivo* phosphorylation sites of the *Arabidopsis* Brassinosteroid-Insensitive1 receptor kinase, *The Plant Cell 17*, 1685-1703.
88. Hink, M.A.**,** Shah, K., Russinova, E., de Vries, S.C., Vissar, A.J. (2008) Fluorescence fluctuation analysis of *Arabidopsis thaliana* somatic embryogenesis receptor-like kinase and brassinosteroid insensitive 1 receptor oligomerization, *Biophys. J. 94***,** 1052-1062.
89. Giranton, J.L., Dumas, C., Cock, J.M., Gaude, T. (2000) The integral membrane S-locus receptor kinase of Brassica has serine/threonine kinase activity in a membranous environment and spontaneously forms oligomers in planta, *Proc. Natl. Acad. Sci. USA 97*, 3759-3764.
90. Wang, X., Kota, U., He, K., Blackburn, K., Li, J., Goshe, M.B., Huber, S.C., Clouse, S.D. (2008) Sequential transphosphorylation of the BRI1/BAK1 receptor kinase complex impacts early events in brassinosteroid signaling, *Developmental Cell 15*, 220-235.

Tables

Table 1. Primers used in cloning and mutagenesis experiments.

Primer	Mutation	Sequence (5' > 3')
1	-	GTGGTGGTGGATCCGAGGTACAGATTGAGGAATTG
2	-	GCGCGTCGACTCAGAAATTATGATGCAAG
3	K540A	CCACTGTTGCAGTGGCGAGAGCGATAATGTC
4	D641A	CTCCCGTGATTCACCGGGCCATTAAATCATCAAACATTC
5	S663A	GCTGATTTTGGTCTCGCCTTACTTGGTCCTGTCG
6	S670A	CTTGGTCCTGTCGATGCCGGCTCTCCTTTGGC
7	S672A	CCTGTCGATAGCGGCGCTCCTTTGGCAGAAC
8	T681A	GAACTACCAGCAGGAGCTCTCGGTTACCTTG
9	Y684F	GCAGGAACTCTCGGTTTCCTTGATCCCGAGTAC
10	T681D	GAACTACCAGCAGGAGATCTCGGTTACCTTG
11	Y684D	GCAGGAACTCTCGGTGACCTTGATCCCGAGTAC
12	Y684S	GCAGGAACTCTCGGTTCCCTTGATCCCGAGTAC
13	Y684T	GCAGGAACTCTCGGTACCCTTGATCCCGAGTAC
14	S663D	GCTGATTTTGGTCTCGACTTACTTGGTCCTGTCG
15	S670D	CTTGGTCCTGTCGATGACGGCTCTCCTTTGGC
16	S672D	CCTGTCGATAGCGGCGATCCTTTGGCAGAAC

Table 2. Site-discriminating ions for phosphorylated residues (in red) in phosphopeptides. The percentage of maximum intensity for each site-discriminating ion in the averaged high resolution CID spectrum are shown in parenthesis (supporting ion information is available for underlined peptide sequences).

Peptide	b ion	Phosphorylated b ion	y ion	Phosphorylated y ion
^{471}SSKDSAFTK^{479}	b4 (+1, 0.14)	b5 (+1, 27.6)	y4 (+1, 1.14)	y5 (+2, 1.62)
^{474}DSAFTKDNGK^{483}	b4 (--)	b5 (+1, 4.9)	y5 (+1, 10.7)	y6 (+2, 2.5)
^{499}VFTYEELEK^{507}	b2 (+1, 6.04)	b3 (+1, 5.77)	y6 (+1, 12.82)	y7 (+1, 22.62)
^{508}AADGFKEESIVGK^{520}	b8 (+1, 0.77)	b9 (+1, 1.07)	y4 (+1, 0.45)	y5 (+1, 0.54)
^{508}AADGFKEESIVGKGSFSCVYK^{528}	b14 (+2, 0.82)	b15 (+2, 3.92)	y6 (+1, 6.07)	y7 (+1, 1.85)
^{533}DGTTVAVK^{540}	b2 (+1, 1.54)	b3 (+1, 1.34)	y5 (+1, 097)	y6 (+2, 2.91)
^{533}DGTTVAVK^{540}	b3 (+1, 2.03)	b4 (--)	y4 (+1, 3.51)	y5 (+1, 1.79)
^{549}QKNSNEFR^{556}	b3 (+1, 0.31)	b4 (--)	y4 (+2, 2.50)	y5 (+2, 1.46)
^{551}NSNEFRTELDLLSR^{564}	b6 (+1, 0.71)	b7 (+1, 2.59)	y7 (+1, 3.33)	y8 (+1, 0.55)
^{557}TELDLLSR^{564}	b6 (+1, 3.16)	b7 (+1, 3.64)	y1 (--)	y2 (--)
^{641}DIKSSNILIDEEHNAR^{656}	b3 (+1, 2.82)	b4 (+1, 2.63)	y12 (+3, 8.75)	y13 (+2, 26.46)
^{641}DIKSSNILIDEEHNAR^{656}	b4 (+1, 3.62)	b5 (--)	y11 (+2, 9.37)	y12 (+2, 6.06)
^{826}SGSENTEFR^{834}	b5 (+1, 2.38)	b6 (+1, 0.42)	y3 (+1, 5.06)	y4 (+1, 5.44)
^{835}GGSWITFPSVTSSQR^{849}	b2 (--)	b3 (--)	y12 (+2, 5.39)	y13 (+2, 4.55)
^{875}SLEEEIGPASPGQSLFLHHNF^{895}	(--)	b1 (--)	y20 (+2, 0.15)	y21 (--)
^{875}SLEEEIGPASPGQSLFLHHNF^{895}	b13 (--)	b14 (+1, 0.32)	y7 (+1, 0.48)	y8 (--)

Figures

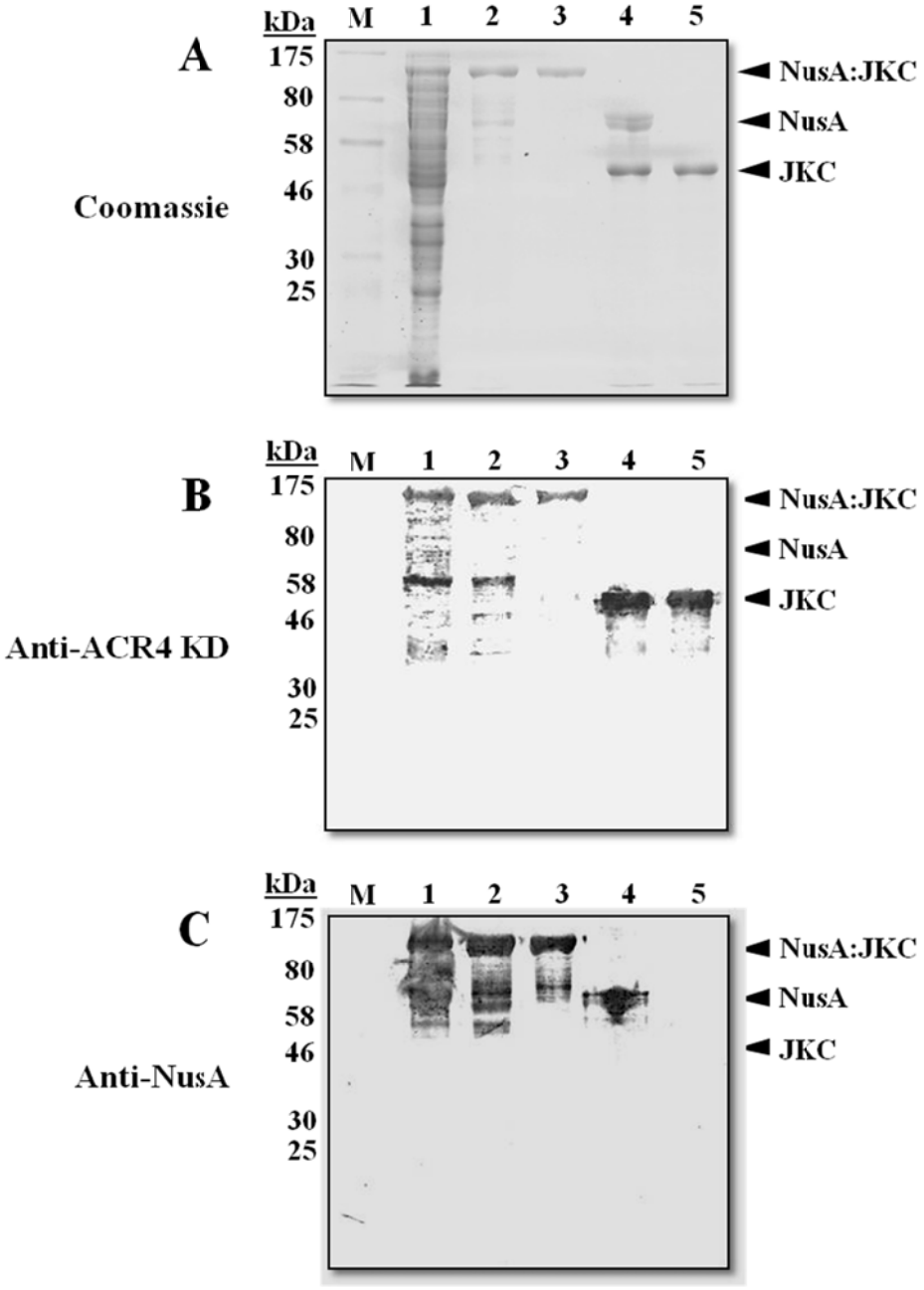

Figure 1. Analysis of protein purification by SDS-PAGE and western blot. (A) 10% SDS-PAGE gel stained with Coomassie Blue stain (B) western blot analysis using polyclonal antibody to the ACR4 kinase domain and (C) western blot analysis using monoclonal antibody to the NusA tag. ***Lane* M**, MW standards; ***lane 1***, total protein from *E. coli* lysate; ***lane 2***, affinity-enriched NusA:JKC; ***lane 3***, NusA:JKC purified by gel filtration; ***lane 4***, thrombin-cleaved NusA:JKC; ***lane 5***, JKC purified by anion-exchange chromatography.

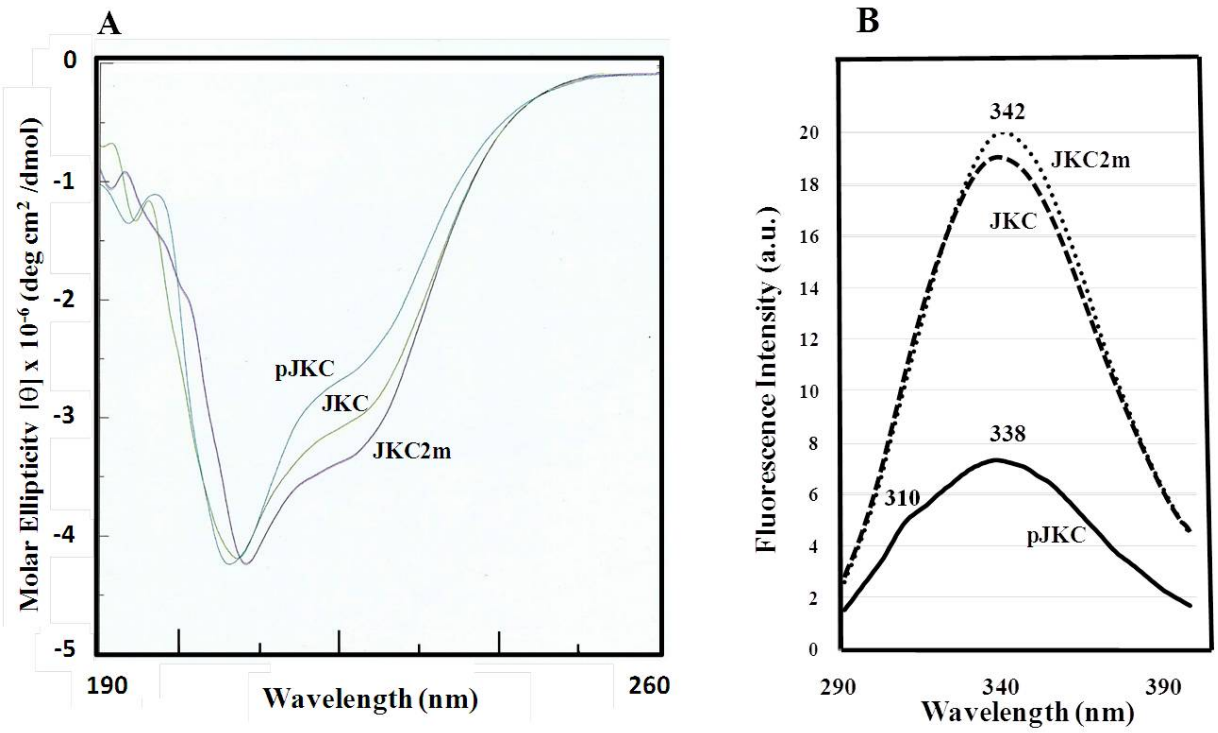

Figure 2. Conformational analysis of JKC proteins. (A) Far-UV CD spectra of the inactive JKC2m, naïve JKC, and autophosphorylated pJKC in 10 mM Tris, pH 7.4 and 0.1 mM TCEP with an A_{280} value of ~1.0. (B) Intrinsic fluorescence spectra of JKC2m, JKC, and pJKC in the same buffer with an A_{280} of 0.1. Measurements were made in a 1cm cuvette at room temperature with a Cary Eclipse spectrofluorometer (Varian) at an excitation wavelength of 280 nm.

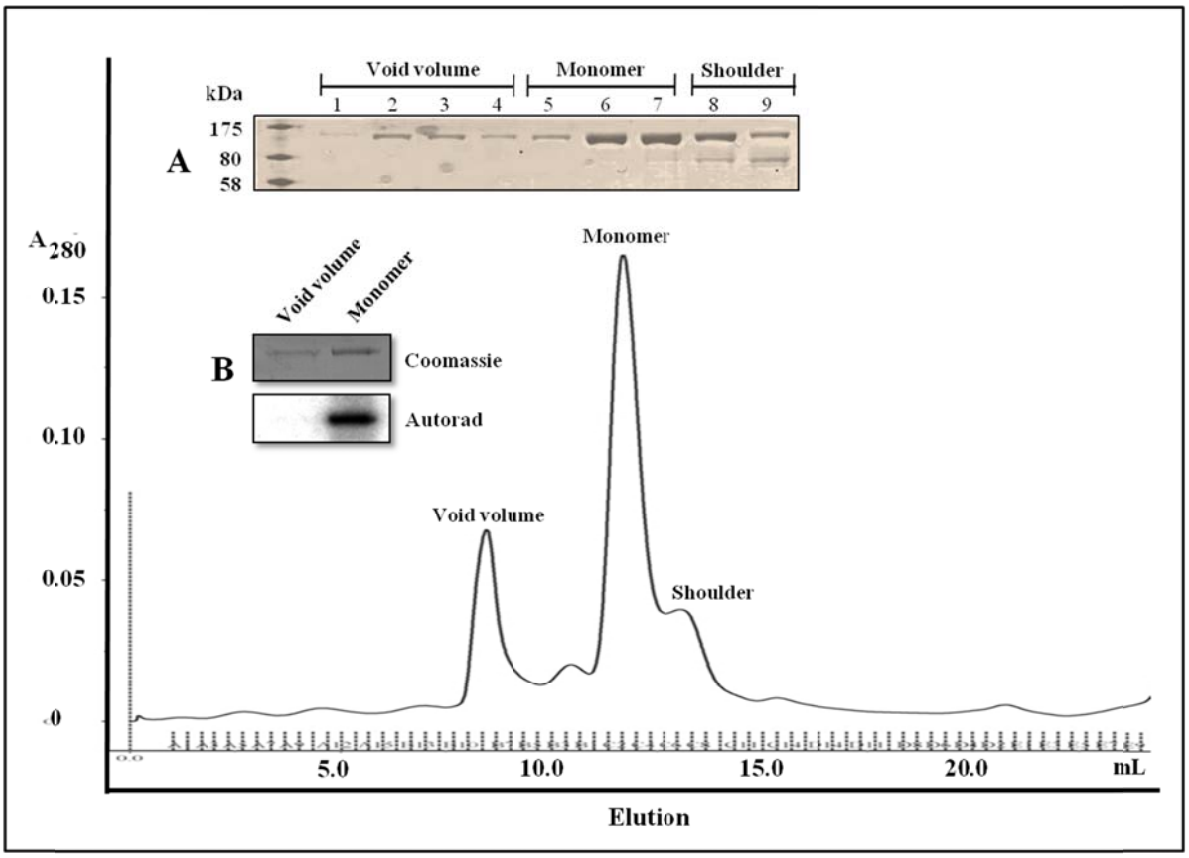

Figure 3. Gel filtration profile of affinity-enriched NusA:JKC in 50 mM Tris, pH 8.0, 150 mM NaCl during the protein purification scheme. The positions of the aggregate peak in the void volume, the monomer peak and the shoulder are indicated. *Insets:* (A) SDS-PAGE of void volume (lanes 1-4), monomer (lanes 5-7) and shoulder fractions (lanes 8-9) (B) NusA:JKC isolated from the void volume and monomer fractions were subjected to an *in vitro* autophosphorylation assay. NusA:JKC from the monomeric fraction was fully active, whereas NusA:JKC from the void volume fraction had little or no activity.

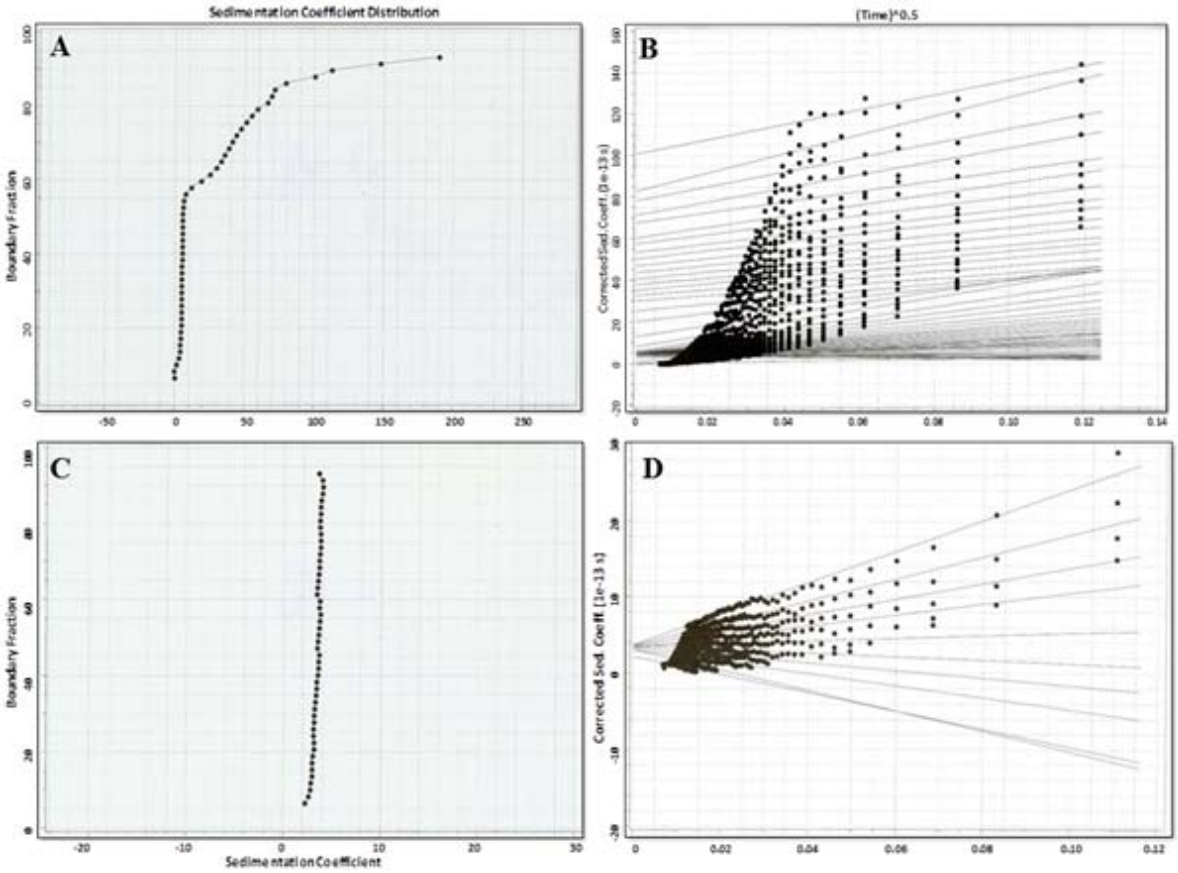

Figure 4. Sedimentation velocity analysis of NusA:JKC (panel A) and autophosphorylatedNusA:JKC (panel C) performed on an XL-A analytical ultracentrifuge using a protein sample with an Abs_{280} of 0.6. The sample was spun at 40,000 rpm at 20 ˚C for a total of 400 scans with a scan rate of 1 scan/min. van Holde-Weischet analysis of NusA:JKC and autophosphorylated NusA:JKC, respectively (panels B &D).

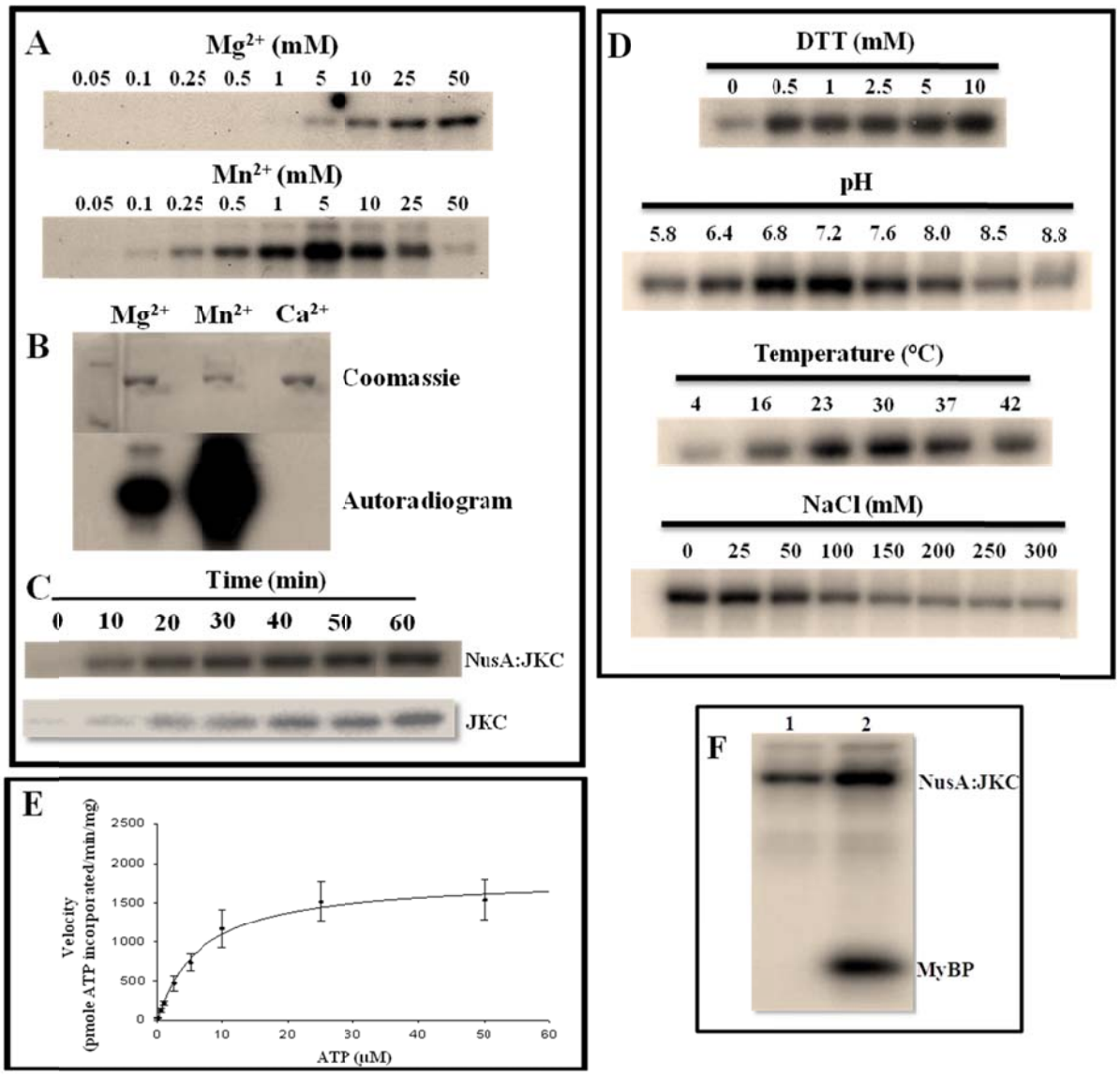

Figure 5. Optimal conditions for *in vitro* autophosphorylation activity as described in materials and methods**.** 2 µg of NusA:JKC was incubated in 20 µl of kinase buffer containing 5µCi of [γ-^{32}P]ATP (6000Ci/mmol). Reactions were terminated by adding SDS sample buffer and proteins were resolved by 10% SDS-PAGE followed by Coomassie Blue staining and phosphorimaging. *Left panel* (A) Concentration dependence of divalent cations. (B) Comparison of 10mM Mg^{2+}, Mn^{2+}, and Ca^{2+}. (C) Time course of autophosphorylation for NusA:JKC (upper panel) and JKC (lower panel). (D) Effect of reducing agent (DTT), pH, temperature and ionic strength on autophosphorylation. (E) Plot of enzyme velocity *vs.* ATP concentration. Data were fitted directly to the Michaelis-Menten equation using SigmaPlot 11.2 and the Enzyme Kinetics 1.3 module. The value of the Km for ATP was 6.68 µM ± 1.62 µM and the Vmax was 193.8 ± 15.14 pmole/min/mg. Data are the mean ± S.E. (n = 4). (F) NusA:JKC can phosphorylate the exogenous substrate MyBP. **Lane 1**, NusA:JKC and **lane 2**, NusA:JKC incubated with MyBP.

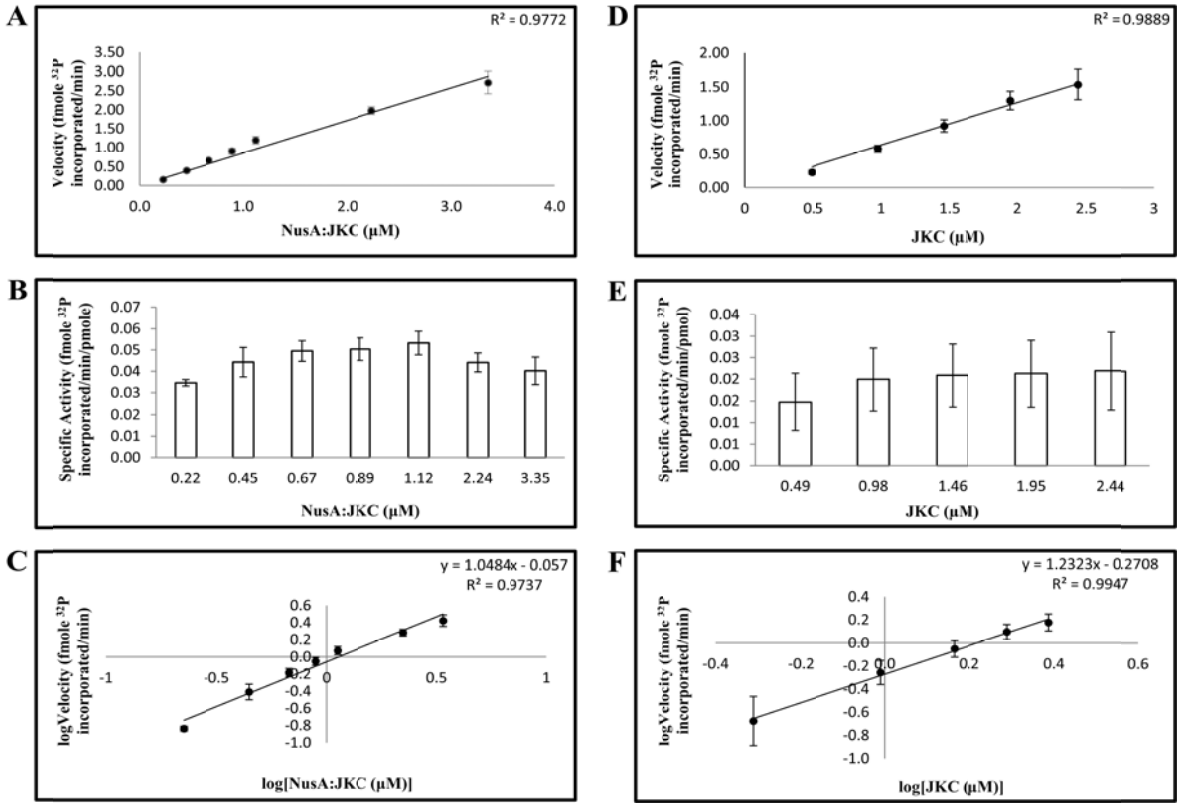

Figure 6. ACR4 autophosphorylates via an intramolecular mechanism. NusA:JKC (A-C) and JKC (D-F) were incubated at increasing enzyme concentrations in an autophosphorylation assay. (A and D) Plot of velocity *vs.* enzyme concentration. (B and E) Plot of specific activity *vs.* enzyme concentration. (C and F) van't Hoff plot of the logarithm of enzyme velocity *vs.* the logarithm of enzyme concentration. Linear regression of the data in C and F estimates a slope of 1.05 for NusA:JKC and a slope of 1.23 for JKC. In A-F, data are the mean ± S.E (n = 4).

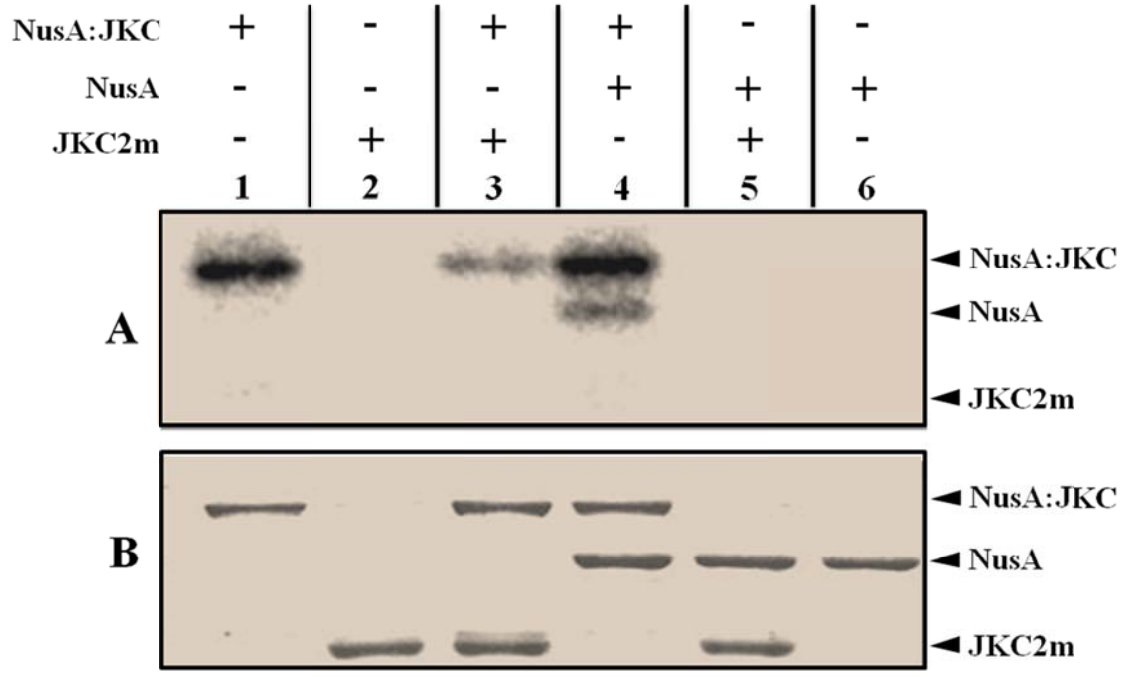

Figure 7. Intramolecular mechanism established by autophosphorylation assay**.** Active NusA:JKC and kinase inactive JKC2m were incubated together in an *in vitro* autophosphorylation assay. ***Lane 1,*** active NusA:JKC; ***lane 2,*** kinase inactive JKC2m; ***lane* 3**, active NusA:JKC and inactive JKC2m; ***lane 4,*** NusA:JKC and the NusA tag; ***lane 5,***kinase inactive JKC2m and the NusA tag; ***lane 6,*** NusA tag. Proteins were resolved by 10% SDS PAGE and analyzed by phosphorimaging (panel A) and Coomassie Blue staining (panel B).

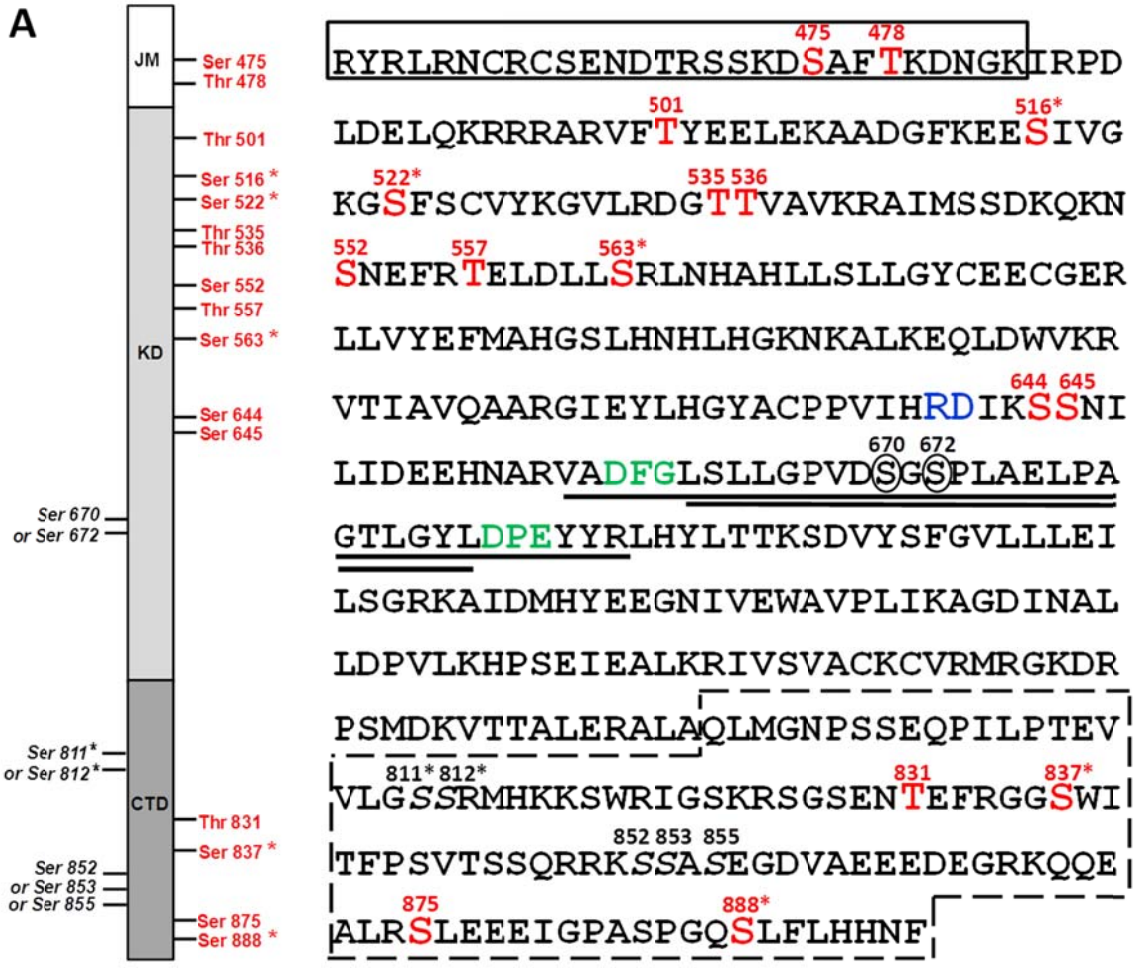
A
JM
KD
CTD
Ser 475
Thr 478
Thr 501
Ser 516 *
Ser 522 *
Thr 535
Thr 536
Ser 552
Thr 557
Ser 563 *
Ser 644
Ser 645
Ser 670
or Ser 672
Ser 811*
or Ser 812*
Thr 831
Ser 837 *
Ser 852
or Ser 853
or Ser 855
Ser 875
Ser 888 *
RYRLRNCRCSENDTRSSKDSAFTKDNGKIRPD
LDELQKRRRARVFTYEELEKAADGFKEESIVG
KGSFSCVYKGVLRDGTTVAVKRAIMSSDKQKN
SNEFRTELDLLSRLNHAHLLSLLGYCEECGER
LLVYEFMAHGSLHNHLHGKNKALKEQLDWVKR
VTIAVQAARGIEYLHGYACPPVIHRDIKSSNI
LIDEEHNARVADFGLSLLGPVDSGSPLAELPA
GTLGYLDPEYYRLHYLTTKSDVYSFGVLLLEI
LSGRKAIDMHYEEGNIVEWAVPLIKAGDINAL
LDPVLKHPSEIEALKRIVSVACKCVRMRGKDR
PSMDKVTTALERALAQLMGNPSSEQPILPTEV
VLGSSRMHKKSWRIGSKRSGSENTEFRGGSWI
TFPSVTSSQRRKSSASEGDVAEEEDEGRKQQE
ALRSLEEEIGPASPGQSLFLHHNF

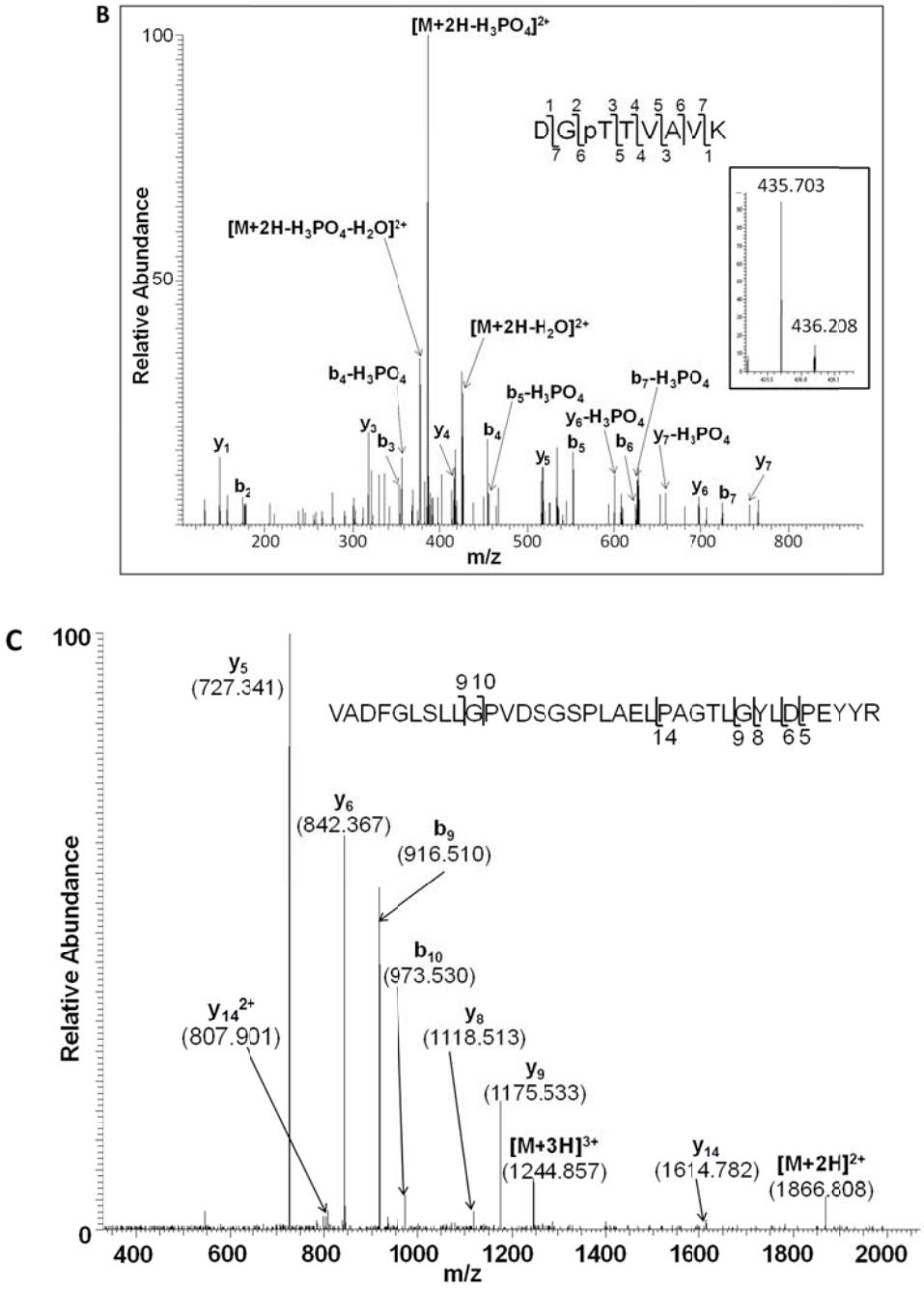

Figure 8. (A) Diagram showing the identified phosphorylation sites. *Left panel*: schematic of the ACR4 ICD showing the boundaries of the JM, KD and CTD. Confirmed phosphorylated residues in the autophosphorylated protein are in red and those that are found in the naïve protein are indicated with an asterisk. *Right panel*: Amino acid sequence of the ICD showing the N-terminal JM region (boxed rectangle), the central KD with the 35 aa tryptic peptide (underlined) and the activation loop sequence (double underlined) between the DFG and DPE motif (in green), the "RD" motif characteristic of RD-type kinases (in

blue) and the CTD (box with dashed lines). Confirmed phosphorylated sites are numbered and highlighted in red and those that are found in the naïve protein are denoted with an asterisk. Potential phosphorylation sites are numbered in black and the two Ser residues (670 & 672) within the activation loop are circled. (B) Collision-induced low resolution fragmentation spectrum of the phosphopeptide DGpTTVAVK (Mascot ion score 41), encompassing residues 533-540 of the ACR4 sequence. The presence of phosphorylated b_3 (theor. *m/z* 354.1; obs'd 354.1) and y_6 (theor. *m/z* 698.3; obs'd 698.2) ions, along with nonphosphorylated b_2 (theor. *m/z* 173.1; obs'd 173.1) and y_5 (theor. *m/z* 517.3; obs'd 517.3) ions, confirms Thr^{535} as the site of phosphorylation. The inset panel shows the MS spectrum of the doubly charged protonated molecular ion $[M+2H]^{2+}$. Isotope clusters are separated by 0.505 Da, confirming the charge state of the peptide. (C) Mass spectrum of the 35-residue tryptic peptide ^{657}VADFGLSLLGPVDSGSPLAELPAGTLGYLDPEYYR^{691} supporting a singly-phosphorylated residue with a mass of 3731.81 corresponding to the identification of $[M+2H]^{2+}$ (*m/z* = 1866.81) and $[M+3H]^{3+}$ (*m/z* = 1244.94) ions.

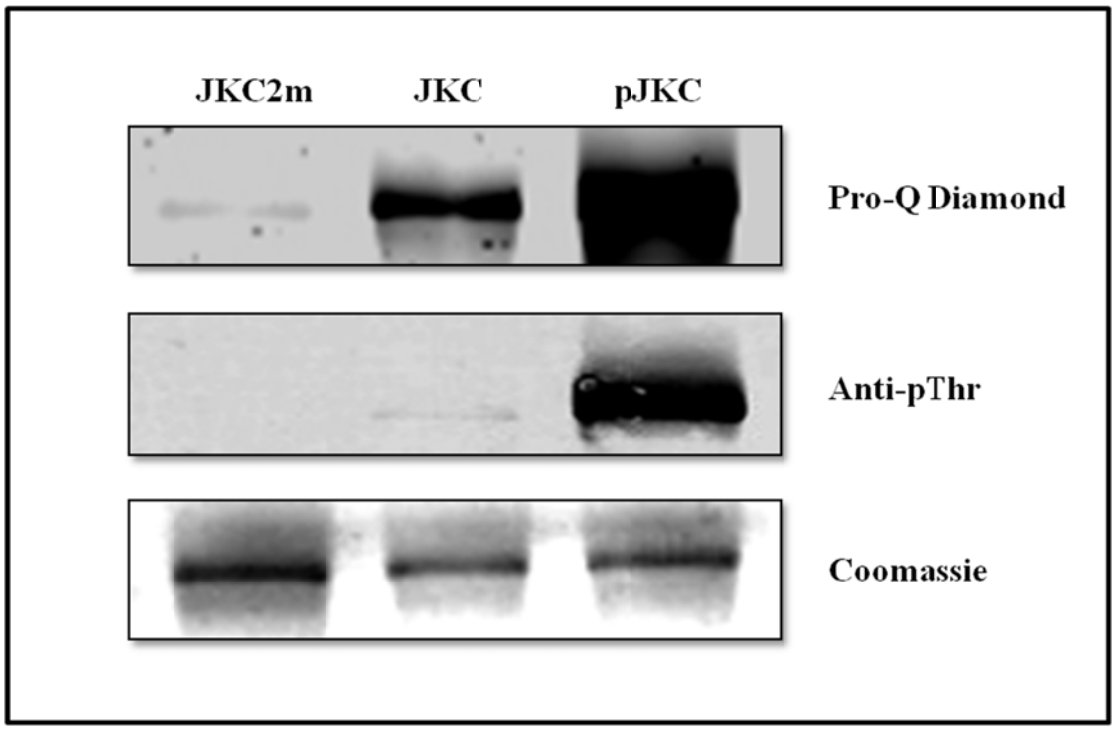

Figure 9. The phosphorylation status of the inactive mutant (JKC2m), naïve JKC (JKC) and the autophosphorylated JKC (pJKC) determined by staining with Pro-Q Diamond (upper panel) and western blot using anti-phosphothreonine antibody (middle panel). The corresponding Coomassie Blue stained gel of the proteins is shown in the lower panel.

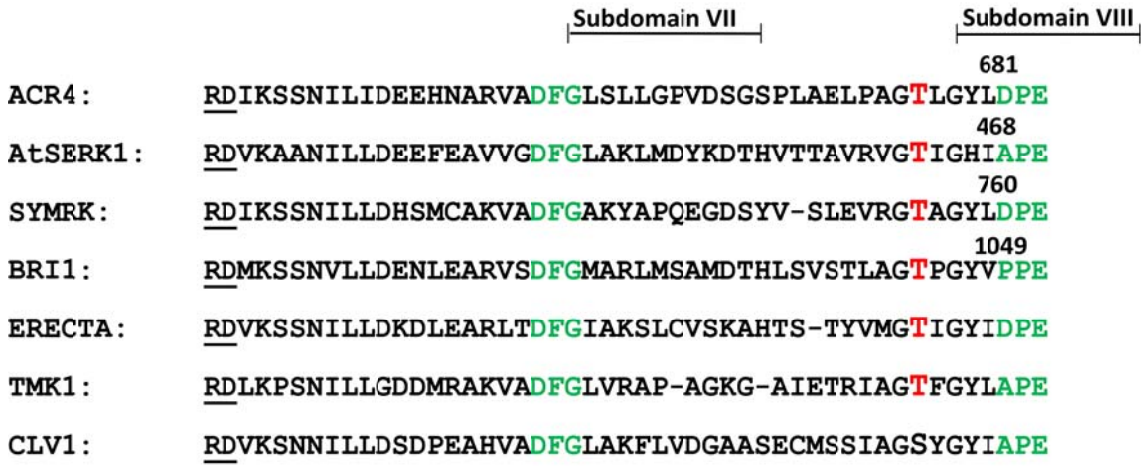

Figure 10. Alignment of the sequences of select RLKs belonging to the RD kinase family showing the Arg residue preceding the invariant Asp in the catalytic subdomain VI, the activation loop sequence in between the "DFG" in subdomain VII and "APE" in subdomain VIII, and the conserved Thr residue. The Gen Bank accession numbers of the sequences are: ACR4 (AB074762), AtSERK1/BAK1 (AT4G33430), SYMRK (AF492655), BRI1 (AT4G39400), ERECTA (AT2G26330), TMK1 (AT1G66150), CLV1 (AT1G75820).

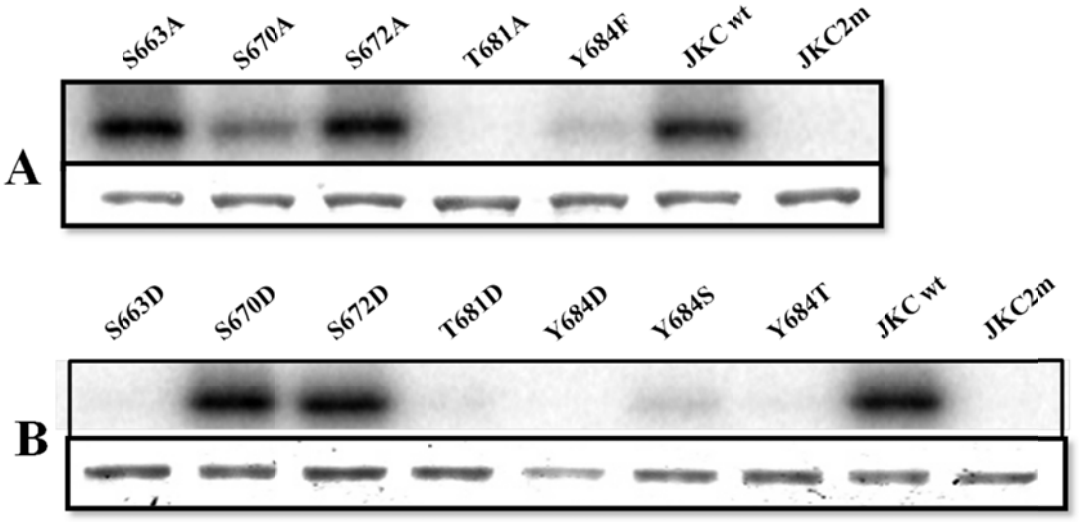

Figure 11. Effect of mutating activation loop phosphorylation sites on kinase activity. (A) Mutations of S^{663}, S^{670}, S^{672}, T^{681} to Ala and Y^{684} to Phe (B) Mutations of S^{663}, S^{670}, S^{672}, T^{681} to Asp and Y^{684} to Asp, Ser and Thr. Each mutant was purified and subjected to *in vitro* kinase assay as described in Materials & Methods. Equal amounts of recombinant proteins were loaded and separated by SDS-PAGE followed by autoradiography. In A and B, the top panel shows the autoradiogram and the bottom panel the corresponding Coomassie Blue stained gel. Wild type JKC and the mutant, JKC2m, were used as controls.

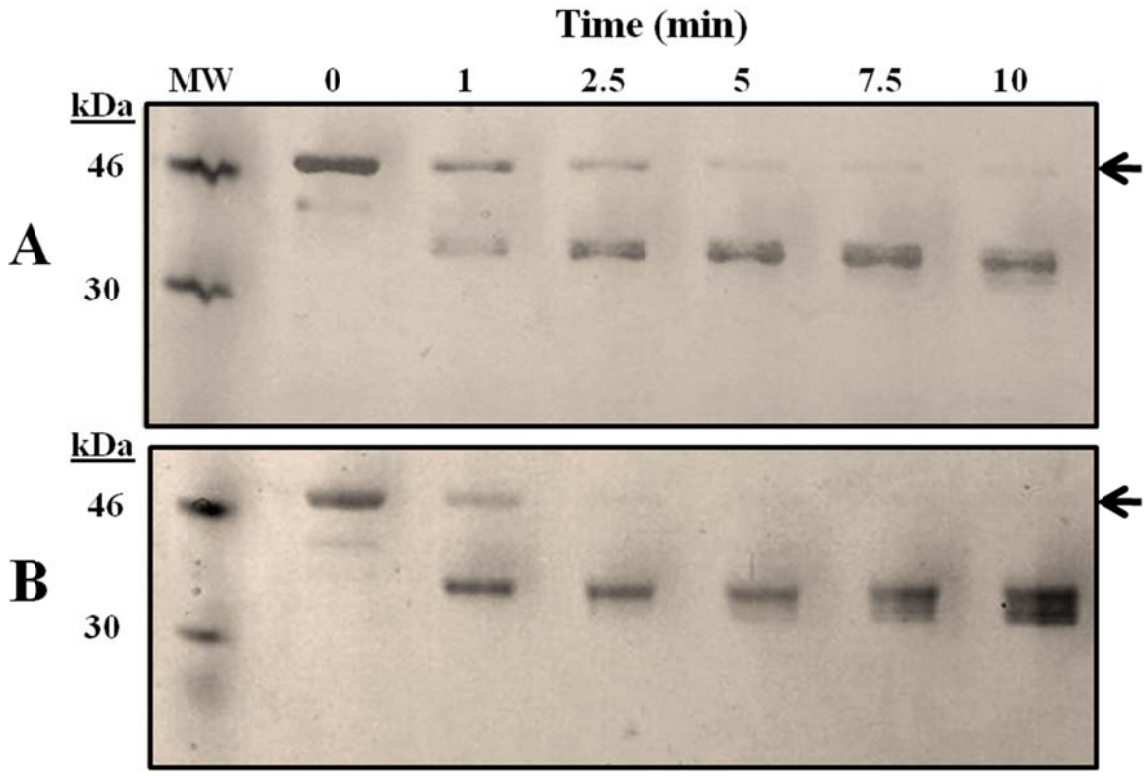

Figure 12. Time course of the tryptic digest of (A) naïve JKC and (B) autophosphorylated pJKC. Proteins were incubated at room temperature for the indicated times with a 1:1000 wt:wt ratio of enzyme to substrate followed by SDS-PAGE analysis. Arrow indicates the mobility of the undigested protein and MW is the lane with molecular mass markers of 46 kDa and 30 kDa.

CHAPTER 3. RECOMBINANT EXPRESSION AND PURIFICATION OF SOLUBLE CYTOPLASMIC KINASE DOMAINS OF THE ACR4, ACR4 HOMOLOGS, AND ALE2 RECEPTOR-LIKE KINASES FROM *ARABIDOPSIS*

Matthew R. Meyer and A. Gururaj Rao

Abstract

Arabidopsis CRINKLY4 (ACR4) is a receptor-like kinase (RLK) involved in the proper formation of epidermis in the leaves and reproductive tissues of the plant and is necessary for stem cell differentiation in the root meristem. Importantly, there are five additional RLKs, four of which are homologs of ACR4 (AtCRR1, AtCRR2, AtCRR3 and AtCRK1 termed *Arabidopsis* Crinkly4 Related, AtCRRs) that contain similar sequence and structural features while the remaining RLK, ABNORMAL LEAF SHAPE 2 (ALE2), is involved in proper epidermal layer formation. ALE2 is also known to synergistically enhance ACR4 kinase activity *in vitro.* However, the precise signaling pathway mediated by these RLKs and the molecular basis of their biological role remain to be elucidated. There is little understanding of the biochemical functions of these RLKs although genetic and cell biology studies implicate their critical role in cellular differentiation and patterning. *In vitro* biochemical and biophysical studies of recombinant proteins can often provide important clues for understanding *in vivo* physiological functions. To this end, we have recombinantly expressed and purified milligram quantities of the intracellular domains (ICD) of ACR4, the AtCRRs, and ALE2 as C-terminal fusions to the Small Ubiquitin like MOdifier (SUMO) protein and describe some biochemical properties of the proteins. Additionally, we demonstrate Ala substitutions of the ACR4 autophosphorylation sites have differential effects on kinase autophosphorylation activity.

Abbreviations

ACR4, *Arabidopsis* CRINKLY4; AEBSF, 4-(2-aminoethyl) benzenesulfonyl fluoride hydrochloride; ALE2, ABNORMAL LEAF SHAPE2; ATP, adenosine triphosphate; BRI1, brassinosteroid insensitive 1; BAK1, BRI1 associated receptor kinase 1; CR4, maize CRINKLY4; AtCRR, *Arabidopsis* CRINKLY4 related; DTT, dithiothreitol; ICD, intracellular domain; IPTG, isopropyl β-D-1-thiogalactopyranoside; KD, kinase domain; Ni-NTA, nickel-nitrilotriacetic acid; PVDF, polyvinylidene fluoride; RLK, receptor-like kinase; SUMO, small ubiquitin-related modifier; TCEP, tris (2-carboxyethyl) phosphine hydrochloride

Introduction

Maize CRINKLY4 (CR4) was initially described as a growth factor like receptor-like kinase (RLK) affecting the epidermal layer in leaves and aleurone layer of the kernel (1, 2). Subsequent genomic studies revealed orthologs to CR4 in *Arabidopsis* (ACR4) and rice (OsCR4) that were similar in both sequence and domain architecture (3). Genetic and cell biology investigations of ACR4 have shown this receptor to affect epidermal layer formation in the leaves and reproductive tissues in the aerial organs of the plant (4-6). Additionally, ACR4 has been described as a central player in the dual processes of maintaining stem cell identity and lateral root initiation during development (7). Another key RLK, ABNORMAL LEAF SHAPE 2 (ALE2), is also involved in proper formation of epidermal tissue in the leaves (8). In addition to ACR4, four homologs with structural features analogous to ACR4 have been described (3). Referred to as *Arabidopsis thaliana* Crinkly4-related proteins (AtCRRs), they represent the ACR4 receptor kinase gene family in *Arabidopsis* and consist of AtCRRs 1, 2 and 3, and AtCRK1. In investigations on the role of ACR4 in root development, De Smet et al. (7) demonstrated that double and triple-mutant combinations of ACR4 with mutations in the AtCRRs caused uncharacteristic lateral root formation and mutant plants showed increased formation and irregular patterning of lateral root meristems.

To complement ongoing *in planta* studies in various laboratories, our laboratory is focused on the *in vitro* biochemical and biophysical analyses of RLKs involved in cell-fate specification and proper development of the plant. To this end, we have recently characterized the biochemical properties of the intracellular domain of ACR4 expressed in *E. coli,* including its Ser/Thr kinase activity (9). However, investigations to address fundamental questions about protein structure and function and protein-protein interactions require

milligram quantities of protein. It is well established that detailed *in vitro* structural and mechanistic studies of recombinantly expressed proteins can provide key insights into our understanding of physiological/cellular functions, generate testable models and facilitate development of protein reagents for the dissection of signaling pathways. In this paper, we report on the expression of milligram quantities of the ICDs of ACR4, the AtCRRs, and ALE2 in fusion with the yeast SUMO protein in an *E. coli* system. The SUMO tag has been successfully used in the overexpression and solubilization of insoluble target proteins (10-12).

Materials and Methods

Materials.

Platinum pfx polymerase, TOP10 cells, dNTPs, and Pro-Q Diamond stain were purchased from Invitrogen. The pE-SUMO vector was acquired from Life Sensors. T4 DNA ligase, T4 DNA polymerase, T7 Express cells, and restriction enzymes, except *AarI* (Fermentas), were purchased from New England Biolabs. Deoxyoligonucleotide primers were purchased from Integrated DNA Technologies Inc. The Rosetta2 (DE3) pLysS expression cells were obtained from Novagen. Ni-NTA Superflow resin was purchased from Qiagen. γ-^{32}P labeled ATP, 6000Ci/mmol, was acquired from Perkin Elmer. All other chemicals were from local sources.

Vector Construction.

The ICDs of ACR4, the AtCRRs, and ALE2 were PCR amplified using Platinum *pfx* and the appropriate primers (Table 1). The amplified genes of interest were then cloned into the pE-SUMO (Kan) vector (Life Sensors) according the manufacturer's instructions and

using the appropriate set of enzymes for each gene (Table 1). The resulting ligated vectors were transformed into chemically competent TOP10 cells and spread onto LB agar plates supplemented with 50 μg/ml Kanamycin. The plates were incubated overnight at 37 °C. Positive colonies for each construct were selected for DNA sequencing to verify correct insertion of the desired gene into the pE-SUMO vector. To generate the Ala point mutations of the ACR4 autophosphorylation sites, the vector encoding the SUMO-tagged ACR4 intracellular domain was mutagenized using the QuickChange Lightning Multi Site-Directed Mutagenesis Kit (Stratagene) using the corresponding primers outlined in Table 2.

Recombinant protein expression.

The recombinant vector was transformed into Rosetta2 (DE3) pLysS cells, plated on LB agar plates supplemented with 50 μg/ml Kanamycin, and incubated overnight at 37 °C. For a typical expression, a single colony was used to inoculate a 5 ml LB-broth starter culture supplemented with 50 μg/ml kanamycin and allowed to incubate overnight at 37 °C with shaking. The starter culture was then used to inoculate, 1:100, a 100 ml LB-broth culture supplemented with the appropriate antibiotic, described above. The culture was grown at 37 °C with shaking until an OD_{600} = 0.6-0.8 was reached, ~2-3 h. The cultures were then cooled to 20 °C followed by induction with 1 mM IPTG and allowed to incubate for 5h with shaking. Cells were then harvested by centrifugation at 6000 rpm for 10 min at 4 °C. Cell pellets were then used immediately or stored at -80 °C until needed.

Purification of recombinant proteins.

The SUMO constructs encode an N-terminal His_6-tag for one-step purification of the proteins by Ni^{2+} metal affinity enrichment chromatography. A 100 ml cell pellet was resuspended in 10 ml of ice-cold Lysis Buffer (50mM Tris-HCl pH 7.4, 150mM NaCl, 1mM

DTT, 30 mM imidazole and 0.1% Triton X-100) supplemented with 1mM AEBSF. Cells were lysed by sonication with chilling on ice in between sonication rounds. The lysate was then centrifuged at 13,200 rpm for 30 min at 4 °C to pellet insoluble material. The soluble lysate was transferred to a 10 ml disposable column containing a 200 µl bed volume of Ni-NTA Superflow resin equilibrated with Lysis Buffer. The lysate/resin mixture was incubated for 1 h at 4 °C with rocking. After incubation, the lysate containing the unbound protein was allowed to flow through. The resin containing the bound recombinant protein was washed with 10 ml of ice-cold Wash Buffer (50mM Tris-HCl pH 7.4, 150mM NaCl, 1mM DTT, 30 mM imidazole) to remove unbound protein. The recombinant fusion proteins were eluted from the resin with three consecutive 200 µl aliquots of ice-cold Elution Buffer (50 mM Bis-Tris pH 7.2, 50 mM NaCl, 1mM DTT, and 150 mM imidazole) and pooled. Resulting protein fractions were analyzed by 12% SDS-PAGE and coomassie staining. Protein quantification was performed by the Bradford method (13). Densitometric analysis with ImageJ v1.45b of the SDS-PAGE gels was used to determine the quantity of fusion protein in the crude lysate and purified protein fractions. For the crude lysate fraction, total protein amount was determined by a Bradford assay. Quantification of the SUMO fusion in the crude lysate was determined by multiplying the ratio of the density of the SUMO fusion protein band to the density of the total crude lysate. The amount of SUMO fusion in the purified fraction was determined by the same method.

Protein Detection by Western Blot.

To assess the fidelity of protein expressions, the recombinant SUMO fused proteins were analyzed by western blot. Briefly, 1 µg of each purified protein was separated by 12% SDS-PAGE and blotted to a PVDF membrane and blocked with milk protein. The proteins

were incubated with either polyclonal rabbit, anti-SUMO (yeast) antibody (Rockland Immunochemicals, 1:10,000) or anti-ACR4 KD (1:2,000) (9). The membrane was washed then probed with anti-rabbit IgG conjugated to Alkaline Phosphatase (Sigma) at a 1:30,000 dilution. Colorimetric detection the proteins was performed with an AP Substrate Kit (Bio-Rad).

Gel Filtration Analysis.

The oligomerization property of each fusion protein was assessed by gel filtration using a Superdex G200 column (GE Healthcare) coupled to an AKTA FPLC (Amersham). Each protein was diluted to a concentration of 5 μM in 500 μl with Column Buffer (50 mM Tris-HCl, 100 mM NaCl, 1 mM DTT) and allowed to incubate at room temperature 30 min prior to injection onto the column. The column was equilibrated with Column Buffer prior to each run. Proteins were eluted off the column at a flow rate of 0.5 ml/min and 1 ml fractions corresponding to the peak fractions were collected. Each fraction was TCA precipitated and proteins were analyzed by 12% SDS-PAGE and Coomassie Blue staining.

Determination of autophosphorylation activity.

The recombinant proteins were subjected to an *in vitro* autophosphorylation assay to determine if the recombinant proteins had kinase activity (9). Briefly, 1 μg of each purified kinase was incubated in a 20 μl reaction of Kinase Buffer (20mM Bis-Tris pH 7.2, 25 mM NaCl, 5mM $MnCl_2$, and 1mM DTT) containing 25 μM ATP and 2 μCi of γ-^{32}P ATP. The reactions were allowed to proceed for 1 h at room temperature followed by termination with 6 μl of 4X SDS sample buffer and boiling for 5 min. Proteins were resolved by 12% SDS-PAGE and radioactive bands were monitored by phosphorimaging. Alanine mutants of the ACR4 autophosphorylation sites were expressed, purified, and assayed for

autophosphorylation activity as described above. Densities of the bands in the autoradiogram were quantified with the UN-Scan-It software v6.1.

Analysis of Phosphorylation status by staining with Pro-Q Diamond.

Approximately 1 µg of each protein was separated by 12% SDS-PAGE. The gel was first fixed for 2 x 30 min with solution containing 50% methanol and 10% acetic acid then washed three times with deionized water. It was then stained with Pro Q diamond stain for 90 min in the dark and then destained using 50 mM sodium acetate buffer pH 4.0 containing 20% acetonitrile. Images of the stained gel were acquired on a Molecular Dynamics Typhoon scanner (Amersham Biosciences) with an excitation source of 532 nm laser and a 580 nm bandpass emission filter.

Intrinsic Fluorescence measurements

SUMO fusion proteins were dialyzed against 10 mM Tris-HCl pH7.4, 0.1 mM TCEP and diluted to an A_{280} of 0.1. Measurements were made in a 1 cm cuvette at room temperature with a Cary Eclipse spectrofluorimeter (Varian) as described previously (9). Scans were executed at an excitation wavelength of 280 nm and a band width of 5 nm and a scan speed of 120 nm/min.

Results

Cloning and expression of SUMO fusion proteins

Fig.1A shows the schematic for the expression of the ICDs of ACR4, the AtCRRs, and ALE2 as C-terminal fusions to the yeast SUMO protein. The ICD of each gene was PCR amplified using appropriate primers (Table 1) and further processed for ligation into the pE-SUMO vector according to the instruction manual using standard ligation procedures.

The SUMO fusion vectors were transformed into Rosetta2 (DE3) pLysS cells for expression of the recombinant proteins followed by a one-step protein purification as described in Materials and Methods. Figure 2 shows the SDS-PAGE analysis of protein fractions at each step of the purification protocol starting with the total E. coli lysate (L), unbound proteins from the Ni-NTA column (U), proteins removed at the washing step (W) and the final step of purification (E). Typical yields of the purified SUMO fusions ranged from 0.5 to 2.4 milligrams from 100 ml cultures and the overall yield of pure protein from the crude lysate ranged from 60 to 85% (Table 3). Western blot analysis of the purified proteins using antibody to the SUMO protein demonstrated >95% purity (Fig. 3 upper panel).

Analysis of kinase activity

We have previously optimized the *in vitro* kinase assay conditions for ACR4 (9). Kinase activity of the recombinantly expressed fusion proteins was assessed using the same protocol by incubating the proteins in kinase buffer in the presence of γ-^{32}P ATP followed by separation by SDS-PAGE and phosphorimaging. It is evident from this study (Fig.4A, top panel) that in addition to SUMO:ACR4 (*lane 1*), the kinase domains of AtCRR3 (*lane 4*), AtCRK1 (*lane 5*) and ALE2 (*lane 6*) are active kinases whereas AtCRR1 (*lane 2*) and AtCRR2 (*lane 3*) are inactive. We also assessed the phosphorylation status of the proteins by staining with Pro-Q Diamond, a phosphospecific stain used extensively in the characterization of kinase activity (14, 15) and identification of phosphoproteins (16). In accordance with their demonstrated kinase activity, ACR4, AtCRR3, AtCRK1 and ALE2 showed intense bands with ProQ Diamond staining (Fig. 4B, top panel *lanes 1, 4, 5 and 6*) whereas the inactive kinases AtCRR1 and AtCRR2 showed no staining (Fig. 4B, top panel *lanes 2 and 3*) as would be expected from an inactive protein undergoing little or no

phosphorylation. The bottom panels in Fig. 4 represent the corresponding Coomassie Blue stained gels to demonstrate equivalent protein loading amounts.

Gel filtration analysis

The hydrodynamic properties of the naïve, unphosphorylated proteins were examined by gel filtration on a Sephadex G200 column (Fig. 5). At a concentration of 5 μM, SUMO:CRR1 eluted predominantly in the void volume. Analysis of these fractions by SDS-PAGE (inset) indicates that the void volume fraction consists entirely of aggregates of the monomer. Similarly, a small proportion of SUMO:ACR4 elutes as an aggregate in the void volume as reported earlier (9). There was no evidence of oligomerization of SUMO:CRR2, SUMO:CRR3 and SUMO:CRK1.

Intrinsic Fluorescence

Fluorescence spectroscopy is a sensitive technique for comparing conformational states of proteins or conformational changes within a given protein and is dependent on the presence of tyrosine (Tyr) and tryptophan (Trp) (17). At 280 nm both these aromatic residues absorb and contribute to the emission spectra. The intrinsic fluorescence spectra of SUMO-fused proteins, acquired by excitation at 280 nm, are depicted in Fig. 6 and the inset table indicates the number of Trp and Tyr residues within each protein. In all cases, the number of Tyr residues exceeds the number of Trp residues but there is no evidence of an emission peak attributable to Tyr residues. The SUMO protein itself has just one Tyr residue and no Trp residue and has low fluorescence intensity.

Effect of point mutants on ACR4 autophosphorylation

Autophosphorylation of a receptor intracellular kinase domain is critical for maximal activation and for recruitment of downstream signaling components. Phosphorylation in

subdomains such as the juxtamembrane domain (JMD), activation loop, and the C-terminal domain (CTD) are required to relieve *cis* inhibitory elements, thus allowing for enhanced kinase activity (18-21). To determine the effects the ACR4 autophosphorylation sites on kinase autophosphorylation, 15 individual point mutants were generated in which the phosphorylation site Ser/Thr was substituted with Ala (Table 2). Multiple attempts to transform the S:ACR4 S837A vector into Rosetta (DE3) pLysS cell were made, however no colonies grew and the mutation appeared to be *E. coli* lethal. Therefore, this mutation was not considered in our study. Each protein was expressed and purified as described in Materials and Methods. The yields of individual mutant proteins were comparable to the S:ACR4 wild-type protein, indicating proper folding of each enzyme. Proteins were then subjected to an *in vitro* phosphorylation assay in the presence of [γ-32] ATP. The autoradiogram in Fig. 7A demonstrates that each mutant had varying effects on ACR4 kinase autophosphorylation. The majority of the mutants, encompassing the JMD, KD, and CTD, displayed decreased autophosphorylation activity when compared to the wild-type enzyme (Fig. 7B), suggesting that phosphorylation at these sites is critical for maximum kinase activity. Interestingly, the S645A in the kinase domain showed enhanced activity when compared to wild-type. This may indicate that phosphorylation in this region is involved in repression of kinase activity. Point mutants of the ACR4 autophosphorylation sites substituted with the phosphomimetic Asp residue may provide some insight into the regulatory nature of phosphorylation at individual positions within the JMD, KD, and CTD.

Discussion

Multicellular organisms require a highly regulated array of signal transduction networks to promote cell fate specification and differentiation. Strict control of these networks ensures proper cell patterning and tissue development within the organism. Thus, in both animal and plant cells, directed cell differentiation, growth and development are facilitated via a variety of external stimuli that are appropriately interpreted by a multitude of cell-surface receptors. Over 400 putative RLKs are encoded in the *Arabidopsis* genome (22-25). However, although the biological functions of several RLKs are known, very few of the RLKs have been characterized in detail at the molecular level and there is little or no knowledge of the biochemical basis of the regulatory network mediated by ACR4, its homologs, and ALE2 in plant development and signaling. It is possible that receptor activation and autophosphorylation of ACR4 kinase could be stimulated by heteromeric interactions with the AtCRR proteins as has been reported for other mammalian receptors (26-28) and *Arabidopsis* brasssinosteroid receptor BRI1 and BAK1 (29). Similarly, genetic studies indicate that pathways involving ALE2 and ACR4 might act positively to regulate the specification of the protoderm and/or protoderm specific genes in the formation of leafy organs . Intriguingly, in the same study, in *in vitro* experiments, the kinase domains of ACR4 have been demonstrated to phosphorylate each other (8).

In light of the studies described above it becomes important to study the structural and functional aspects of the cell-surface RLKs as potential predictors of *in vivo* function. In this regard, the inability to purify these proteins from natural sources in sufficient quantities for biochemical and cell biological experimentation has been a major constraint. We have

now removed this constraint by recombinant expression of the proteins in *E. coli* in fusion with the SUMO-tag.

One measure of proper folding and functional integrity of the produced protein is its solubility in aqueous buffers since misfolded proteins generally tend to precipitate. We have developed a relatively simple one-step affinity purification scheme to obtain a >95% pure protein preparation (Fig. 2 and Fig. 3). As shown in Table 2, we have recovered high yields (60-85%) of soluble protein using small volumes (100 ml) of expression medium and have also not encountered any loss of efficiency in scaling it up to larger volumes (data not shown).

Biological activity is yet another paradigm of a correctly folded protein. The cytoplasmic domains of ACR4, AtCRR3, AtCRK1 and ALE2 have kinase domains (KD) that are predicted to be functional and indeed we have demonstrated that the recombinantly expressed proteins possess kinase activity *in vitro* (Fig. 4A top panel, lanes 1, 4, 5 and 6). These results confirm the previously reported kinase activity of the proteins (3, 8, 9). On the other hand, the cytoplasmic domains of AtCRR1 and AtCRR2 are predicted to harbor inactive kinases owing to the deletion of key residues within subdomain VIII (3). Accordingly, the recombinant fusion proteins showed no autophosphorylation activity (Fig. 4A top panel, lanes 1 and 2).

Importantly, receptor kinase autophosphorylation also leads to enhanced activity and the ability to recruit substrate proteins. Indeed in the classic example of the EGF receptor, receptor activation and kinase autophosphorylation promotes conformational changes that allow the recruitment of co-receptors and/or substrate proteins (30, 31). Among RLKs, BRI1 autophosphorylation leads to potential conformational changes in the C-terminal domain that

allow for binding to the co-receptor BAK1 and to recruit intracellular targets (32, 33). Our results indicate that individual ACR4 autophosphorylation sites make a partial contribution to maximal kinase activity (Fig. 7) and concomitant conformational changes (9) may be important for regulation of activity *in vivo*.

It is pertinent to point out that the kinase domains of AtCRR1, AtCRR2, AtCRR3, AtCRK1 share an amino acid sequence identity of 41%, 40%, 43%, 42% respectively with the ACR4 kinase domain. In contrast, in the case of ALE2, the primary structure is less well conserved and the kinase domain exhibits only a 33% identity to the ACR4 KD. Proteins with similar primary structure can be expected to show topographic or functional similarities and in the case of kinases the basic fold of the protein family is remarkably well conserved (34). It is therefore not entirely unreasonable to expect that the homologs would also have specific epitopes that would be cross-reactive to antibody raised to the ACR4 kinase domain. Indeed, in western blot analysis all the ACR4 homologs react positively to the anti-ACR4 KD polyclonal antibody (data not shown). However, no cross-reactivity was observed with the KD of ALE2 or the SUMO protein, indicating possible differences in linear and/or conformational epitopes (data not shown).

Fluorescence spectroscopy is a widely used technique to study structural features and conformations of protein molecules (17). In particular, the fluorescence of Trp residues is sensitive to the polarity of the local environment and is reflected in the λ_{max} of the emission spectrum. In tryptophan containing proteins, five different spectral classes have been described, each exhibiting significantly different emission peak maxima and quantum yields (35). When the Trp residues in the protein are buried in the three-dimensional structure in a low-polar hydrophobic environment and protected from the aqueous phase, the λ_{max} can be as

low as 308 nm with a low quantum yield (Class A). On the other hand, in proteins containing exposed Trp residues in a high-polar aqueous environment, the λ_{max} can be $\geq$ 350 nm with a quantum yield equal to or greater than that of free aqueous tryptophan (Class III). The three other classes, S, I and II exhibit emission spectra with λ_{max} values in between 308 and 350 nm accompanied by varying spectral shapes and widths (35). Therefore, in proteins containing multiple Trp residues, the emission spectrum is reflective of multiple contributions of the five spectral classes. In relative terms, the emission spectra of ACR4, AtCRR1, AtCRR2, AtCRR3 and AtCRK1 (λ_{max} 323-336 nm) are supportive of Trp residues being in a more non-polar environment compared with the red-shifted λ_{max} of 346 nm observed in the emission spectra of ALE2, indicative of a more polar environment for the Trp residues (Fig. 6). These studies therefore suggest subtle differences in the conformations of the folded state of the ICDs.

The movement of proteins through a gel filtration matrix is related to its mass, aggregation state and shape. Generally, a narrow and symmetrical elution peak is observed for a protein that is folded as a single compact entity, whereas a broader non-symmetrical peak is more illustrative of a conformationally flexible molecule that exists as a heterogeneous population of species (36). Thus, the symmetrical, single-peak elution profiles for SUMO fused ACR4, CRR2, CRR3, CRK1 and ALE2 (Fig. 5) suggest that they have well defined compact conformations. In contrast, the elution profile of SUMO:CRR1 is more irregular and indicative of a heterogeneous mixture of conformers, some of which could be contributing to the aggregated form that elutes close to the void volume. Potentially, this behavior could be attributed to a misfolded SUMO:CRR1 with exposed hydrophobic

surfaces although the solubility of the protein and the fluorescence emission spectrum are contrarian indicators.

In conclusion, in this paper we describe for the first time a scheme for the expression and purification of the ICDs of some plant RLKs implicated in cell fate specification in the aerial organs of plants as well as maintenance of stem cell identity at the root tip meristem. Ongoing and future experiments in our laboratory will address fundamental questions related to protein-protein interactions and regulation of phosphorylation activity by members of this group. We expect that these *in vitro* studies will complement genetic approaches and contribute to an overall understanding of signal transduction events mediated by ACR4, the ACR4 homologs, and ALE2. In the larger context, we yet do not know the functions of hundreds of RLKs and their putative ligands. Our focused effort exemplifies the need for the development of technologies for production and characterization of the RLKs that will further catalyze the generation of other reagents and enable systems biology investigations in plant biology.

References

1. Becraft, P.W., P.S. Stinard, and D.R. McCarty, *CRINKLY4: A TNFR-like receptor kinase involved in maize epidermal differentiation.* Science, 1996. **273**(5280): p. 1406-9.
2. Jin, P., T. Guo, and P.W. Becraft, *The maize CR4 receptor-like kinase mediates a growth factor-like differentiation response.* Genesis, 2000. **27**(3): p. 104-16.
3. Cao, X., K. Li, S.G. Suh, T. Guo, and P.W. Becraft, *Molecular analysis of the CRINKLY4 gene family in Arabidopsis thaliana.* Planta, 2005. **220**(5): p. 645-57.
4. Tanaka, H., M. Watanabe, D. Watanabe, T. Tanaka, C. Machida, and Y. Machida, *ACR4, a putative receptor kinase gene of Arabidopsis thaliana, that is expressed in the outer cell layers of embryos and plants, is involved in proper embryogenesis.* Plant and Cell Physiology, 2002. **43**(4): p. 419-428.

5. Gifford, M.L., S. Dean, and G.C. Ingram, *The Arabidopsis ACR4 gene plays a role in cell layer organisation during ovule integument and sepal margin development.* Development, 2003. **130**(18): p. 4249-58.
6. Watanabe, M., H. Tanaka, D. Watanabe, C. Machida, and Y. Machida, *The ACR4 receptor-like kinase is required for surface formation of epidermis-related tissues in Arabidopsis thaliana.* Plant Journal, 2004. **39**(3): p. 298-308.
7. De Smet, I., V. Vassileva, B. De Rybel, M.P. Levesque, W. Grunewald, D. Van Damme, G. Van Noorden, M. Naudts, G. Van Isterdael, R. De Clercq, J.Y. Wang, N. Meuli, S. Vanneste, J. Friml, P. Hilson, G. Jurgens, G.C. Ingram, D. Inze, P.N. Benfey, and T. Beeckman, *Receptor-like kinase ACR4 restricts formative cell divisions in the Arabidopsis root.* Science, 2008. **322**(5901): p. 594-7.
8. Tanaka, H., M. Watanabe, M. Sasabe, T. Hiroe, T. Tanaka, H. Tsukaya, M. Ikezaki, C. Machida, and Y. Machida, *Novel receptor-like kinase ALE2 controls shoot development by specifying epidermis in Arabidopsis.* Development, 2007. **134**(9): p. 1643-1652.
9. Meyer, M.R., C.F. Lichti, R.R. Townsend, and A.G. Rao, *Identification of in vitro autophosphorylation sites and effects of phosphorylation on the Arabidopsis CRINKLY4 (ACR4) receptor-like kinase intracellular domain: insights into conformation, oligomerization, and activity.* Biochemistry, 2011. **50**(12): p. 2170-86.
10. Malakhov, M.P., M.R. Mattern, O.A. Malakhova, M. Drinker, S.D. Weeks, and T.R. Butt, *SUMO fusions and SUMO-specific protease for efficient expression and purification of proteins.* J Struct Funct Genomics, 2004. **5**(1-2): p. 75-86.
11. Marblestone, J.G., S.C. Edavettal, Y. Lim, P. Lim, X. Zuo, and T.R. Butt, *Comparison of SUMO fusion technology with traditional gene fusion systems: enhanced expression and solubility with SUMO.* Protein Science, 2006. **15**(1): p. 182-9.
12. Esposito, D. and D.K. Chatterjee, *Enhancement of soluble protein expression through the use of fusion tags.* Current Opinion in Biotechnology, 2006. **17**(4): p. 353-358.
13. Bradford, M.M., *A rapid and sensitive method for the quantitation of microgram quantities of protein utilizing the principle of protein-dye binding.* Anal Biochem, 1976. **72**: p. 248-54.
14. Schulenberg, B., T.N. Goodman, R. Aggeler, R.A. Capaldi, and W.F. Patton, *Characterization of dynamic and steady-state protein phosphorylation using a fluorescent phosphoprotein gel stain and mass spectrometry.* Electrophoresis, 2004. **25**(15): p. 2526-2532.
15. Burza, A.M., I. Pekala, J. Sikora, P. Siedlecki, P. Malagocki, M. Bucholc, L. Koper, P. Zielenkiewicz, M. Dadlez, and G. Dobrowolska, *Nicotiana tabacum osmotic stress-activated kinase is regulated by phosphorylation on Ser-154 and Ser-158 in the kinase activation loop.* Journal of Biological Chemistry, 2006. **281**(45): p. 34299-34311.
16. Agrawal, G.K. and J.J. Thelen, *A high-resolution two dimensional Gel- and Pro-Q DPS-based proteomics workflow for phosphoprotein identification and quantitative profiling.* Methods in Molecular Biology, 2009. **527**: p. 3-19.
17. Lakowicz, J.R., *Principles of Fluorescence Spectroscopy*. Second Ed. ed. 1999: Plenum Publishing Corporation.

18. Hubbard, S.R., *Protein tyrosine kinases: autoregulation and small-molecule inhibition.* Curr Opin Struct Biol, 2002. **12**(6): p. 735-41.
19. Hubbard, S.R., *Juxtamembrane autoinhibition in receptor tyrosine kinases.* Nat Rev Mol Cell Biol, 2004. **5**(6): p. 464-71.
20. Pike, A.C., P. Rellos, F.H. Niesen, A. Turnbull, A.W. Oliver, S.A. Parker, B.E. Turk, L.H. Pearl, and S. Knapp, *Activation segment dimerization: a mechanism for kinase autophosphorylation of non-consensus sites.* Embo Journal, 2008. **27**(4): p. 704-14.
21. Lochhead, P.A., *Protein kinase activation loop autophosphorylation in cis: overcoming a Catch-22 situation.* Sci Signal, 2009. **2**(54): p. pe4.
22. Shiu, S.H. and A.B. Bleecker, *Plant receptor-like kinase gene family: diversity, function, and signaling.* Sci STKE, 2001. **2001**(113): p. re22.
23. Becraft, P.W., *Receptor kinase signaling in plant development.* Annu Rev Cell Dev Biol, 2002. **18**: p. 163-92.
24. Haffani, Y.Z., N.F. Silva, and D.R. Goring, *Receptor kinase signalling in plants.* Canadian Journal of Botany-Revue Canadienne De Botanique, 2004. **82**(1): p. 1-15.
25. Afzal, A.J., A.J. Wood, and D.A. Lightfoot, *Plant receptor-like serine threonine kinases: roles in signaling and plant defense.* Mol Plant Microbe Interact, 2008. **21**(5): p. 507-17.
26. Saito, Y., J. Haendeler, Y. Hojo, K. Yamamoto, and B.C. Berk, *Receptor heterodimerization: essential mechanism for platelet-derived growth factor-induced epidermal growth factor receptor transactivation.* Mol Cell Biol, 2001. **21**(19): p. 6387-94.
27. Pfeiffer, M., T. Koch, H. Schroder, M. Laugsch, V. Hollt, and S. Schulz, *Heterodimerization of somatostatin and opioid receptors cross-modulates phosphorylation, internalization, and desensitization.* J Biol Chem, 2002. **277**(22): p. 19762-72.
28. Morgillo, F., J.K. Woo, E.S. Kim, W.K. Hong, and H.Y. Lee, *Heterodimerization of insulin-like growth factor receptor/epidermal growth factor receptor and induction of survivin expression counteract the antitumor action of erlotinib.* Cancer Res, 2006. **66**(20): p. 10100-11.
29. Russinova, E., J.W. Borst, M. Kwaaitaal, A. Cano-Delgado, Y. Yin, J. Chory, and S.C. de Vries, *Heterodimerization and endocytosis of Arabidopsis brassinosteroid receptors BRI1 and AtSERK3 (BAK1).* Plant Cell, 2004. **16**(12): p. 3216-29.
30. Cadena, D.L., C.L. Chan, and G.N. Gill, *The intracellular tyrosine kinase domain of the epidermal growth factor receptor undergoes a conformational change upon autophosphorylation.* J Biol Chem, 1994. **269**(1): p. 260-5.
31. Schulze, W.X., L. Deng, and M. Mann, *Phosphotyrosine interactome of the ErbB-receptor kinase family.* Molecular Systems Biology, 2005. **1**.
32. Wang, X., X. Li, J. Meisenhelder, T. Hunter, S. Yoshida, T. Asami, and J. Chory, *Autoregulation and homodimerization are involved in the activation of the plant steroid receptor BRI1.* Dev Cell, 2005. **8**(6): p. 855-65.
33. Ye, H.X., L. Li, and Y.H. Yin, *Recent Advances in the Regulation of Brassinosteroid Signaling and Biosynthesis Pathways.* Journal of Integrative Plant Biology, 2011. **53**(6): p. 455-468.

34. Scheeff, E.D. and P.E. Bourne, *Structural evolution of the protein kinase-like superfamily.* PLoS Comput Biol, 2005. **1**(5): p. e49.
35. Reshetnyak, Y.K. and E.A. Burstein, *Decomposition of protein tryptophan fluorescence spectra into log-normal components. II. The statistical proof of discreteness of tryptophan classes in proteins.* Biophys J, 2001. **81**(3): p. 1710-34.
36. Corbett, R.J. and R.S. Roche, *Use of high-speed size-exclusion chromatography for the study of protein folding and stability.* Biochemistry, 1984. **23**(8): p. 1888-94.

Tables

Table 1. Primer design of respective fusion proteins

Construct	Residues Cloned[a]	Restriction Enzymes	Primer	Primer Sequence (5' → 3')
SUMO:ACR4	456-895	BbsI, XbaI	Forward Reverse	GGTGGTGAAGACTTAGGTAGGTACAGATTGAGGAATTG GGTGGTTCTAGATCAGAAATTATGATGCAAGAACAAG
SUMO:CRR1	462-775	BsaI, XbaI	Forward Reverse	GGAGGAGGAGGTCTCGAGGTCGGATTGTCACTAGTCCTAAT GGTGGTGGTTCTAGATCATCAGAAGATCAATGCATCTCTTGC
SUMO:CRR2	455-776	BsaI. XbaI	Forward Reverse	GGAGGAGGAGGTCTCGAGGTAAGATGACAAAAGGTAGTAAAC GGTGGTGGTTCTAGATCATCAAAAAGTGAGGCCAGACTTGA
SUMO:CRR3	419-814	BsaI	Forward Reverse	GGAGGAGGAGGTCTCGAGGTACTGGAGTTTGCTTGGGGA GGAGGAGGTCTCTCTAGATCATCAATCAGAGACAATAGAACAAATG
SUMO:CRK1	388-751	AarI	Forward Reverse	GGAGGAGGACACCTGCGAGAAGGTAAAAGCCACTGTCGATGCC GGTGGTCACCTGCGAGTCTAGATCATCAATAAGTGTTTGATCGAGATACG
SUMO:ALE2	282-744	AarI	Forward Reverse	GGAGGAGGACACCTGCGAGAAGGTAAATGGAAGAAAATTGGGAAGTC GGTGGTCACCTGCGAGTCTAGATCATCAGAGCCAGTCACCATTGCCG

Table 2. Mutagenesis primer design for ACR4 autophosphorylation site point mutants.

Subdomain	Mutation	Primer Sequence (5' → 3')
JMD	S475A	CAAGGTCTTCTAAAGATGCAGCCTTTACGAAAGAT
JMD	T478A	CTAAAGATTCAGCCTTTGCGAAAGATAATGGCAAAATCCG
KD	T501A	GAAGGGCTAGAGTTTTCGCTTATGAGGAACTTG
KD	S516A	GGATTCAAAGAAGAAGCAATAGTGGGGAAAGGG
KD	S522A	ATAGTGGGGAAAGGGGCTTTCTCATGTGTGTACAA
KD	T535A	GTACTGAGAGATGGAGCCACTGTTGCAGTGAAG
KD	T536A	CTGAGAGATGGAACCGCTGTTGCAGTGAAGAG
KD	S552A	GACAAACAGAAGAATGCAAATGAGTTTCGCACG
KD	T557A	AATGAGTTTCGCGCGGAGCTTGATCTGTTA
KD	S563A	GAGCTTGATCTGTTAGCAAGACTCAACCATGCTC
KD	S644A	CACCGGGATATTAAAGCATCAAACATTCTTATAGATG
KD	S645A	CCGGGATATTAAATCAGCAAACATTCTTATAGATGAAG
CTD	T831A	TCTGGTTCCGAGAACGCGGAATTCAGAGG
CTD	S837A	GAATTCAGAGGCGGAGCATGGATAACATTCC
CTD	S875A	GAATTCAGAGGCGGAGCATGGATAACATTCC
CTD	S888A	CCAGCTTCTCCTGGACAGGCCTTGTTCTTGCATCAT

Table 3. Protein recovery at each step of the protein purification scheme as outlined in Materials & Methods.

Protein	Crude Lysate Total Protein (mg)[a]	Crude Lysate SUMO Fusion (mg)[b]	Crude Lysate % SUMO Fusion	Ni-NTA Total Protein (mg)[a]	Ni-NTA SUMO Fusion (mg)[b]	Ni-NTA % SUMO Fusion	% Yield
SUMO:ACR4	13.00	0.83	6	0.51	0.50	98	60.2
SUMO:CRR1	15.05	0.57	4	0.48	0.47	99	83.3
SUMO:CRR2	18.25	2.02	11	1.63	1.61	99	79.7
SUMO:CRR3	15.15	2.37	16	1.99	1.94	97	81.7
SUMO:CRK1	19.35	2.36	12	1.84	1.81	98	76.7
SUMO:ALE2	21.45	2.83	13	2.60	2.41	93	85.4

[a] Protein amounts were estimated using the Bradford assay

[b] Densitometric analysis of SDS-PAGE gels using Image J 1.45b software as described in Materials & Methods.

Figures

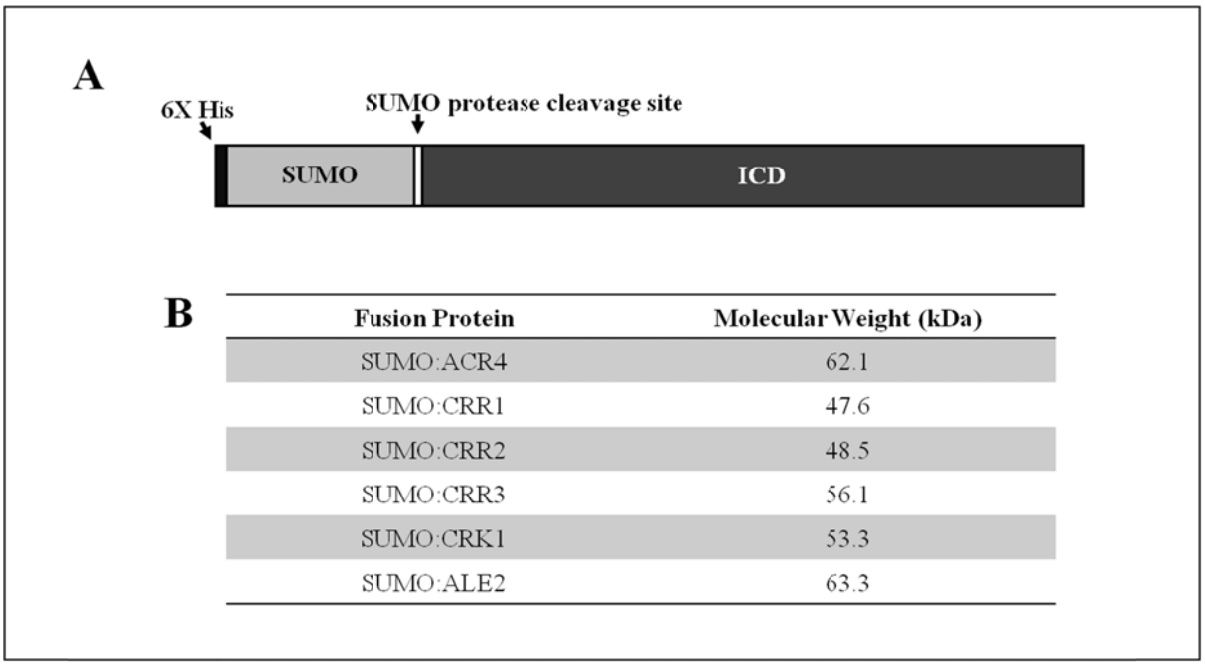

B

Fusion Protein	Molecular Weight (kDa)
SUMO:ACR4	62.1
SUMO:CRR1	47.6
SUMO:CRR2	48.5
SUMO:CRR3	56.1
SUMO:CRK1	53.3
SUMO:ALE2	63.3

Figure 1. Fusion protein design. (A) Diagram of SUMO fusion protein design containing an N-terminal His_6 tag followed by the yeast SUMO protein and the ICD. (B) Table of the molecular weights of each SUMO fusion protein. Molecular weights were estimated from the primary amino acid sequence in the Vector NTI software, v11.0.

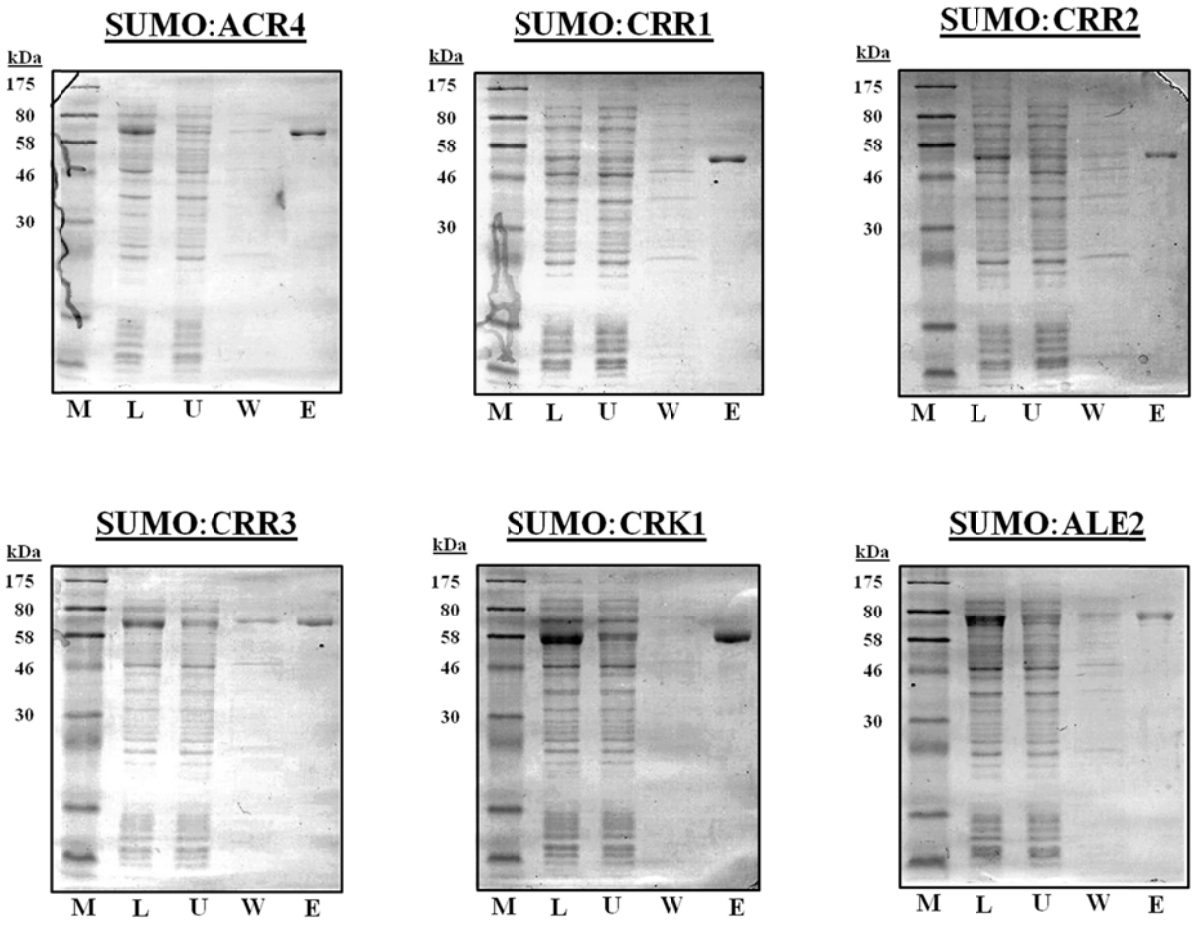

Figure 2. Purification of SUMO-fused proteins as analyzed by SDS-PAGE. Each protein was purified by a one step protocol using Ni-NTA. (M): Molecular weight marker; (L): Soluble *E. coli* lysate; (U) Unbound proteins after incubation with Ni-NTA; (W) Proteins removed by washing step; (E) Eluted fraction, purified SUMO fused protein, indicated by an arrow. Protein loaded in Lane E represents ~1 μg of fusion protein.

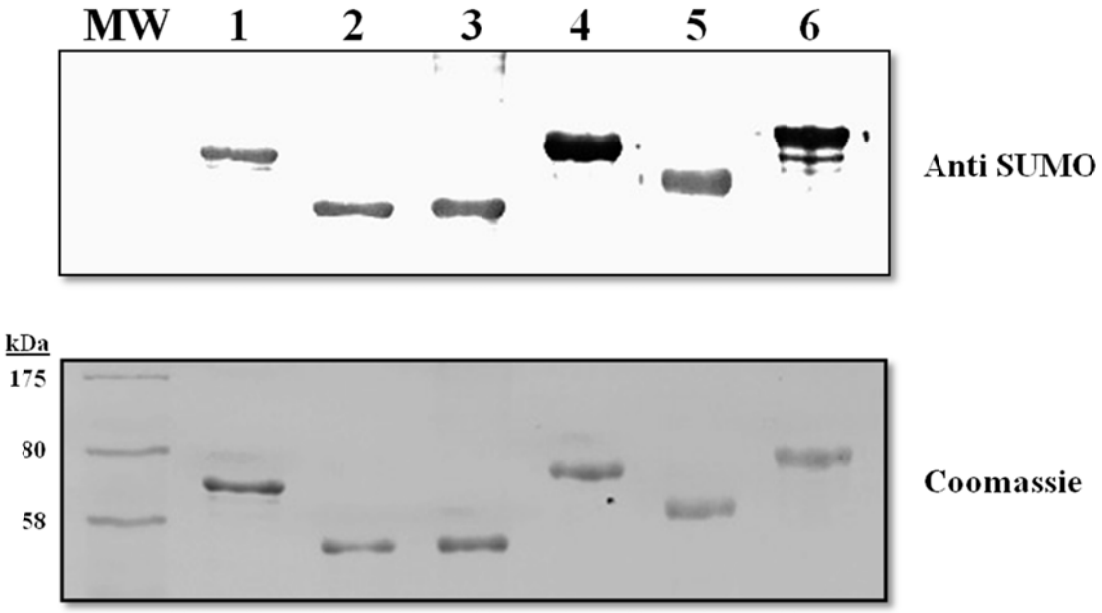

Figure 3. Analysis of SUMO fusion proteins by western blot. Approximately 1 μg of each purified protein was blotted to PVDF membrane and probed with antibody to the SUMO tag. Colorimetric detection was performed with anti-rabbit IgG conjugated with alkaline phosphatase and a colorimetric substrate kit (Bio-Rad). *Upper panel*: western blot of SUMO fusions, *lower panel*: the corresponding Coomassie stained gel. *Lane* MW, molecular weight markers, *lane 1*, SUMO:ACR4; *lane 2*, SUMO:CRR1; *lane 3*, SUMO:CRR2; *lane 4*, SUMO:CRR3; *lane 5*, SUMO:CRK1; *lane 6*, SUMO:ALE2.

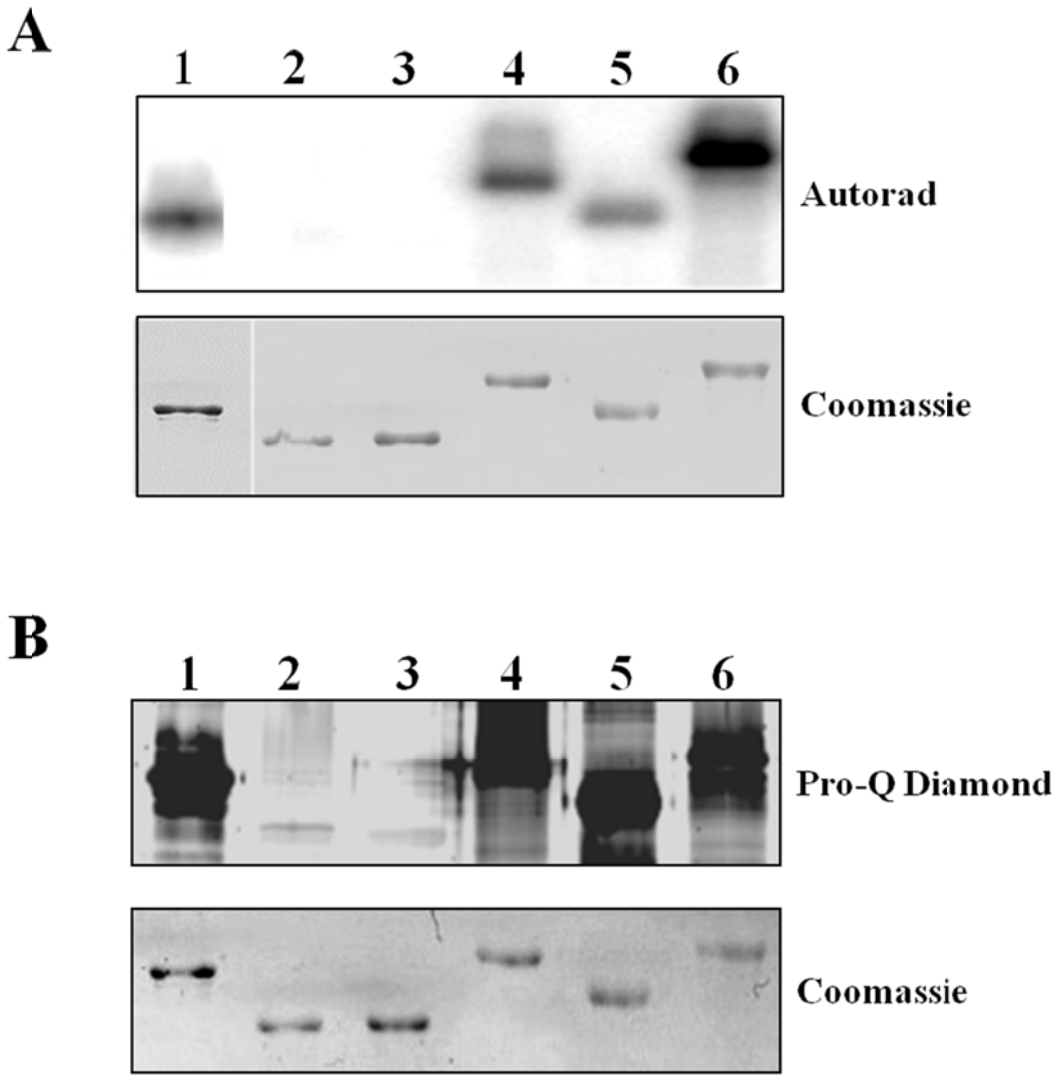

Figure 4. Analysis of kinase activity. (A) To determine kinase activity, proteins were subjected to an *in vitro* autophophosphorylation assay. ~1μg of each protein was incubated in kinase buffer in the presence of γ-^{32}P ATP. Reactions were allowed to proceed for 1h at room temperature, then terminated with the addition of SDS sample buffer and boiled. Proteins were resolved by 12% SDS-PAGE (lower panel) and analyzed by phosphorimaging (upper panel). *Lane 1,* SUMO:ACR4; *lane 2,* SUMO:CRR1; *lane 3*, SUMO:CRR2; *lane 4,* SUMO:CRR3; *lane 5, S*UMO:CRK1; *lane 6,* SUMO:ALE2. (B) Autophosphorylation activity determine by Pro-Q Diamond staining. ~1 μg of the autophosphorylated proteins was resolved by 12% SDS-PAGE and stained with Pro-Q Diamond fluorescent stain. Fluorescence was analyzed on a Typhoon 9400 scanner with an excitation of 532 nm and detected emission at 580 nm. *Upper panel:* Pro-Q Diamond staining of autophosphorylated proteins. *Lower panel:* Coomassie Blue stained gel to demonstrate protein loading.

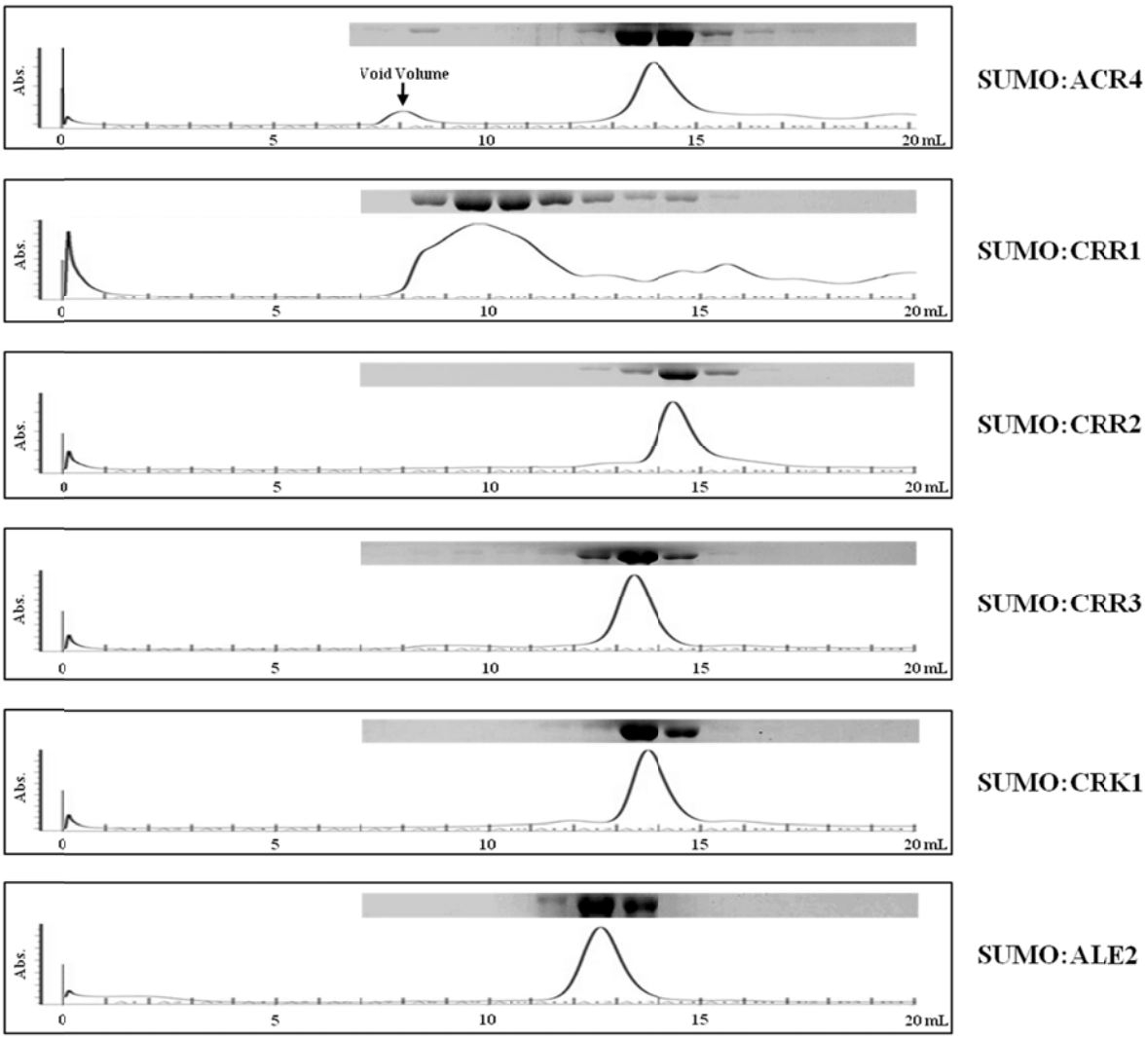

Figure 5. Gel filtration analysis of SUMO fusion proteins on a Sephadex G200 column. Purified proteins were diluted to a concentration of 5 μM in 500 μl of Column Buffer. Proteins were eluted at a flow rate of 0.5 ml/min and 1 ml fractions were collected from the peak volumes indicated. All of the proteins were predominantly monomeric *except* for SUMO:CRR1 which existed mostly as soluble aggregates. *Insets:* Fractions were TCA precipitated and proteins were subsequently resolved by 12% SDS-PAGE and stained with Coomassie Blue stain.

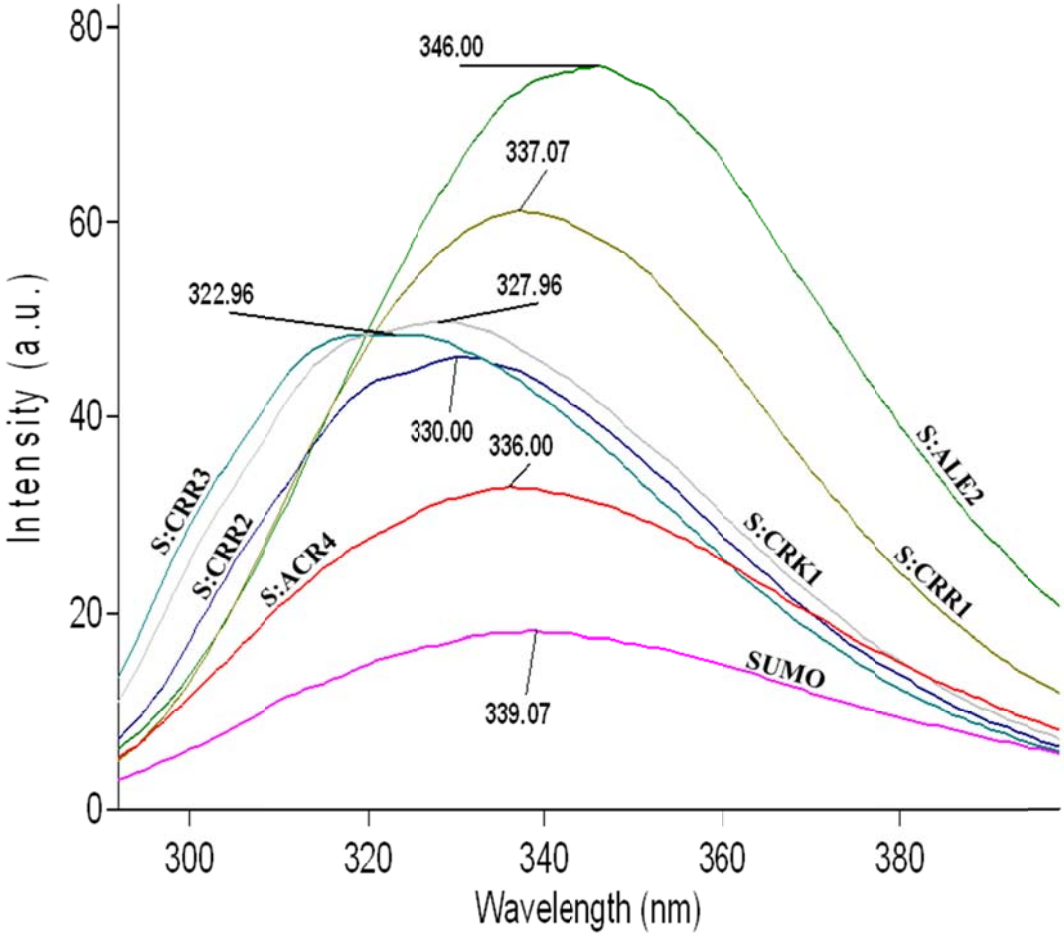

Figure 6. Intrinsic fluorescence spectra of the SUMO fusion proteins. The purified proteins were dialyzed overnight in 10mM Tris, pH 7.4, 0.1 mM TCEP and adjusted to an A_{280} of 0.1. Measurements were made in a 1cm cuvette at room temperature with a Cary Eclipse spectrophotometer (Varian) at an excitation wavelength of 280 nm with an emission scan range of 290-400 nm. The λ_{max} of emission for each protein is also shown and the inset table indicates the number of Trp and Tyr residues.

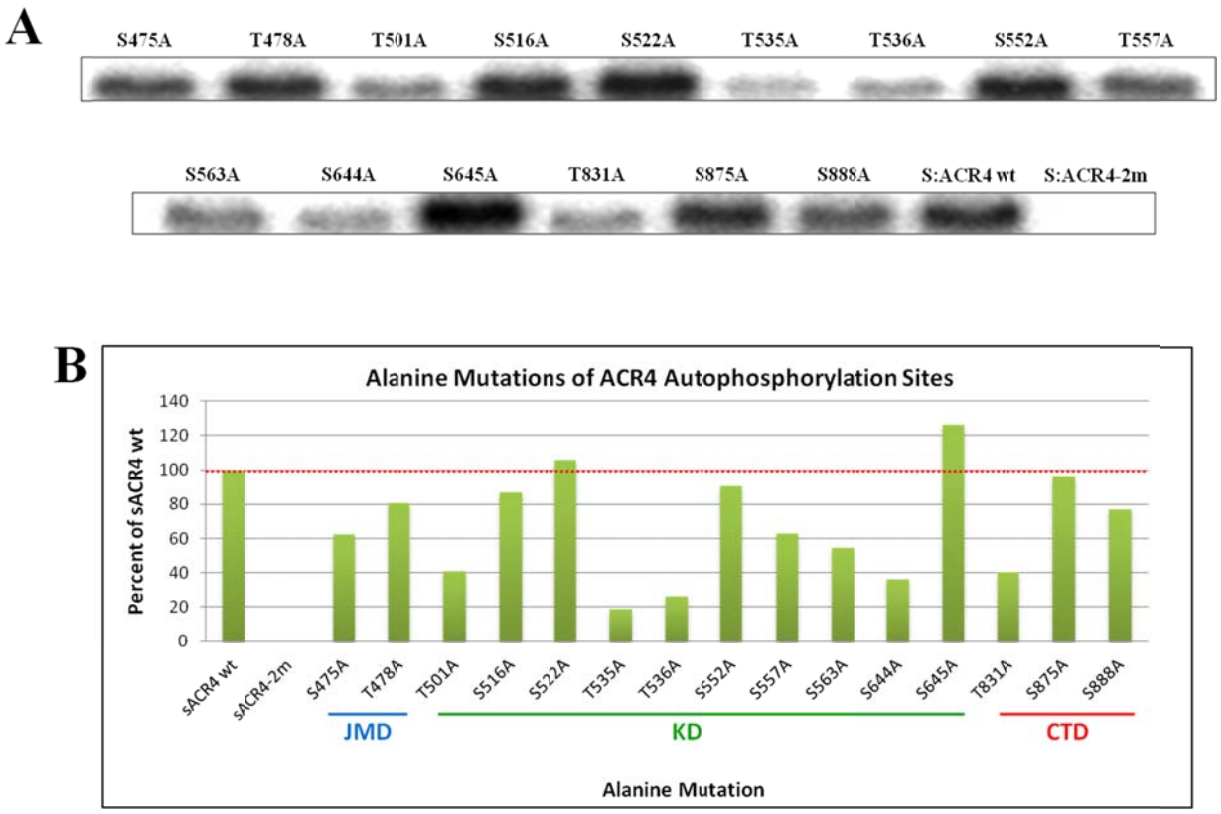

Figure 7. Effect of mutations on ACR4 autophosphorylation. (A) Alanine scanning mutagenesis was performed on the ACR4 autophosphorylation sites. To determine autophosphorylation activity, proteins were subjected to an *in vitro* autophophosphorylation assay. 1µg of each protein was incubated in kinase buffer in the presence of [γ-^{32}P] ATP. Reactions were allowed to proceed for 1 h at room temperature, then terminated with the addition of SDS sample buffer and boiled. Proteins were resolved by 12% SDS-PAGE and activity was monitored by phosphorimaging. (B) Plot of density *versus* point mutation. Densities are represented as a percent of sACR4 wild-type. Densities of the bands in the autoradiogram were quantified with the UN-Scan-It software v6.1.

CHAPTER 4. EVIDENCE FOR AN INTRAMOLECULAR INTERACTION BETWEEN THE JUXTAMEMBRANE AND KINASE SUBDOMAINS IN ACR4 AND IMPLICATIONS FOR REGULATION OF KINASE ACTIVITY

A paper to be submitted for publication.

M.R. Meyer, S. Shah, and A.G. Rao

Abstract

Arabidopsis CRINKLY4 (ACR4) is a receptor-like kinase required for the proper development of both aerial and underground organs of the plant. Loss of ACR4 function results in epidermal defects in the leaves and reproductive tissues and is necessary for stem cell differentiation in the root apical meristem. ACR4 is a Type 1 membrane protein and has architecture analogous to receptor tyrosine kinases (RTK). ACR4 includes an extracellular ligand binding domain, a transmembrane helix, and an intracellular kinase domain. The intracellular domain contains the juxtamembrane domain (JMD) and the C-terminal domain (CTD) subdomains, which flank the core kinase domain (KD). While the salient *in vitro* biochemical properties of the ACR4 intracellular domain have been previously described, the role of the flanking JMD and CTD in the structure and function of the kinase domain remains to be ascertained. In this study, we provide evidence for an intramolecular interaction between the ACR4 JMD and the amino-terminal region of the KD and its potential role in the regulation of kinase activity. We demonstrate that peptides derived from the JMD region can repress kinase activity of the KD in the unphosphorylated state. Importantly, the peptides are able to bind to ACR4 *in vitro*. To gain further insight into the nature of this interaction, we screened the unphosphorylated and phosphorylated JMD peptides against a combinatorial

peptide library expressed on M13 phage pIII coat protein and have identified the sequence LLSLL in the N-terminal region of the KD as preferred interaction motif for the phosphorylated peptide. Furthermore, we also show through kinetic analyses of JMD mutants that autophosphorylated JMD may be important for efficient substrate phosphorylation.

Abbreviations

ACR4, *Arabidopsis* CRINKLY4; ATP, adenosine triphosphate; BRI1, Brassinosteroid insensitive 1; CR4, maize CRINKLY4; CD, circular dichroism; AtCRR, *Arabidopsis* CRINKLY4 related; CTD, carboxy-terminal domain; DTT, dithiothreitol; EGFR, epidermal growth factor receptor; ICD, intracellular domain; KC, kinase + carboxy terminal domain; JM, juxtamembrane; KD, kinase domain; MyBP, myelin basic protein; NusA, N-utilization substance A; PDGF, platelet derived growth factor; RLK, receptor-like kinase; RTK, receptor tyrosine kinase; SERK, somatic embryogenesis receptor-like kinase; TCEP, Tris (2-carboxyethyl) phosphine hydrochloride; UV, ultraviolet; WOX5, WUSCHEL RELATED HOMEOBOX 5; PBS, phosphate buffered saline; pNPP, p-nitrophenyl phosphate.

Introduction

Higher organisms are required to maintain a controlled equilibrium between cell proliferation and differentiation throughout their growth and development. Failure to retain this balance results in developmental problems which leads to increased disease states and decreased survival. Organisms make use of cell-surface receptors to detect external or internal signals that impact cellular function. Mammalian systems have acquired signal transduction mechanisms via the use of receptor tyrosine kinases (RTK) to regulate cellular processes such as proliferation, migration, differentiation, and cell-cycle control (1). RTKs consist of an extracellular ligand binding domain, a single transmembrane helix, and an intracellular tyrosine kinase domain. The general paradigm of RTK activation entails ligand binding to the extracellular domain of the receptor, followed by receptor oligomerization, and activation of the kinase domains via *trans* phosphorylation (2, 3). Activation of the intracellular kinase domain of the receptor initiates a signal transduction cascade involving cytoplasmic components that eventually regulate gene transcription in the nucleus (1, 4). Importantly, structural, biochemical and biophysical studies of a variety of RTKs have revealed the effects of phosphorylation and the regulatory role of non-catalytic domains such as the JMD and the CTD on kinase activity and function (5-13).

The CRINKLY4 (CR4) gene was first identified in maize and encodes a receptor-like kinase (RLK) that is involved in the proper specification of epidermal tissues in the leaves and the aleurone of the kernel (14). Architectural features of the RLK include an extracellular domain containing seven repeating regions, termed ‘Crinkly’ repeats, and three cysteine-rich repeats similar to the extracellular motifs found in the tumor necrosis factor receptor, a membrane spanning region, and an intracellular serine/threonine kinase domain

(14, 15). An ortholog to CR4 has been identified in *Arabidopsis* that retains all of the features of maize CR4 (16), including a functional serine/threonine kinase domain (17-19). The *Arabidopsis* genome encodes four homologs to ACR4, termed *Arabidopsis* CRINKLY4-Related proteins (AtCRRs), which contain sequence similarity and architectural features analogous to ACR4 (19). Genetic and biological studies have characterized the functional properties of ACR4 in some detail. ACR4 primarily effects epidermal formation in the leaves and reproductive tissues of the plant, similar to CR4 function (16-18). Furthermore, ACR4 has been demonstrated to affect root growth and morphology. Examination of developing roots has shown that ACR4 is required for proper columella stem cell differentiation in the root apical meristem and is essential for proper lateral root formation (20, 21). ACR4 mutant plants lacking ACR4 function show increased numbers of columella stem cells in the root tip. A signaling module has been suggested involving a postulated peptide ligand, CLE40, the ACR4 RLK, and the WOX5 transcription factor that engage in a possible feedback mechanism controlling stem cell differentiation (21, 22). Molecular biology investigations have revealed that ACR4 requires the extracellular 'Crinkly' repeat domain for receptor function (23). However, the importance of the active, intracellular kinase domain is being debated (18, 23). Biochemical studies involving the transmembrane domains (TMD) of CR4, ACR4, and the AtCRRs demonstrate their ability to homodimerize and that residues within the TMDs of ACR4 and CR4 can significantly influence dimer propensity (24, 25). However, biochemical knowledge regarding the mechanisms of receptor activation and intracellular KD activation and regulation is needed in order to fully understand receptor function.

We have recently reported on some salient *in vitro* biochemical properties of the ACR4 intracellular domain including its kinase activity and identification of 16 autophosphorylation sites encompassing the JMD, KD, CTD (26). In RTKs, the importance of the JM region in the regulation of kinase function is well documented (5, 9). However, the role of the JMD in regulating ACR4 kinase activity is unclear. To this end, we have undertaken this *in vitro* study to delineate the contribution of the JMD in ACR4 kinase activity and establish the ground for more detailed characterization. Thus, we provide evidence for an intramolecular interaction between the ACR4 JMD and KD and its potential role in the regulation of kinase activity. We demonstrate that peptides derived from the JMD region can repress kinase activity of the KD in the unphosphorylated state. Importantly, the JMD peptides are able to bind to ACR4 *in vitro*. To gain further insight into the nature of this interaction, we screened the unphosphorylated and phosphorylated JMD peptides against a combinatorial peptide library expressed on M13 phage pIII coat protein and have identified the sequence LLSLL in the N-terminal region of the KD as preferred interaction motif for the phosphorylated peptide. Furthermore, we also show through kinetic analyses of JMD mutants that prior autophosphorylation of the JMD may contribute to more efficient substrate phosphorylation of myelin basic protein.

Materials and Methods

Protein Mutagenesis

The SUMO fused ACR4 intracellular domain (sACR4) was prepared as previously described (Chapter 2). The sACR4 KC protein which lacks the intracellular juxtamembrane domain, residues 456-483 (26), was cloned into the pE-SUMO vector (Life Sensors) using

the forward primer 5'-GGTGGTGAAGACTTAGGTATCCGTCCGGATCTTGATG-3' and the reverse primer 5'-GGTGGTTCTAGATCATGCAAGCGCTCGTTCCAAT-3' containing a BbsI and a XbaI site, respectively. Standard cloning procedures were followed according to the instruction manual that was provided with the vector. The resulting construct was verified by sequencing to ensure protein was in frame and no mutations had occurred.

To generate the JMD mutant proteins, the vector encoding the SUMO-tagged ACR4 intracellular domain was mutagenized using the QuickChange Lightning Multi Site-Directed Mutagenesis Kit (Stratagene). Sequential mutagenesis was required to produce the JMD double alanine (JMD-2A) and double aspartate (JMD-2D) mutants. To generate the JMD-2A mutant, first S475 was mutated to alanine using the S475A primer, 5'-CAAGGTCTTCTAAAGATGCAGCCTTTACGAAAGAT-3'. The mutation was verified by sequencing and the resulting vector was subjected to a second round of mutagenesis using the T478A primer, 5'-CTAAAGATGCAGCCTTTGCGAAAGATAATGGCAAAATCCG-3'. The double alanine mutant vector was verified by sequencing. The JMD-2D was produced using the same method using the S475D primer, 5'-GATACAAGGTCTTCTAAAGATGACGCCTTTACGAAAGATAATGGC-3', followed by the T478D primer, 5'-CTTCTAAAGATTCAGCCTTTGACAAAGATAATGGCAAAATCCGTC-3'. Sequencing verified the correct mutations.

Protein expression and purification

Vectors encoding the SUMO fused kinase domains of ACR4 were transformed into Rosetta2 (DE3) pLysS (Novagen) cells and plated on Kanamycin plates. Luria Broth cultures supplemented with 50 μg/ml Kanamycin were initiated by standard procedures.

Cultures were grown with shaking at 37 °C for ~3 h until an OD_{600} = 0.6-0.8 was reached. The temperature was reduced to 20 °C and cultures were induced with 1 mM IPTG. The cultures were incubated for 5 h, harvested by centrifugation, and stored at -80 °C until needed. To purify the SUMO fused proteins, frozen pellets from 250 ml cultures were thawed on ice and resuspended in 10 ml Lysis Buffer (50 mM Tris-HCl pH7.4, 150 mM NaCl, 40 mM imidazole, 0.1% Triton X-100, 1 mM DTT, and 1 mM AEBSF). Cells were lysed by sonication on ice and the resulting lysate was centrifuged at 13,200 rpm for 15 min at 4°C. Supernatants were then transferred to a 10 ml column containing 250 µl of Ni-NTA Superflow resin (Qiagen) equilibrated with Lysis Buffer. The resin/lysate mixture was incubated on a rocker at 4°C for 1 h. After incubation, the unbound proteins were allowed to flow through the column. The resin was washed with 10 ml of Wash Buffer (50 mM Tris-HCl pH7.4, 150 mM NaCl, 50 mM imidazole, 1 mM DTT). Bound proteins were eluted into individual microfuge tubes with three successive 250 µl aliquots of Elution Buffer (50 mM Bis-Tris pH7.2, 50 mM NaCl, 150 mM imidazole, 1 mM DTT) on ice. Protein quantities were determined by the Bradford method.

Autophosphorylation time course assays

Autophosphorylation time course assays were performed to determine the effect of mutations in the JMD on sACR4 autophosphorylation. First, 300 µl reaction volumes of Kinase Buffer (20 mM Bis-Tris pH 7.2, 25 mM NaCl, 5 mM $MnCl_2$, 1 mM DTT, 25 µM ATP) supplemented with 30 µCi of [γ-^{32}P] ATP (Perkin Elmer, 6,000 Ci/mmol) were prepared. Subsequnetly, reactions were initiated with the appropriate enzyme to a final concentration of 1 µg/20 µl of reaction. 20 µl aliquots were taken at the time points indicated

and terminated with the addition of 4X SDS Laemmli buffer and boiled. Proteins were separated by 12% SDS-PAGE and gels were analyzed by phosphorimaging.

Peptide synthesis

The JMD peptides and the carboxy-terminal domain peptides (CTD) were chemically synthesized (Genscript) with a biotin tag at the amino terminus (Table 1).

Peptide inhibition assays

Inhibition of sACR4 kinase activity was assessed by incubating 20 μl reaction volume of Kinase Buffer containing 2 μCi [γ-^{32}P] ATP, 1 μg of sACR4 KC, and increasing concentrations of JMD1 peptide (0-200 μM) for 20 min at room temperature. Reactions were initiated with the enzyme followed by incubation at room temperature for 30 min before terminating the reaction by the addition of 4X Laemmli buffer and boiling. Proteins were separated by 12% SDS-PAGE and resulting gels were analyzed by phosphorimaging.

Substrate phosphorylation assays

Phosphorylation of MyBP by ACR4 (26) was assessed with or without prior autophosphorylation. 240 μl reactions were set up as described above containing 12 μg of sACR4, 24 μg of MyBP, and 24 μCi of [γ-^{32}P] ATP. For the reaction requiring autophosphorylation of the kinase, the reaction was set up without [γ-^{32}P] ATP and MyBP, initiated with the kinase, and incubated at room temperature for 1 h. After autophosphorylation, the reaction was spiked with the [γ-^{32}P] ATP and MyBP. For the experiment with no prior autophosphorylation, all reaction components were mixed and the reaction was initiated with the addition of the enzyme. 20 μl aliquots were taken at the indicated time points, stopped and processed as described above. Densities of the protein

bands from the autoradiogram were quantified using the UN-Scan-It v6.1 software (Silk Scientific, Inc.) and plots of density versus time were generated.

In order to determine if the JMD affects substrate phosphorylation, sACR4 wild-type and JMD mutant proteins were incubated with increasing concentrations of MyBP. A series of 20 µl reactions were prepared with Kinase Buffer containing 0.5 µg (0.3 µM) of kinase, 2 µCi of [γ-^{32}P] ATP, and MyBP (0.7-54.3 µM). Reactions were initiated with the addition of the enzyme and incubated at room temperature for 15 min. Reactions were terminated with the addition of 4X SDS Laemmli buffer and boiled. Proteins were separated by 12% SDS-PAGE and resulting gels bands were stained with Coomassie blue. Protein bands corresponding to MyBP were excised from the gel and radioactive counts quantified by liquid scintillation counting. Phosphate incorporation was calculated using a [γ-^{32}P] ATP standard curve and the radioactive counts. Kinetic analysis was performed as described (26).

Phage peptide library construction

The phagemid vector pCANTAB 5E (GE healthcare) was used to construct a random 21-amino acid library fused to the pIII coat protein (Rao laboratory, unpublished data). Briefly, two oligonucleotide primers were first synthesized (Integrated DNA Technologies). The forward primer 5'-CGTGGT**GGCCCAGCCGGCC**$(NNK)_{21}$**GCGGCCGC**AGCACGACAG-3' contained the degenerate codon NNK encoding all 20 amino acids and the TAG stop codon. The oligonucleotide also incorporated *Sfi*1 and *Not*1 restriction enzyme sites at the 5' and 3' ends respectively. A complementary reverse primer 5'-CTGTCGTGCTGCGGCCGC-3' was used for double-strand synthesis, followed by digestion with Sfi1/Not1 and ligation into the similarly digested phagemid vector. Multiple transformations of highly electro-competent

(competency > $1.0x10^{10}$) SS320 *E. coli* cells and phage preparation resulted in a phage-peptide library with a diversity of ~ $1x10^{9}$. The library was validated by first screening against the anti-FLAG monoclonal antibody that recognizes the sequence epitope DYKDDDDK. Four rounds of screening against the antibody yielded >95% clones containing the core sequence DYKxxD

Phage peptide library screening of JMD1 peptides

Biotinylated peptides were immobilized on 20 µl of streptavidin coated beads (Dynabeads® MyOne™ Streptavidin T1, Invitrogen) and dispersed in 100 µl of phosphate buffer saline pH, 7.4 (PBS) at room temperature with gentle rotation for 45 mins. The beads were washed three times with PBS containing 0.1 % BSA. Peptide coated beads were blocked with PBS containing 0.1 % BSA for 30 mins followed by 2 washes with PBS containing 0.1 % BSA. Beads were then incubated with phage (100 µl diluted in 900 µl of PBS containing 0.1 % BSA) for 3 h at room temperature with gentle rotation. The unbound phage was washed 3 times with PBS and then the beads were transferred into fresh eppendorf tubes. The bound phage was eluted by incubating with 500 µl of 0.1 M HCl for 5 mins at room temperature with the aid of shaking. The eluted phage was immediately neutralized by the addition of 167 µl of 1M Tris-HCl buffer pH 8.0, followed by infection of XL1-Blue cells (grown to < 0.6 OD in 10 µg/ml tetracycline) with the phage. Infected XL1-Blue cells were incubated at 37 °C for 20 mins followed by addition of helper phage and again incubating at 37 °C for 30 mins. The phage infected XL1-Blue cells were transferred into a conical flask containing 50 ml of 2YT media containing 10 µg/ml of tetracycline and 100 µg/ml ampicillin and was further incubated at 37 °C overnight with shaking at 210 rpm.

Phage preparation was carried out by centrifuging the overnight culture at 8000 rpm for 10 mins. The supernatant was collected into another centrifuge tube and the phage was precipitated by adding 12.5 ml of 20 % PEG 8000 and 2.5 M NaCl solution at room temperature. The precipitated phage were collected by centrifugation at 12,000 rpm for 20 mins and diluted with 1 ml of PBS. This was the first round of enriched phage. The entire process was repeated for four rounds and for each subsequent round of biopanning, enriched phage from previous round was used. During the 3rd and 4th round of panning, the wash buffer contained 0.01 % Tween 20. Following 3rd and 4th round panning, phage infected XL1-Blue cells were grown on 2YT ampicillin plates and 50 colonies were characterized by DNA sequencing after plasmid preparation.

Phage ELISA for binding specificity

For phage ELISAs, streptavidin coated plates were washed three times with PBS containing 0.05 % Tween 20 (PBST). Juxtamembrane peptides (10ug/ml in PBS) were immobilized on streptavidin coated plate by incubating 100 µl of peptide per well at room temperature for 1 h. Plate was washed two times with PBST followed by blocking with PBST containing 0.1 % BSA for 1 h. The plate was then washed three times with PBST followed by incubation with the appropriate phage-peptide (pd-LHSLL phage, pd-AHALA phage) and helper phage for 2 h at room temperature with gentle shaking. Then the plate was washed three times with PBST followed by incubation with anti-M13 HRP conjugated antibody for 1h. Again the plate was washed four times with PBST. The bound phage in each well was detected by incubating with 50 µl of substrate solution (0.01 % hydrogen peroxide + 0.8 mg/ml o-Phenylenediamine dihydrochoride) for ~10 min. Reactions were terminated

by the addition of 50 µl of 3 M HCl and measuring the absorbance of the developed yellow color at 405 nm. In the case of ACR4 kinase peptide derived phage (acr4-LLSLL and acr4-ALALA), all the washing steps before phage binding were performed using TBS containing 0.05 % Tween 20 and thereafter only with TBS.

Peptide overlay assays

The JMD1 peptides were diluted in 2.5 mM in Tris-HCl buffer, pH 8.0. To demonstrate peptide binding to sACR4 KC protein, 2 µg of sACR4 KC and 2 µg of SUMO protein were separated by 12% SDS-PAGE and blotted to nitrocellulose membrane. Blots were briefly stained with a 0.1% Ponceau S solution to locate the protein bands. Bands were then cut from the blot, appropriately labeled, then destained in successive washes with distilled water and a final wash in 1X TBS (50 mM Tris-HCl pH 7.4, 150 mM NaCl) to remove Ponceau S staining. Blots were then blocked with 5% milk protein in TBS + 0.1% Tween 20 for 1 h. After blocking, blots were washed three times with TBS + 0.1% Tween 20, 5 min each wash. They were then placed in individual microfuge tubes containing 1 ml of TBS, followed by addition of the appropriate peptide to a final concentration of 100 µM. To demonstrate specific binding to ACR4, peptides were also incubated with SUMO protein as a control. Blots were incubated on a rotating platform for 2 h at room temperature, followed by two washes with 1.5 ml of TBS at 5 min intervals. To detect peptide binding, 1 ml of TBS containing 1:500 streptavidin conjugated Alkaline Phosphatase (AP) (Pierce) was added to each tube. Blots were incubated on a rotator for 1 h at room temperature, washed as described above to remove excess streptavidin-AP followed by colorimetric detection of peptide binding using the AP Substrate kit (Bio-Rad). The presence of sACR4 and SUMO proteins were confirmed in separate blots probed with anti-SUMO primary antibody

(Rockland Immunochemicals, 1:1000) and polyclonal anti-rabbit secondary antibody (Sigma, 1:15,000).

Peptide binding assays

The binding of JMD1 peptides to sKC protein was demonstrated as follows. First, a 96 well nickel coated plate (XpressBio) was washed three times with TBS + 0.1% Tween 20. A 0.8 μM solution of sKC (5 μg/100 μl) or SUMO protein (1 μg/100 μl) was prepared in TBS + 0.1% Tween 20. 100 μl of appropriate protein solution was added to individual wells and incubated on an orbital shaker for 1 h at room temperature to allow protein to bind to the plate through the His tag. Wells containing immobilized sKC or SUMO protein were washed three times with TBS + 0.1% Tween 20 to remove unbound material. JMD1 peptide solutions were prepared in TBS to a final concentration of 200 μM. 50 μl of the peptide solutions were added to appropriate wells and allowed to incubate on an orbital shaker for 2 h at room temperature. After incubation, excess peptide solution in the wells was discarded. Wells were then washed with TBS two times with gentle shaking to remove unbound peptides. 50 μl of a streptavidin-AP solution (1:500) was added to each well and incubated on an orbital shaker for 1 h at room temperature. Streptavidin-AP solution was discarded and the wells were washed twice with TBS using gentle shaking. Colorimetric detection of peptide binding was initiated by adding 100 μl of a p-nitrophenyl phosphate (pNPP) solution (100 mM ethanolamine pH 9.8, 10 mM pNPP) to each well. The reactions were allowed to incubate for 5 min with occasional manual shaking. Reactions were terminated with the addition of 50 μl of 2N NaOH to each well. 100 μl of each reaction was diluted with 400 μl of water and absorbance at 405 nm measured. Data were generated by accounting for the dilution factor and subtracting the absorbance of the control (SUMO) wells from the

experimental (sACR4 KC) wells. Each peptide binding experiment was performed in triplicate.

CD analysis of JMD1 peptides

Circular dichroism (CD) analysis of JMD1 peptides was carried out by dissolving the JMD1 peptides in CD Buffer (10 mM Tris pH 7.2, and 0.1 mM TCEP) to a final concentration of 125 μM. For assays involving TFE, peptides were dissolved in CD Buffer containing either 15 or 40 % TFE. Far-UV spectra of each peptide were obtained on a Jasco J-710 spectropolarimeter, in a 0.1 cm path length cuvette with excitation wavelengths ranging from 190-260 nm.

Homology model of ACR4 kinase domain

Homology modeling was used to build the model for the ACR4 kinase domain encompassing the sequence of residues starting from 512 through 785 in the whole receptor. The Discovery Studio v 3.1 (Accelrys, San Diego, USA) was used for homology model construction. Sequence analysis identified Interleukin-1 receptor associated kinase (PDB identification 2NRU_B) as the optimal template based on 50% homology and 34% identity in the amino acid sequence. The protein model was generated by MODELER, which was originally developed by Sali (27) and the refined model was validated using the Verify Protein (Profiles-3D) protocol, which assesses the compatibility of the 3D structure of the protein model with its amino acid sequence.

Results

Effect of the JMD on ACR4 autophosphorylation

We have previously reported on the autophosphorylation activity of ACR4 kinase domain, its mechanism and the identification of 16 autophosphorylation sites, including two sites, Ser^{475} and Thr^{478}, in the JM region (26). Protein kinases are often regulated by *cis*-acting elements outside the catalytic domain i.e. the juxtamembrane domain and the carboxy terminal domain (8, 28-30). Therefore, to determine if the JM region and the two autophosphorylation sites within are important for kinase activity an autophosphorylation time course experiment was carried out using the sACR4 wt, sACR4 KC (missing the JM) and sACR4 JMD mutants in which both Ser^{475} and Thr^{478} were replaced with Ala (sACR4 JMD-2A) or Asp, a phosphomimetic residue (sACR4 JMD-2D) (Fig. 1A). All proteins were prepared as described in Materials & Methods and assayed as previously described (26). It is evident from the autoradiograms (Fig. 1B) that there is no difference in the time course of autophosphorylation activity between the wild type and mutant proteins, suggesting that the JMD has little effect on kinase autophosphorylation.

We therefore decided to test whether the addition of exogenous peptides from the JMD could act in *trans* to either repress or enhance the kinase activity of sACR4 KC. Thus, four different 15mer peptides corresponding to residues 468-482 of the ACR4 primary amino acid sequence were generated. The wild type peptide, JMD1, contains the unmodified Ser^{475} and Thr^{478} residues. In the mutant peptide JMD1m, both sites of autophosphorylation have been replaced with Ala. In the peptide pJMD1 Ser^{475} is phosphorylated and in ppJMD1 both Ser^{475} and Thr^{478} are phosphorylated (Fig. 2A). Our results (Fig. 2B) indicate that when sACR4 KC is incubated with increasing concentrations of these peptides (0-200 μM), the

singly (pJMD1) and doubly (ppJMD1) phosphorylated derivatives have only slight inhibitory effects (~10% decrease) on autophosphorylation even at the highest concentration (Fig. 2A and B). On the other hand, the JMD1 reduced sACR4 KC autophosphorylation efficiency ~20% when incubated at the highest concentration of 200 μM and, interestingly, the mutant peptide JMD1m, was able to inhibit kinase activity by as much as 40% at a concentration of 200 μM (Fig. 2A and B). These results indicate that the JMD of ACR4 may contribute to the regulation of kinase activity although, given that full inactivation of the kinase was not observed, other regions of the protein such as the activation loop (26) and the C-terminal domain may play a significant role.

Effect of JMD on substrate phosphorylation

It has been noted in the case of the Brassinosteroid Insensitive1 (BRI1) receptor kinase that mutations in the JM region have little or no effect on autophosphorylation but dramatically affect substrate phosphorylation in vitro (31). We therefore assessed the role of the JMD on ACR4 kinase substrate phosphorylation using the exogenous substrate Myelin Basic Protein (MyBP) as reported previously (26). To this end, we incubated each of the ACR4 JMD mutants with MyBP (0.7-54 μM) and examined the kinetics of substrate phosphorylation. The data, fitted to a Michaelis-Menten equation (using the Enzyme Kinetics Module in SigmaPlot v11.2), showed typical Michaelis-Menten kinetics for all proteins (Fig. 3). The wild-type sACR4 protein kinetics exhibited V_{max} and K_m values of 6.37 ± 0.47 nmol min^{-1} mg^{-1} and 0.68 ± 0.29 μM, respectively (Table 2) whereas the sACR4 JMD-2A mutant showed a dramatic decrease in the efficiency of substrate phosphorylation activity (V_{max} and K_m values of 4.57 ± 0.18 nmol min^{-1} mg^{-1} and 0.92 ± 0.20 μM, respectively), suggesting that autophosphorylation of Ser^{475} and Thr^{478} is required for full

activity against substrate proteins. Support for this comes from the kinetics data for the sACR4 JMD-2D protein in which the two Asp residues may be regarded as mimicking the negatively charged phosphorylated Ser^{475} and Thr^{478} residues in the JMD of ACR4. Clearly, the phosphomimetic derivative is able to restore the efficiency of substrate phosphorylation to wild-type levels (Fig. 3D, Table 2). The sACR4, JMD-2A and 2D mutants have similar binding affinities for MyBP and are comparable to the wild-type enzyme, regardless of the type of mutation present (Table 2). Interestingly, substrate phosphorylation is also significantly enhanced in the absence of the JMD in the sACR4 KC protein (V_{max} = 7.50 ± 0.38 nmol min^{-1} mg^{-1}) although the binding affinity (K_m = 1.98 ± 0.46 μM), which is >2-fold higher than that of sACR4 wt (K_m = 0.68 ± 0.29 μM) suggests that residue(s) within the JMD may play a critical role in binding to substrates. Taken together, these results indicate that autophosphorylation of Ser^{475} and Thr^{478} in the ACR4 JMD may be necessary for optimal substrate phosphorylation *in vitro*. We also examined whether prior autophosphorylation was necessary for efficient substrate phosphorylation. Thus, the time course of MyBP phosphorylation (Fig. 4) shows that the autophosphorylated sACR4 (+AutoP) has a subtle but distinct ability to phosphorylate at an earlier time point (0.5 min) than the protein that is not autophosphorylated (2 min) (-AutoP) suggesting that substrate recognition may be regulated by autophosphorylation.

Phage panning of JMD1 peptides

Structural studies on several receptor tyrosine kinases have established that activation and inhibition of kinase activity is often mediated by the juxtamembrane domain through intramolecular interactions with residues in the active site (9, 32-36). Based on our observation that the unphosphorylated JMD1 peptide inhibits kinase activity, we invoked the

possibility that the JMD in the ACR4 kinase could serve a similar structural role via an intramolecular interaction. Ideally, knowledge of the x-ray or NMR derived three-dimensional structure of ACR4 kinase domain would provide the necessary atomic level detail to unequivocally delineate specificity of interactions within the molecule. However, this is not a trivial exercise. In the absence of structural information, phage display screening of random peptide libraries has become a widely used method to identify peptide ligands, probe structure-function relationships in proteins and map protein-protein interaction sites (37-39). Typically, phage-display screening yield peptides that harbor linear sequences/motifs that have the potential to interact with the target molecule. *A priori*, the probability of finding an *exact* match to the sequence of a binding partner is rather low. Consequently, consensus analysis provides the basis for identifying candidate natural sequences that may interact with the protein.

Thus, we used a random 21-mer phage peptide library to identify potential interaction sites for the JMD1 peptides. The target peptides JMD1 (^{468}DTRSSKDSAFTKDNG^{482}) and the phosphorylated pJMD1 peptide (^{468}DTRSSKDpSAFTKDNG^{482}) were immobilized through their N-terminal biotin tag on streptavidin coated plates and subjected to four rounds of panning as described in Materials & Methods. Phage isolated from the fourth round were enriched in clones harboring peptides with specificity and affinity for the target JMD1 peptides.

In panning against the nonphosphorylated JMD1 peptide, 46 clones were randomly chosen from the 4th round and amino acid sequences of displayed peptides were deduced by DNA sequence analysis. While there was no single dominating sequence, some sequences

were represented multiple times (Fig. 5). Significantly, the majority of the peptides contained the consensus tripeptide motif 'SXL'. There were miscellaneous other sequences.

Fig. 6 shows the amino acid sequences of 46 randomly chosen clones from the 4th round of panning against the phosphorylated peptide, pJMD1. A single dominant sequence, YRWWDSAINLHSLLFSPPLFG, was represented 16 times. Interestingly, this peptide contains the sequence NLHSLLF (and there are three other peptides with a sequence of amino acids that are similar, LLHSNDF, NLSLSYL AND KLHTSPW). The sequence N**L**HS**LL**F harbors the motif LXXLL that is known to be involved in numerous protein-protein interactions in plants and animals, most notably in mammalian nuclear receptor signaling (40-43).

The results of our phage panning experiments highlights the discriminatory power of the method in distinguishing the subtle differences in the binding interactions of JMD1 and pJMD1. Whereas the JMDI appears to have an affinity for sequences containing the SXL motif, the pJMD1 appears to favor the LHSLL sequence. However, the fact that clones containing this sequence are also seen in the panning against JMD1 (Fig. 5) underscores the plasticity in the conformations of JMD1 and pJMD1 that differ only by one phosphorylation. We employed a phage ELISA to confirm the interaction between JMD1, JMD2, their phosphorylated derivatives and the phage displaying the "LHSLL" motif (pd-LHSLL). First, a homogenous population of pd-LHSLL phage particles was generated and tested for binding to JMD1, pJMD1, ppJMD1, JMD2, pJMD2, and the control peptides CTD2 and its phosphorylated form, pCTD2 derived from the C-terminal domain of ACR4 kinase (Table 1). In Figs. 7A and B, it is evident that all of the JMD1 peptides bind to the pd-LHSLL phage, thus reconfirming our phage panning results. Furthermore, pd-LHSLL also bound the JMD2

peptides. This was not entirely surprising, since the JMD1 and JMD2 peptides share overlapping sequences and differ by only three amino acids. The fact that little or no color was produced in the phage ELISA using the control peptides CTD2 and pCTD2 (Fig. 7), is an affirmation of the specificity of the LHSLL motif to the JMD peptides. To further confirm the specificity of interaction between LHSLL and the JMD peptides, we created a mutant motif AHALA in which the first Leu, the middle Ser and the last Leu residues of LHSLL motif were replaced with Ala. Subsequently, a homogenous population of phage particles displaying the mutant peptide sequence YRWWDSAINAHALAFSPPLFG (pd-AHALA) was produced and used in the phage ELISA. Relative binding affinities were reduced ~60-80 % compared to pd-LHSLL phage binding, thus indicating the mutated residues are essential for efficient binding to the JMD1 peptides.

LLSLL motif in ACR4 binds to the ACR4 JMD peptides

As mentioned earlier, consensus peptide sequences identified in phage display experiments can be searched against protein sequence databases to identify natural sequences that represent interaction partners with biological relevance. The predominant peptide (YRWWDSAINLHSLLFSPPLFG) isolated from panning against pJMD1 peptide contains the sequence LHSLL or the LXXLL motif. Searching the *Arabidopsis* protein database with the motif LXXLL, retrieved a number of potential interacting proteins, including ACR4 and two of its homologs AtCRR3 and AtCRK1. Indeed, the sequence LHSLL is almost identical to the sequence LLSLL found within the N-lobe of the ACR4 kinase domain. The similarity in residues on either side of this sequence is even more striking (AINLHSLLFS identified in the phage panning versus HAHLLSLLGY in ACR4). This region in ACR4 is located on the back side of the kinase distal to the active site and comprises part of the β4 strand in the

model structure (Fig.8). Interestingly, it is also worth noting that ACR4 contains a GLSLL sequence comprised of the Gly residue in the conserved DFG motif and the N-terminus of the activation loop (Fig. 8). Crystal structures of the kinase domains of the Eph receptor family have shown that the juxtamembrane region is able to form intramolecular contacts with the kinase N-lobe and activation loop to stabilize the kinase in an inactive conformation (36, 44). Therefore, we considered the intriguing possibility that the JMD of ACR4 may participate in intramolecular interactions involving the LLSLL motif and possibly via the LSLL sequence in the proximity of the activation loop.

To test this hypothesis, we also performed phage ELISAs (Fig. 9A) on immobilized JMD1, JMD2, and CTD2 peptides using a homogeneous population of phage displaying a 15mer peptide LNHAHLLSLLGYCEE, corresponding to the LLSLL motif in ACR4 (acr4-LLSLL) as well as the triple Ala mutant in which the first and last Leu and the central Ser of the LLSLL motif (acr4-ALALA) were changed to Ala. The assays demonstrated the best binding between pJMD1 and acr4-LLSLL phage whereas affinity for the JMD1 and ppJMD1 peptides was ~20% lower compared to pJMD1 (Fig. 9B). The JMD2 peptide was also able to bind to the acr4-LLSLL phage, again indicating that the binding motif is conserved among the JMD1 and JMD2 peptides, as would be expected from their overall identity. However, the binding of the acr4-ALALA mutant phage to the JMD1 and JMD2 series of peptides was distinctly less, once more demonstrating the importance of the mutated residues in binding to JMD peptides (Fig. 9A and B). Thus, our results indicate that JMD specific peptides can distinctively bind to the LLSLL motif within the ACR4 kinase N-lobe.

JMD1 peptide binding to ACR4 KC

Although we have demonstrated peptide-peptide interactions between JMD1 peptides and the ACR4 LLSLL peptide, the binding in the context of the full-length kinase domain remained to be ascertained. Therefore, we performed peptide overlay assays to determine whether the JMD1 peptides could bind to the ACR4 kinase. To ensure no interference from the juxtamembrane domain we used the sACR4 KC protein lacking the JMD. As described in Materials & Methods, peptide binding to the blotted protein was assessed by colorimetric assay using streptavidin conjugated Alkaline Phosphatase. All the peptides, JMD1, pJMD1, and ppJMD1 peptides bound to sACR4 KC (Fig. 10A, *upper panel*) but did not bind to the SUMO protein which was blotted as a control (Fig. 10A, *lower panel*). Western blots using SUMO antibodies confirmed the presence of the sACR4 KC and SUMO proteins. In parallel experiments, we assessed peptide binding to sACR4 KC that was immobilized on Ni^{2+} coated plates via the N-terminal 6X His tag and incubated with either JMD1, pJMD1, or ppJMD1 (Fig. 10B). It is evident from this experiment that the phosphorylation state of the JMD1 peptide has an effect on the binding efficiency with the doubly phosphorylated peptide (ppJMD1) exhibiting the strongest binding followed by the singly phosphorylated peptide (pJMD1) and the naïve peptide (JMD1). This influence of phosphorylation on JMD1 peptide binding was not obvious in the experiments involving peptide-peptide interactions and phage ELISAs and strongly suggests that structural features other than just the LLSLL motif in ACR4 may play an additional role in JMD1 peptide binding.

Conformation of JMD1 peptides by circular dichroism

Structure analyses of the kinase domains of several RTKs have shown that the JM regions adopt secondary structures that promote interactions with regions on the kinase domain (8, 29, 33, 45). We determined the secondary structures of the JMD1 peptides by CD

analysis in aqueous buffer and in the presence of the helix inducer 2,2,2-trifluoroethanol (TFE). In the absence of TFE, the JMD1 peptides form an extended coil conformation with the lowest negative molar ellipticity at 200 nm (Fig. 11A). Phosphorylation at the two autophosphorylation sites does not appear to affect JMD1 conformation but a shallower minimum at ~222 nm indicates that the peptides can form some α-helical structure. Although the extended coil conformation is dominant among the three JMD1 peptides in aqueous buffer, it does not preclude the possibility that the JMD may form ordered secondary structures when in context of the full-length intracellular domain when anchored at the inner membrane surface.

To determine if we could promote an ordered conformation within the JMD1 peptides, we measured the CD spectra in the presence of increasing concentrations of trifluoroethanol (TFE). TFE is considered a helix inducer and has been used to monitor helical formation in oligopeptides (46-48). In the presence of increasing concentrations of TFE, the minimum absorption peak shifts from 200 to 204 nm and there is an obvious increase in the negative ellipticity at 222 nm, indicating the adoption of a helical conformation in the phosphorylated peptides (Fig. 11B and C). The shape of the curves is also increasingly characteristic of a helical conformation. Interestingly, pJMD1 shows the greatest increase in negative molar ellipticity at 222 nm, implying that the singly phosphorylated peptide can adopt a more ordered structure. These results suggest that the JMD1 peptides have the capacity to adopt a more ordered conformation depending on the phosphorylation status. However, further studies of the entire 28 amino acid JMD need to be conducted to better understand the conformational dynamics of this region.

Discussion

Multicellular organisms require a highly regulated array of signal transduction networks to promote cell fate specification and growth. Strict control of these networks ensures proper cell patterning and tissue development within the organism. In both animals and plant cells, directed cell differentiation, growth and development are facilitated via a variety of external stimuli that are appropriately interpreted by a multitude of cell surface receptors. In animal cells, this response is mediated predominantly through RTKs and in plants by RLKs. The classical paradigm of signal transduction involves ligand binding to receptor, activation/autophosphorylation of kinase domain and subsequent activation of downstream signaling pathways.

However, the regulation of kinase activity through reversible phosphorylation is of critical importance to maintaining cellular homeostasis and ensuring the fidelity of physiological processes. There are a multitude of mechanisms that regulate kinase activity and important insights into the molecular basis of regulation have come from crystallographic studies of several RTK kinase domains (7, 49). One common mechanism involves the ordered phosphorylation of key residues in the activation loop or segment (50, 51). Autophosphorylation at these sites causes a conformational change that relieves *cis*-autoinhibitory constraints (52-54). Importantly, other biochemical and structural studies provide evidence for the involvement of non-catalytic regions in regulation of kinase activity. Thus, in several receptors such as the ephrin binding receptor (EpH) family (29), platelet-derived growth factor (PDGF) receptor family (33), and the epidermal growth factor receptor (EGFR) family (55), the juxtamembrane domain, proximal to the N-terminus of the kinase domain, is a major regulatory domain (9). Similarly, a domain on the carboxyl side of the

kinase domain can be autoinhibitory as has been demonstrated for the receptor TIE2 (56). Among plant RLK's, the CTD of BRI1 is a negative regulator of kinase activity and the phosphorylation of this domain enhances the activity (11).

In the absence of structural information, we have probed the role of the JMD in ACR4 kinase through mutagenesis and peptide binding studies. On this basis, we present evidence for a model that strongly suggests that the JMD is involved in an intramolecular interaction that may inhibit the activation segment in the kinase domain from adopting the activated conformation for optimal activity. Thus, in kinetic experiments, the significant decrease in the efficiency of substrate phosphorylation (Fig. 3 and Table 2) by the JMD-2A mutant (phosphorylation sites Ser^{475} and Thr^{478} knocked out with Ala substitutions) and the restoration of wild-type activity levels in JMD-2D (Ser^{475} and Thr^{478} replaced with the phosphomimetic Asp residue) attests to the importance of phosphorylation at these two sites for kinase activity against substrates. This is not surprising since it is well established in many receptor kinases that phosphorylation of sites within the JM and CTD regions not only serve a regulatory function but are a prerequisite for efficient substrate binding and phosphorylation (30, 31, 57). Alanine scanning mutagenesis studies with the BRI1 intracellular domain has demonstrated that loss of autophosphorylation sites in the JMD can in fact decrease BR13 peptide substrate phosphorylation *in vitro* without any noticeable effect on autophosphorylation (31). On the other hand, removal of the JMD in ACR4 kinase enhances substrate phosphorylation compared to the wild-type protein (Fig. 3B). These observations can be correlated with a model in which the JM region, in the unphosphorylated state, occludes the active site and prevents efficient substrate binding. Significantly, this negative effect is relieved by phosphorylation of Ser^{475} and Thr^{478} in the JMD. Indeed,

biochemical and structural information on RTKs such as FLT3, cKIT, cFMS-1, MuSK and members of the Eph receptor family demonstrate a similar mode of regulation in which the unphosphorylated JMD allosterically regulates kinase activity by making extensive contacts across the kinase domain causing disruption of the αC helix and/or sterically hindering the activation loop from adopting an active conformation. Maximal kinase activity is restored when the phosphorylated juxtamembrane moves away from the active site (29, 32-34, 36, 44, 53). Interestingly, in the case of ErbB2, mutational studies indicate that the αC-β4 loop functions as an intramolecular switch in controlling the kinase activity (58). This region is analogous to the LLSLL region in the ACR4 kinase domain as shown in Fig.8.

However, our kinetic experiments do not provide information about the molecular details or the mechanism of the proposed intramolecular interaction. It is also well known that short linear motifs or SLiMS, which consist of a peptide sequence less than 10 residues long, often mediate protein-protein interactions and are found predominantly in signaling and regulatory networks (59-61). Linear peptide-peptide interactions are governed not only by primary sequence, but spatial arrangements of side chains within peptide secondary structures that can act as “hot points” for specific interactions (62). Some of the best exemplified linear motifs are those interacting with the Src Homology 2 (SH2), phosphotyrosine-binding (PTB) and 14-3-3 domains. Typically, interactions mediated by linear motifs are transient in nature and are characterized by weak affinities with dissociation constants in the micromolar range, perhaps attributable to the small number of residues that are involved in direct contact. Screening with phage-peptide libraries offers a facile way of identifying short peptides with varying affinities and specificities owing to the control that can be exercised in the binding and washing steps in each cycle of panning (63).

Our phage display experiments have defined consensus peptide binding motifs for the unphosphorylated and phosphorylated JMD peptides. The two peptides differ only in the phosphorylated Ser^{475} in pJMD1. The predominant peptide sequences binding to the unphosphorylated JMD1 contained an SXL motif whereas the pJMD1 preferred the consensus binding sequence LXSLL. This suggests that phosphorylation at Ser^{475} promotes a structural change that shifts the affinity of the phosphorylated peptide to a similar but subtly different target sequence. The specificity of interaction between the phage-selected peptide pd-LHSLL and pJMD1 was confirmed in our phage ELISA assays (Fig. 7). Furthermore, mutations in the LHSLL motif (i.e. AHALA) significantly diminished binding to the pJMD1 sequence indicating the critical role of the two Leu and one Ser residues. Most intriguingly, the sequence NHAHLLSLLGY found in the ACR4 kinase N-lobe, contains the LXSLL motif and, indeed, the phage displayed peptide corresponding to the LLSLL region of ACR4 (acr4-LLSLL) recognizes and binds to the JMD1 peptides in a phage ELISA (Fig. 9). Significantly, mutations of the LLSLL motif to ALALA drastically reduce the efficiency of binding. These observations reinforce the contention that there is an interaction between the juxtamembrane region and the kinase domain.

In addition, it is particularly interesting that the SXL signature is found in the sequence GLSLL at the beginning of the activation loop just after the DFG sequence in the kinase domain. This, along with the fact that the unphosphorylated JMD1 has a preferential interaction with the SXL sequence, hints to the GLSLL region as a possible site of interaction for the unphosphorylated JMD with the kinase domain. On the basis of these experiments, we invoke a possible mechanism for the regulation of ACR4 kinase activity modulated by autophosphorylation of Ser^{475} and Thr^{478} of the JMD. In our model, in the unphosphorylated

state, the juxtamembrane domain holds the kinase in a 'closed' inactive conformation perhaps through interactions with the GLSLL sequence located in the proximity of the catalytically important αC helix and the activation loop. Upon autophosphorylation, the phosphorylated juxtamembrane undergoes a conformational change, which switches its affinity to the LLSLL region towards the back side of the kinase (Fig. 12). Based on the proximity of the LLSLL and the GLSLL regions to one another in the modeled kinase tertiary structure (Fig. 8), it would not be unreasonable to speculate that the JMD can move back and forth between these two positions. Thus, phosphorylation-dephosphorylation of Ser^{475} and/or Thr^{478} in JMD could act as a molecular switch to regulate ACR4 kinase activity through conformational changes in the activation segment and the N-lobe of the kinase. The ability of the JMD peptides, in particular pJMD1 and ppJMD1, to adopt an α-helical structure in the presence of TFE (Fig. 11B and C) is supportive of the intrinsic ability of this region to switch from an unordered to an ordered state subsequent to phosphorylation. Further support for a conformational switch mechanism comes from our peptide inhibition studies (Fig. 2) in which we have demonstrated the *inability* of the phosphorylated JMD1 to repress the autophosphorylation activity in comparison with the distinct *ability* of the unphosphorylated and mutant JMD1 to exert significant repression. Our observation is analogous to that observed for the inhibition of the Kit RTK kinase activity by the wild type JM region but not by the phosphorylated derivative (8).

In this body of work, we have described a putative model for the intramolecular regulation of ACR4 kinase activity by the juxtamembrane region. Clearly, however, more detailed experiments are needed to provide the contextual specificity of this model in conjunction with the potential role of the 105 amino acid carboxyl terminal domain which

has at least 6 autophosphorylation sites (26). Indeed, the carboxy-terminal tail is known to function as a negative regulator of receptor kinase activity in the RLK BRI1 (11) and the RTK TIE2 (56, 64). Phosphorylations within the JMD/CTD may also be responsible for recruitment of substrate proteins (65-68) by creating docking sites for the recruitment of downstream interaction partners. It is therefore important to understand the connection between kinase activation and the sequestration or release of phosphorylation sites. Complementary mutagenesis studies *in vivo,* which may drive varied phenotypic effects, will also help understand the molecular basis of kinase function and the ACR4 mediated signaling network. Finally, the determination of the three dimensional structure of the kinase in the activated and inhibited state will provide atomic level detail of the mechanistic aspects of regulation and help elucidate the role of the subdomains on kinase activity.

References

1. Lemmon, M.A. and J. Schlessinger, *Cell signaling by receptor tyrosine kinases.* Cell, 2010. **141**(7): p. 1117-34.
2. Ullrich, A. and J. Schlessinger, *Signal Transduction by Receptors with Tyrosine Kinase-Activity.* Cell, 1990. **61**(2): p. 203-212.
3. Schlessinger, J., *Cell signaling by receptor tyrosine kinases.* Cell, 2000. **103**(2): p. 211-25.
4. Scott, J.D. and T. Pawson, *Cell signaling in space and time: where proteins come together and when they're apart.* Science, 2009. **326**(5957): p. 1220-4.
5. Huse, M., T.W. Muir, L. Xu, Y.G. Chen, J. Kuriyan, and J. Massague, *The TGF beta receptor activation process: an inhibitor- to substrate-binding switch.* Mol Cell, 2001. **8**(3): p. 671-82.
6. Hubbard, S.R., *Protein tyrosine kinases: autoregulation and small-molecule inhibition.* Curr Opin Struct Biol, 2002. **12**(6): p. 735-41.
7. Huse, M. and J. Kuriyan, *The conformational plasticity of protein kinases.* Cell, 2002. **109**(3): p. 275-82.
8. Chan, P.M., S. Ilangumaran, J. La Rose, A. Chakrabartty, and R. Rottapel, *Autoinhibition of the kit receptor tyrosine kinase by the cytosolic juxtamembrane region.* Mol Cell Biol, 2003. **23**(9): p. 3067-78.

9. Hubbard, S.R., *Juxtamembrane autoinhibition in receptor tyrosine kinases.* Nat Rev Mol Cell Biol, 2004. **5**(6): p. 464-71.
10. Roskoski, R., Jr., *Structure and regulation of Kit protein-tyrosine kinase--the stem cell factor receptor.* Biochem Biophys Res Commun, 2005. **338**(3): p. 1307-15.
11. Wang, X., X. Li, J. Meisenhelder, T. Hunter, S. Yoshida, T. Asami, and J. Chory, *Autoregulation and homodimerization are involved in the activation of the plant steroid receptor BRI1.* Dev Cell, 2005. **8**(6): p. 855-65.
12. Chen, X., M. Chern, P.E. Canlas, C. Jiang, D. Ruan, P. Cao, and P.C. Ronald, *A conserved threonine residue in the juxtamembrane domain of the XA21 pattern recognition receptor is critical for kinase autophosphorylation and XA21-mediated immunity.* J Biol Chem, 2010. **285**(14): p. 10454-63.
13. Mirza, A., M. Mustafa, E. Talevich, and N. Kannan, *Co-conserved features associated with cis regulation of ErbB tyrosine kinases.* PLoS One, 2010. **5**(12): p. e14310.
14. Becraft, P.W., P.S. Stinard, and D.R. McCarty, *CRINKLY4: A TNFR-like receptor kinase involved in maize epidermal differentiation.* Science, 1996. **273**(5280): p. 1406-9.
15. Jin, P., T. Guo, and P.W. Becraft, *The maize CR4 receptor-like kinase mediates a growth factor-like differentiation response.* Genesis, 2000. **27**(3): p. 104-16.
16. Tanaka, H., M. Watanabe, D. Watanabe, T. Tanaka, C. Machida, and Y. Machida, *ACR4, a putative receptor kinase gene of Arabidopsis thaliana, that is expressed in the outer cell layers of embryos and plants, is involved in proper embryogenesis.* Plant and Cell Physiology, 2002. **43**(4): p. 419-428.
17. Gifford, M.L., S. Dean, and G.C. Ingram, *The Arabidopsis ACR4 gene plays a role in cell layer organisation during ovule integument and sepal margin development.* Development, 2003. **130**(18): p. 4249-58.
18. Watanabe, M., H. Tanaka, D. Watanabe, C. Machida, and Y. Machida, *The ACR4 receptor-like kinase is required for surface formation of epidermis-related tissues in Arabidopsis thaliana.* Plant Journal, 2004. **39**(3): p. 298-308.
19. Cao, X., K. Li, S.G. Suh, T. Guo, and P.W. Becraft, *Molecular analysis of the CRINKLY4 gene family in Arabidopsis thaliana.* Planta, 2005. **220**(5): p. 645-57.
20. De Smet, I., V. Vassileva, B. De Rybel, M.P. Levesque, W. Grunewald, D. Van Damme, G. Van Noorden, M. Naudts, G. Van Isterdael, R. De Clercq, J.Y. Wang, N. Meuli, S. Vanneste, J. Friml, P. Hilson, G. Jurgens, G.C. Ingram, D. Inze, P.N. Benfey, and T. Beeckman, *Receptor-like kinase ACR4 restricts formative cell divisions in the Arabidopsis root.* Science, 2008. **322**(5901): p. 594-7.
21. Stahl, Y., R.H. Wink, G.C. Ingram, and R. Simon, *A signaling module controlling the stem cell niche in Arabidopsis root meristems.* Curr Biol, 2009. **19**(11): p. 909-14.
22. Stahl, Y. and R. Simon, *Is the Arabidopsis root niche protected by sequestration of the CLE40 signal by its putative receptor ACR4?* Plant Signal Behav, 2009. **4**(7): p. 634-5.
23. Gifford, M.L., F.C. Robertson, D.C. Soares, and G.C. Ingram, *ARABIDOPSIS CRINKLY4 function, internalization, and turnover are dependent on the extracellular crinkly repeat domain.* Plant Cell, 2005. **17**(4): p. 1154-66.

24. Stokes, K.D. and A. Gururaj Rao, *Dimerization properties of the transmembrane domains of Arabidopsis CRINKLY4 receptor-like kinase and homologs.* Arch Biochem Biophys, 2008. **477**(2): p. 219-26.
25. Stokes, K.D. and A.G. Rao, *The role of individual amino acids in the dimerization of CR4 and ACR4 transmembrane domains.* Arch Biochem Biophys, 2010. **502**(2): p. 104-11.
26. Meyer, M.R., C.F. Lichti, R.R. Townsend, and A.G. Rao, *Identification of in vitro autophosphorylation sites and effects of phosphorylation on the Arabidopsis CRINKLY4 (ACR4) receptor-like kinase intracellular domain: insights into conformation, oligomerization, and activity.* Biochemistry, 2011. **50**(12): p. 2170-86.
27. Sali, A., L. Potterton, F. Yuan, H. van Vlijmen, and M. Karplus, *Evaluation of comparative protein modeling by MODELLER.* Proteins, 1995. **23**(3): p. 318-26.
28. Sicheri, F. and J. Kuriyan, *Structures of Src-family tyrosine kinases.* Curr Opin Struct Biol, 1997. **7**(6): p. 777-85.
29. Wybenga-Groot, L.E., B. Baskin, S.H. Ong, J. Tong, T. Pawson, and F. Sicheri, *Structural basis for autoinhibition of the Ephb2 receptor tyrosine kinase by the unphosphorylated juxtamembrane region.* Cell, 2001. **106**(6): p. 745-57.
30. Binns, K.L., P.P. Taylor, F. Sicheri, T. Pawson, and S.J. Holland, *Phosphorylation of tyrosine residues in the kinase domain and juxtamembrane region regulates the biological and catalytic activities of Eph receptors.* Mol Cell Biol, 2000. **20**(13): p. 4791-805.
31. Wang, X., M.B. Goshe, E.J. Soderblom, B.S. Phinney, J.A. Kuchar, J. Li, T. Asami, S. Yoshida, S.C. Huber, and S.D. Clouse, *Identification and functional analysis of in vivo phosphorylation sites of the Arabidopsis BRASSINOSTEROID-INSENSITIVE1 receptor kinase.* Plant Cell, 2005. **17**(6): p. 1685-703.
32. Mol, C.D., D.R. Dougan, T.R. Schneider, R.J. Skene, M.L. Kraus, D.N. Scheibe, G.P. Snell, H. Zou, B.C. Sang, and K.P. Wilson, *Structural basis for the autoinhibition and STI-571 inhibition of c-Kit tyrosine kinase.* J Biol Chem, 2004. **279**(30): p. 31655-63.
33. Griffith, J., J. Black, C. Faerman, L. Swenson, M. Wynn, F. Lu, J. Lippke, and K. Saxena, *The structural basis for autoinhibition of FLT3 by the juxtamembrane domain.* Mol Cell, 2004. **13**(2): p. 169-78.
34. Schubert, C., C. Schalk-Hihi, G.T. Struble, H.C. Ma, I.P. Petrounia, B. Brandt, I.C. Deckman, R.J. Patch, M.R. Player, J.C. Spurlino, and B.A. Springer, *Crystal structure of the tyrosine kinase domain of colony-stimulating factor-1 receptor (cFMS) in complex with two inhibitors.* J Biol Chem, 2007. **282**(6): p. 4094-101.
35. Li, S., N.D. Covino, E.G. Stein, J.H. Till, and S.R. Hubbard, *Structural and biochemical evidence for an autoinhibitory role for tyrosine 984 in the juxtamembrane region of the insulin receptor.* J Biol Chem, 2003. **278**(28): p. 26007-14.
36. Wiesner, S., L.E. Wybenga-Groot, N. Warner, H. Lin, T. Pawson, J.D. Forman-Kay, and F. Sicheri, *A change in conformational dynamics underlies the activation of Eph receptor tyrosine kinases.* Embo Journal, 2006. **25**(19): p. 4686-96.
37. Sidhu, S.S., W.J. Fairbrother, and K. Deshayes, *Exploring protein-protein interactions with phage display.* Chembiochem, 2003. **4**(1): p. 14-25.

38. Tonikian, R., Y. Zhang, C. Boone, and S.S. Sidhu, *Identifying specificity profiles for peptide recognition modules from phage-displayed peptide libraries.* Nat Protoc, 2007. **2**(6): p. 1368-86.
39. Molek, P., B. Strukelj, and T. Bratkovic, *Peptide Phage Display as a Tool for Drug Discovery: Targeting Membrane Receptors.* Molecules, 2011. **16**(1): p. 857-887.
40. Cubas, P., N. Lauter, J. Doebley, and E. Coen, *The TCP domain: a motif found in proteins regulating plant growth and development.* Plant Journal, 1999. **18**(2): p. 215-222.
41. Savkur, R.S. and T.P. Burris, *The coactivator LXXLL nuclear receptor recognition motif.* Journal of Peptide Research, 2004. **63**(3): p. 207-212.
42. Plevin, M.J., M.M. Mills, and M. Ikura, *The LxxLL motif: a multifunctional binding sequence in transcriptional regulation.* Trends in Biochemical Sciences, 2005. **30**(2): p. 66-69.
43. Kim, J.G., X.Y. Li, J.A. Roden, K.W. Taylor, C.D. Aakre, B. Su, S. Lalonde, A. Kirik, Y.H. Chen, G. Baranage, H. McLane, G.B. Martin, and M.B. Mudgett, *Xanthomonas T3S Effector XopN Suppresses PAMP-Triggered Immunity and Interacts with a Tomato Atypical Receptor-Like Kinase and TFT1.* Plant Cell, 2009. **21**(4): p. 1305-1323.
44. Davis, T.L., J.R. Walker, P. Loppnau, C. Butler-Cole, A. Allali-Hassani, and S. Dhe-Paganon, *Autoregulation by the juxtamembrane region of the human ephrin receptor tyrosine kinase A3 (EphA3).* Structure, 2008. **16**(6): p. 873-884.
45. Irusta, P.M., Y. Luo, O. Bakht, C.C. Lai, S.O. Smith, and D. DiMaio, *Definition of an inhibitory juxtamembrane WW-like domain in the platelet-derived growth factor beta receptor.* Journal of Biological Chemistry, 2002. **277**(41): p. 38627-38634.
46. Sonnichsen, F.D., J.E. Vaneyk, R.S. Hodges, and B.D. Sykes, *Effect of Trifluoroethanol on Protein Secondary Structure - an Nmr and Cd Study Using a Synthetic Actin Peptide.* Biochemistry, 1992. **31**(37): p. 8790-8798.
47. Altschuler, E.L., N.V. Hud, J.A. Mazrimas, and B. Rupp, *Random coil conformation for extended polyglutamine stretches in aqueous soluble monomeric peptides.* Journal of Peptide Research, 1997. **50**(1): p. 73-75.
48. Defossez, P.A., J.L. Baert, M. Monnot, and Y. deLaunoit, *The ETS family member ERM contains an alpha-helical acidic activation domain that contacts TAFII60.* Nucleic Acids Research, 1997. **25**(22): p. 4455-4463.
49. Landau, M., S.J. Fleishman, and N. Ben-Tal, *A putative mechanism for downregulation of the catalytic activity of the EGF receptor via direct contact between its kinase and C-terminal domains.* Structure, 2004. **12**(12): p. 2265-2275.
50. Krupa, A., G. Preethi, and N. Srinivasan, *Structural modes of stabilization of permissive phosphorylation sites in protein kinases: distinct strategies in Ser/Thr and Tyr kinases.* J Mol Biol, 2004. **339**(5): p. 1025-39.
51. Nolen, B., S. Taylor, and G. Ghosh, *Regulation of protein kinases: Controlling activity through activation segment conformation.* Molecular Cell, 2004. **15**(5): p. 661-675.
52. Murray, B.W., E.S. Padrique, C. Pinko, and M.A. McTigue, *Mechanistic effects of autophosphorylation on receptor tyrosine kinase catalysis: enzymatic characterization of Tie2 and phospho-Tie2.* Biochemistry, 2001. **40**(34): p. 10243-53.

53. Till, J.H., M. Becerra, A. Watty, Y. Lu, Y.L. Ma, T.A. Neubert, S.J. Burden, and S.R. Hubbard, *Crystal structure of the MuSK tyrosine kinase: Insights into receptor autoregulation.* Structure, 2002. **10**(9): p. 1187-1196.
54. Lew, E.D., C.M. Furdui, K.S. Anderson, and J. Schlessinger, *The Precise Sequence of FGF Receptor Autophosphorylation Is Kinetically Driven and Is Disrupted by Oncogenic Mutations.* Science Signaling, 2009. **2**(58).
55. Thiel, K.W. and G. Carpenter, *Epidermal growth factor receptor juxtamembrane region regulates allosteric tyrosine kinase activation.* Proceedings of the National Academy of Sciences of the United States of America, 2007. **104**(49): p. 19238-19243.
56. Niu, X.L., K.G. Peters, and C.D. Kontos, *Deletion of the carboxyl terminus of Tie2 enhances kinase activity, signaling, and function. Evidence for an autoinhibitory mechanism.* J Biol Chem, 2002. **277**(35): p. 31768-73.
57. Nuhse, T.S., A. Stensballe, O.N. Jensen, and S.C. Peck, *Phosphoproteomics of the Arabidopsis plasma membrane and a new phosphorylation site database.* Plant Cell, 2004. **16**(9): p. 2394-405.
58. Fan, Y.X., L. Wong, J. Ding, N.A. Spiridonov, R.C. Johnson, and G.R. Johnson, *Mutational activation of ErbB2 reveals a new protein kinase autoinhibition mechanism.* J Biol Chem, 2008. **283**(3): p. 1588-96.
59. Pawson, T. and P. Nash, *Assembly of cell regulatory systems through protein interaction domains.* Science, 2003. **300**(5618): p. 445-452.
60. Diella, F., N. Haslam, C. Chica, A. Budd, S. Michael, N.P. Brown, G. Trave, and T.J. Gibson, *Understanding eukaryotic linear motifs and their role in cell signaling and regulation.* Frontiers in Bioscience, 2008. **13**: p. 6580-6603.
61. Neduva, V., R. Linding, I. Su-Angrand, A. Stark, F. de Masi, T.J. Gibson, J. Lewis, L. Serrano, and R.B. Russell, *Systematic discovery of new recognition peptides mediating protein interaction networks.* Plos Biology, 2005. **3**(12): p. 2090-2099.
62. Stein, A. and P. Aloy, *Contextual Specificity in Peptide-Mediated Protein Interactions.* PLoS One, 2008. **3**(7).
63. Kay, B.K., J. Winter, and J. McCafferty, *Phage display of peptides and proteins.* 1996, Academic Press, San Diego.
64. Shewchuk, L.M., A.M. Hassell, B. Ellis, W.D. Holmes, R. Davis, E.L. Horne, S.H. Kadwell, D.D. McKee, and J.T. Moore, *Structure of the Tie2 RTK domain: self-inhibition by the nucleotide binding loop, activation loop, and C-terminal tail.* Structure, 2000. **8**(11): p. 1105-13.
65. He, W., A. Craparo, Y. Zhu, T.J. O'Neill, L.M. Wang, J.H. Pierce, and T.A. Gustafson, *Interaction of insulin receptor substrate-2 (IRS-2) with the insulin and insulin-like growth factor I receptors. Evidence for two distinct phosphotyrosine-dependent interaction domains within IRS-2.* J Biol Chem, 1996. **271**(20): p. 11641-5.
66. Holland, S.J., N.W. Gale, G.D. Gish, R.A. Roth, Z. Songyang, L.C. Cantley, M. Henkemeyer, G.D. Yancopoulos, and T. Pawson, *Juxtamembrane tyrosine residues couple the Eph family receptor EphB2/Nuk to specific SH2 domain proteins in neuronal cells.* Embo Journal, 1997. **16**(13): p. 3877-88.

67. Park, C.J., Y. Peng, X. Chen, C. Dardick, D. Ruan, R. Bart, P.E. Canlas, and P.C. Ronald, *Rice XB15, a protein phosphatase 2C, negatively regulates cell death and XA21-mediated innate immunity.* Plos Biology, 2008. **6**(9): p. e231.
68. Deheuninck, J., G. Goormachtigh, B. Foveau, Z. Ji, C. Leroy, F. Ancot, V. Villeret, D. Tulasne, and V. Fafeur, *Phosphorylation of the MET receptor on juxtamembrane tyrosine residue 1001 inhibits its caspase-dependent cleavage.* Cell Signal, 2009. **21**(9): p. 1455-63.

Tables

Table 1. Synthetic peptides generated for phage ELISAs and peptide binding assays. Sequences are derived from the ACR4 primary amino acid sequence.

Peptide	Sequence
JMD1	^{468}DTRSSKD**S**AFTKDNG^{482}
pJMD1	^{468}DTRSSKD**pS**AFTKDNG^{482}
ppJMD1	^{468}DTRSSKD**pS**AFpTKDNG^{482}
JMD2	^{471}SSKDSAF**T**KDNGKIR^{485}
pJMD2	^{471}SSKDSAF**pT**KDNGKIR^{485}
CTD2	^{824}KRSGSEN**T**EFRGGSW^{838}
pCTD2	^{824}KRSGSEN**pT**EFRGGSW^{838}

Table 2. Effect of ACR4 JMD mutants on substrate phosphorylation

Protein	Vmax (nmole/min/mg)	Km (μM)
sACR4 wt	6.37 ± 0.47	0.68 ± 0.29
sACR4 KC	7.50 ± 0.38	1.98 ± 0.46
sACR4 JMD-2A	4.57 ± 0.18	0.92 ± 0.20
sACR4 JMD-2D	6.30 ± 0.16	0.93 ± 0.13

Figures

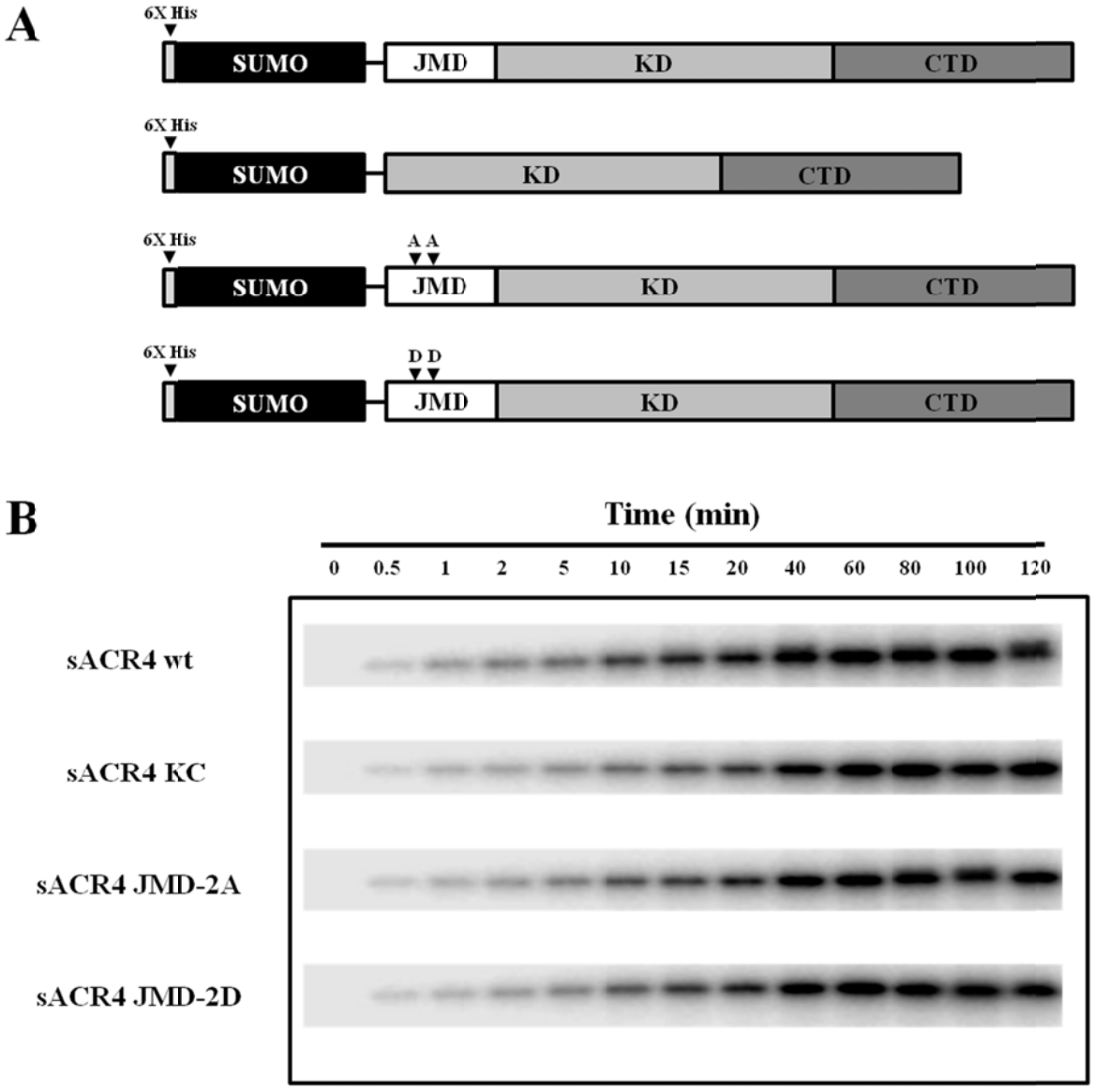

Figure 1. Effect of JMD mutants of autophosphorylation activity of ACR4. (A) Schematic of the SUMO fused intracellular domain of ACR4 and the JMD mutants. Constructs were generated lacking the JMD residues 456-482 (sACR4 KC) or double point mutants in which S^{475}/Thr^{478} were substituted with Ala (sACR4 JMD-2A) or with Asp (sACR4 JMD-2D). (B) An autoradiogram of the autophosphorylation time courses of the sACR4 JMD mutants. Reactions were incubated at the times indicated. Proteins were resolved by 12% SDS-PAGE and radioactive bands were analyzed by phosphorimaging.

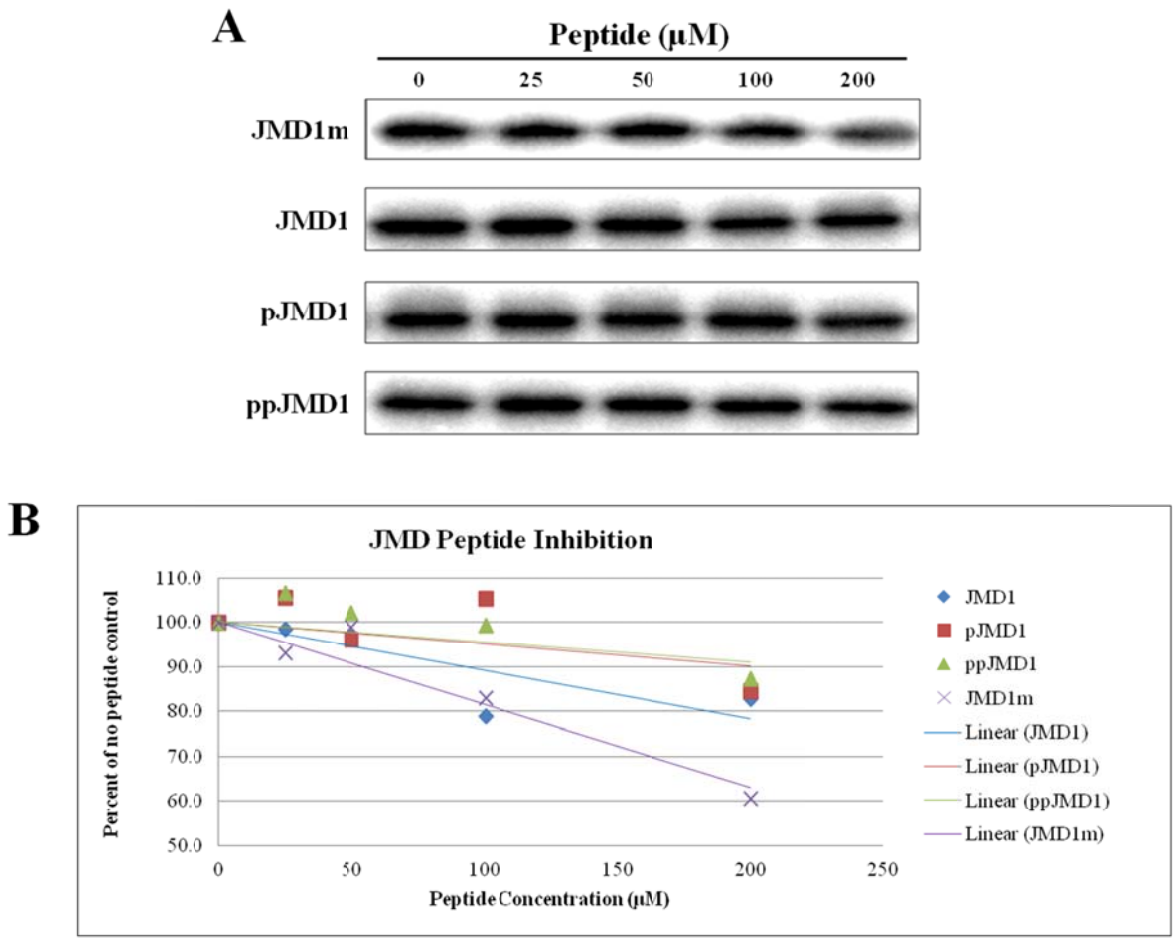

Figure 2. JMD1 peptide inhibition of the ACR4 kinase. (A) An autoradiogram showing the autophosphorylation activity of the sACR4 KC protein incubated with increasing concentrations of the JMD1 peptides (0-200 µM). (B) Plot of density *versus* peptide concentration quantified from the autoradiogram in *panel A*. Density analysis shows the greatest inhibition for the JMD1m peptide and the least inhibition with the ppJMD1 peptide. Densities are represented as a percentage of the no peptide control and were quantified with the UN-Scan-It software v6.1.

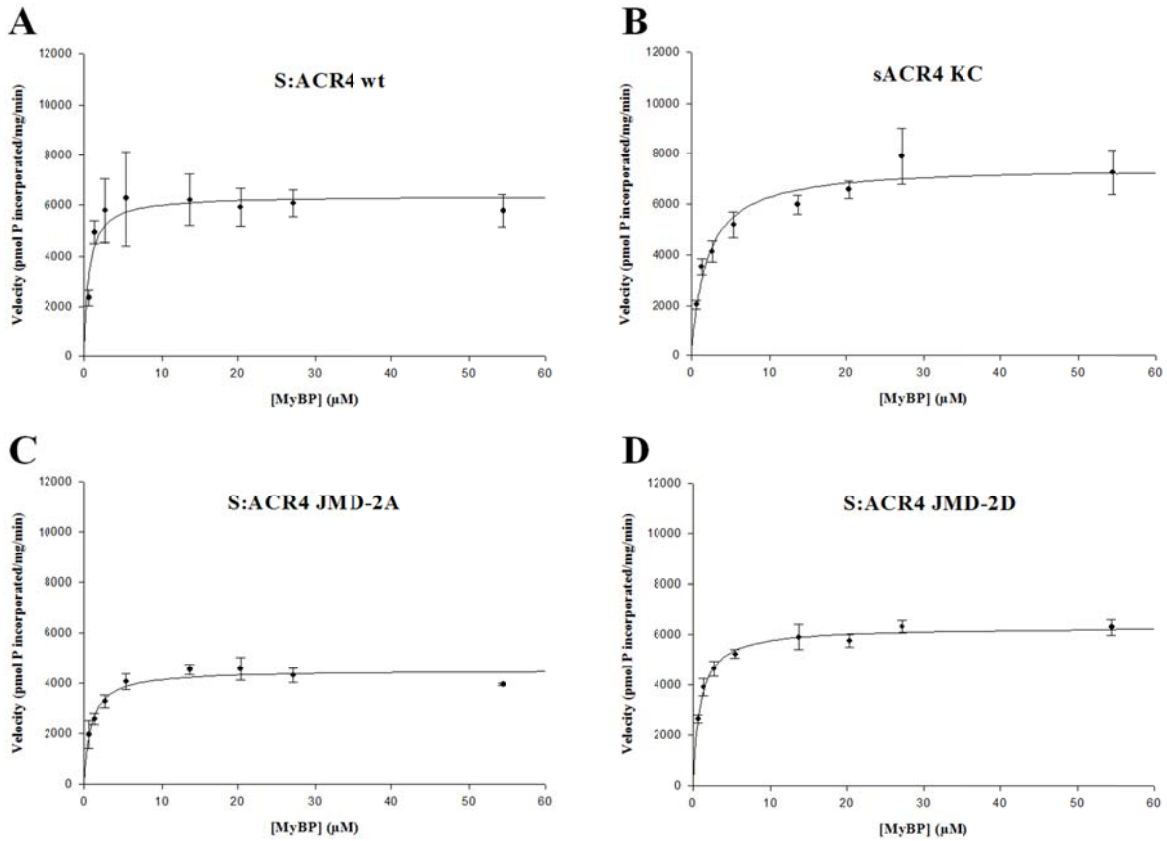

Figure 3. Effect of JMD mutants on substrate phosphorylation. Kinetic analysis of MyBP substrate phosphorylation was performed by incubating the sACR4 wild-type enzyme or the JMD mutants with increasing concentrations of MyBP (0.7-54.4 µM). Plots of phosphate incorporation *versus* substrate concentration were generated using the SigmaPlot v11.2 Enzyme Kinetics Module 1.3. Curves are sACR4 wild-type (A), sACR4 KC (B), sACR4 JMD-2A (C), and sACR4 JMD-2D (D). Data are plotted as the mean ± the S.E (n=3).

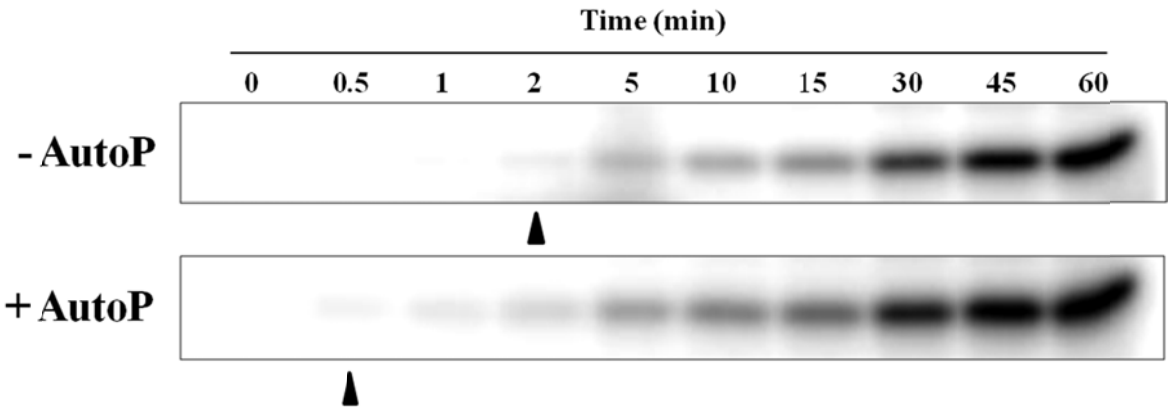

Figure 4. Effect of ACR4 autophosphorylation on substrate phosphorylation. An autoradiogram showing the effect of ACR4 autophosphorylation on activity against the MyBP substrate. sACR4 enzyme was incubated with (+AutoP) or without (–AutoP) ATP prior to addition of substrate. Reactions were incubated at times indicated. Proteins were resolved by 12% SDS-PAGE and radioactive bands were monitored by phosphorimaging. The appearance of MyBP phosphorylation is indicated by the arrows

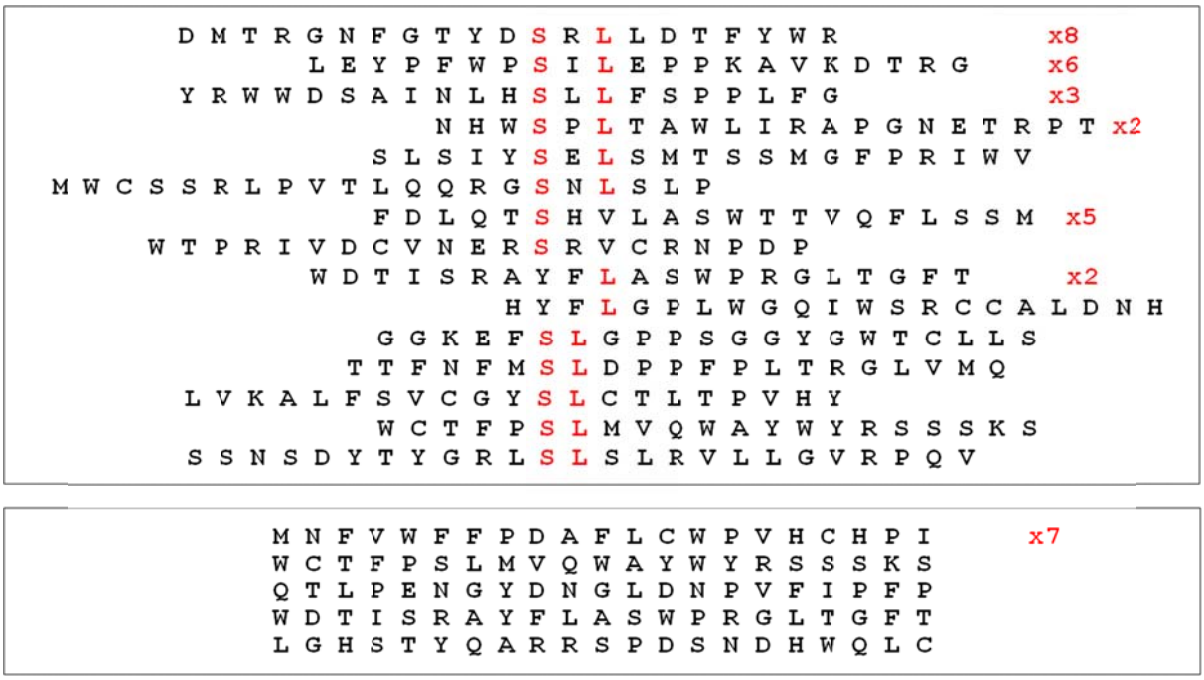

Figure 5. Phage panning of JMD1 peptide. The immobilized JMD1 peptide was screened with a random 21-aa linear peptide library encoded in the pIII protein of filamentous phage. Phage peptide binders were enriched by successive binding, washing, and elution steps. After four rounds, 46 clones were randomly selected for DNA sequencing. The table represents the peptide sequences binding specifically to JMD1 peptide and their frequency of occurrence. A consensus tripeptide SXL motif was enriched.

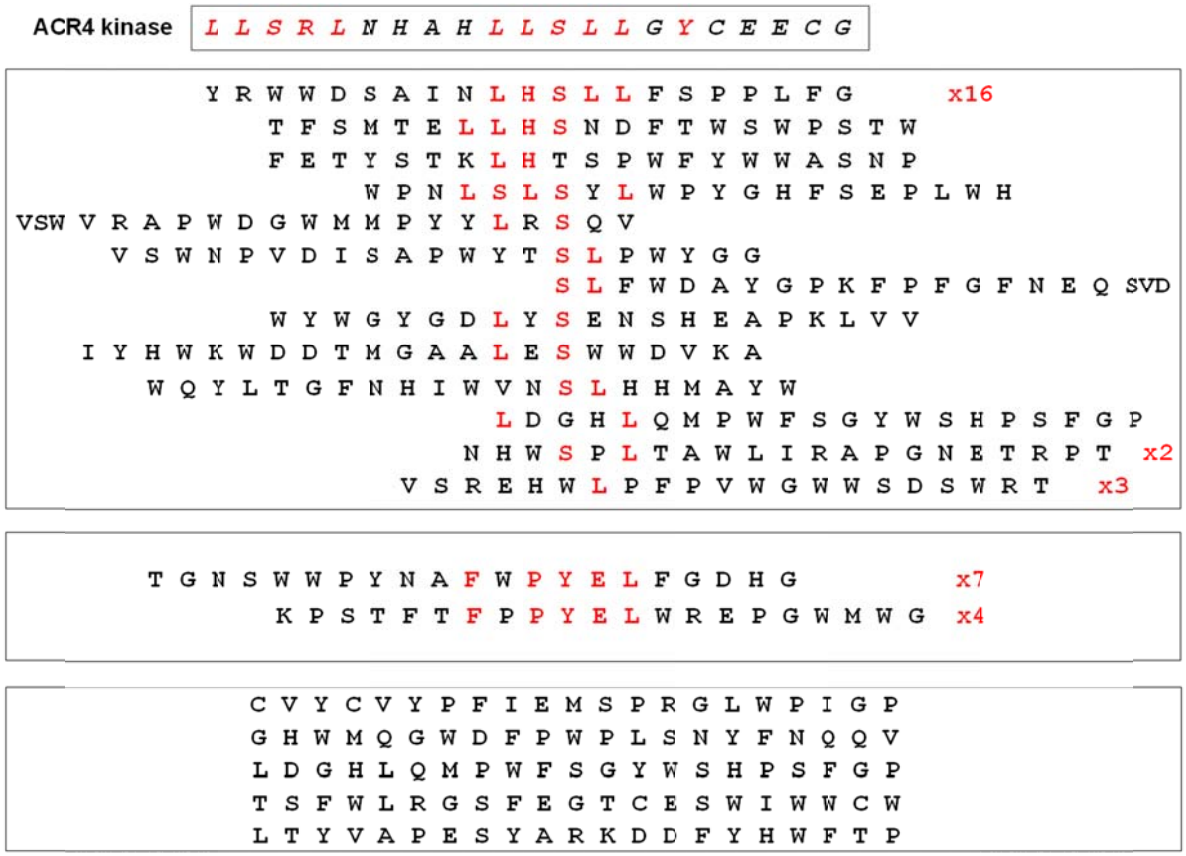

Figure 6. Phage panning of pJMD1 peptide. The immobilized JMD1 peptide was screened with a random 21-aa linear peptide library encoded in the pIII protein of filamentous phage. Phage peptide binders were enriched by successive binding, washing, and elution steps. After four rounds, 47 clones were randomly selected for DNA sequencing. The table represents the peptide sequences binding specifically to JMD1 peptide and their frequency of occurrence. A consensus LXSLL motif was enriched from the phage library.

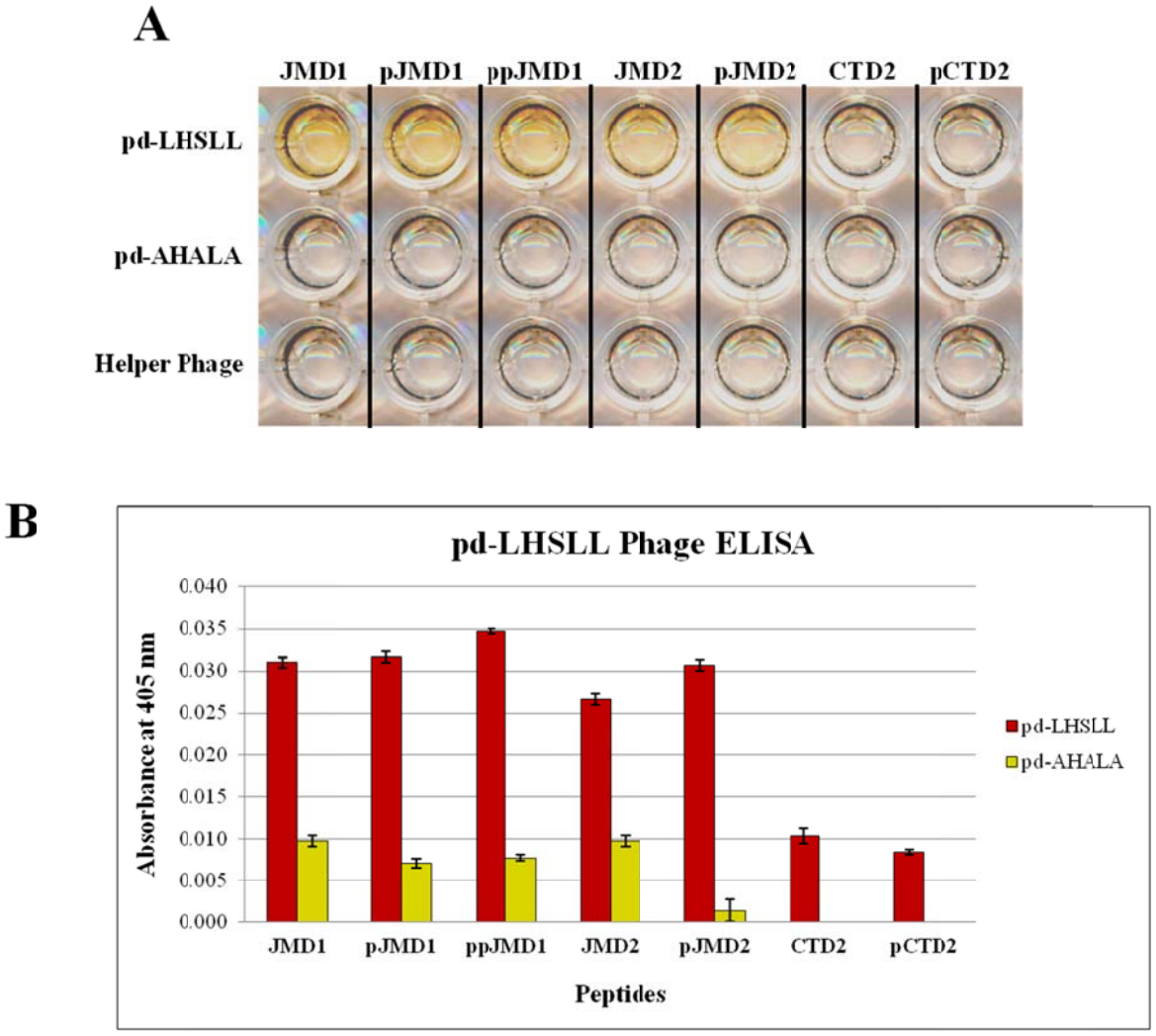

Figure 7. Specificity of phage derived 'LHSLL' for JMD1 peptides. Specificity of the phage derived peptide 'YRWWDSAINLHSLLFSPPLFG' was determined by phage ELISAs. Synthetic JMD1 or control peptides (Table 1) were immobilized to streptavidin plates via their N-terminal biotin tag. (A) Homogenous phage libraries displaying the wild-type sequence pd-LHSLL or the triple mutant pd-AHALA were screened for binding to the various ACR4 specific peptides. pd-LHSLL specificity was demonstrated against all JMD series of peptides. pd-AHALA binding to the JMD series of peptides was highly diminished demonstrating the importance of these mutated residues in JMD peptide binding. (B) Bar graph showing the quantification of phage peptide binding. Absorbance was measured at 405 nm. Data are the mean ± the S.E. (n=3).

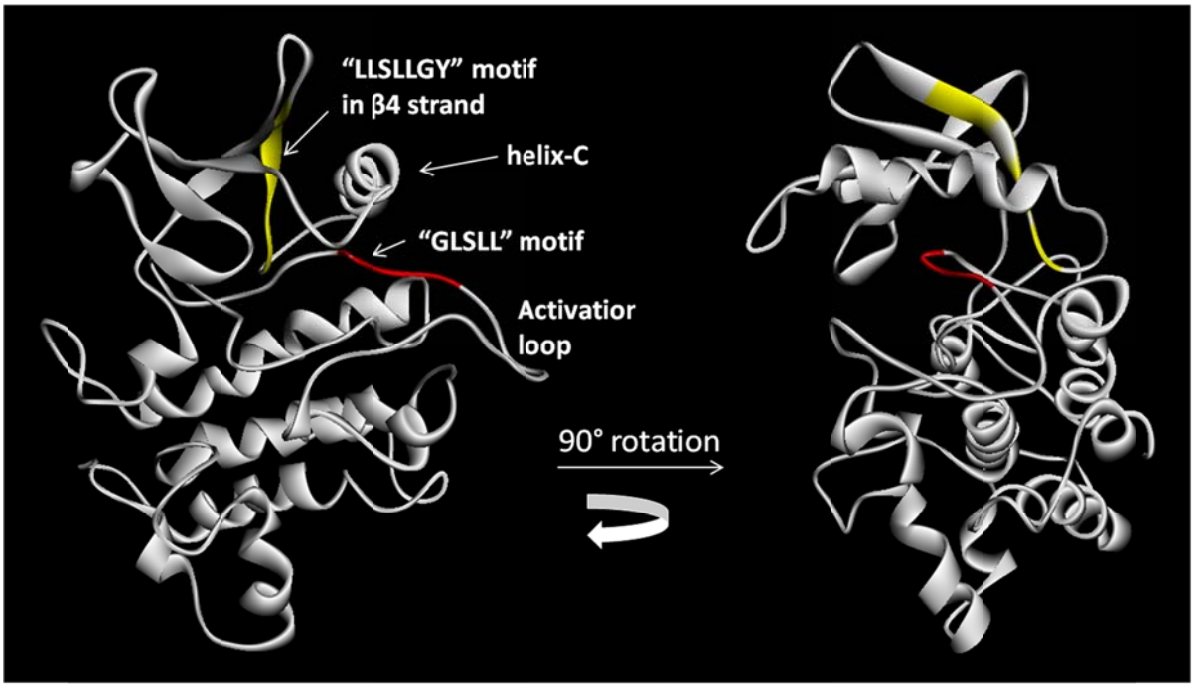

Figure 8. Model of the ACR4 kinase domain. The ACR4 kinase domain, residues 512-785, was modeled after the Interleukin-1 receptor associated kinase structure (PDB: 2NRU_B) which was 50% similar and 34% identical to the ACR4 sequence. The homology model was prepared using the Discovery Studio v 3.1 (Accelrys) software. The protein model was generated by MODELER and was validated using the Verify Protein (Profiles-3D) protocol. The modeled ACR4 tertiary fold has features of a typical kinase domain comprising of a N-terminal and C-terminal lobe. The 'LLSLLGY' motif (yellow) and the 'GLSLL' motif (red) are key regions thought to be involved in an intramolecular contact with the JMD.

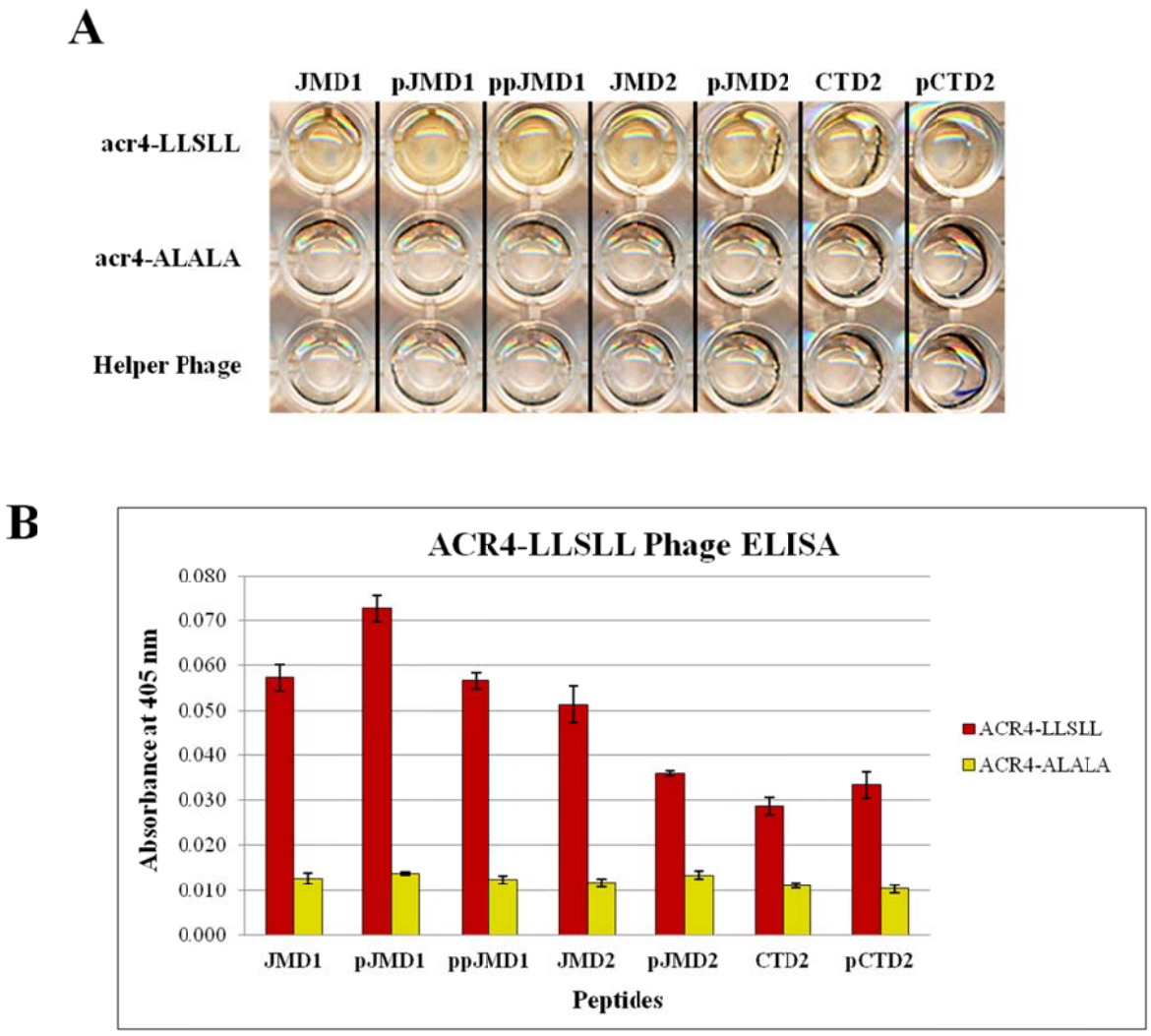

Figure 9. Specificity of ACR4 'LLSLL' motif for JMD1 peptides. Specificity of ACR4 derived 'LNHAHLLSLLGYCEE' for the JMD series of peptides was determined by phage ELISAs. Synthetic JMD1 or control peptides (Table 1) were immobilized to streptavidin plates via their N-terminal biotin tag. (A) Homogenous phage libraries displaying the wild-type sequence (acr4-LLSLL) or the triple mutant (acr4-ALALA) were screened for binding to the various ACR4 specific peptides. acr4-LLSLL specificity was demonstrated against all JMD series of peptides. acr4-ALALA binding to the JMD series of peptides was abrogated, demonstrating the importance of these mutated residues in JMD peptide binding. (B) Bar graph showing the quantification of phage peptide binding. Absorbance was measured at 405 nm. Data are the mean ± the S.E. (n=3).

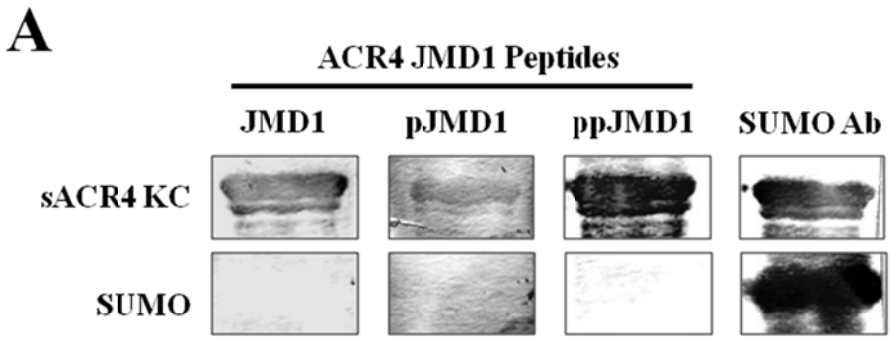

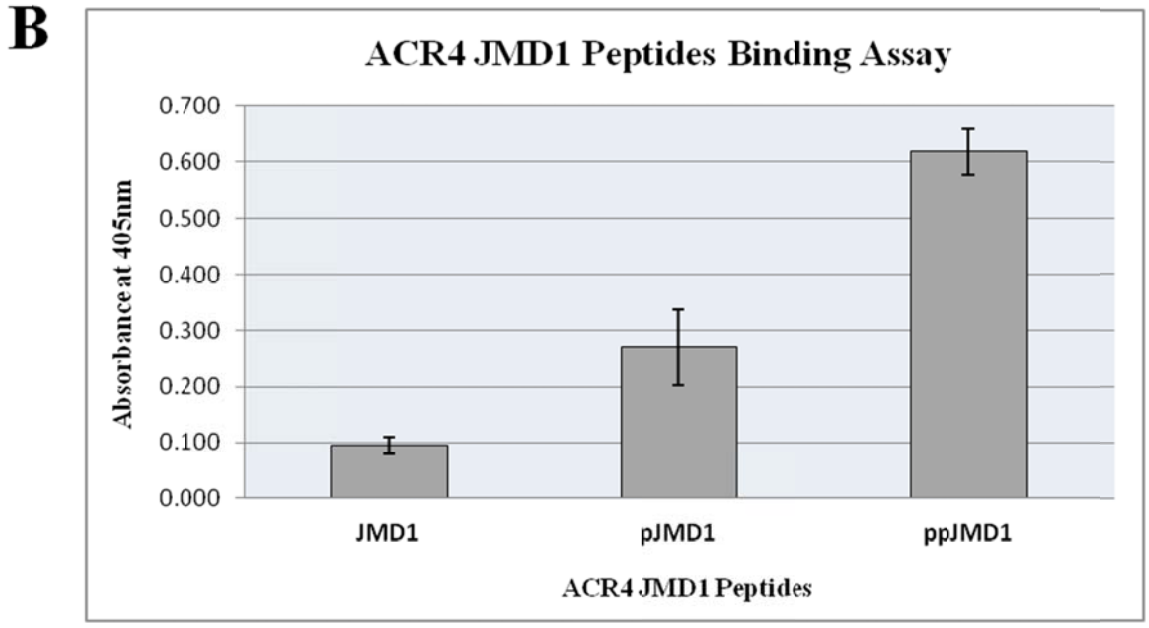

Figure 10. JMD1 peptide binding assays. The JMD1 series of peptides was incubated with the sACR4 KC protein to demonstrate specificity of binding towards the ACR4 kinase. (A) A peptide overlay assay showing that the unphosphorylated JMD1, the singly phosphorylated pJMD1, and the doubly phosphorylated ppJMD1 can bind to sACR4 KC (upper panel). Controls blots show no specificity towards the SUMO solubility tag (lower panel). To confirm the presence of each protein, anti-SUMO western blots were performed. (B) JMD1 peptide binding assay demonstrating the JMD1 series of peptides can bind to the natively folded sACR4 KC protein. Phosphorylation of the JMD1 peptide at Ser^{475} or at both Ser^{475} and Thr^{478} increases its capacity to bind sACR4 KC, more so with the doubly phosphorylated peptide.

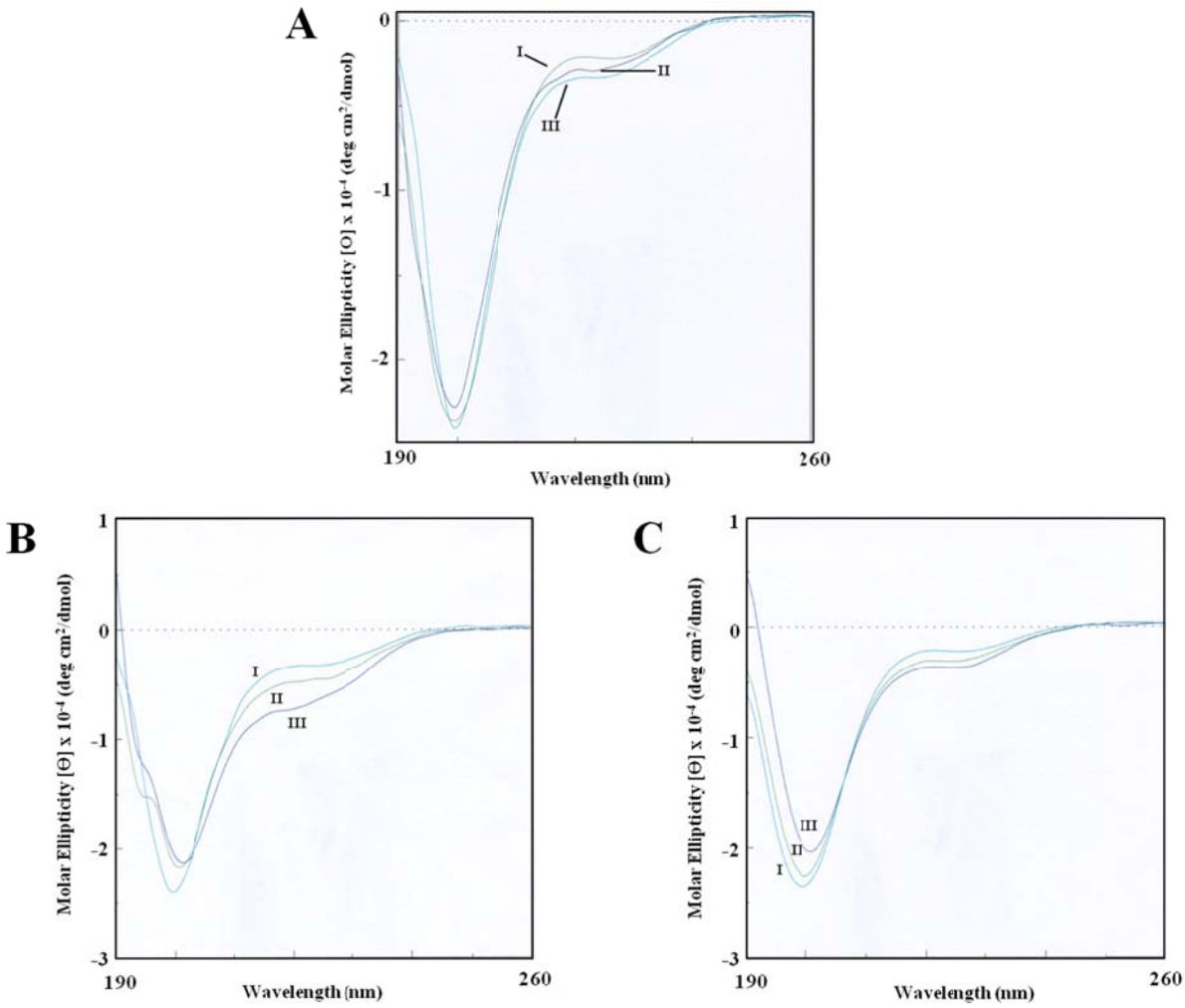

Figure 11. Conformational analysis of synthetic JMD1 peptides. The secondary structure of JMD1, pJMD1, and ppJMD1 peptides was determined by CD analaysis. (A) Far-UV CD spectra of the JMD1 (I), pJMD1 (II), ppJMD1 (III) peptides in 10 mM Tris (pH 7.2) and 0.1 mM TCEP. (B) Far-UV CD spectra of pJMD1 peptide in increasing concentrations of trifluoroethanol (TFE): 0 % (I), 15 % (II), and 40 % (III) TFE. (C) Far-UV CD spectra of ppJMD1 peptide in increasing concentrations of TFE: 0 % (I), 15 % (II), and 40 % (III) TFE.

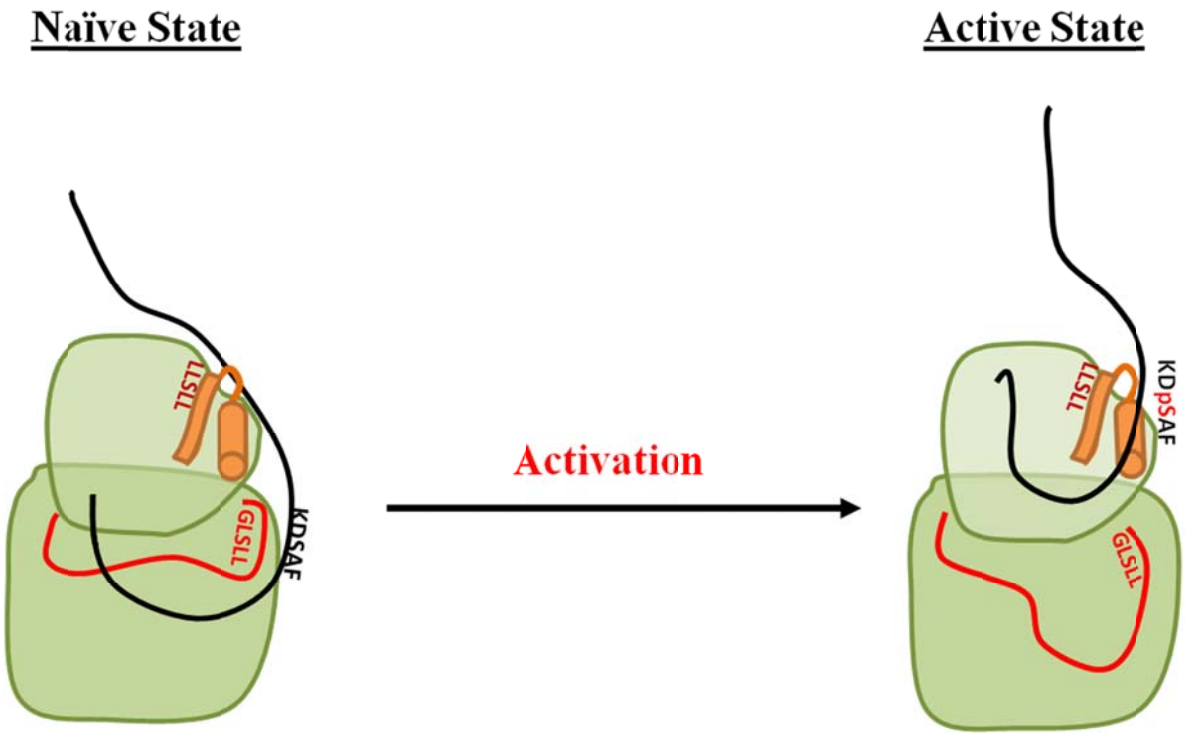

Figure 12. JMD regulation of the ACR4 kinase by a potential intramolecular mechanism. Diagram of a postulated intramolecular contact between the JMD the ACR4 N-lobe and/or activation loop to regulate kinase activity. In the naïve, basal state the unphosphorylated JMD potentially interacts with the 'GLSLL' motif at the N-terminal region of the activation loop, preventing it from adopting a productive conformation. During activation the JMD is autophosphorylated at Ser^{475} and Thr^{478}. Phosphorylation induces structural changes and possibly electrostatic repulsion at the active site causing the JMD to swing to the back side of the kinase N-lobe and bind to the 'LLSLL' region. The JMD (black), the activation loop (red), the kinase domain (blue), and the CTD (green) are shown. The labels for each motif are respectively color coded to match. The C-terminal domain of ACR4 is not shown.

CHAPTER 5. INTERMOLECULAR INTERACTIONS BETWEEN THE INTRACELLULAR DOMAINS OF ACR4 AND THE AtCRRs SIGNIFIES POTENTIAL CROSSTALK AMONG THE RECEPTOR FAMILY

A paper to be submitted for publication in *ACS Biochemistry*.

M.R. Meyer, S. Shah, J. Zhang, C.F. Lichti, R.R. Townsend, and A.G. Rao

Abstract

Arabidopsis CRINKLY4 (ACR4) is a receptor-like kinase (RLK) involved in the global development of the plant. *acr4* mutant plants show disorganized epidermal formation in leaves and reproductive tissues consequentially affecting aerial organ development. Additionally, loss of ACR4 function results in proliferation of columella stem cells (CSC) in the root tip and increased lateral root initiation in developing roots. A negative feedback mechanism has been proposed between the CLE40 peptide, ACR4, and the WOX5 transcription factor to regulate CSC differentiation. The *Arabidopsis* genome encodes four homologs to ACR4 that contain sequence similarity and analogous architectural elements to ACR4, termed *Arabidopsis* CRINKLY4 Related (AtCRRs) proteins. Genetic and cell biology studies have suggested potential communication between members of the ACR4 gene family. However, little biochemical evidence is available to ascertain the molecular aspects of receptor hetero-oligomerization and the role of phosphorylation in these interactions. Therefore, we have undertaken an investigation of the *in vitro* interactions between the intracellular domains (ICD) of ACR4 and the CRRs and an additional RLK involved in epidermis formation, ALE2. We demonstrate that ACR4 can interact with all four CRRs in a phosphorylation independent manner. Furthermore, sequence analysis of the

ACR4 gene family has revealed a conserved 'KDSAF' motif that may be involved in protein-protein interactions among the receptor family. We demonstrate that CRR3, CRK1, and ALE2 peptides harboring this conserved motif are able to bind to the ACR4 kinase domain, presumably through the LLSLL motif in the kinase N-lobe. We also employed multiple techniques to characterize a potential interaction between ACR4 and WOX5 and, show for the first time, that WOX5 is able to bind to ACR4 in a phosphorylation independent fashion. Furthermore, mass spectrometry analysis shows WOX5 is phosphorylated by ACR4 at four different sites *in vitro.* Lastly, phage display panning of a phosphorylated peptide in the juxtamembrane domain has identified two consensus interaction motifs, LXSLL and FXPYEL.

Abbreviations

ACR4, *Arabidopsis* CRINKLY4; ALE2, ABNORMAL LEAF SHAPE 2; AP, alkaline phosphatase; AtCRR, *Arabidopsis* CRINKLY4-Related; ATP, adenosine triphosphate; BRI1, Brassinosteroid insensitive 1; CR4, maize CRINKLY4; CD, circular dichroism; AtCRR, *Arabidopsis* CRINKLY4 related; CTD, carboxy-terminal domain; DTT, dithiothreitol; EGFR, epidermal growth factor receptor; ICD, intracellular domain; KC, kinase + carboxy terminal domain; JM, juxtamembrane; KD, kinase domain; MyBP, myelin basic protein; NusA, N-utilization substance A; PBS, phosphate buffered saline; PDGF, platelet derived growth factor; pNPP, p-nitrophenyl phosphate; RLK, receptor-like kinase; RTK, receptor tyrosine kinase; SERK, somatic embryogenesis receptor-like kinase; TCEP, Tris (2-carboxyethyl) phosphine hydrochloride; TFE, trifluoracetic acid; TBS, tris buffered saline; UV, ultraviolet; WOX5, WUSCHEL RELATED HOMEOBOX 5.

Introduction

Mammalian systems have acquired signal transduction mechanisms via the use of receptor tyrosine kinases (RTK) to coordinate cellular processes such as proliferation, migration, differentiation, and cell-cycle control (1). RTKs are comprised of an extracellular ligand binding domain, a single membrane spanning region, and an intracellular tyrosine kinase domain. The classical paradigm of RTK activation involves ligand binding to the extracellular domain and receptor homo- or heterodimerization through interactions among receptor subdomains (1-5).

Similar to RTKs in architecture, plant RLKs contain an extracellular ligand binding domain, a transmembrane helix, and an intracellular serine/threonine kinase domain and are involved in various plant signaling processes (6-9). It is evident from structural and biochemical studies that mechanisms of RLK signaling are similar to RTKs where ligand binding leads to receptor activation and initiation of an intracellular signaling cascade. Furthermore, it has been demonstrated in RTKs that homo- or heterodimeric receptor complexes can elicit differential signaling cascades based on intracellular kinase autophosphorylation and recruitment of specific signaling molecules as classically exemplified by the EGF receptor family (10-12). Among RLKs, the heterodimeric interactions between BRI1 and BAK1 and its effects on downstream signaling are well documented (13, 14).

Arabidopsis CRINKLY4 (ACR4) is a RLK involved in the proper growth and development of the plant (15-18). We have recently reported on some significant *in vitro* biochemical properties of the ACR4 intracellular domain including its kinase activity, its oligomerization properties, and the identification of at least 16 autophosphorylation sites

encompassing all three subdomains (19). Genetic and biological experiments have detailed the functional properties of ACR4 in developing and mature tissues. The RLK primarily effects epidermal formation in the leaves, sepal margins, and reproductive tissues of the plant (15, 16, 18). Another RLK, ALE2, has been shown to affect epidermis related tissues and to function in the same genetic pathway as ACR4. Furthermore, recombinant kinase domains of both receptors have been shown to synergistically enhance their activities in an *in vitro* kinase assay (20). ACR4 is also known to influence root development and morphology. Thus, ACR4 is required for columella stem cell differentiation in the root apical meristem and is essential for proper lateral root formation (21, 22). A signaling module has been proposed including a postulated peptide ligand, CLE40, the ACR4 RLK, and the WOX5 transcription factor that engage in a possible feedback mechanism controlling stem cell differentiation similar to CLAVATA signaling in the shoot apical meristem (22-24).

The *Arabidopsis* genome encodes four homologs to ACR4, termed *Arabidopsis* CRINKLY4-Related proteins (AtCRRs), which are similar in sequence and architecture to ACR4 (17). Both CRR1 and CRR2 have been described as kinase-defective due to the absence of the activation loop, a stretch of sequence critical for activity (17, 25). Recombinant CRR2 kinase domain has been shown to have little to no activity *in vitro* (17) but can be phosphorylated by ACR4 kinase, suggesting a possible intermolecular interaction. Functional redundancy has been suggested to account for the five members of the ACR4 gene family (17). Developing *Arabidopsis* roots showed significant enhancement of lateral root densities in *acr4*/*crr* triple mutant backgrounds compared to *acr4* single mutants, suggesting that the CRRs may be able to compensate for loss of ACR4 function in restricting lateral root initiation (21). Various genetic and cell biology experiments have hinted at

multiple players/interactions potentially involved in the ACR4 signaling network. However, the molecular aspects of these interactions with potential membrane-associated or cytosolic protein targets at the cell surface is vaguely understood.

To better understand the role of protein-protein interactions mediated by ACR4, we have undertaken an *in vitro* study of the interactions between the intracellular domains (ICD) of ACR4 and the CRRs. We have utilized *in vitro* kinase assays to show that the ACR4 can phosphorylate the CRRs and ALE2. Furthermore, the ACR4 ICD can interact with all of the CRR ICDs in a phosphorylation independent manner. Notably, interactions seen between ACR4 and CRR3 and CRK1 are mitigated by kinase autophosphorylation. Additionally, peptide binding assays demonstrate a conserved 'KDSAF' motif in the helix-C region of CRR3, CRK1, and ALE2 bind to the ACR4 kinase domain. Phage display screening of 'KDSAF' motif peptide has identified two consensus motifs, LXSLL and FXPYEL, as interaction sequences. For the first time, we also provide evidence for the direct interaction of ACR4 ID with WOX5 in the absence of autophosphorylation. Importantly, ACR4 can phosphorylate WOX5 *in vitro* and mass spectrometry analysis has identified four phosphorylation sites within the WOX5 protein sequence.

Materials and Methods

Protein expression and purification

Vectors encoding the SUMO fused kinase domains of ACR4, the CRRs, and ALE2 were transformed into Rosetta2 (DE3) pLysS (Novagen) cells and plated on Kanamycin plates. Luria Broth cultures supplemented with 50 μg/ml Kanamycin were initiated by standard procedures. Cultures were grown with shaking at 37 °C for ~3 h until an OD_{600} =

0.6-0.8 was reached. The temperature was reduced to 20 °C and cultures were induced with 1 mM IPTG. The cultures were incubated for 5 h, harvested by centrifugation, and stored at -80 °C until needed. To purify the SUMO fused proteins, frozen pellets from 250 ml cultures were thawed on ice and resuspended in 10 ml Lysis Buffer (50 mM Tris-HCl pH 7.4, 150 mM NaCl, 40 mM imidazole, 0.1% Triton X-100, 1 mM DTT, and 1 mM AEBSF). Cells were lysed by sonication on ice and the resulting lysate was centrifuged at 13,200 rpm for 15 min at 4°C. Supernatants were then transferred to a 10 ml column containing 250 µl of Ni-NTA Superflow resin (Qiagen) equilibrated with Lysis Buffer. The resin/lysate mixture was incubated on a rocker at 4°C for 1 h. After incubation, the unbound proteins were allowed to flow through the column. The resin was washed with 10 ml of Wash Buffer (50 mM Tris-HCl pH 7.4, 150 mM NaCl, 50 mM imidazole, 1 mM DTT). Bound proteins were eluted into individual microfuge tubes with three successive 250 µl aliquots of Elution Buffer (50 mM Bis-Tris pH 7.2, 50 mM NaCl, 150 mM imidazole, 1 mM DTT) on ice. Protein quantities were determined by the Bradford method. Protein yields depended on the protein being purified and typically ranged from 1-5 mg of protein.

To isolate the mACR4 protein, the vector encoding the MBP fused ACR4 kinase was transformed into T7 Express cells (New England Biolabs) and plated on Ampicillin plates. Protein expression and purification was performed as described above, except Ampicillin (100 µg/ml) was used in cultures. Further purification of the IMAC enriched protein was required. Enriched protein, ~1 mg in 500 µl, was passed over a Global 10/300 Superdex G200 column (GE Healtchare) equilibrated with Column Buffer (50 mM Tris-HCl 7.4, 100 mM NaCl, 1 mM DTT). Protein was eluted at a rate of 0.4 ml/min and fractions

corresponding to the full length mACR4 protein were collected and pooled to be used for further study.

Pull-down assays

The mACR4 kinase (20 µg per reaction) was used as bait to pull out sCRR/ALE2 kinase domains (30 µg per reacton). Depending on the assay conditions, proteins were autophosphorylated in proteins 200 µl Kinase Buffer (20 mM Bis-Tris pH 7.2, 25 mM NaCl, 5 mM MnCl2, 1 mM DTT) and 100 µM ATP. Proteins were allowed to autophosphorylate for 1 h prior to pull-down experiments. Potential binding partners were added to each reaction and Binding Buffer (50 mM Tris-HCl pH 7.4, 150 mM NaCl, 1 mM DTT, 0.02% NP-40) was added to a final volume of 500 µl. Proteins were incubated on a rotator for 1 h at room temperature. 25 µl bed volume of amylose resin was added to each reaction and incubated an additional 1 h on a rotator at room temperature. Reactions were spun down at 1,000 rpm for 30 sec to pellet the resin. The resin was washed three times with Binding Buffer to remove unbound protein. After the third wash, the supernatant was removed and 100 µl of Laemmli buffer was added to the resin. The resin/protein mixture was boiled at 95 ºC for 5 min then centrifuged at max speed to pellet resin. 10 µl of supernatant from each reaction was separated by 12% SDS-PAGE and proteins were analyzed by coomassie staining or by western blots with polyclonal anti-MBP (Rockland Immunochemicals, 1:3,000 dilution) or anti-SUMO (Rockland Immunochemials, 1:2,000 dilution)

The kinase active proteins were used for conditions requiring phosphorylated or unphosphorylated proteins of both interacting partners (Fig. 2, panels A and D). The inactive kinase mutants were used for conditions which required one protein of the interaction pair to be unphosphorylated (Fig. 2, B and C). A special case was made for the sALE2 protein for

which an inactive mutant was unstable (Fig. 2B). First, mACR4 protein was autophosphorylated as described above, immobilized on 25 µl of amylose resin, and washed three times with Binding Buffer to remove excess ATP. Binding of naïve, active sALE2 then proceeded as described above.

mWOX5 protein was used to pull down sACR4 protein similar to the protocol outlined above. Briefly, 20 µg of mWOX5 protein was incubated with 30 µg of sACR4 protein. Depending on the assay conditions, sACR4 was autophosphorylated as described above. mWOX5 and sACR4 were added to a reaction and Binding Buffer was added to a final volume of 500 µl. Proteins were incubated and pulled-down as described above. 10 µl of supernatant from each reaction was separated by 10% SDS-PAGE and proteins were analyzed by coomassie staining or by western blots with polyclonal anti-MBP (Rockland Immunochemicals, 1:3,000 dilution) or anti-SUMO antibody (Rockland Immunochemicals, 1:2000 dilution).

Gel filtration studies

Purified sACR4 protein was incubated with a sCRR/ALE2 protein at equimolar concentrations to determine possible interactions. 5 µM sACR4 was incubated with 5 µM of binding partner in 500 µl of Column Buffer (50 mM Tris pH 7.4, 100 mM NaCl, 1 mM DTT, and 100 µM $MnCl_2$) for 1 h at room temperature. Protein mixtures were then loaded onto a Global 10/300 Superdex G-200 Column (GE Healthcare) coupled to an AKTA FPLC system. Prior to protein loading the column was equilibrated with Column Buffer. Proteins were passed through the column at a flow rate of 0.5ml/min and 1 ml fractions were collected. Proteins in subsequent fractions were analyzed by 12% SDS-PAGE.

In vitro phosphorylation assays

Active sACR4 protein was incubated with the inactive sCRRm/ALE2m proteins. For each reaction 1 µg of sACR4 was incubated with ~1 µg of sCRRm/ALE2m in 20 µl of Kinase Buffer (20 mM Bis-Tris pH 7.2, 25 mM NaCl, 5 mM $MnCl_2$, 1 mM DTT, 25 µM ATP) supplemented with 2 µCi of [γ-^{32}P] ATP (Perkin Elmer, 6,000 Ci/mmol). Proteins were incubated at room temperature for 1 h. Reactions were then terminated with the addition of 4X SDS sample buffer and boiled. Proteins were separated by 12% SDS-PAGE and radioactive bands were analyzed by phosphorimaging.

A modified *in vitro* phosphorylation assay was used for sACR4 and mWOX5 since they migrate similarly on an SDS-PAGE gel. Phosphorylation proceeded in a 50 µl reaction containing 2 µg of sACR4 and 30 µg of mWOX5 (or 30 µg of MBP as a control) in Kinase Buffer as described above. Following incubation, mWOX5 protein was pulled-down using amylose resin. The phosphorylation reactions were brought up to 500 µl with Wash Buffer (50 mM Tris-HCl pH 7.4, 150 mM NaCl, 1 mM DTT, and 0.5% NP-40). 25 µl bed volume of amylose resin was added to each reaction and incubated an additional 1 h on a rotator at room temperature. Reactions were spun down to pellet the resin and the supernatant was removed. The resin was washed five times with 500 µl of Wash Buffer to remove unbound protein. After washing, the supernatant was removed and 100 µl of Laemmli buffer was added to the resin. The resin/protein mixture was boiled at 95 ºC for 5 min then centrifuged to pellet resin. Proteins from each reaction were separated by 10% SDS-PAGE and analyzed by phosphorimaging.

To examine sACR4 phosphorylation of the CRR3, CRK1, and ALE2 hC peptides, a similar assay was used as described above. For each reaction 1 µg of sACR4 was incubated with 10 µg of peptide in 20 µl of Kinase Buffer supplemented with 2 µCi of [γ-^{32}P] ATP.

Proteins/peptide reactions were incubated at room temperature for 1 h. Reactions were then terminated with the addition of 4X SDS sample buffer and boiled. Proteins/peptides were separated by 16.5% Tris/tricine gel (Bio-Rad). Peptide bands were fixed into the gel by incubating in 12.5% glutaraldehyde for 30 min. The gel was then washed three times with distilled water then stained with coomassie blue. Radioactive bands were analyzed by phosphorimaging.

Identification of WOX5 phosphorylation sites by mass Spectrometry.

This was performed as described by Meyer et al. (19). Briefly, tryptic peptides were generated from the reduced-alkylated protein using Sequencing Grade Modified Trypsin (Promega). The resulting peptides were desalted on a SOURCE 15 RPC column (GE Healthcare) and eluted in 90% acetonitrile, 0.1% TFA. The eluted peptides were then dried down in a vacuum centrifuge. Phosphopeptides were enriched using the PHOS-Select Ga^{3+} Silica Spin Column kit (Supelco) according to the kit instructions. The complex peptide mixtures were analyzed using high-resolution nano-LC-MS on a hybrid mass spectrometer consisting of a linear quadrupole ion-trap and an Orbitrap (LTQ-Orbitrap XL, Thermo Fisher Scientific). Chromatographic separations were performed using a NanoLC-1D™ Plus (Eksigent) for gradient delivery and a cHiPLC-nanoflex (Eksigent) containing a 15 cm x 75 μm C18 column (ChromXP C18-CL, 3 μm, 120 Å, Eksigent). The liquid chromatograph was interfaced to the mass spectrometer with a nanospray source (PicoView PV550; New Objective). The survey scans (*m/z* 350-2000) (MS1) were acquired at high resolution (60,000 at *m/z* = 400) in the Orbitrap and the MS/MS spectra (MS2) were acquired in the linear ion trap at low resolution, both in profile mode. The MS1 scan was followed by one MS2 event with collision activation in the ion trap (parent threshold = 10000; isolation width = 4.0 Da;

normalized collision energy = 30%; activation Q = 0.250; activation time = 30 ms). The following ion source parameters were used: capillary temperature 200 ºC, source voltage 3.3 kV, source current 100 μA, capillary voltage 34 V, and the tube lens at 125 V.

Data Analysis.

The MS2 spectra were analyzed by searching against the WOX5 sequence and expert manual interpretation. The exact masses of the phosphopeptide and fragmentation ions were calculated using the MS-Product utility within Protein Prospector (http://prospector.ucsf.edu). For database searches, the LC-MS files were processed using MASCOT Distiller (Matrix Science, version 2.3.0.0) with the settings previously described (20). The resulting MS2 centroided files were used for database searching with MASCOT, version 2.1.6, against a custom, in-house database containing the WOX5 sequence using the following parameters: enzyme, trypsin; MS tolerance = 15 ppm, MS/MS tolerance = 0.8 Da with a fixed carbamidomethylation of Cys residues and the following variable modifications: oxidation (Met) and phosphorylation (Ser, Thr, and Tyr); Maximum Missed Cleavages = 9; and 1+, 2+ and 3+ charge states. For analysis of the tandem spectra from spectral acquisitions in the Orbitrap (MS2), the raw files were processed using MASCOT Distiller (Matrix Science, Oxford, UK) with the following settings: 1) as described previously (19).

Hydrogen/Deuterium Exchange Mass Spectrometry

Differential, solution phase HDX experiments were performed to detect the conformational change of sACR4 induced by the addition of sALE2 or sCRK1. Each exchange reaction was initiated by incubating 4 μl of protein complex (with or without ALE2 or CRK1) with 16 μl of D_2O protein buffer (50 mM Bis Tris pH 7.2, 25 mM NaCl, 0.1 mM $MnCl_2$, 1 mM DTT) for a predetermined time (10, 30, 60, 120, 900, and 3600 s) at 4 °C. The

exchange reaction was quenched by mixing with 30 μl of 3 M urea, 1% TFA at 1 °C. The mixture was passed across an in-house packed pepsin column (2 mm X 2 cm) at 200 μl/min and digested peptides were captured onto a 2mm X 1cm C_8 trap column (Agilent) and desalted (total time for digestion and desalting was 3 min). Peptides were then separated across a 2.1 mm X 5 cm C_{18} column (1.9μ Hypersil Gold, Thermo Scientific) with linear gradient of 4%–40% CH_3CN, 0.1% formic acid, over 5 min. Protein digestion and peptide separation were performed within a ice water bath to reduce D/H back exchange. Mass spectrometric analyses were carried out with capillary temperature at 225 °C, and data were acquired with a measured resolving power of 100,000 at m/z 400. Three replicates were performed for each on-exchange time point.

Peptide Identification and HDX Data Processing

MS/MS experiments were performed with a LTQ Orbitrap mass spectrometer (ThermoFisher). Product ion spectra were acquired in a data-dependent mode and the six most abundant ions were selected for the product ion analysis. The MS/MS *.raw data files were converted to *.mgf files and then submitted to Mascot (Matrix Science, London, UK) for peptide identification. Peptides included in the peptide set used for HDX had a MASCOT score of 20 or greater. The MS/MS MASCOT search was also performed against a decoy (reverse) sequence and ambiguous identifications were ruled out. The MS/MS spectra of all of the peptide ions from the MASCOT search were further manually inspected, and only those verifiable are used in the coverage. The intensity weighted average m/z value (centroid) of each peptide isotopic envelope was calculated with HD Desktop (26). The deuterium level was calculated as described previously (27). Deuterium level (%) = {[m(P) - m(N)]/[m(F) - m(N)]} X 100%, where m(P), m(N) and m(F) are the centroid value of partly deuterated

peptide, nondeuterated peptide, and fully deuterated peptide, respectively. The correction of accounting for the known 80% deuterium content of the on-exchange buffer was made. No back exchange correction was made and all values are therefore reported as relative.

Homology models of ACR4 and AtCRK1 kinase domains

Homology models for the ACR4 kinase domain (residues 512 through 785 in the whole receptor) and the AtCRK1 kinase domain (residues 444 through 729 in the whole receptor) were built using Discovery Studio v 3.1 (Accelrys, San Diego, USA). Sequence analysis identified Interleukin-1 receptor associated kinase (PDB identification 2NRU_B) as the optimal template based on ~50% homology and 34% identity in the amino acid sequences. Protein models were generated by MODELER, which was originally developed by Sali (28) and the refined model was validated using the Verify Protein (Profiles-3D) protocol, which assesses the compatibility of the 3D structure of the protein model with its amino acid sequence.

Peptide overlay assays

The 'KDSAF' motif containing peptides (Fig. 7A) were chemically synthesized (Genscript) and engineered with an N-terminal biotin tag. Peptides were diluted 2.5 mM in Tris-HCl buffer, pH8.0. To demonstrate peptide binding to sACR4 KC protein, 2 μg of sACR4 KC and 2 μg of SUMO protein were separated by 12% SDS-PAGE and blotted to nitrocellulose membrane. Blots were briefly stained with a 0.1% Ponceau S solution to locate the protein bands. Bands were then cut from the blot, appropriately labeled, and destained in successive washes with distilled water and a final wash in 1X TBS (50 mM Tris-HCl pH 7.4, 150 mM NaCl) to remove Ponceau S staining. Blots were then blocked with 5% milk protein in TBS + 0.1% Tween 20 for 1 h. After blocking, blots were washed three

times with TBS + 0.1% Tween 20 (5 min each wash) and then added to individual microfuge tubes containing 1 ml of TBS and the appropriate peptide to a final concentration of 100 μM. To demonstrate specific binding to ACR4, peptides were also incubated with SUMO protein as a control. Blots were incubated on a rotating platform for 2 h at room temperature, followed by two washes with 1.5 ml of TBS at 5 min intervals. To detect peptide binding, 1 ml of TBS containing 1:500 streptavidin conjugated Alkaline Phosphatase (AP) (Pierce) was added to each tube. Blots were incubated on a rotator for 1 h at room temperature, washed as described above to remove excess streptavidin-AP followed by colorimetric detection of peptide binding using the AP Substrate kit (Bio-Rad). The presence of sACR4 and SUMO proteins were confirmed in separate blots probed with anti-SUMO primary antibody (1:1000) and polyclonal anti-rabbit secondary antibody (Sigma, 1:15,000).

Peptide binding assays

The binding of 'KDSAF' peptide binding to sACR4 KC protein was demonstrated as follows. First, a 96 well nickel coated plate (XpressBio) was washed three times with TBS + 0.1% Tween20, excess wash buffer was discarded. A 0.8 μM solution of sKC (5 μg/100 μl) or SUMO protein (1 μg/100 μl) was prepared in TBS + 0.1% Tween 20. 100 μl of appropriate protein solution was added to individual wells and incubated on an orbital shaker for 1 h at room temperature to allow protein to bind to the plate. Wells containing immobilized sKC or SUMO protein were washed three times with TBS + 0.1% Tween 20 to remove unbound material. 'KDSAF' peptide solutions were prepared in TBS to a final concentration of 200 μM. 50 μl of the peptide solutions were added to appropriate wells and allowed to incubate on an orbital shaker for 2 h at room temperature. After incubation, excess peptide solution in the wells was discarded. Wells were then washed with TBS two

times with gentle shaking to remove unbound peptides. 50 µl of a streptavidin-AP solution (1:500) was added to each well and incubated on an orbital shaker for 1 h at room temperature. Streptavidin-AP solution was discarded and the wells were washed twice with TBS using gentle shaking, excess wash buffer was discarded. Colorimetric detection of peptide binding was initiated by adding 100 µl of a pNPP solution (100 mM ethanolamine pH 9.8, 10 mM pNPP) to each well. The reactions were allowed to incubate 5 min with occasional manual shaking. Reactions were terminated with the addition of 50 µl of 2N NaOH to each well. 100 µl of each reaction was diluted with 400 µl of water and absorbances at 405 nm were obtained. Bar diagrams were generated by accounting for the dilution factor and subtracting the absorbance of the control (SUMO) wells from the experimental (sACR4 KC) wells. Each peptide binding experiment was performed in triplicate.

Phage peptide library construction

The phagemid vector pCANTAB 5E (GE healthcare) was used to construct a random 21-amino acid library fused to the pIII coat protein (Rao laboratory, unpublished data). Briefly, two oligonucleotide primers were first synthesized (Integrated DNA Technologies). The forward primer 5'-CGTGGT**GGCCCAGCCGGCC**$(NNK)_{21}$**GCGGCCGC**AGCACGACAG-3' contained the degenerate codon NNK encoding all 20 amino acids and the TAG stop codon. The oligonucleotide also incorporated *Sfi*1 and *Not*1 restriction enzyme sites at the 5' and 3' ends respectively. A complementary reverse primer 5'-CTGTCGTGCTGCGGCCGC-3' was used for double-strand synthesis, followed by digestion with Sfi1/Not1 and ligation into the similarly digested phagemid vector. Multiple transformations of highly electro-competent

(competency > $1.0x10^{10}$) SS320 *E. coli* cells and phage preparation resulted in a phage-peptide library with a diversity of ~ $1x10^{9}$. The library was validated by first screening against the anti-FLAG monoclonal antibody that recognizes the sequence epitope DYKDDDDK. Four rounds of screening against the antibody yielded >95% clones containing the core sequence DYKxxD.

Phage peptide library screening of the pJMD1 peptide

Biotinylated peptides were immobilized on 20 µl of streptavidin coated beads (Dynabeads® MyOne™ Streptavidin T1, Invitrogen) and dispersed in 100 µl of phosphate buffer saline pH, 7.4 (PBS) at room temperature with gentle rotation for 45 mins. The beads were washed three times with PBS containing 0.1 % BSA. Peptide coated beads were blocked with PBS containing 0.1 % BSA for 30 mins followed by 2 washes with PBS containing 0.1 % BSA. Beads were then incubated with phage (100 µl diluted in 900 µl of PBS containing 0.1 % BSA) for 3 h at room temperature with gentle rotation. The unbound phage was washed 3 times with PBS and then the beads were transferred into fresh eppendorf tubes. The bound phage was eluted by incubating with 500 µl of 0.1 M HCl for 5 mins at room temperature with the aid of shaking. The eluted phage was immediately neutralized by the addition of 167 µl of 1M Tris-HCl buffer pH 8.0, followed by infection of XL1-Blue cells (grown to < 0.6 OD in 10 µg/ml tetracycline) with the phage. Infected XL1-Blue cells were incubated at 37 °C for 20 mins followed by addition of helper phage and again incubating at 37 °C for 30 mins. The phage infected XL1-Blue cells were transferred into a conical flask containing 50 ml of 2YT media containing 10 µg/ml of tetracycline and 100 µg/ml ampicillin and was further incubated at 37 °C overnight with shaking at 210 rpm.

Phage preparation was carried out by centrifuging the overnight culture at 8000 rpm for 10 mins. The supernatant was collected into another centrifuge tube and the phage was precipitated by adding 12.5 ml of 20 % PEG 8000 and 2.5 M NaCl solution at room temperature. The precipitated phage were collected by centrifugation at 12,000 rpm for 20 mins and diluted with 1 ml of PBS. This was the first round of enriched phage. The entire process was repeated for four rounds and for each subsequent round of biopanning, enriched phage from previous round was used. During the 3rd and 4th round of panning, the wash buffer contained 0.01 % Tween 20. Following 3rd and 4th round panning, phage infected XL1-Blue cells were grown on 2YT ampicillin plates and 50 colonies were characterized by DNA sequencing after plasmid preparation.

Results

In vitro Interactions between the ACR4 and CRR ICDs

We examined potential interactions between the ICDs of ACR4 and the CRRs by gel filtration chromatography (Fig. 1), demonstrated to be useful in the analysis of the hydrodynamic properties of oligomeric kinase protein complexes (29-31). We first recombinantly expressed the intracellular domains of ACR4, its homologs and ALE2, as C-terminal fusions to the yeast SUMO protein, termed sACR4, sCRR, and sALE2. Pairs of unphosphorylated proteins were then incubated together at equimolar concentrations (5 μM each) and subjected to gel filtration. It is evident by this analysis that purified sACR4 protein is predominantly monomeric, although there is evidence of higher order oligomers (Fig. 1A and inset). This is in agreement with our previous gel filtration studies of the NusA fused

ACR4 ICD (19) and indicates that the solubility tag does not influence oligomerization. When sACR4 was incubated with sCRR2 or sCRK1, the gel filtration profile clearly indicated interactions between these proteins. Thus, the elution profiles showed the formation of oligomeric complexes containing sACR4/sCRR2 (Fig. 1B, left panel) and sACR4/sCRK1 (Fig. 1D, left panel) when analyzed by SDS-PAGE (Fig. 1B and D, *left panels inset*). Importantly, neither sCRR2 (Fig. 1B, right panel) nor sCRK1 (Fig. 1D, right panel) by themselves showed any evidence of self-association in the absence of phosphorylation at the concentrations examined during gel filtration. These results suggest that ICDs of CRK1 and CRR2 can interact with the ICD of ACR4 in the absence of phosphorylation. No oligomeric complexes were observed with the sACR4/sCRR3 or the sACR4/sALE2 samples. It is possible that ACR4 ICD has a higher propensity for self-association than for heteromeric association with either sCRR3 or sALE2. Therefore, higher concentrations of sCRR3 or sALE2 may be required to drive a heteromeric association with sACR4. Furthermore, other regions of the receptor, the transmembrane domain or extracellular region, may also be important. The interaction between sACR4 and sCRR1 could not be studied by gel filtration owing to the propensity of sCRR1 to aggregate under these conditions. The reason for this is not entirely clear, although it is possible that other structural elements lacking in the CRR1 ICD may influence its aggregation propensity (17).

Effects of phosphorylation on heteromeric interactions

The kinase domains of many plant receptors are known to undergo phosphorylation during receptor activation and oligomerization (32-34). To determine if the interactions between the ICD of ACR4 and the ICDs of the CRRs and ALE2 was influenced by phosphorylations, *in vitro* pull-down experiments were performed with various combinations

of autophosphorylated kinases. The MBP-fused ICD of ACR4 (mACR4) protein (~0.4 μM) was used as the bait and the sCRRs/sALE2 proteins (~1 μM) were used as the prey. Therefore, the target proteins were in ~ 2.5 molar excess over the mACR4 bait protein. In the naïve, unphosphorylated state, mACR4 was able to pull out all of the naïve sCRR proteins (Fig. 1D). This suggests that these kinases possess the intrinsic propensity to hetero-oligomerize in the unphosphorylated state. It is worth noting that this experiment was able to demonstrate an interaction between the naïve mACR4 and sCRR3 when the concentration of sCRR3 was in excess of sACR4, suggesting that concentration effects may indeed drive hetero-association of these two proteins not seen in our gel filtration studies that was performed at a lower protein concentration. Additionally, the SUMO tagged ACR4 (sACR4) intracellular domain was pulled out by mACR4 confirming previous sedimentation velocity experiments using the NusA fused ACR4 ICD that indicated kinase domain oligomerization in the absence of phosphorylation (19). Control reactions showed these interactions were specific towards the ICDs and were not due to interactions with the SUMO and MBP solubility tags or nonspecific binding of fusion proteins to the amylose resin (data not shown). The presence of mACR4 in each reaction was confirmed with western blots using polyclonal, anti-MBP antibody (Fig. 2, *lower panel*) and the sCRRs were confirmed by western blots probed with a polyclonal, anti-SUMO antibody (Fig. 2A-D).

Interestingly, autophosphorylation of the ICDs had striking effects on ACR4 interactions with the CRR homologs. Loss of interaction occurs between mACR4/sACR4 (Fig. 2A, *lane 1*). The fact that phosphorylated mACR4 does not interact with phosphorylated sACR4 supports our previous observation that ACR4 monomerizes upon autophosphorylation (19). The interaction between phosphorylated mACR4 and

phosphorylated sCRK1 is attenuated but not completely abolished, suggesting this kinase complex may form at the cell surface during receptor activation (Fig. 2A). Intriguingly, the interaction between sACR4 and sCRR3 is completely abolished, demonstrating that autophosphorylation of the ICDs forces disassociation of these two proteins. The dissociation may be due to conformational changes that accompany autophosphorylation (19) and/or electrostatic repulsion due to increases in net negative charge from autophosphorylation.

The interactions observed between the mACR4/sACR4 and mACR4/sCRR3 showed decreased binding ability depending on whether the bait protein (mACR4) or the target protein (sACR4, sCRR3) was in the phosphorylated state (Fig. 2B and C) as compared to the two extremes of where the participating proteins are either in the phosphorylated state (Fig. 2A) or unphosphorylated state (Fig. 2D). These results indicate that autophosphorylation of both partners is required to disrupt the intracellular contact between ACR4/ACR4 and ACR4/CRR3 kinase domains. The fact that mACR4 is able to strongly interact with sCRR1 and sCRR2 regardless of phosphorylation state (Fig. 1A-D), raises the possibility that ACR4 may be able to signal through the use of dead kinase domains (35, 36). We did not observe any interactions between mACR4 and sALE2 in the pull-down experiments regardless of phosphorylation status or using an excess molar ratio of sALE2 compared to mACR4. This observation suggests that the intracellular domains of ACR4 and ALE2 may not interact with each other directly but may do so in the presence of other proteins or could be modulated by the extracellular domains or the transmembrane regions of other RLKs.

ACR4 can phosphorylate the CRR homologs

Receptor activation through homo- or heterodimerization is accompanied by intra and intermolecular phosphorylation reactions, recruitment of proteins to the intracellular domain of the receptor and subsequent activation of signaling events inside the cell (1, 10, 14). Previous studies have proposed that ACR4 can phosphorylate CRR2 in an *in vitro* phosphorylation assay (17). We further assessed the ability of ACR4 to phosphorylate the CRRs by incubating the active mACR4 kinase with the kinase dead, sCRR and sALE2 mutants (sCRRms/sALE2m) (Fig. 3A). Since CRR3, CRK1, and ALE2 have robust kinase activity (Chapter 2), we mutated the catalytic Asp (37) of each kinase to Ala in order to inactivate each enzyme (Materials and Methods). Although CRR1 and CRR2 have intrinsically very weak kinase activity attributable to the absence of the activation loop in each protein (17), in order to completely eliminate autophosphorylation activity, we also mutated the catalytic Asp in both CRR1 and CRR2 to Ala. Inactivity of each mutant was confirmed by an *in vitro* autophosphorylation assay (Fig. 3B). However, in the case of ALE2, mutation of the catalytic Asp to Ala resulted in an unstable protein. Therefore, the essential Lys residue (37) was mutated to Ala to obtain a more stable protein albeit one with weak residual kinase activity (Fig. 3B, *lane 5*). The ACR4 kinase can in fact phosphorylate the intracellular kinase domains of all four CRR homologs *in vitro*. Amongst the CRRs, the weakest phosphorylation activity was seen against sCRR1m (Fig. 3A, *lane 1*) and relatively stronger activity was seen against the sCRK1m ICD (Fig. 3A, *lane 4*). Thus, these *in vitro* experiments suggest that ACR4 may also have the potential to phosphorylate the CRRs *in vivo*. Interestingly, sACR4 showed the strongest phosphorylation activity against the sALE2 ICD (Fig. 3A, *lane 5*) and is in agreement with the observations of Tanaka et al. (20). No

phosphorylation of the yeast SUMO protein was observed when incubated with sACR4 indicating that the phosphorylations of the SUMO-tagged CRRs and ALE2 was specific to the intracellular domain and not to the fusion tag (Fig. 1A, *lane 6*).

Mapping ACR4/CRK1 interaction sites by H/D exchange

Thus far, our interaction studies have shown that ACR4 can interact with all of the CRR homologs in the unphosphorylated state. To assess the molecular basis of these interactions, we used hydrogen-deuterium exchange coupled to mass spectrometry in order to map potential intermolecular interactions sites within the ACR4 ICD. Hydrogen-deuterium exchange (HDX) is an effective tool to map in solution protein-ligand interaction sites and determining conformational dynamics of proteins (38, 39). This technique makes advantageous use of backbone amide hydrogens and their availability for isotopic labeling with deuterium from the solvent. Amide hydrogens undergoing intra- or intermolecular hydrogen bonding have reduced exchange rates when compared to amide hydrogens exposed to the solvent. Therefore, hydrogen exchanged with deuterium can be monitored by mass spectrometry to delineate specific regions within a protein sequence that are solvent accessible. Binding interfaces within a protein complex can be determined by comparing HDX rates of the bound and unbound state (40-42). Consequently, mapping of isotopically labeled peptides along a given protein sequence provides a general idea of potential protein-protein interactions sites.

On the basis of the gel filtration, pull-down, and phosphorylation studies, we determined that CRK1 was a good candidate for mapping potential interactions sites between the unphosphorylated ACR4 and CRK1. The experiment was initially performed with the unbound, *apo*-sACR4 protein to determine individual HDX profiles for all peptides produced

from the in-line pepsin digest of the sample. Overall, 100 peptides with overlapping sequence corresponding to the ACR4 ICD were identified in the mass spectrometry analysis of peptic fragments generated from the *apo*-sACR4 enzyme. Peptide sequence coverage was ~98% of the ACR4 intracellular domain. This data was then compared to peptide HDX profiles generated from the *holo*-sACR4 protein bound to sCRK1 after prior incubation at ratios of 1:1 or 1:3 (see Materials and Methods). Evaluation of the mass spectrometry data revealed two sites of protection within the ACR4 ICD. One site, corresponding to the peptic fragment FRTELDL, is a part of helix-C in the N-terminal lobe of the kinase domain. This region displayed a significant average decrease in percent deuteration of 5%. The second peptide, YRLHY, occurs in the C-lobe of the kinase domain, just downstream of the C-terminal hinge of the activation loop, and showed a 6% average decrease in deuterium uptake compared to the *apo*-ACR4 sample (Fig. 4). The decrease in deuterium uptake is indicative of a significant involvement of these two regions in interfacial contacts between ACR4 and CRK1. Interestingly, as depicted in the modeled structure, both regions fall on the same side of the ACR4 kinase molecule (Fig. 5). Our experiments did not reveal any differences in HD exchange for peptides corresponding to the JMD or CTD of ACR4. However, further studies are needed to ascertain the exact role of these subdomains in potential protein-protein contacts.

Phage panning of pJMD1 peptide

Many cellular functions in eukaryotic cells are mediated by modification-dependent interactions between small protein recognition modules (PRM) and their cognate ligands. Examples of PRMs include the Src homology 2 (SH2) domain binding to phosphotyrosines, Src homology 3 (SH3) and WW domains binding to polyproline motifs (43, 44). In general,

the recognition sequences for the PRMs are short stretches of continuous peptide sequence <10 residues long, called Short Linear Motifs (SLiM) that occur within the cognate interacting protein (45). Peptide ligands have been isolated from phage peptide libraries (46-48) that in many instances show conservation of the motifs in native interacting proteins, facilitating the first step towards identification of natural candidate proteins *in vivo* (49, 50). Phosphorylation of Ser/Thr residues also creates binding surfaces for diverse phosphoamino acid binding modules such as the 14-3-3, WW and forkhead-associated (FHA) (51). However, the structure and mechanism of phosphobinding are quite diverse (52) and combinatorial peptide library screening has been very successful in defining the specificity of these PRMs to identify consensus peptide sequences as well as discover novel binding motifs (53). Furthermore, biochemical studies have demonstrated that phosphorylation of residues within the noncatalytic juxtamembrane and/or C-terminal regions flanking the core kinase domain of several receptors act as recruitment sites for intracellular substrate proteins (54-58). Thus, as described in the previous chapter, we utilized a random 21 amino acid phage peptide library to identify potential binding motifs to the phosphorylated Ser^{475} in the pJMD1 peptide ^{468}DTRSSKDpSAFTKDNG^{482}. The target peptide was immobilized on a streptavidin coated plate via the N-terminal biotin tag and subjected to four rounds of biopanning (see Materials and Methods). Phage binding after the fourth round were enriched for peptides that bind the pJMD1 peptide.

After the fourth round of panning, 46 phage isolates were selected at random and sequenced. Interestingly, 35% of the clones selected had the sequence, YRWWDSAINLHSLLFSPPLFG (Fig. 6). Notably, this peptide contains the sequence LXXLL, a motif that has been identified as regulating protein-protein interactions among the

mammalian nuclear receptors, transcription factors, and coactivators (59-61). Additionally, 30% of the selected sequences contained variations of the LXXLL motif further defining it as the predominant binding motif to the pJMD1 peptide. Recently, identification of a LXXLL motif in the Tomato Atypical Receptor-like Kinase (TARK1) was shown to be responsible for direct binding to the XopN virulence factor (62). In the same study, XopN was shown to also contain a LXXLL motif that is required to bind to TARK1 (62). Remarkably, sequence analysis of ACR4, CRR3, and CRK1 revealed that they all harbor LXXLL motifs within their ICDs. ACR4 houses this motif in two locations, one in the N-lobe (LLSLL) which is most similar to the LXSLL motif found in the YRWWDSAINLHSLLFSPPLFG peptide and one in the C-lobe of the kinase domain (LLELL), while CRR3 and CRK1 contain this motif in the respective kinase C-lobes. A second motif was also preferentially selected through our phage display screening. Two peptides containing the consensus motif, FXPYEL, were selected and represented 24% of the peptides that were sequenced. The observation of this motif indicates an additional linear sequence that is able to recognize the pJMD1 phosphopeptide and potential protein-protein interactions mediated by this motif is addressed later in this article.

'KDSAF' motif binds ACR4 kinase domain

Results from our phage display experiments suggested that conserved features among the JMDs of the CRR homologs or ALE2 could be involved in protein-protein interactions among these proteins. Therefore, we performed sequence similarity searches between the JMD of ACR4 and the intracellular domains of the CRRs and ALE2. Interestingly, a close scrutiny of the amino acid sequences of ACR4, CRR3 and CRK1 revealed a highly conserved 'KD/ESAF' motif and a similar RDREF motif in ALE2 (Fig. 7A). The inactive

CRR1 and CRR2 ICDs do not contain this motif, suggesting that this region may serve a critical role in the kinase-active members of the ACR4 family. Whereas the KDSAF sequence is found in the JMD of ACR4, in CRR3, CRK1, and ALE2 it occurs in the kinase domain towards the N-terminal portion of the presumed helix-C region (Fig. 8). The identification of conserved KDSAF and LXXLL motifs therefore allows us to propose an intriguing model for interaction among these proteins based on the 'KDSAF' motifs of CRR3, CRK1, and ALE2 forming intermolecular contacts between themselves and the LLSLL region in the ACR4 N-lobe.

To test this hypothesis, we synthesized peptides corresponding to the helix-C regions of CRR3, CRK1, and ALE2 (termed hC peptides), and the unphosphorylated JMD1 peptide which contains the 'KDSAF' motif in ACR4, for use in a peptide overlay assays (Fig 7A). The unphosphorylated JMD1 peptide was used in our experiments since we are currently unaware of phosphorylation at the Ser/Thr residue within the 'KDSAF' motif of CRR3, CRK1, or ALE2. As described in Materials and Methods, peptide binding was assessed by colorimetric detection using streptavidin conjugated Alkaline Phosphatase. Our results unequivocally show direct binding of the 'KDSAF' containing peptides to the sACR4 KC, a protein lacking the JMD (Fig. 7B, *upper panel*). Importantly, the peptides do not bind to the SUMO protein used as a control (Fig. 7B, *lower panel*). The presence of blotted sACR4 KC or SUMO protein was verified by independent western blots using anti-SUMO antibody (data not shown).

In a comparable experiment we determined peptide binding to sACR4 KC that was immobilized on Ni^{2+} coated plates through the N-terminal histidine tag to ensure that the 'KDSAF' peptides binding to sACR4 KC was not an artifact caused by nonspecific binding

to a misfolded protein. The data in Fig. 7C, demonstrates that all four 'KDSAF' motif containing peptides are able to bind to the sACR4 KC protein to different extents. The CRR3 and CRK1 hC peptides showed the highest binding affinity to sACR4 KC and had similar binding capacity under our assay conditions. The ALE2 hC peptide also interacted with sACR4 KC, but with ~4-fold less affinity than either CRR3 or CRK1 hC peptides. Interestingly, the JMD1 peptide was capable of binding to sACR4 KC, indicating that the unphosphorylated JMD can make intramolecular contacts with the ACR4 kinase domain. Autoregulation of receptor kinase domains by the neighboring, non-catalytic JMD is a common mechanism to regulate kinase activity (63-69). The differences in binding affinities seen with these peptides suggest that variations in the flanking residues of the core 'KDSAF' motif may influence binding affinity. The peptide binding results provide strong support for the involvement of the 'KDSAF' region in intermolecular contacts among CRR3, CRK1, and ALE2.

ACR4 can phosphorylate 'KDSAF' region of CRR3

We next examined whether ACR4 could phosphorylate the hC peptides as phosphorylation within this region could represent a potential regulatory mechanism for ACR4 association with its binding partners. The CRR3 and CRK1 hC peptides contain a Ser or Thr within their respective 'KDSAF' regions whereas, in ALE2, the central position is replaced with arginine. Nonetheless, it does contain a Thr residue at the N-terminus that could be phosphorylated (Fig. 7A). *In vitro* kinase assays performed with wild-type sACR4 and individual hC peptides showed intermolecular phosphorylation of the CRR3 hC peptide (Fig. 7D). This is commensurate with our phosphorylation assays demonstrating that CRR3 ICD is phosphorylated by ACR4 (Fig. 3). However, in contrast to the kinase assay with the

whole protein (Fig. 3), no phosphorylation signal was seen with CRK1 and ALE2 hC peptides. In part, this may perhaps be attributed to the more important role of distal sequences in phosphorylation.

ACR4 directly interacts with WOX5

Previous reports have suggested a signaling module involving ACR4 and the WOX5 transcription factor. WOX5 expression dynamics are proposed to be influenced by ACR4 acting through the perception of a postulated CLE40 peptide ligand. ACR4 is primarily expressed in the D1-D3 cell layers in the root tip, whereas WOX5 is solely expressed in quiescent center (QC) (22, 23, 70). Overexpression of the CLE40 gene or application of exogenous CLE40 peptide expands the ACR4 expression domain to include the QC (22, 23). We therefore hypothesized that the ACR4 intracellular domain may have the capability to directly interact with WOX5 and phosphorylate it, thus affecting WOX5 function inside the cell. We cloned and expressed milligram quantities of WOX5 as a C-terminal fusion to the maltose binding protein (MBP) with a 6X histidine tag at the C-terminus to aid in purification of full length protein (see Materials and Methods).

To examine the *in vitro* association of ACR4 with WOX5, we first incubated the purified sACR4 and mWOX5 proteins together and used amylose resin to pull-down the mWOX5 protein. Additionally, in a parallel experiment, we determined the effect of autophosphorylation of the ACR4 ICD on interaction with WOX5. Our results demonstrate that mWOX5 is indeed pulled-down by naïve sACR4 protein (Fig. 9A, *upper panel, lane 2, arrow*) but not by phosphorylated protein indicating that autophosphorylation is not a requirement for association. To unequivocally show that mWOX5 is pulling out sACR4 and that the protein band observed (Fig. 9A, *upper panel, lane 2, arrow*) is not a degradation

fragment of mWOX5, we performed separate western blots using anti-SUMO and anti-MBP antibodies to demonstrate the presence or absence of each protein. In addition, control reactions using either the SUMO or MBP solubility tags demonstrate the observed interaction was specifically between the ACR4 ICD and WOX5 (Fig. 9A and B, *lanes 3-5*). Interestingly, the autophosphorylated sACR4 is unable to interact with mWOX5 (Fig. 9B, *lane 2*). However, this is not a complete surprise since WOX5 is a transcription factor that may be phosphorylated by ACR4, thus activating the protein.

Mapping of in vitro WOX5 phosphorylation sites

The in vivo expression patterns of WOX5 and ACR4 have been demonstrated to overlap in the *Arabidopsis* root tip (22, 23). In addition, our pull-down studies indicate that the ICD of ACR4 can interact with WOX5. Therefore, we considered the possibility that the ACR4 kinase domain could phosphorylate WOX5, thus affecting WOX5 function in the root. Transcription factors can be regulated through reversible phosphorylation, therefore regulating their function inside the cell. For example, Stat transcription factors can be directly phosphorylated by the EGF receptor kinase domain to modulate their DNA binding activity (72, 73). Thus, we incubated sACR4 with mWOX5 in an *in vitro* kinase assay in the presence of [γ-^{32}P] ATP. We clearly demonstrate that WOX5 is phosphorylated by sACR4, *in vitro* (Fig. 10, *lanes 2-4*). Since sACR4 and mWOX5 have similar migration patterns on an SDS-PAGE gel, we wanted to ensure the signal in the autoradiogram was due to WOX5 phosphorylation and *not* sACR4 autophosphorylation. Therefore, after incubation, the phosphorylated mWOX5 protein was pulled-down by amylose resin and extensively washed to remove autophosphorylated sACR4. Indeed, the appearance of the radioactive band was due to mWOX5 phosphorylation, as seen by the absence of sACR4 when incubated alone

(Fig. 10, *lane 1*). A separate control reaction performed under the same conditions with sACR4 and MBP confirmed that the phosphorylation was specific towards WOX5 and not the MBP solubility tag (Fig.10, *lanes 5-7*). Thus, ACR4 may also have the potential to phosphorylate WOX5 *in vivo*.

We next determined the sites of phosphorylation within the WOX5 protein by collision induced dissociation (CID) tandem mass spectrometry. The data dependent analysis of tryptic peptides and a search against the mWOX5 protein sequence (Fig. 11) yielded several phosphorylated peptides. Assignment of the phosphorylation site was performed by verifying the presence of diagnostic site-discriminating *y* and *b* series ions. For example, the CID tandem mass spectrum of the phosphopeptide encompassing the junction between the C-terminal end of the solubility tag and the N-terminal sequence of WOX5, GSAGAALG(pS)FSVK, is shown in Fig. 11B. The predominant species is the $[M+2H-98]^{2+}$ ion (*m/z* of 567.3) carrying a +2 charge state. This is characteristic of a neutral loss of phosphoric acid which is indicative of a phosphorylated peptide. Exact assignment of the phosphorylation at Ser^2 (in WOX5 amino acid sequence) was verified by the presence of site-discriminating ions including the phosphorylated b_9 (theoretical *m/z* 654.32, observed *m/z* of 654.33) and y_5 (theoretical *m/z* 549.30, observed *m/z* of 549.33) ions and the unphosphorylated b_8 (theoretical *m/z* 585.30, observed *m/z* of 585.17) and y_4 (theoretical *m/z* 480.28, observed *m/z* of 480.30) ion. The absence of the phosphorylated b series of ions corresponding to b_2-b_8 and y series ions y_3-y_4, further confirmed that phosphorylation occurs at Ser^2. A total of four phosphorylation sites were identified within the WOX5 sequence (Fig. 11A). Table 1 summarizes the site-discriminating ions for the four confirmed sites at Ser^2, Ser^4, Ser^{88}, and Ser^{158} of the WOX5 protein. Intriguingly, phosphorylation at two Ser

residues occurs in a 'GSFS' motif within WOX5. ACR4 also contains a 'GSFS' sequence located within the glycine-rich loop of the kinase structure and is autophosphorylated at the first Ser (19). Furthermore, a third phosphorylation site in WOX5, Ser^{158}, is found in a 'TSFS' motif that is highly similar to the 'GSFS' sequence. These data suggest a potential recognition motif for ACR4 substrate phosphorylation of WOX5 *in vivo*.

Database mining of pJMD1 consensus binding motifs

In our phage-display screening of the pJMD1 peptide, two consensus peptide motifs LXSLL and FXPYEL, were identified. In order to establish potential interacting proteins to the pJMD1 peptide sequence, we queried the consensus binding motifs against the *Arabidopsis* protein database using the Sequence Pattern search function in Scansite 2.0 (MIT, http://scansite.mit.edu/). Queries with the consensus motifs LXSLL, LLXLL and LLXXL yielded a multitude of protein hits. Proteins that had an unknown function or did not have an apparent relevance to signal transduction were disregarded. Our analysis included members of the RLK family, phosphatases, and transcription factors (Table 2). The sequence of each RLK in our query was examined to ensure the consensus motif was located in the intracellular domain. RLKs that contained the consensus motif in the presumed extracellular space were discarded. As mentioned earlier, the AtCRRs were among the more significant RLKs identified in our search. Additionally, some RLKs involved in plant growth and development were also identified including Brassinosteroid receptor kinase 1 (BRI1), somatic embryogenesis receptor kinases 4 and 5 (AtSERK), and ANXUR1 and 2 (14, 74, 75). Inasmuch as the significance and role of these RLKs in ACR4 signaling remains to be elucidated, there is increasing evidence of RLK crosstalk via heterodimer formation to activate differential signaling pathways in plant signaling behavior (14, 34, 74).

A parallel query with the consensus motif FXPYEL, however, yielded no hits. Searching with the overlapping sub-sequences FXPY and PYEL returned a total of 295 matches. The FXPY motif yielded the largest return of 280 proteins, with the PYEL only returning 15 proteins containing this motif. Identified proteins included those specifically involved in signal transduction processes such as protein phosphatases, transcription factors, F-box containing proteins, and ASYMMETRIC LEAVES2/LATERAL ORGAN BOUNDARY (AS2/LOB) domain containing proteins. It is worth noting that 27 of the proteins were members of the AS2/LOB domain containing family. AS2/LOB domain proteins comprise a 42 member family in *Arabidopsis* that have been shown to have influence functions in plant development, most notably lateral organ development in the meristem and cell fate specification in flower petals (76). Interestingly, the WOX5 transcription factor was among the proteins identified with a 'FXPY' motif. WOX5 contains a 'FSPY' motif (residues 159-162) that is localized to the C-terminal end of the protein (Fig. 11A). Moreover, we have identified an *in vitro* ACR4 phosphorylation site at the Ser^{158} positioned just upstream of this motif. However, the functional significance of this motif and the role of phosphorylation at Ser^{158} have yet to be determined.

Discussion

In higher animals and plants, directed cell proliferation, specification, and differentiation during growth and development are guided by a variety of external stimuli that are perceived and interpreted by a multitude of cell surface receptors primarily mediated through RTKs in animals and by RLKs in plants. The accepted paradigm of signal

transduction involves ligand perception/binding to the extracellular domain, activation of the intracellular kinase domain and subsequent activation of downstream signaling pathways through reversible phosphorylation events. Subsequently, downstream signaling components influence transcriptional activity in the nucleus allowing appropriate cellular responses to specific signaling cues.

In recent years, however, it has become apparent that the concept of a single receptor-single ligand interaction is perhaps too simplistic. Thus, structural, biophysical, biochemical and functional studies of several RTKs such as the Epidermal Growth Factor Receptor (EGFR) family (10-12, 56), Somatostatin and Opioid receptors (77), Insulin-like Growth Factor Receptor (78), and Platelet-derived Growth Factor (PDGF) (79) have demonstrated the capacity of these RTKs to assemble as homo- or heterodimeric complexes with distinct ligand specificity/affinities and downstream signaling activity. Similar heteromeric interactions occur among RLKs such as FLS2 and BAK1 (80), CLAVATA2 (81), and BRI1 (13, 14) and their impact on downstream signaling cascades is well established. Among the five members of the ACR4 receptor family, limited genetic and cell biology analyses have suggested these receptors may act in the same genetic pathway through functional redundancy based upon gene duplication and/or through activation of signaling cascades via receptor heterodimerization (15, 17, 21). Furthermore, RT-PCR studies of ACR4 and CRR transcript levels in varying tissues encompassing the entire *Arabidopsis* plant demonstrate all family members are expressed within all tissues examined, except for CRR2 and CRK1 which are not expressed in the siliques (17). Therefore, based upon their overlapping expression patterns in a variety of tissues, it is tempting to speculate that these proteins may also have the capacity to functionally interact *in vivo*.

In this study we have analyzed the *in vitro* interactions between the ICDs of ACR4 and the CRRs to elucidate the molecular aspects of protein-protein interactions within this receptor family. Ideally, crystal structure determination of complexes between ACR4 and the CRRs would facilitate an atomistic level understanding of these interactions. In the absence of structural information, we utilized hydrodynamic analyses, peptide binding studies, pull-down assays and phage display to demonstrate protein-protein interactions among members of the ACR4 family. Our gel filtration studies and pull-downs show that, in the unphosphorylated state, the ICD of ACR4 can self-associate (Fig. 1A and Fig. 2D, *lane 1*) and also bind to all four CRR ICDs (Fig. 1B and D and Fig. 2D), thus indicating that the intracellular regions of these receptors have the potential to form inactive, heteromeric complexes. Indeed, examples exist in which RTKs are capable of preformed, inactive heterodimer complexes in a ligand independent manner. For instance, the EGFRs are able to form homo- or heterodimeric structures in the absence of external signaling molecules (82, 83). Furthermore, the intracellular kinase domains of the EGF receptor family also contribute to receptor oligomerization (83-86). Among RLKs, an example of receptor homodimerization is seen for the BRI1 receptor in the absence of the brassinosteroid ligand (87) and the *Arabidopsis* Somatic Embroygenesis Receptor Kinase 1 (AtSERK1) is also able to form homodimers in protoplasts (88). Interestingly, the ICDs of CRR2, CRR3, and CRK1 do not show evidence of homodimerization (Fig. 1B, C, and D, *right panels*) although it is possible that they may have the capacity to form heteromers within the family. Indeed, precedent for such a heteromeric interaction exists in the five member AtSERK family, wherein AtSERK1 is able to heterodimerize with AtSERK2 in cowpea protoplasts (74).

The effect of phosphorylation on the interactions between the ICD's of ACR4 and the CRRs in the pull-down assays raises some intriguing questions about regulation of *in vivo* receptor activity. Thus, the inability of ACR4 to self-associate or even interact with CRR3 after phosphorylation (Fig. 2A), suggests that pre-existing complexes may be activated upon ligand binding, allowing dissociation to monomeric receptors and subsequent engagement with other receptors/membrane bound proteins to induce a signaling cascade. Alternatively, in the activated state, the heteromeric complex could still be maintained through interactions between the transmembrane domains as well as the extracytoplasmic domains, as has been reported for the EGFR family (89-93). In this model, it would be conformational changes in the cytoplasmic domain that would disrupt the protein-protein interactions. On the other hand, the interaction between ACR4 and CRK1 is attenuated but not completely eliminated in the phosphorylated state, indicating that active kinase domains may transduce signal via an active heterodimer complex. Indeed, signaling from the BRI-BAK1 receptor complex is achieved through *trans* phosphorylation of receptor partners to fully activate the receptors (14). Furthermore, it has recently been shown that fully active cytoplasmic domains of the FLS2 receptor and BAK1 (80) are required for immune responses in the plant (34, 94). We have also demonstrated that the ICD of ACR4 is capable of binding to the kinase-dead CRR1 and CRR2 ICDs regardless of the phosphorylation status (Fig. 2A and D). This observation is particularly interesting in light of the fact that in animals there are atypical RTKs with kinase-inactive domains that signal through phosphorylation-independent mechanisms (Kroiher et al., 2001). A classic example is the ErbB3 receptor in the EGFR family that has a weakly active or non-functional kinase domain but is nevertheless a critical component of the EGFR signaling mechanism since it can form heterodimers with other members of the family

that phosphorylate it (12, 95). Atypical RLKs, functioning in an analogous manner, have also been reported in plants. Sequence analysis suggests that ~20% of the >600 RLKs encoded in the *Arabidopsis* genome are inactive, atypical RLKs, and it is likely that activation of differential signaling pathways can occur through heterodimerization among this RLK subfamily (36, 96, 97). Therefore, it is quite possible for ACR4 to expand its signaling cascade through interactions with the kinase-dead homologs. Futhermore, the fact that ACR4 kinase can phosphorylate both CRR1 and CRR2 ICDs (Fig. 3), parallels the mechanism described in kinase-defective ErbB3 signaling in complex with active members of the EGF receptor family (12, 95).

During ligand binding and receptor activation among the RTKs, the intracellular kinases are activated and autophosphorylated via a *trans* mechanism (1). Our *in vitro* kinase assays demonstrate the active ACR4 kinase domain can phosphorylate the ICDs of all the CRR homologs, therefore indicating that ACR4 signaling can occur through heterodimerization with CRR family members. Similar mechanisms have been determined in plant RLKs in which cytoplasmic domains in heterodimeric receptor complexes can undergo *trans* phosphorylation. For instance, the BRI1 RLK can transphosphorylate members of the AtSERK family, AtSERK1 and AtSERK3 (BAK1) (33, 98). Additionally, the FLS2, BIK1, and BAK1 require transphosphorylation for signaling during plant defense responses (99). Importantly, binding of different ligands to the ACR4 extracellular domain may also promote preferred heterodimerization with CRR family members to initiate a diverse array of signaling pathways and alter the signaling output and duration. For instance, members of the EGF receptor family can bind a variety of ligands which promotes homo- or heterodimerization that can activate multiple downstream signaling cascades (10, 12).

Indeed, an extra layer of complexity and dimension is conferred through cross-talk mediated by activation of EGFR signaling pathways by G-protein coupled receptor (GPCR) agonists (100, 101). Although one peptide, CLE40, has been proposed to be the ligand for ACR4 (22, 23), it does not preclude the possibility that other ligands may act in ACR4 signaling. Indeed, there are 32 members of the CLE peptide family in *Arabidopsis* that affect developmental functions in the plant (102, 103). However, the role of these presumed peptide ligands in ACR4 or CRR signaling has yet to be determined. Our gel filtration and pull-down assays show that the ICD of ACR4 *cannot* interact with the ALE2 ICD regardless of phosphorylation status but it *can* phosphorylate ALE2 *in vitro* (Fig. 3, *lane 5*). This may be attributed to an intrinsic low affinity between the ACR4 and ALE2 kinase domains but the apparent binding affinity may be increased by distal contacts found outside of the consensus phosphorylation sites harbored in the ALE2 substrate protein. This is illustrated in the low affinity, kinase-substrate complex formed between the yeast Sky1P kinase and its substrate, nuclear protein localization 3 (npl3). Here, a fast phosphoryl transfer step due to efficient 'clamping' of the npl3 substrate produces a decreased apparent K_m of binding (104, 105). Thus, this may explain the observation of enhanced substrate phosphorylation without observing a stable protein-protein interaction.

Both intramolecular and intermolecular protein-protein interactions are driven by contacts between specific residues on the interfacial faces of the participating domains. In contrast to stable complexes, biological signal transduction is regulated in large part by transiently formed states in which the proteins may switch between bound and unbound forms through modification-dependent conformational changes. While it is not possible to accurately define the state of the ACR4/AtCRR interactions based on current data,

nevertheless our phage-display, peptide-binding and HD exchange experiments provide us a basis to propose a model for a molecular level understanding of the heteromeric interactions. In this model (Fig. 12), in the naïve heterodimeric state, the KDSAF sequence in the C-helix of CRK1/CRR3 (Fig. 8) contacts the LLSLL site in the β4 strand of the ACR4 kinase domain. Upon activation, phosphorylation of residues in ACR4, including Ser^{475} in the juxtamembrane region, induces a conformational change and dissociation of the complex. In this monomeric state, the phosphorylated KDSAF in the JM region of ACR4 now forms intramolecular contacts with the LLSLL site on the β4 strand within its N-lobe. This model is supported by the following facts: (i) the ICD of ACR4 exists as monomers in the phosphorylated state (19) (Chapter 2) (ii) in pull-down assays ACR4 is incapable of binding to sCRR3 and sALE2 in the fully autophosphorylated state (Fig. 2A, *lanes 4 and 6*) (iii) 'KDSAF' motif containing peptides generated from the CRR3, CRK1, and ALE2 sequences are able to bind to the ACR4 kinase domain (Fig. 7B and C) and (iv) although our HDX results did not show a direct interaction between CRK1 and the ACR4 LLSLL region, the FRTELDL sequence is in close proximity to the 'LLSLL' region at the helix-C of ACR4 (Fig. 5). Taken together, these results point to the importance of the N-lobe region of ACR4 in heteromeric interactions in general, and with CRK1 in particular. In fact, the N-lobe of some RTKs is implicated in the modulation of intermolecular interactions and kinase activity. For example, the FKBP12 protein binds to the N-lobe of the TGFβ receptor-I kinase domain, holding it in an inactive conformation (106, 107). However, additional mutational studies are needed to elucidate the function of the KDSAF motif in the ACR4 JMD and the helix-C regions of CRR3, CRK1, and ALE2 in protein-protein interactions.

In planta investigations in the root tip have suggested a signaling module involving a putative peptide ligand, CLE40, the ACR4 RLK, and the WOX5 transcription factor [22-23]. In this study, we provide evidence that, for the first time, establishes a link between ACR4 and WOX5 in the proposed module. The two proteins can not only interact with each other (Fig. 9) but the WOX5 transcription factor is phosphorylated by the ACR4 kinase (Fig. 10). This is similar to the example of the EGF receptor which can recruit and phosphorylate the Stat3 transcription factor, therefore modulating Stat3 activity inside the cell [72-73, 109]. Furthermore, inactive G protein coupled receptors (GPCR) are able to bind the alpha subunit of G proteins through their intracellular GEF domains [71]. GPCR activation promotes the dissociation of G proteins in order to continue the signaling cascade inside the cell. Thus, our data invokes a possible mechanism in which WOX5 and ACR4 may associate in a preformed complex at the cell surface. WOX5 could presumably be activated by phosphorylation and move to the nucleus to influence transcriptional activity in an analogous manner.

Phosphorylation sites within receptor molecules not only recruit substrate proteins but also create docking sites for downstream interaction partners (54-58). The identification of such cellular proteins will lend significant context to the potential involvement of diverse multi-protein complexes in the functions of ACR4. Phage display peptide screening affords a rapid tool for the identification of potential interaction partners through consensus peptide binding motifs (49, 50). Our phage display studies identified two consensus peptide binding motifs for the phosphorylated JMD1 peptide, LXSLL and FXPYEL. Database mining of these sites yielded numerous proteins containing Leu-rich consensus sequences (Table 2). Intriguingly, both the LXXLL motif and the FXPYEL submotifs, FXPY and PYEL, returned

proteins that can be classified into distinct signal transduction categories i.e. RLKs, phosphatases, transcription factors, and adapter proteins (F-box containing proteins). It should of course be emphasized that, as with any high throughput screening procedures, while this data constitutes a significant collection of potential interacting proteins, their biological relevance need further confirmation and validation. Given this as it may, it is worth noting that the guidance to further study interactions with the AtCRRs was provided by the identification of the LXXLL motif by our phage display screening. Interestingly, only ACR4 contains an LXSLL motif (LLSLL) in the N-lobe, whereas CRK1 contains a LVRLL motif at an analogous position. All members of the ACR4 family also contain an LLEL/IL motif in the C-lobes of their respective kinase domains. However, this conserved motif is required for structural stabilization of the kinase domain (109) and is therefore unlikely to be important for protein-protein interactions. The WOX5 transcription factor was also found in our database search and contained an FXPY motif.

In summary, we have provided evidence for heteromeric interactions between the ICDs of ACR4 and CRR3, CRK1, and ALE2 and described a potential mechanism for these interactions. However, further *in vivo* and *in vitro* structure-function experiments, involving mutagenesis of binding site and phosphorylation site residues, are required to provide a more detailed view of the molecular aspects that modulate the interaction between these proteins. Importantly, to better understand heterologous signaling mechanisms and cross-talk, it will also be necessary to pursue the identification of key elements of the "ACR4 network" using complementary approaches such as yeast 2-hybrid screening, affinity pull-downs and phage display screening, followed by genetic validation *in planta* using knockout strains.

References

1. Lemmon, M.A. and J. Schlessinger, *Cell signaling by receptor tyrosine kinases.* Cell, 2010. **141**(7): p. 1117-34.
2. Ullrich, A. and J. Schlessinger, *Signal Transduction by Receptors with Tyrosine Kinase-Activity.* Cell, 1990. **61**(2): p. 203-212.
3. Jiang, G. and T. Hunter, *Receptor signaling: When dimerization is not enough.* Current Biology, 1999. **12**(9): p. R568-71.
4. Schlessinger, J., *Cell signaling by receptor tyrosine kinases.* Cell, 2000. **103**(2): p. 211-25.
5. Scott, J.D. and T. Pawson, *Cell signaling in space and time: where proteins come together and when they're apart.* Science, 2009. **326**(5957): p. 1220-4.
6. Shiu, S.H. and A.B. Bleecker, *Plant receptor-like kinase gene family: diversity, function, and signaling.* Sci STKE, 2001. **2001**(113): p. re22.
7. Haffani, Y.Z., N.F. Silva, and D.R. Goring, *Receptor kinase signalling in plants.* Canadian Journal of Botany-Revue Canadienne De Botanique, 2004. **82**(1): p. 1-15.
8. Afzal, A.J., A.J. Wood, and D.A. Lightfoot, *Plant receptor-like serine threonine kinases: roles in signaling and plant defense.* Mol Plant Microbe Interact, 2008. **21**(5): p. 507-17.
9. Kim, T.W., S. Guan, Y. Sun, Z. Deng, W. Tang, J.X. Shang, A.L. Burlingame, and Z.Y. Wang, *Brassinosteroid signal transduction from cell-surface receptor kinases to nuclear transcription factors.* Nat Cell Biol, 2009. **11**(10): p. 1254-60.
10. Olayioye, M.A., R.M. Neve, H.A. Lane, and N.E. Hynes, *The ErbB signaling network: receptor heterodimerization in development and cancer.* Embo Journal, 2000. **19**(13): p. 3159-67.
11. Prenzel, N., O.M. Fischer, S. Streit, S. Hart, and A. Ullrich, *The epidermal growth factor receptor family as a central element for cellular signal transduction and diversification.* Endocrine-Related Cancer, 2001. **8**(1): p. 11-31.
12. Wieduwilt, M.J. and M.M. Moasser, *The epidermal growth factor receptor family: biology driving targeted therapeutics.* Cell Mol Life Sci, 2008. **65**(10): p. 1566-84.
13. Clouse, S.D., *Brassinosteroid signal transduction: from receptor kinase activation to transcriptional networks regulating plant development.* Plant Cell, 2011. **23**(4): p. 1219-30.
14. Ye, H.X., L. Li, and Y.H. Yin, *Recent Advances in the Regulation of Brassinosteroid Signaling and Biosynthesis Pathways.* Journal of Integrative Plant Biology, 2011. **53**(6): p. 455-468.
15. Gifford, M.L., S. Dean, and G.C. Ingram, *The Arabidopsis ACR4 gene plays a role in cell layer organisation during ovule integument and sepal margin development.* Development, 2003. **130**(18): p. 4249-58.
16. Watanabe, M., H. Tanaka, D. Watanabe, C. Machida, and Y. Machida, *The ACR4 receptor-like kinase is required for surface formation of epidermis-related tissues in Arabidopsis thaliana.* Plant Journal, 2004. **39**(3): p. 298-308.
17. Cao, X., K. Li, S.G. Suh, T. Guo, and P.W. Becraft, *Molecular analysis of the CRINKLY4 gene family in Arabidopsis thaliana.* Planta, 2005. **220**(5): p. 645-57.

18. Tanaka, H., M. Watanabe, D. Watanabe, T. Tanaka, C. Machida, and Y. Machida, *ACR4, a putative receptor kinase gene of Arabidopsis thaliana, that is expressed in the outer cell layers of embryos and plants, is involved in proper embryogenesis.* Plant and Cell Physiology, 2002. **43**(4): p. 419-428.
19. Meyer, M.R., C.F. Lichti, R.R. Townsend, and A.G. Rao, *Identification of in vitro autophosphorylation sites and effects of phosphorylation on the Arabidopsis CRINKLY4 (ACR4) receptor-like kinase intracellular domain: insights into conformation, oligomerization, and activity.* Biochemistry, 2011. **50**(12): p. 2170-86.
20. Tanaka, H., M. Watanabe, M. Sasabe, T. Hiroe, T. Tanaka, H. Tsukaya, M. Ikezaki, C. Machida, and Y. Machida, *Novel receptor-like kinase ALE2 controls shoot development by specifying epidermis in Arabidopsis.* Development, 2007. **134**(9): p. 1643-1652.
21. De Smet, I., V. Vassileva, B. De Rybel, M.P. Levesque, W. Grunewald, D. Van Damme, G. Van Noorden, M. Naudts, G. Van Isterdael, R. De Clercq, J.Y. Wang, N. Meuli, S. Vanneste, J. Friml, P. Hilson, G. Jurgens, G.C. Ingram, D. Inze, P.N. Benfey, and T. Beeckman, *Receptor-like kinase ACR4 restricts formative cell divisions in the Arabidopsis root.* Science, 2008. **322**(5901): p. 594-7.
22. Stahl, Y., R.H. Wink, G.C. Ingram, and R. Simon, *A signaling module controlling the stem cell niche in Arabidopsis root meristems.* Curr Biol, 2009. **19**(11): p. 909-14.
23. Stahl, Y. and R. Simon, *Is the Arabidopsis root niche protected by sequestration of the CLE40 signal by its putative receptor ACR4?* Plant Signal Behav, 2009. **4**(7): p. 634-5.
24. Miwa, H., A. Kinoshita, H. Fukuda, and S. Sawa, *Plant meristems: CLAVATA3/ESR-related signaling in the shoot apical meristem and the root apical meristem.* J Plant Res, 2009. **122**(1): p. 31-9.
25. Nolen, B., S. Taylor, and G. Ghosh, *Regulation of protein kinases: Controlling activity through activation segment conformation.* Molecular Cell, 2004. **15**(5): p. 661-675.
26. Pascal, B.D., M.J. Chalmers, S.A. Busby, and P.R. Griffin, *HD desktop: an integrated platform for the analysis and visualization of H/D exchange data.* J Am Soc Mass Spectrom, 2009. **20**(4): p. 601-10.
27. Zhang, Z. and D.L. Smith, *Determination of amide hydrogen exchange by mass spectrometry: a new tool for protein structure elucidation.* Protein Science, 1993. **2**(4): p. 522-31.
28. Sali, A., L. Potterton, F. Yuan, H. van Vlijmen, and M. Karplus, *Evaluation of comparative protein modeling by MODELLER.* Proteins, 1995. **23**(3): p. 318-26.
29. Berenstein, D., J.F. Christensen, T. Kristensen, R. Hofbauer, and B. Munch-Petersen, *Valine, not methionine, is amino acid 106 in human cytosolic thymidine kinase (TK1) - Impact on oligomerization, stability, and kinetic properties.* Journal of Biological Chemistry, 2000. **275**(41): p. 32187-32192.
30. Hansson, H., M.P. Okoh, C.I.E. Smith, M. Vihinen, and T. Hard, *Intermolecular interactions between the SH3 domain and the proline-rich TH region of Bruton's tyrosine kinase.* Febs Letters, 2001. **489**(1): p. 67-70.
31. Levinson, N.M., P.R. Visperas, and J. Kuriyan, *The Tyrosine Kinase Csk Dimerizes through Its SH3 Domain.* PLoS One, 2009. **4**(11).

32. Stone, J.M., A.E. Trotochaud, J.C. Walker, and S.E. Clark, *Control of meristem development by CLAVATA1 receptor kinase and kinase-associated protein phosphatase interactions.* Plant Physiology, 1998. **117**(4): p. 1217-1225.
33. Wang, X., U. Kota, K. He, K. Blackburn, J. Li, M.B. Goshe, S.C. Huber, and S.D. Clouse, *Sequential transphosphorylation of the BRI1/BAK1 receptor kinase complex impacts early events in brassinosteroid signaling.* Dev Cell, 2008. **15**(2): p. 220-35.
34. Schulze, B., T. Mentzel, A.K. Jehle, K. Mueller, S. Beeler, T. Boller, G. Felix, and D. Chinchilla, *Rapid Heteromerization and Phosphorylation of Ligand-activated Plant Transmembrane Receptors and Their Associated Kinase BAK1.* Journal of Biological Chemistry, 2010. **285**(13): p. 9444-9451.
35. Kim, H.H., U. Vijapurkar, N.J. Hellyer, D. Bravo, and J.G. Koland, *Signal transduction by epidermal growth factor and heregulin via the kinase-deficient ErbB3 protein.* Biochemical Journal, 1998. **334**: p. 189-195.
36. Castells, E. and J.M. Casacuberta, *Signalling through kinase-defective domains: the prevalence of atypical receptor-like kinases in plants.* Journal of Experimental Botany, 2007. **58**(13): p. 3503-3511.
37. Hanks, S.K. and T. Hunter, *Protein kinases 6. The eukaryotic protein kinase superfamily: kinase (catalytic) domain structure and classification.* FASEB J, 1995. **9**(8): p. 576-96.
38. Yan, X. and C.S. Maier, *Hydrogen/Deuterium Exchange Mass Spectrometry*, in *Mass Spectrometry of Proteins and Peptides*, M. Lipton and L. Pasa-Tolic, Editors. 2009, Humana Press. p. 255-271.
39. Konermann, L., J.X. Pan, and Y.H. Liu, *Hydrogen exchange mass spectrometry for studying protein structure and dynamics.* Chemical Society Reviews, 2011. **40**(3): p. 1224-1234.
40. Busenlehner, L.S. and R.N. Armstrong, *Insights into enzyme structure and dynamics elucidated by amide H/D exchange mass spectrometry.* Archives of Biochemistry and Biophysics, 2005. **433**(1): p. 34-46.
41. Zhou, B., J.L. Zhang, S.J. Liu, S. Reddy, F. Wang, and Z.Y. Zhang, *Mapping ERK2-MKP3 binding interfaces by hydrogen/deuterium exchange mass spectrometry.* Journal of Biological Chemistry, 2006. **281**(50): p. 38834-38844.
42. Zhou, B. and Z.Y. Zhang, *Application of hydrogen/deuterium exchange mass spectrometry to study protein tyrosine phosphatase dynamics, ligand binding, and substrate specificity.* Methods, 2007. **42**(3): p. 227-233.
43. Pawson, T. and P. Nash, *Assembly of cell regulatory systems through protein interaction domains.* Science, 2003. **300**(5618): p. 445-452.
44. Cesareni, G., M. Gimona, M. Sudol, and M. Yaffe, *Modular Protein Domains*. 2005: Wiley-VCH.
45. Ren, S., V.N. Uversky, Z.J. Chen, A.K. Dunker, and Z. Obradovic, *Short Linear Motifs recognized by SH2, SH3 and Ser/Thr Kinase domains are conserved in disordered protein regions.* Bmc Genomics, 2007. **9**.
46. Sidhu, S.S., W.J. Fairbrother, and K. Deshayes, *Exploring protein-protein interactions with phage display.* Chembiochem, 2003. **4**(1): p. 14-25.

47. Tonikian, R., Y. Zhang, C. Boone, and S.S. Sidhu, *Identifying specificity profiles for peptide recognition modules from phage-displayed peptide libraries.* Nat Protoc, 2007. **2**(6): p. 1368-86.
48. Molek, P., B. Strukelj, and T. Bratkovic, *Peptide Phage Display as a Tool for Drug Discovery: Targeting Membrane Receptors.* Molecules, 2011. **16**(1): p. 857-887.
49. Kay, B.K., J. Kasanov, S. Knight, and A. Kurakin, *Convergent evolution with combinatorial peptides.* Febs Letters, 2000. **480**(1): p. 55-62.
50. Smothers, J.F. and S. Henikoff, *The HP1 chromo shadow domain binds a consensus peptide pentamer.* Current Biology, 2000. **10**(1): p. 27-30.
51. Yaffe, M.B. and A.E.H. Elia, *Phosphoserine/threonine-binding domains.* Current Opinion in Cell Biology, 2001. **13**(2): p. 131-138.
52. Joughin, B.A., B. Tidor, and M.B. Yaffe, *A computational method for the analysis and prediction of protein: phosphopeptide-binding sites.* Protein Science, 2005. **14**(1): p. 131-139.
53. Yaffe, M.B. and S.J. Smerdon, *The use of in vitro peptide-library screens in the analysis of phosphoserine/threonine-binding domain structure and function.* Annual Review of Biophysics and Biomolecular Structure, 2004. **33**: p. 225-244.
54. He, W., A. Craparo, Y. Zhu, T.J. O'Neill, L.M. Wang, J.H. Pierce, and T.A. Gustafson, *Interaction of insulin receptor substrate-2 (IRS-2) with the insulin and insulin-like growth factor I receptors. Evidence for two distinct phosphotyrosine-dependent interaction domains within IRS-2.* J Biol Chem, 1996. **271**(20): p. 11641-5.
55. Holland, S.J., N.W. Gale, G.D. Gish, R.A. Roth, Z. Songyang, L.C. Cantley, M. Henkemeyer, G.D. Yancopoulos, and T. Pawson, *Juxtamembrane tyrosine residues couple the Eph family receptor EphB2/Nuk to specific SH2 domain proteins in neuronal cells.* Embo Journal, 1997. **16**(13): p. 3877-88.
56. Schulze, W.X., L. Deng, and M. Mann, *Phosphotyrosine interactome of the ErbB-receptor kinase family.* Molecular Systems Biology, 2005. **1**.
57. Park, C.J., Y. Peng, X. Chen, C. Dardick, D. Ruan, R. Bart, P.E. Canlas, and P.C. Ronald, *Rice XB15, a protein phosphatase 2C, negatively regulates cell death and XA21-mediated innate immunity.* Plos Biology, 2008. **6**(9): p. e231.
58. Deheuninck, J., G. Goormachtigh, B. Foveau, Z. Ji, C. Leroy, F. Ancot, V. Villeret, D. Tulasne, and V. Fafeur, *Phosphorylation of the MET receptor on juxtamembrane tyrosine residue 1001 inhibits its caspase-dependent cleavage.* Cell Signal, 2009. **21**(9): p. 1455-63.
59. Cubas, P., N. Lauter, J. Doebley, and E. Coen, *The TCP domain: a motif found in proteins regulating plant growth and development.* Plant Journal, 1999. **18**(2): p. 215-222.
60. Savkur, R.S. and T.P. Burris, *The coactivator LXXLL nuclear receptor recognition motif.* Journal of Peptide Research, 2004. **63**(3): p. 207-212.
61. Plevin, M.J., M.M. Mills, and M. Ikura, *The LxxLL motif: a multifunctional binding sequence in transcriptional regulation.* Trends in Biochemical Sciences, 2005. **30**(2): p. 66-69.
62. Kim, J.G., X.Y. Li, J.A. Roden, K.W. Taylor, C.D. Aakre, B. Su, S. Lalonde, A. Kirik, Y.H. Chen, G. Baranage, H. McLane, G.B. Martin, and M.B. Mudgett, *Xanthomonas T3S Effector XopN Suppresses PAMP-Triggered Immunity and*

Interacts with a Tomato Atypical Receptor-Like Kinase and TFT1. Plant Cell, 2009. **21**(4): p. 1305-1323.

63. Mol, C.D., D.R. Dougan, T.R. Schneider, R.J. Skene, M.L. Kraus, D.N. Scheibe, G.P. Snell, H. Zou, B.C. Sang, and K.P. Wilson, *Structural basis for the autoinhibition and STI-571 inhibition of c-Kit tyrosine kinase.* J Biol Chem, 2004. **279**(30): p. 31655-63.
64. Griffith, J., J. Black, C. Faerman, L. Swenson, M. Wynn, F. Lu, J. Lippke, and K. Saxena, *The structural basis for autoinhibition of FLT3 by the juxtamembrane domain.* Mol Cell, 2004. **13**(2): p. 169-78.
65. Schubert, C., C. Schalk-Hihi, G.T. Struble, H.C. Ma, I.P. Petrounia, B. Brandt, I.C. Deckman, R.J. Patch, M.R. Player, J.C. Spurlino, and B.A. Springer, *Crystal structure of the tyrosine kinase domain of colony-stimulating factor-1 receptor (cFMS) in complex with two inhibitors.* J Biol Chem, 2007. **282**(6): p. 4094-101.
66. Li, S., N.D. Covino, E.G. Stein, J.H. Till, and S.R. Hubbard, *Structural and biochemical evidence for an autoinhibitory role for tyrosine 984 in the juxtamembrane region of the insulin receptor.* J Biol Chem, 2003. **278**(28): p. 26007-14.
67. Hubbard, S.R., *Juxtamembrane autoinhibition in receptor tyrosine kinases.* Nat Rev Mol Cell Biol, 2004. **5**(6): p. 464-71.
68. Roskoski, R., Jr., *Structure and regulation of Kit protein-tyrosine kinase--the stem cell factor receptor.* Biochem Biophys Res Commun, 2005. **338**(3): p. 1307-15.
69. Wiesner, S., L.E. Wybenga-Groot, N. Warner, H. Lin, T. Pawson, J.D. Forman-Kay, and F. Sicheri, *A change in conformational dynamics underlies the activation of Eph receptor tyrosine kinases.* Embo Journal, 2006. **25**(19): p. 4686-96.
70. Sarkar, A.K., M. Luijten, S. Miyashima, M. Lenhard, T. Hashimoto, K. Nakajima, B. Scheres, R. Heidstra, and T. Laux, *Conserved factors regulate signalling in Arabidopsis thaliana shoot and root stem cell organizers.* Nature, 2007. **446**(7137): p. 811-4.
71. Dorsam, R.T. and J.S. Gutkind, *G-protein-coupled receptors and cancer.* Nature Reviews Cancer, 2007. **7**(2): p. 79-94.
72. Park, O.K., T.S. Schaefer, and D. Nathans, *In vitro activation of Stat3 by epidermal growth factor receptor kinase.* Proc Natl Acad Sci U S A, 1996. **93**(24): p. 13704-8.
73. Quesnelle, K.M., A.L. Boehm, and J.R. Grandis, *STAT-mediated EGFR signaling in cancer.* J Cell Biochem, 2007. **102**(2): p. 311-9.
74. Albrecht, C., E. Russinova, B. Kemmerling, M. Kwaaitaal, and S.C. de Vries, *Arabidopsis SOMATIC EMBRYOGENESIS RECEPTOR KINASE proteins serve brassinosteroid-dependent and -independent signaling pathways.* Plant Physiol, 2008. **148**(1): p. 611-9.
75. Boisson-Dernier, A., S. Roy, K. Kritsas, M.A. Grobei, M. Jaciubek, J.I. Schroeder, and U. Grossniklaus, *Disruption of the pollen-expressed FERONIA homologs ANXUR1 and ANXUR2 triggers pollen tube discharge.* Development, 2009. **136**(19): p. 3279-88.
76. Matsumura, Y., H. Iwakawa, Y. Machida, and C. Machida, *Characterization of genes in the ASYMMETRIC LEAVES2/LATERAL ORGAN BOUNDARIES (AS2/LOB)*

family in Arabidopsis thaliana, and functional and molecular comparisons between AS2 and other family members. Plant Journal, 2009. **58**(3): p. 525-37.
77. Pfeiffer, M., T. Koch, H. Schroder, M. Laugsch, V. Hollt, and S. Schulz, *Heterodimerization of somatostatin and opioid receptors cross-modulates phosphorylation, internalization, and desensitization.* J Biol Chem, 2002. **277**(22): p. 19762-72.
78. Morgillo, F., J.K. Woo, E.S. Kim, W.K. Hong, and H.Y. Lee, *Heterodimerization of insulin-like growth factor receptor/epidermal growth factor receptor and induction of survivin expression counteract the antitumor action of erlotinib.* Cancer Res, 2006. **66**(20): p. 10100-11.
79. Saito, Y., J. Haendeler, Y. Hojo, K. Yamamoto, and B.C. Berk, *Receptor heterodimerization: essential mechanism for platelet-derived growth factor-induced epidermal growth factor receptor transactivation.* Mol Cell Biol, 2001. **21**(19): p. 6387-94.
80. Chinchilla, D., C. Zipfel, S. Robatzek, B. Kemmerling, T. Nurnberger, J.D. Jones, G. Felix, and T. Boller, *A flagellin-induced complex of the receptor FLS2 and BAK1 initiates plant defence.* Nature, 2007. **448**(7152): p. 497-500.
81. Guo, Y., L. Han, M. Hymes, R. Denver, and S.E. Clark, *CLAVATA2 forms a distinct CLE-binding receptor complex regulating Arabidopsis stem cell specification.* Plant Journal, 2010. **63**(6): p. 889-900.
82. Liu, P., T. Sudhaharan, R.M. Koh, L.C. Hwang, S. Ahmed, I.N. Maruyama, and T. Wohland, *Investigation of the dimerization of proteins from the epidermal growth factor receptor family by single wavelength fluorescence cross-correlation spectroscopy.* Biophys J, 2007. **93**(2): p. 684-98.
83. Tao, R.H. and I.N. Maruyama, *All EGF(ErbB) receptors have preformed homo- and heterodimeric structures in living cells.* Journal of Cell Science, 2008. **121**(19): p. 3207-3217.
84. Chantry, A., *The Kinase Domain and Membrane Localization Determine Intracellular Interactions between Epidermal Growth-Factor Receptors.* Journal of Biological Chemistry, 1995. **270**(7): p. 3068-3073.
85. Yu, X.C., K.D. Sharma, T. Takahashi, R. Iwamoto, and E. Mekada, *Ligand-independent dimer formation of epidermal growth factor receptor (EGFR) is a step separable from ligand-induced EGFR signaling.* Molecular Biology of the Cell, 2002. **13**(7): p. 2547-2557.
86. Monsey, J., W. Shen, P. Schlesinger, and R. Bose, *Her4 and Her2/neu tyrosine kinase domains dimerize and activate in a reconstituted in vitro system.* J Biol Chem, 2010. **285**(10): p. 7035-44.
87. Wang, X., X. Li, J. Meisenhelder, T. Hunter, S. Yoshida, T. Asami, and J. Chory, *Autoregulation and homodimerization are involved in the activation of the plant steroid receptor BRI1.* Dev Cell, 2005. **8**(6): p. 855-65.
88. Shah, K., T.W. Gadella, Jr., H. van Erp, V. Hecht, and S.C. de Vries, *Subcellular localization and oligomerization of the Arabidopsis thaliana somatic embryogenesis receptor kinase 1 protein.* J Mol Biol, 2001. **309**(3): p. 641-55.
89. Spivak-Kroizman, T., D. Rotin, D. Pinchasi, A. Ullrich, J. Schlessinger, and I. Lax, *Heterodimerization of c-erbB2 with different epidermal growth factor receptor*

mutants elicits stimulatory or inhibitory responses. J Biol Chem, 1992. **267**(12): p. 8056-63.
90. Ferguson, K.M., P.J. Darling, M.J. Mohan, T.L. Macatee, and M.A. Lemmon, *Extracellular domains drive homo- but not hetero-dimerization of erbB receptors.* Embo Journal, 2000. **19**(17): p. 4632-43.
91. Gerber, D., N. Sal-Man, and Y. Shai, *Two motifs within a transmembrane domain, one for homodimerization and the other for heterodimerization.* Journal of Biological Chemistry, 2004. **279**(20): p. 21177-21182.
92. Ferguson, K.M., *Structure-based view of epidermal growth factor receptor regulation.* Annu Rev Biophys, 2008. **37**: p. 353-73.
93. Mineev, K.S., E.V. Bocharov, Y.E. Pustovalova, O.V. Bocharova, V.V. Chupin, and A.S. Arseniev, *Spatial Structure of the Transmembrane Domain Heterodimer of ErbB1 and ErbB2 Receptor Tyrosine Kinases.* Journal of Molecular Biology, 2010. **400**(2): p. 231-243.
94. Gomez-Gomez, L., Z. Bauer, and T. Boller, *Both the extracellular leucine-rich repeat domain and the kinase activity of FLS2 are required for flagellin binding and signaling in arabidopsis.* Plant Cell, 2001. **13**(5): p. 1155-1163.
95. Hynes, N.E. and G. MacDonald, *ErbB receptors and signaling pathways in cancer.* Current Opinion in Cell Biology, 2009. **21**(2): p. 177-184.
96. Shiu, S.H. and A.B. Bleecker, *Expansion of the receptor-like kinase/Pelle gene family and receptor-like proteins in Arabidopsis.* Plant Physiol, 2003. **132**(2): p. 530-43.
97. Llompart, B., E. Castells, A. Rio, R. Roca, A. Ferrando, V. Stiefel, P. Puigdomenech, and J.M. Casacuberta, *The direct activation of MIK, a germinal center kinase (GCK)-like kinase, by MARK, a maize atypical receptor kinase, suggests a new mechanism for signaling through kinase-dead receptors.* J Biol Chem, 2003. **278**(48): p. 48105-11.
98. Karlova, R., S. Boeren, W. van Dongen, M. Kwaaitaal, J. Aker, J. Vervoort, and S. de Vries, *Identification of in vitro phosphorylation sites in the Arabidopsis thaliana somatic embryogenesis receptor-like kinases.* Proteomics, 2009. **9**(2): p. 368-79.
99. Lu, D., S. Wu, X. Gao, Y. Zhang, L. Shan, and P. He, *A receptor-like cytoplasmic kinase, BIK1, associates with a flagellin receptor complex to initiate plant innate immunity.* Proc Natl Acad Sci U S A, 2010. **107**(1): p. 496-501.
100. Gschwind, A., E. Zwick, N. Prenzel, M. Leserer, and A. Ullrich, *Cell communication networks: epidermal growth factor receptor transactivation as the paradigm for interreceptor signal transmission.* Oncogene, 2001. **20**(13): p. 1594-1600.
101. Filardo, E.J., *Epidermal growth factor receptor (EGFR) transactivation by estrogen via the G-protein-coupled receptor, GPR30: a novel signaling pathway with potential significance for breast cancer.* Journal of Steroid Biochemistry and Molecular Biology, 2002. **80**(2): p. 231-238.
102. Fiers, M., K.L. Ku, and C.M. Liu, *CLE peptide ligands and their roles in establishing meristems.* Current Opinion in Plant Biology, 2007. **10**(1): p. 39-43.
103. Wang, G. and M. Fiers, *CLE peptide signaling during plant development.* Protoplasma, 2010. **240**(1-4): p. 33-43.

104. Aubol, B.E., L. Ungs, R. Lukasiewicz, G. Ghosh, and J.A. Adams, *Chemical clamping allows for efficient phosphorylation of the RNA carrier protein Npl3.* Journal of Biological Chemistry, 2004. **279**(29): p. 30182-30188.
105. Lieser, S.A., B.E. Aubol, L. Wong, P.A. Jennings, and J.A. Adams, *Coupling phosphoryl transfer and substrate interactions in protein kinases.* Biochim Biophys Acta, 2005. **1754**(1-2): p. 191-9.
106. Huse, M., Y.G. Chen, J. Massague, and J. Kuriyan, *Crystal structure of the cytoplasmic domain of the type I TGF beta receptor in complex with FKBP12.* Cell, 1999. **96**(3): p. 425-36.
107. Huse, M., T.W. Muir, L. Xu, Y.G. Chen, J. Kuriyan, and J. Massague, *The TGF beta receptor activation process: an inhibitor- to substrate-binding switch.* Mol Cell, 2001. **8**(3): p. 671-82.
108. Shao, H., H.Y. Cheng, R.G. Cook, and D.J. Tweardy, *Identification and characterization of signal transducer and activator of transcription 3 recruitment sites within the epidermal growth factor receptor.* Cancer Res, 2003. **63**(14): p. 3923-30.
109. Kornev, A.P., S.S. Taylor, and L.F. Ten Eyck, *A helix scaffold for the assembly of active protein kinases.* Proc Natl Acad Sci U S A, 2008. **105**(38): p. 14377-82.

Tables

Table 1. Site-discriminating ions for phosphorylated residues (red) from WOX5 phosphopeptides[a]

Peptide	Residue Position in WOX5	b ion	Phosphorylated b ion	y ion	Phosphorylated y ion
GSAGAALG**S**FSVK	2	b8 (+1, 6.45)	b9 (+1, 4.42)	y4 (+1, 6.50)	y5 (+2.41)
GSAGAALGSF**S**VKGR	4	b10 (+1, 5.22)	b11 (--) *	y4 (+2, 2.54)	y5 (+2, 1.79)
KI**S**IDFDHHHHQPSTR	88	b2 (+1, 0.40)	b3(+1, 0.92)	y13 (+2, 1.30)	y14 (+2, 3.74)
ETTTT**S**FSPYSSCGAEMEHPPPLDLR	158	b5 (+1, 2.50)	b6 (--) *	y20 (+2, 16.59)	y21 (+2, 4.06)

[a] The percentage of maximal intensity for each site-discriminating ion in the averaged low-resolution CID spectrum is shown in parentheses.
* Supporting ion information is available.

Table 2. Potential ACR4 interaction partners

Motif Searched	Uniprot ID	Entry name	Protein name	Function	Localization
LXSLL, LLXLL, LLXXL	Q9LX29	ACR4	Ser/Thr-protein kinase-like protein, ACR4	RLK	PM
	Q9S7D9	ACRR1	Ser/Thr-protein kinase-like protein, AtCRR1	RLK, low activity	PM
	O80963	ACRR2	Ser/Thr-protein kinase-like protein, AtCRR2	RLK, low activity	PM
	Q9LY50	ACRR3	Ser/Thr-protein kinase-like protein, AtCRR3	RLK	PM
	Q9FIJ6	ACCR4	Ser/Thr-protein kinase-like protein, AtCRK1	RLK	PM
	O22476	BRI1	Protein BRASSINOSTEROID INSENSITIVE 1, BRI1	RLK	PM
	Q9M021	LRKA1	L-type lectin-domain containing receptor kinase VI.2	RLK	PM
	Q9M020	LRKA2	Lectin-domain containing receptor kinase VI.3	RLK	PM
	Q9SR05	ANX1	Receptor-like protein kinase ANXUR1	RLK	PM
	Q3E8W4	ANX2	Receptor-like protein kinase ANXUR2	RLK	PM
	Q9SKG5	SERK4	Somatic embryogenesis receptor kinase 4	RLK	PM
	Q8LPS5	SERK5	Somatic embryogenesis receptor kinase 5	RLK	PM
	P43298	TMK1	Probable receptor protein kinase TMK1	RLK	PM
	Q9FHK7	Y5516	Probable leucine-rich repeat receptor-like protein kinase At5g05160	RLK	PM
	Q9C9Y8	Y3868	Probable inactive receptor kinase At3g08680	RLK, no activity	PM
	Q9FK10	Y5332	Probable inactive receptor kinase At5g53320	RLK, no activity	PM
	Q9FMD7	Y5659	Probable inactive receptor kinase At5g16590	RLK, no activity	PM
	Q9LP77	Y1848	Probable inactive receptor kinase At1g48480	RLK, no activity	PM
	Q9LVM0	Y5830	Probable inactive receptor kinase At5g58300	RLK, no activity	PM
	P49333	ETR1	Ethylene receptor 1	R	PM
	O04660	GLR21	Glutamate receptor 2.1	R, IC	PM, M
	Q93YV6	2A5I	Ser/Thr protein phosphatase 2A 57 kDa regulatory subunit B' iota isoform	P	n.a.
	Q9LR65	P2C01	Probable protein phosphatase 2C 1	P	PM, M
	Q9M9W3	PP19	Ser/Thr-protein phosphatase PP1 isozyme 9	P	n.a.
	P48482, P48483, P48484, P48485, P48486, O82733, O82734, Q9M9W3	PP1	Ser/Thr-protein phosphatase PP1	P	C
	Q07099, Q07098, P48578, Q07100, O04951	PP2A	Serine/threonine-protein phosphatase PP2A catalytic subunit	P	PM, N, C
	Q9LR78	BSU1	Serine/threonine-protein phosphatase BSU1	P	N
	Q8LDQ4	PP2A	PP2A regulatory subunit TAP46	P	C
	Q9FX31	HDG11	Homeobox-leucine zipper protein HDG11	TF	N
	Q9LMT8	HDG12	Homeobox-leucine zipper protein HDG12	TF	N
	O04291	ATB14	Homeobox-leucine zipper protein ATHB-14	TF	N
	Q9SLB6	LBD17	LOB domain-containing protein 17	TR	n.a.

Table 2. Potential ACR4 interaction partners (continued)

Motif Searched	Uniprot ID	Entry name	Protein name	Function	Localization
FXPY	Q9S9M3	WAKLC	Wall-associated receptor kinase-like 3	RLK	PM
	Q8RY67	WAKLO	Wall-associated receptor kinase-like 14	RLK	PM
	Q9LHP4	RCH2	Receptor-like protein kinase 2	RLK	PM
	Q9M8W7	GLR11	Glutamate receptor 1.1	R, IC	PM, M
	Q9C8E7	GLR33	Glutamate receptor 3.3	R, IC	PM, M
	Q9SDQ4	GLR37	Glutamate receptor 3.7	R, IC	PM, M
	Q38846	ERS1	Ethylene response sensor 1	R	ER
	Q9SA51, Q9SHE9, O04479, O82198, O64836, Q8L8W3, Q9AT61, Q9SJW5, Q8L5T5, Q9SLB7, Q9SLB6, O22131, O22132, Q9SRL8, P59467, P59468, Q8L8Q3, Q9SCS4, Q9M2J7, O81323, O81322, Q9LHS8, P59469, Q9FKZ3	LBD	LOB domain-containing protein; ASYMMETRIC LEAVES 2-like protein	TR	n.a.
	Q9LU89	2A5N	Ser/Thr protein phosphatase 2A 59 kDa regulatory subunit B' eta	P	C, N
	Q8LF36	2A5T	Ser/Thr protein phosphatase 2A 57 kDa regulatory subunit B' theta	P	PX
	Q38950	2AAB	Ser/Thr protein phosphatase 2A 65 kDa regulatory subunit A beta	P	PM, C
	Q940A2	P2C31	Protein kinase and PP2C-like domain-containing protein	P	n.a.
	A0MES8	ABI4	Ethylene-responsive transcription factor ABI4	TF	N
	Q9LZR0	ATB51	Putative homeobox-leucine zipper protein ATHB-51	TF	N
	Q8W2F2	BH011	Transcription factor bHLH11	TF	N
	A4D998	BH075	Transcription factor bHLH75	TF	N
	Q9LK48	BH077	Transcription factor bHLH77	TF	N
	Q8LFV3	DOF33	Dof zinc finger protein DOF3.3	TF	N
	O82804	ELF3	Protein EARLY FLOWERING 3	TF	N
	Q8LC79	GAT18	GATA transcription factor 18	TF	N
	O82632	GATA9	GATA transcription factor 9	TF	N
	Q9FFX4	KNU	Zinc finger protein KNUCKLES	TF	N
	Q00958	LFY	Protein LEAFY	TF	N
	Q9FML4	LOB	Protein LATERAL ORGAN BOUNDARIES	TF	n.a.
	Q9LXV2	MYB46	Transcription factor MYB46	TF	N
	Q9LXV5	NFYA1	Nuclear transcription factor Y subunit A-1	TF	N
	Q945M9	NFYA9	Nuclear transcription factor Y subunit A-9	TF	N
	Q9LDL7	PAT1	Scarecrow-like transcription factor PAT1	TF	C
	Q9S7H5	SCL21	Scarecrow-like protein 21	TF	N
	Q8H125	SCL5	Scarecrow-like protein 5	TF	C, N
	Q8H1D2	WOX5	WUSCHEL-related homeobox 5, WOX5	TF	N
	Q93WV4	WRK71	Probable WRKY transcription factor 71	TF	N
	Q9FHB0	Y5014	B3 domain-containing protein At5g60140	TF	N
	Q9FHH1	Y5772	B3 domain-containing protein At5g57720	TF	N
	Q9FT50, Q6AWW4, Q9FYJ1, Q9FMT5, Q3ECR3, Q9XIR1, O82378, Q9LM75 , Q9LXR4, Q93ZX6, O82379, Q9FL99, Q0V7S6	FB202	F-box protein	n.a.	n.a.
PYEL	Q9FF23	FB268	Putative F-box protein At5g38390	n.a.	n.a.
	Q8S8F2	FBL11	LRR and BTB/POZ domain-containing protein FBL11	n.a.	PR
	Q9C8V8, Q9ZUP0	LBD	LOB domain-containing protein; ASYMMETRIC LEAVES 2-like protein	TR	n.a.

Figures

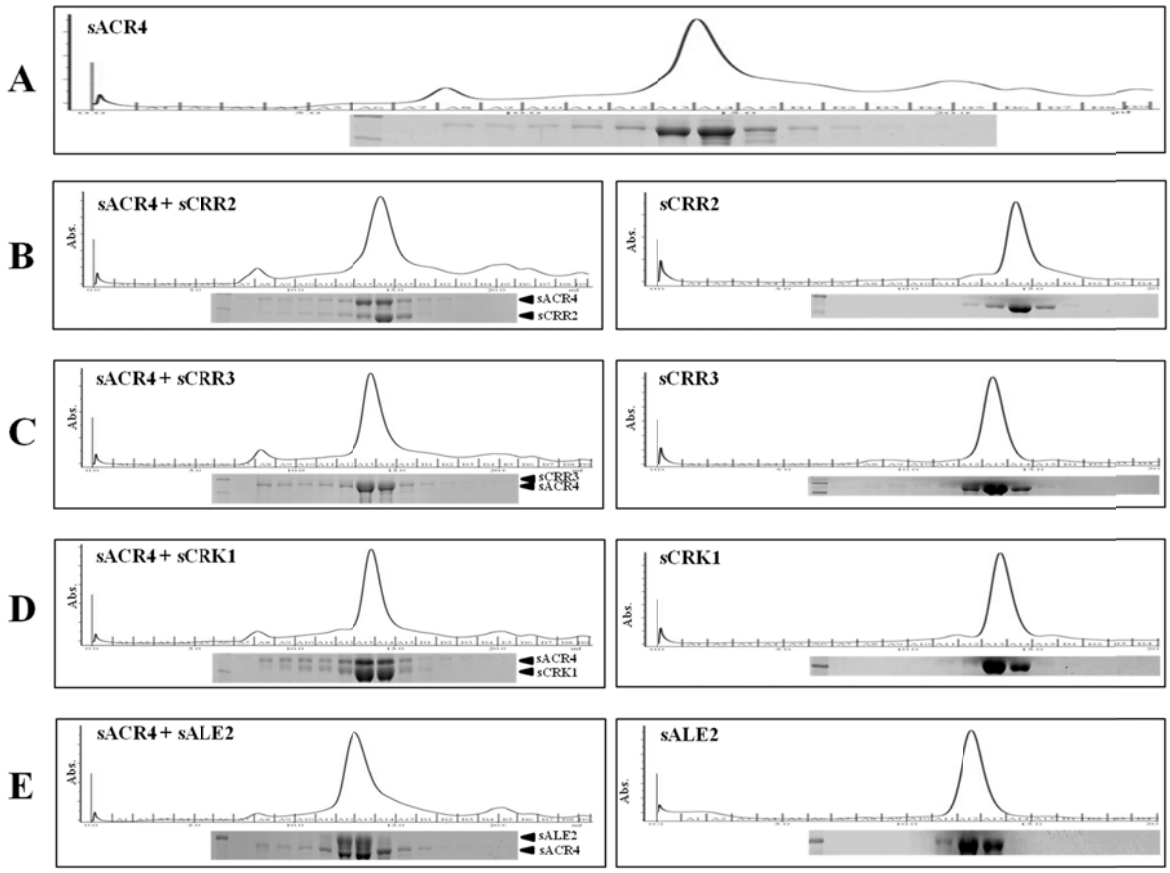

Figure 1. Gel filtration analysis of ICD interactions. Protein-protein interactions between the ICDs of ACR4 and the CRR/ALE2 binding partners were assessed by gel filtration on a Superdex G-200 column. (A) ACR4 elution profile demonstrating the protein primarily elutes as a monomer, but has the propensity to form higher order oligomers. (B-E) the elution profiles of the CRRs /ALE2 incubated alone (*right panels*) or with ACR4 (*left panels*). Insets depict 12% SDS-PAGE gels of eluted protein fractions.

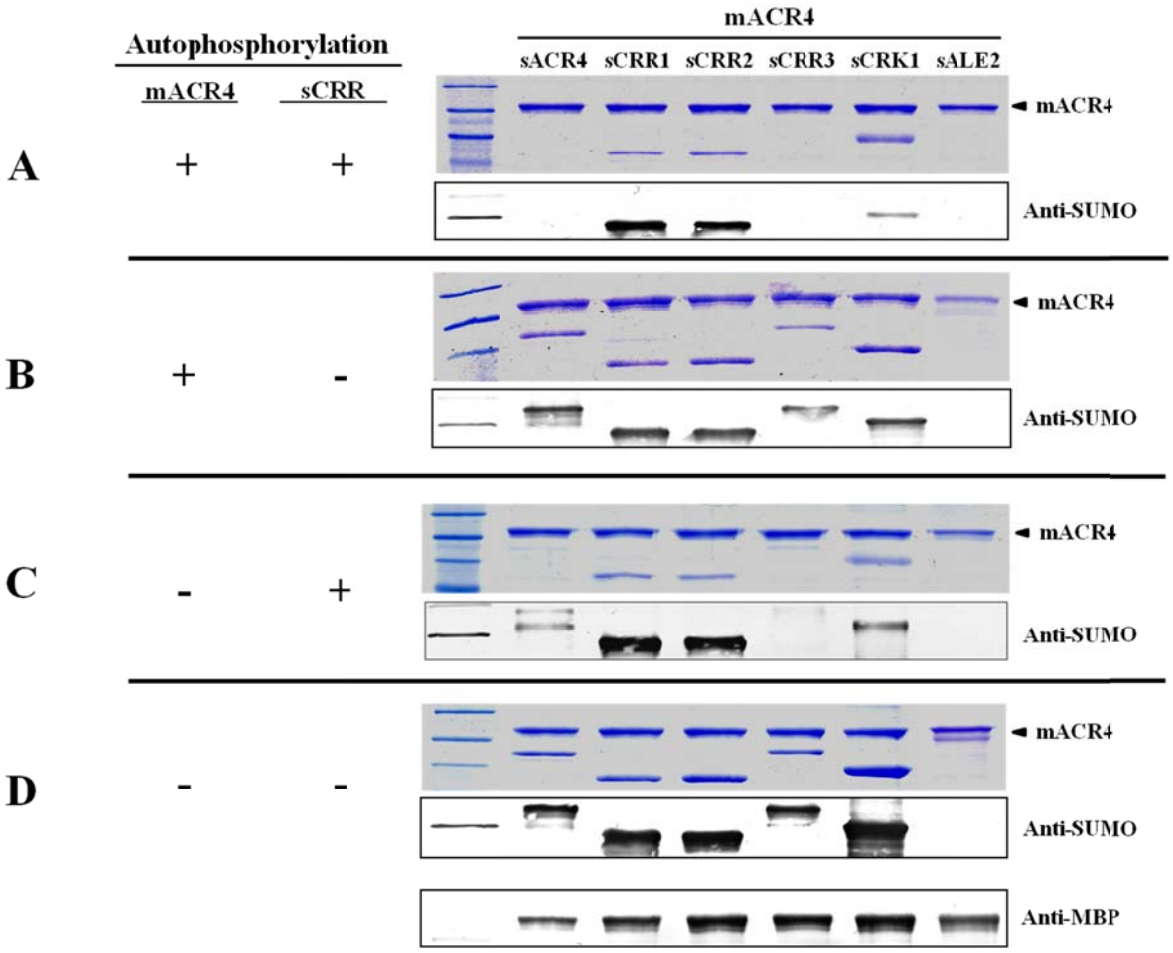

Figure 2. Effect of autophosphorylation on ICD interactions. Pull-down assays were performed to determine the effects of phosphorylation on interactions between the ICDs of ACR4 and the CRRs/ALE2. The autophosphorylation status of each protein was varied for individual experiments, (+) denotes autophosphorylated protein, (-) denotes unphosphorylated protein. In (A), mACR4 (+) and sCRRs/sALE2 (+), (B) mACR4 (+) and sCRRs/sALE2 (-), (C) mACR4 (-) and sCRRs/sALE2 (+), (D) mACR4 (-) and sCRRs/sALE2 (-). In A-D, proteins were separated by 12% SDS-PAGE (*top panels*) and the presence of interacting proteins was determined by anti-SUMO western blot (*lower panels*). In bottom panel, anti-MBP western blot demonstrates the presence of mACR4 in each reaction.

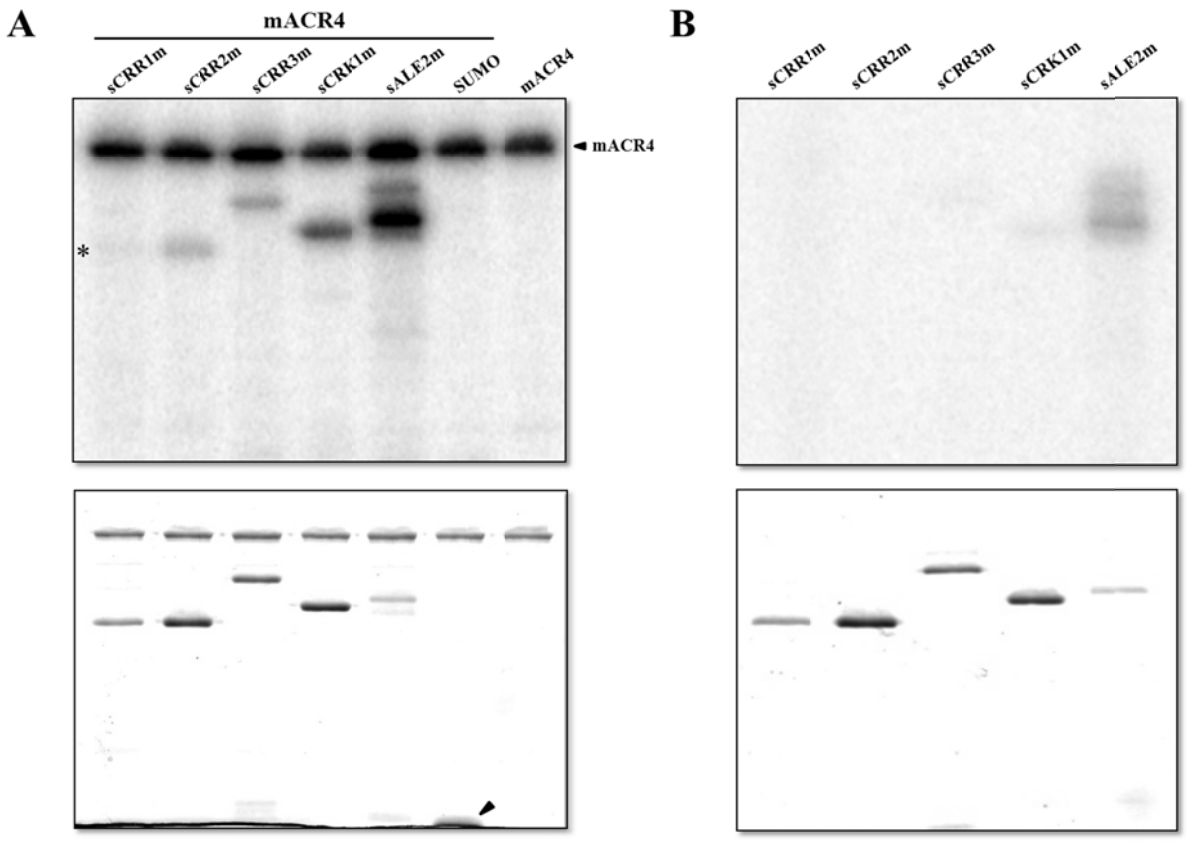

Figure 3. ACR4 can phosphorylate the ICDs of the CRRs and ALE2. Active mACR4 was incubated with the inactive sCRRs/ALE2 in an *in vitro* kinase assay. (A) *Upper panel* shows an autoradiogram demonstrating ACR4 can phosphorylate the ICDs of the CRRs and ALE2. ACR4 *cannot* phosphorylate the SUMO tag. *Lower panel* shows the corresponding coomassie stained gel. The arrow indicates the SUMO protein band. (B) *Upper panel* depicts an autoradiogram showing the inactivity of the sCRR mutants in which their respective catalytic Asp residues have been mutated to Ala. For sALE2m, the essential Lys^{377} was mutated to Ala, but protein retained weak activity. *Lower panel* is the corresponding coomassie stained gel showing the presence of each protein.

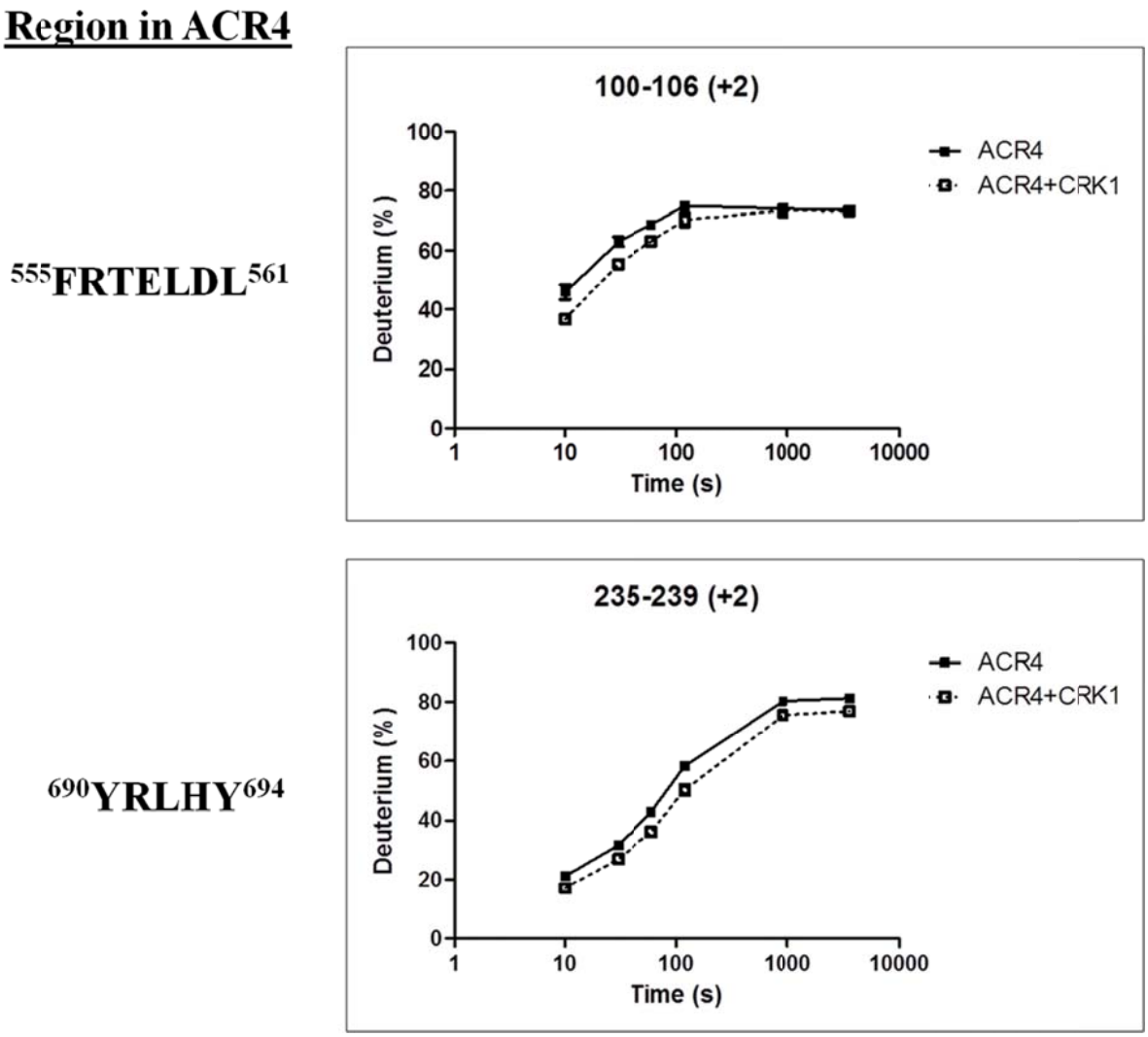

Figure 4. HDX-MS analysis of ACR4/CRK1. Time course of deuterium uptake for two ACR4 peptides, FRTELDL and YRLHY, that demonstrated significant hydrogen-deuterium exchange rates between the free ACR4 (closed squares) and the ACR4/CRK1 bound (open squares) states. Data represent the mean (n=3).

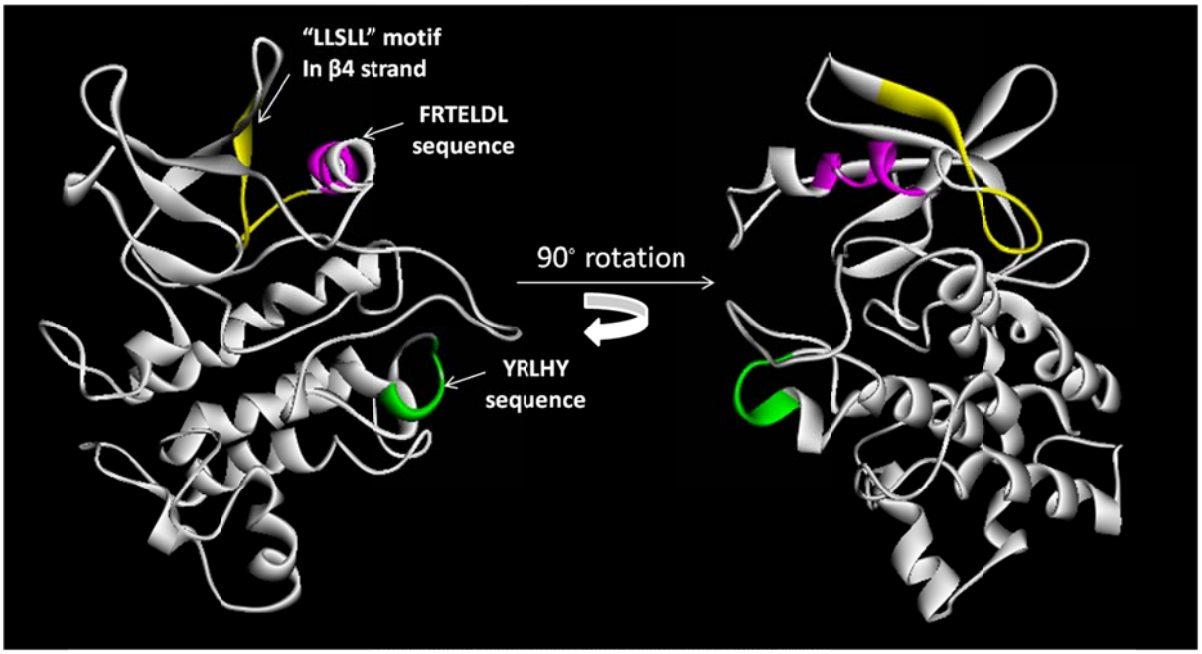

Figure 5. Mapping of the HDX sites. Structural model of the ACR4 kinase domain depicting the regions showing significant H-D exchange rates. The ACR4 kinase domain, residues 512-785, was modeled after the Interleukin-1 receptor associated kinase structure (PDB: 2NRU_B) which was 50% similar and 34% identical to the ACR4 sequence. The homology model was prepared using the Discovery Studio v 3.1 (Accelrys) software. The protein model was generated by MODELER and was validated using the Verify Protein (Profiles-3D) protocol. The model shows the kinase is a two lobed structure (gray). Peptides showing significant HDX are highlighted; the peptide, FRTELDL (magenta) and the peptide, YRLHY (green). The presumed protein-protein interaction site, LLSLL, is highlighted in yellow.

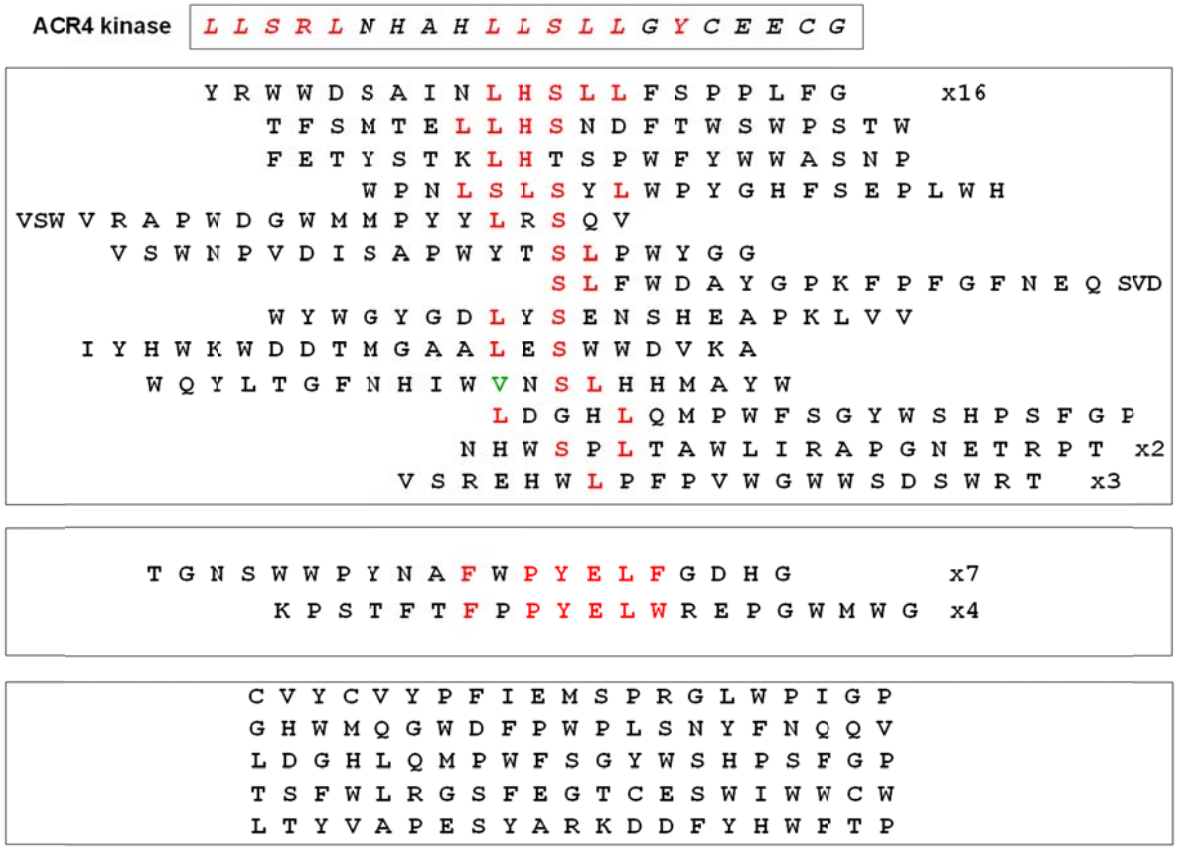

Figure 6. Phage panning of pJMD1 peptide. The immobilized JMD1 peptide was screened with a random 21-aa linear peptide library encoded in the pIII protein of filamentous phage. Phage peptide binders were enriched by successive binding, washing, and elution steps. After four rounds, 47 clones were randomly selected for DNA sequencing. The table represents the peptide sequences binding specifically to JMD1 peptide and their frequency of occurrence. A consensus LXSLL motif was enriched from the phage library.

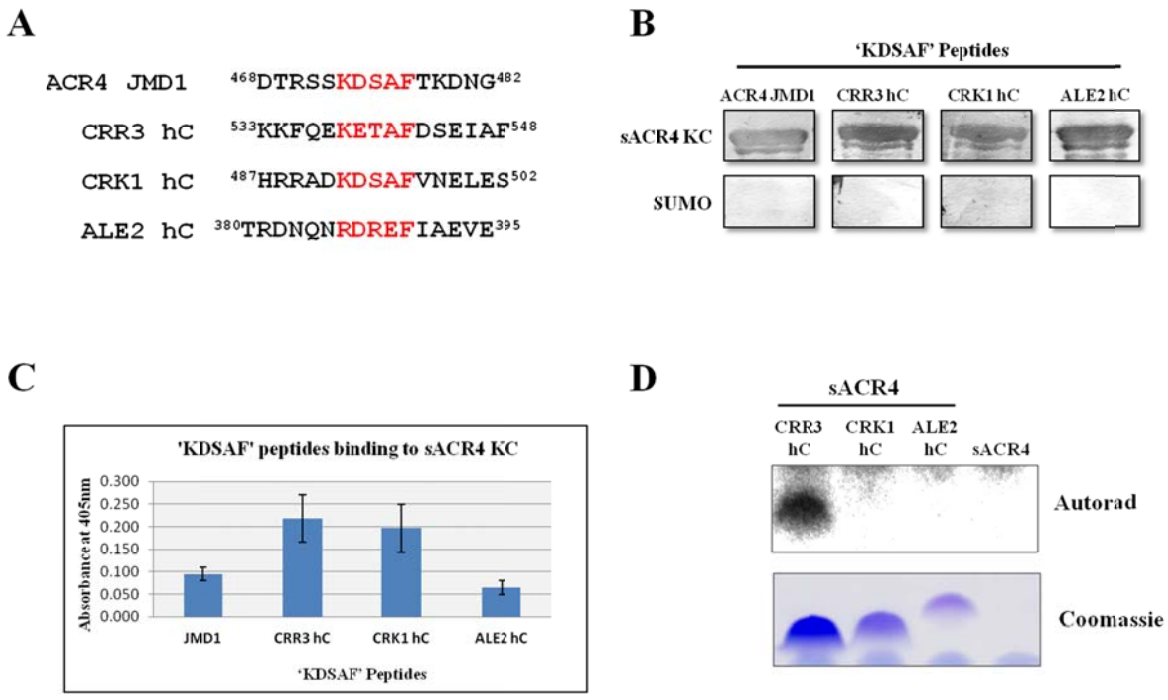

Figure 7. 'KDSAF' peptides bind to the ACR4 kinase. The 'KDSAF' motif containing peptides were incubated with the sACR4 KC protein to demonstrate specificity of binding towards the ACR4 kinase. (A) Peptide alignment of the ACR4 JMD1, CRR3 hC, and CRK1 hC demonstrating the conserved 'KDSAF' motif (red). In ALE2, the sequence is 'RDREF'. (B) A peptide overlay assay showing that the unphosphorylated JMD1, the CRR3 hC, CRK1 hC, and the ALE2 hC peptides can bind to sACR4 KC (*upper panel*). Control blots show no specificity towards the SUMO solubility tag (*lower panel*). To confirm the presence of each protein, anti-SUMO western blots were performed. (C) Peptide binding assay demonstrating the 'KDSAF' containing peptides can bind to the natively folded sACR4 KC protein immobilized on a Ni^{2+} coated plate. (D) Autoradiogram (*upper panel*) demonstrating that ACR4 can phosphorylate the CRR3 hC peptide, but not the CRR3 or ALE2 hC peptides. The presence of each peptide was confirmed by coomassie staining (*lower panel*).

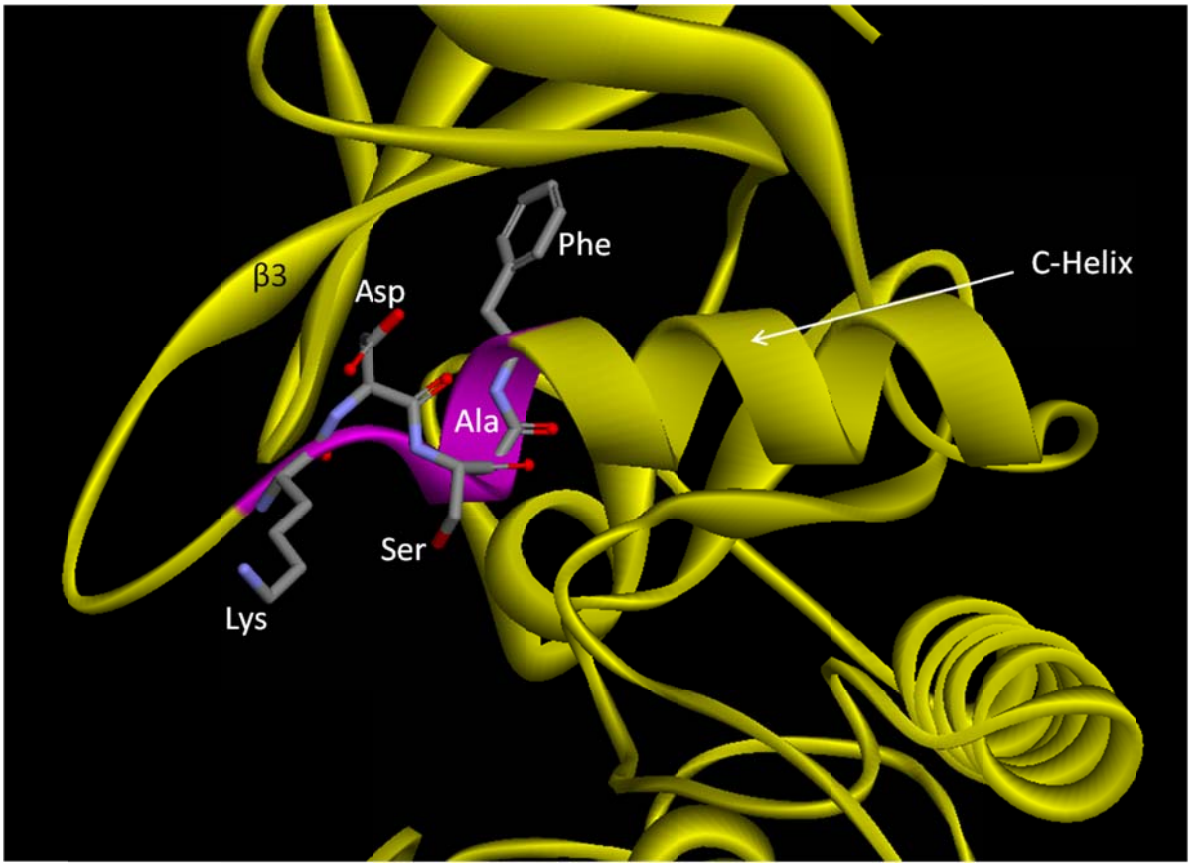

Figure 8. Model of the KDSAF motif. The CRK1 kinase domain, residues 444-729, was modeled after the Interleukin-1 receptor associated kinase structure (PDB: 2NRU_B). The homology model was prepared using the Discovery Studio v 3.1 (Accelrys) software. The protein model was generated by MODELER and was validated using the Verify Protein (Profiles-3D) protocol. The region depicted is a close up view of the alpha-C helix. The peptide backbone is highlighted in yellow. The 'KDSAF' motif (purple) is a key region thought to be involved in an intermolecular contact with the ACR4 N-lobe at the 'LLSLL' motif. Orientation of the sidechains of the residues involved in the KDSAF motif are shown (gray).

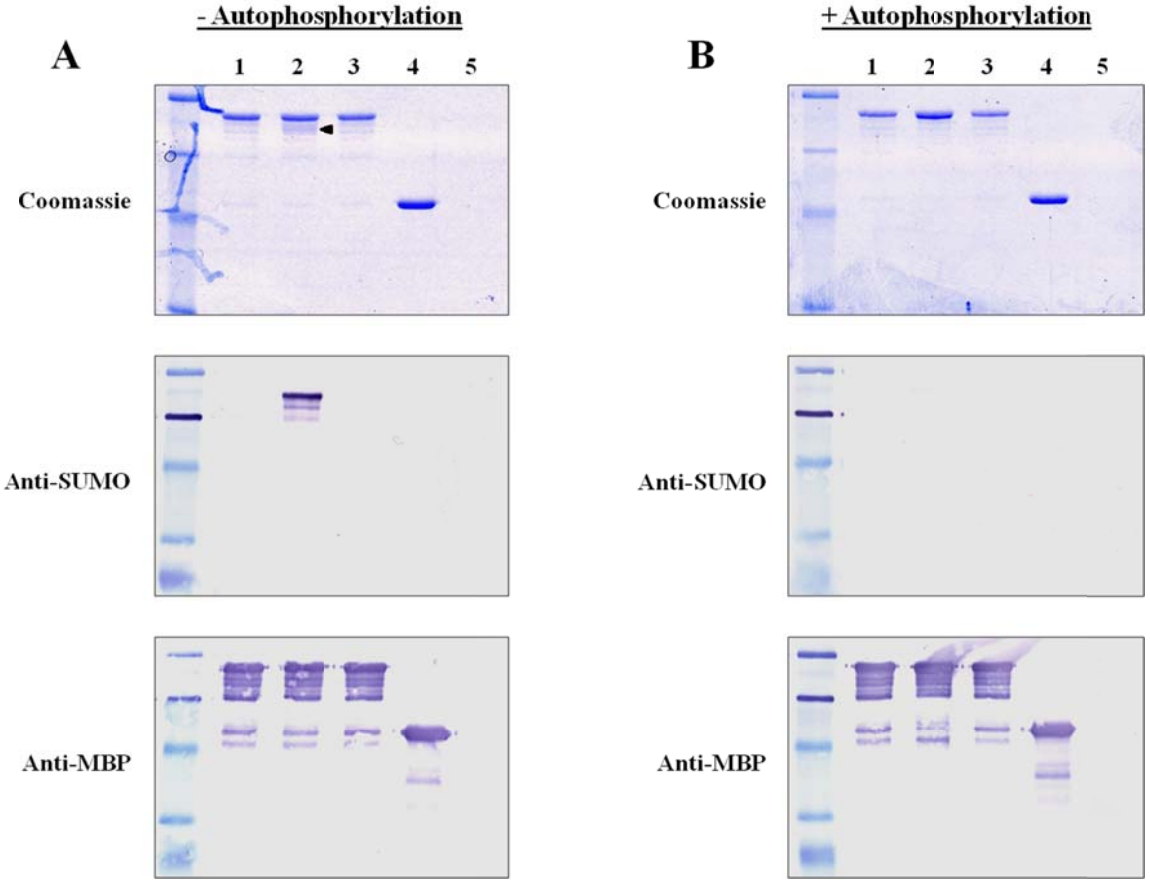

Figure 9. ACR4 ICD interaction with WOX5. The interaction between sACR4 and mWOX5 was determined by an *in vitro* pull-down assay. (A), mWOX5 can specifically bind naïve sACR4 (*arrow*). (B) mACR4 *cannot* interact with autophosphorylated sACR4. In A an B, 12% SDS-PAGE separation of interacting proteins (*top panels*), anti-SUMO western blots of proteins from each reaction (*middle panels*), anti-MBP western blots of proteins in each reaction (*bottom panels*). ***Lane 1***, mWOX5 only; ***lane 2***, mWOX5 + sACR4; ***lane 3***, mWOX5 + SUMO tag; ***lane 4***, MBP + sACR4; ***lane 5***, sACR4 only.

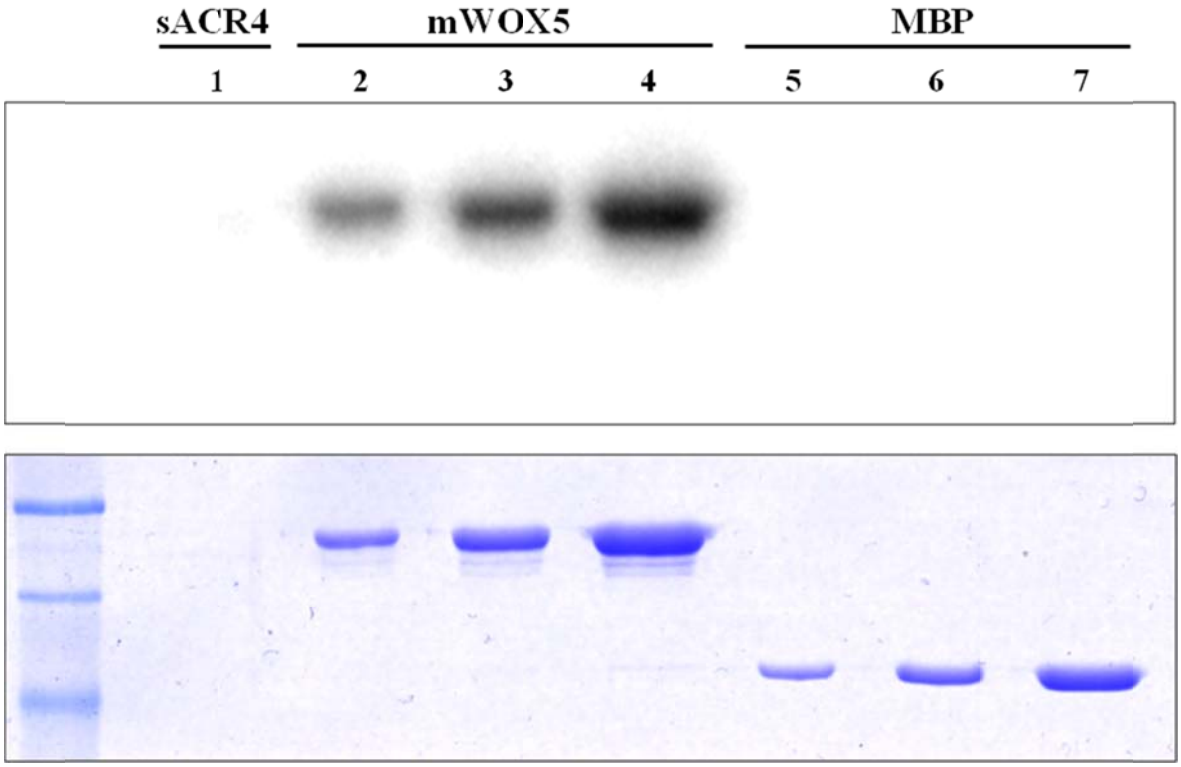

Figure 10. ACR4 can phosphorylate WOX. To demonstrate ACR4 phosphorylation of WOX5, sACR4 was incubated with mWOX5 in an *in vitro* kinase assay. *Upper panel*: An autoradiogram demonstrating phosphorylation of WOX5. The absence of sACR4 (10 µl load) is shown in *lane 1*. Phosphorylated mWOX5 (*lanes 2-4*) was loaded at increasing amounts, 2, 5, and 10 µl of reaction per lane, respectively. A control reaction showing MBP *cannot* be phosphorylated by ACR4 (*lanes 5-7*) was loaded at increasing amounts, 2, 5, and 10 µl of reaction per lane, respectively. *Lower panel*: Corresponding coomassie stained gel.

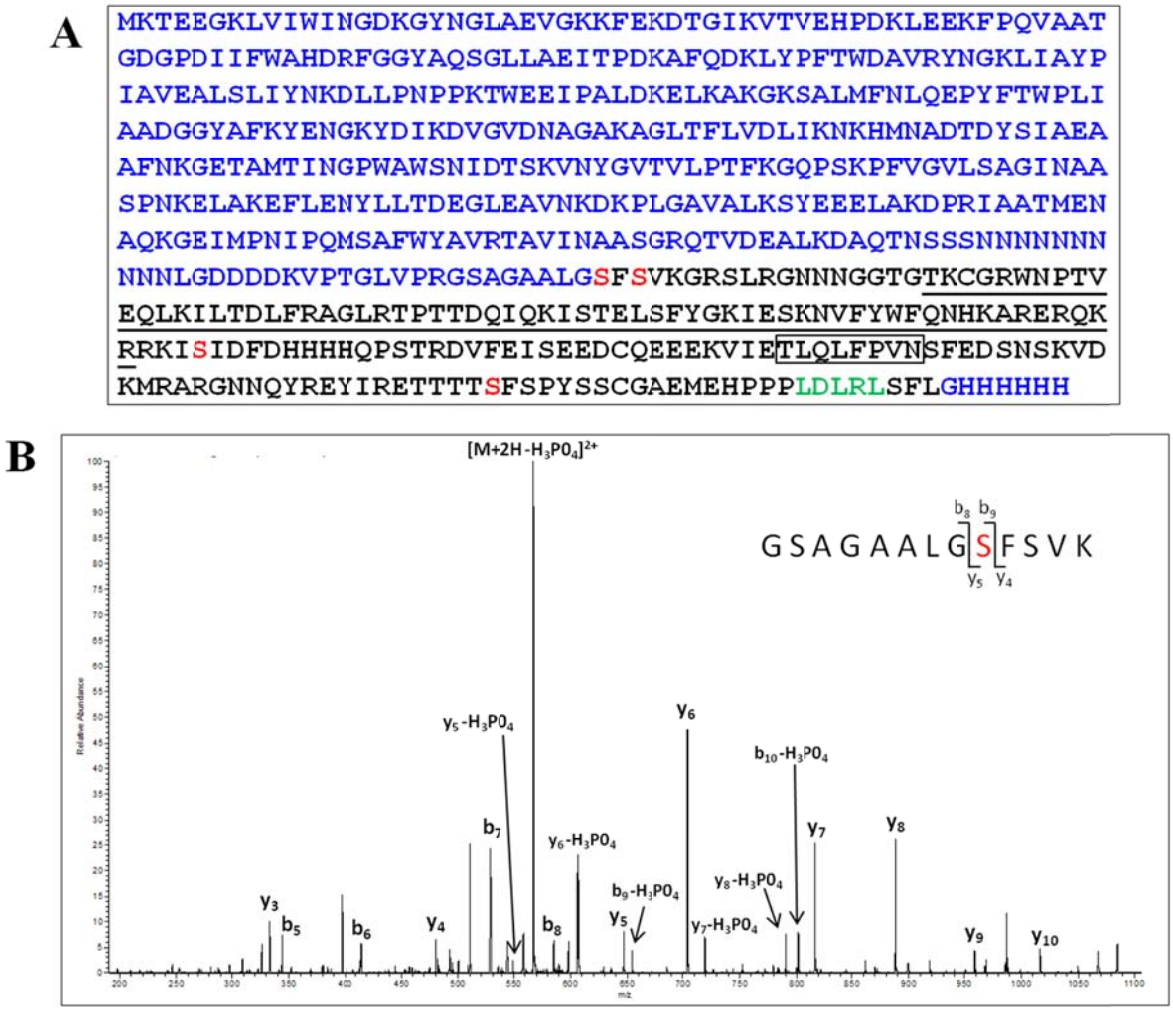

Figure 11. Identification of *in vitro* WOX5 phosphorylation sites. (A) The sequence of the MBP fused WOX5 protein is shown: the N-terminal MBP fusion tag and the C-terminal 6X His tag (blue) and the 182aa WOX5 sequence (black). Note, the N-terminal Met residue of WOX5 was changed to Gly. Key features of the WOX5 protein are the homeobox domain (underlined), the WUS box (boxed) and the EAR domain (green). Confirmed phosphorylation sites, Ser^{2}, Ser^{4}, Ser^{88}, and Ser^{158} are highlighted in red. (B) Collision-induced low resolution fragmentation spectrum of the phosphopeptide GSAGAALGSFSVK, encompassing the C-terminal end of the fusion tag and the N-terminal end of WOX5. The presence of the phosphorylated b_9 (theoretical *m/z* 654.32, observed *m/z* of 654.33) and y_5 (theoretical *m/z* 549.30, observed *m/z* of 549.33) ions, and the unphosphorylated b_8 (theoretical *m/z* 585.30, observed *m/z* of 585.17) and y_4 (theoretical *m/z* 480.28, observed *m/z* of 480.30) ions, confirms Ser^{2} as the site of phosphorylation.

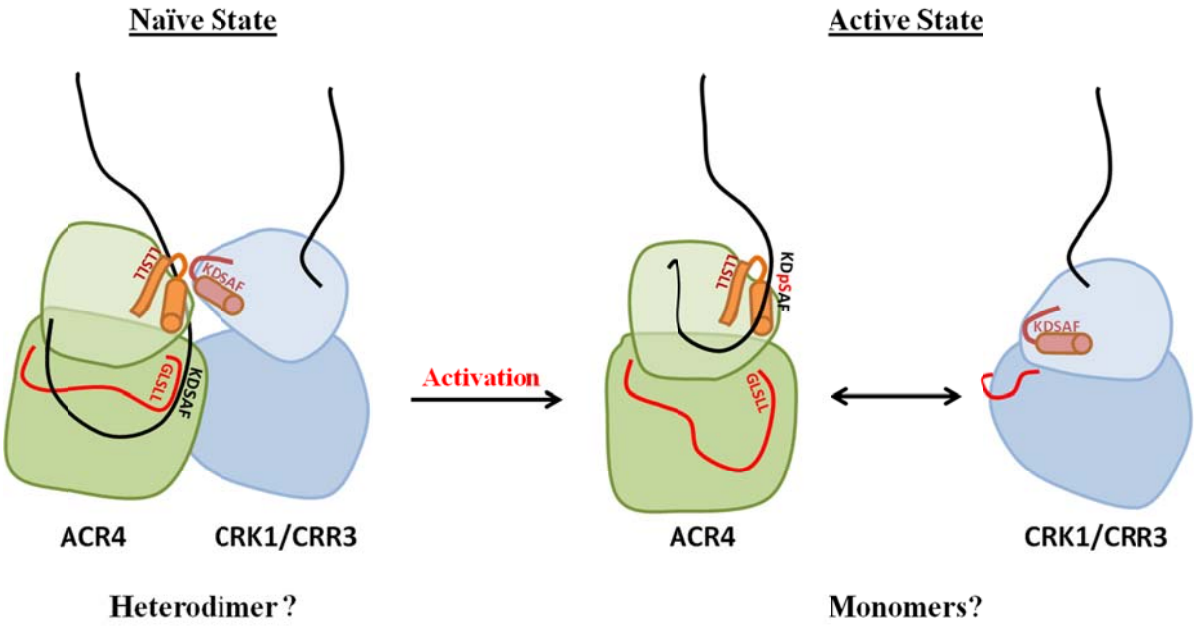

Figure 12. Potential intermolecular interaction mechanism among the ACR4 family. Diagram of a potential intermolecular contact between the KDSAF region of CRR3/CRK1/ALE2 and the LLSLL region in the ACR4 N-lobe. In the naïve, basal state the ACR4 JMD potentially interacts with the 'GLSLL' region at the N-terminal section of the activation loop preventing an active conformation. During kinase activation autophosphorylation at Ser^{475} and Thr^{478} in the JMD drives a conformational change in the JMD provoking an intramolecular interaction between the ACR4 JMD and kinase N-lobe at the LLSLL region. Intramolecular binding of the ACR4 JMD forces dissociation of the CRR3, CRK1, or ALE2 intracellular domain. Different regions of the proteins are highlighted: the JMDs (black), the activation loops (red), the ACR4 LLSLL motif (orange), and the CRR3/CRK1/ALE2 KDSAF motif (pink). The labels for each motif are respectively color coded to match. The C-terminal domain of ACR4 or the CRR is not shown.

CHAPTER 6: CONCLUSIONS AND FUTURE WORK

General Conclusion

Since the discovery of the CRINKLY4 gene in maize over 15 years ago (1), salient advancements have been made in understanding the function of the CRINKLY4 gene in both maize and *Arabidopsis*. Genetic and cell biology studies have shed light on the function of maize CR4 pertaining to the morphogenesis of epidermal tissues in the plant (1-3). The identification of an ortholog of maize CR4 in *Arabidopsis* (ACR4) has facilitated the examination of CRINKLY4 function in this model organism (4). Phenotypic analyses of *acr4* knockout plants have provided a large amount of information about receptor function in both the aerial and underground organs of the plant (5-8). Additionally, molecular and cell biology studies of truncation mutants have revealed information on receptor localization and internalization that have led to a basic understanding of domains within the ACR4 receptor that are critical for cellular functions (6, 9, 10). Recent biochemical studies have started to elucidate the role of the transmembrane domains of the CR4, ACR4, and AtCRR receptors in protein function (11, 12). However, the molecular basis for ligand binding, activation of the receptor and concomitant activation of the intracellular kinase domain, and the components of the downstream signaling pathway remains largely a mystery.

In this dissertation we provide the first fundamental biochemical analysis of the intracellular domain of the ACR4 receptor and its interaction with homologs. In concert with concurrent genetic and biological investigations from other laboratories, this study lays the foundation for a more comprehensive exploration of the central role of this important receptor in plant growth and development. Significant new information includes:

- The ACR4 kinase domain was recombinantly expressed in a bacterial system and its biochemical properties including autophosphorylation mechanism, oligomerization, and conformational dynamics were studied in detail (13) (Chapter 2).
- To study the interactions between members of the ACR4 receptor family, we have recombinantly expressed and purified milligram quantities of the ICDs of ACR4, the AtCRRs, and ALE2 as C-terminal fusions to the Small Ubiquitin like MOdifier (SUMO) protein (Chapter 3).
- We provide evidence for an intramolecular interaction between the ACR4 JMD and the amino-terminal region of the KD and its potential role in the regulation of kinase activity. Phage display and peptide binding studies demonstrate that the 'KDSAF' motif harbored in the ACR4 JMD can make intramolecular contacts with the N-lobe of the kinase via a 'LLSLL' motif. Furthermore, we also show that autophosphorylation of the JMD may be important for efficient substrate phosphorylation (Chapter 4).
- We demonstrate that ACR4 can interact with all four CRRs in a phosphorylation independent manner. Sequence comparison, phage display, and peptide binding studies are indicative of an intermolecular interaction mechanism between a highly conserved 'KDSAF' region in CRR3, CRK1, and ALE2 and the 'LLSLL' motif in the ACR4 kinase N-lobe (Chapter 5).
- Phage display panning of a phosphorylated peptide in the juxtamembrane domain has allowed us to compile a significant list of potential interacting proteins that can be classified into distinct signal transduction categories i.e. RLKs, phosphatases, transcription factors, and other adapter proteins that will have to await further confirmation and establishment of biological relevance.
- Lastly, we demonstrate, for the first time, that the intracellular domain of ACR4 can interact with the WOX5 transcription factor and phosphorylate it *in vitro*. Thus, signifying a potential

interaction between the ACR4 RLK and a putative downstream signaling component within the ACR4 signaling pathway.

Future Work

The role of subdomains on kinase activity

The studies in this dissertation provide evidence for a mechanism of ACR4 juxtamembrane autoinhibition of the kinase domain (KD) but the intriguing question is how the kinase is retained in a basal, inactive state at the cell surface. Our studies indicate that phosphorylation at Ser^{475} and Thr^{478} are necessary for maximal kinase activity (Chapter 4, Fig. 3). However, the exact roles of individual autophosphorylation sites in JMD autoregulation remain to be ascertained. Furthermore, there is an additional phosphorylation site at Thr^{501} that shows a significant effect on kinase autophosphorylation when mutated to Ala (Chapter 3, Fig. 7). Although this site is outside our defined region of the JMD, it lies immediately N-terminal to the kinase subdomain.

Thus far, little is known about the role of the C-terminal domain (CTD) in kinase autoregulation and activation. Individual Ala mutations of autophosphorylation sites within the CTD have been shown to be inhibitory to maximal kinase activity (Chapter 3, Fig. 7), suggesting that the CTD performs a similar role to JMD. Future studies must emphasize detailed biochemical and biophysical analysis that includes kinetic analyses of CTD autophosphorylation site mutants and substrate phosphorylation. These studies will provide the mechanistic details of CTD autoregulation and aid in the development of an overall mechanism of intracellular subdomain autoinhibition of the ACR4 kinase.

Ultimately, the three-dimensional structure of the ACR4 kinase domain, in the phosphorylated and unphosphorylated state, will provide a better understanding of the finer aspects of kinase activity and its regulation.

Intermolecular interactions in the ACR4 family

Our studies have shown that the ACR4 ICD can interact with all four of the CRR ICDs in the absence of phosphorylation (Chapter 5, Fig. 1 and 2). A potential mechanism for these interactions involves the conserved 'KDSAF' motif in the CRRs and 'LLSLL' region in ACR4. Yet, we do not know the precise role of these residues/regions in protein-protein interactions within the family. Mutational studies of these interaction sites in ACR4 and the CRRs will need to be assessed *in vitro.* Concomitant phenotypic analysis of mutant plants will provide valuable clues regarding the relationship between heteromeric interactions and potential activation of differential signaling events. It may be possible to tailor specific combinations of heteromers to influence new signaling pathways and produces novel phenotypes. It is also enticing to speculate that an entirely different mechanism regulates the interactions of ACR4 with the dead kinases, CRR1 and CRR2. Interestingly, both of these proteins contain an 'IVNLL'motif in the analogous position to the 'LLSLL' motif in ACR4. Our HDX data with CRK1 shows other regions that may also be involved in protein-protein contacts between the ICDs (Chapter 5, Fig. 5). Further HDX analysis of these protein-protein interactions, especially with membrane bound ICDs, can be utilized to characterize the interaction interface on both the ACR4 and CRRs in more detail.

Other members of the "ACR4 network"

Phage display screening of phosphorylated JMD peptides has yielded consensus sequences that preferentially bind to these linear peptides. Subsequently, database mining for

proteins that harbor these consensus motifs revealed a multitude of hits to proteins (Chapter 5, Table 2) that are potentially involved in signal transduction. However, the relevance of these proteins in the ACR4 signaling network remains to be clarified. With at least 18 autophosphorylation sites in ACR4 (13) (Chapter 2), it is a daunting challenge to delineate the function of each phosphorylation site during ACR4 signaling. For instance, one site may be involved in activation of the kinase domain by driving conformational changes in the protein versus a phosphorylation site that acts as a recruitment point for downstream targets in the ACR4 signaling pathway. Further increasing this complexity, are the potential for the CRRs and ALE2 to transphosphorylate the ACR4 intracellular domain (Chapter 3, Fig. 4) and the ability of ACR4 to phosphorylate all of the CRRs and ALE2 (Chapter 5, Fig. 3). Thus, increasing the number of potential phosphorylation sites correspondingly increases the complexity and the challenge of delineating their specific roles. Phage display screening of phosphorylated peptides and/or domains corresponding to ACR4 phosphorylation sites coupled to yeast 2-hybrid screening would provide an excellent means to overcome this obstacle.

As of yet, there are no known proteins that interact with the C-terminal domain (CTD). It is common among RTKs to have their CTDs phosphorylated at tyrosine residues in response to receptor activation. These sites can then recruit SH2 or PTB domain containing target proteins. As exemplified in the four-member EGF receptor family, multiple sites within their respective CTDs are phosphorylated and act to attract downstream targets (14, 15). Therefore, we can invoke the likelihood that some of the six autophosphorylation sites in the ACR4 receptor can serve to recruit downstream signaling targets. Therefore, phage display screening of phosphorylated peptide targets would be advantageous in

identifying consensus binding motifs that potentially signify 14-3-3, WW, FHA, or WD40 domain containing proteins that recognize phosphoserine or phosphothreonine residues (16).

It appears that ACR4 is involved in at least two distinct signaling pathways with overlapping themes. In one pathway, ACR4 has been proposed to be the mediator of stem cell differentiation in the root tip (8, 17). Here, ACR4 is described to perceive the extracellular CLE40 peptide ligand which promotes stem cell differentiation. Presumed activation of ACR4 then influences the expression domain of the WOX5 transcription factor, a protein that promotes stem cell proliferation (described in Chapter 1). Our experiments have demonstrated that the ACR4 kinase can interact with and phosphorylate WOX5 *in vitro*. At this time, the relevance of these phosphorylation sites is not known. Complementary *in vivo* experiments knocking out the potential phosphorylation sites in the WOX5 protein may drive phenotypic effects in transformed *wox5* mutant plants aiding in the characterization of the functional significance of these phosphorylated residues. In the second pathway, ACR4 is described to be involved in the proper differentiation of epidermis in vegetative and reproductive tissues (described in Chapter 1). Currently, the list of proteins known to be involved in epidermal development is rather limited. The major players such as AtDEK1, ALE1, ALE2, ACR4, and SAL1 are all known to affect different aspects of epidermal specification, differentiation, and maintenance (described in Chapter 1). Recently, maize Thk1 has been identified as a negative regulator of aluerone cell identity and has been proposed to function downstream of maize DEK1 (18). However, little is known about the interplay among these proteins (Fig. 1) and how they network together to regulate epidermis formation. One of our long term goals is to understand the relationship between ACR4 and other members of epidermal cell fate, namely, signaling components that can directly interact

with ACR4 in the intracellular or extracellular region. *In vitro* biochemical and biophysical studies of recombinant proteins can often provide valuable clues towards an understanding of *in vivo* physiological functions. However, this is not a trivial task and characterization of proteins involved in epidermal cell fate will require large amounts of soluble protein. For example, we have attempted to clone and express the extracellular domain of the ACR4 receptor in eukaryotic and prokaryotic systems with no success thus far. This is likely due to the overall complexity of the extracellular 'crinkly' repeats and the 26 cysteine residues found in the extracellular domain (Chapter 1, Fig. 1). Cloning and expressing other proteins classified to be involved in epidermal formation may be a task within itself. Indeed, the production of milligram quantities of the ACR4 intracellular domain itself was quite challenging.

The grand challenges of the 21st century are health, food, water and energy. The world population is growing at an annual rate of 80 million per year and, at this rate, will increase from the current 6 billion to >10 billion people by the 2030's (19). Simultaneous decline of arable agricultural land continues to challenge our ability to meet increasing demands for food, feed and fuel. To meet these demands, it is necessary to achieve a comprehensive understanding of plant function to enable knowledge-driven manipulation of pathways and regulatory networks for crop improvement. Towards this goal, *Arabidopsis* has served as a model for identifying genes and discovering their function in plant growth and development for application to crop species (20). Therefore, on a broader basis, given the existence of ACR4 equivalents in both maize and rice, there is high probability of the conservation of signaling components in these agriculturally important crops. The potential therefore exists to advantageously regulate plant development for improved agronomic value

via manipulation of signal transduction pathways. ACR4 is one of the central players in this effort.

References

1. Becraft, P.W., P.S. Stinard, and D.R. McCarty, *CRINKLY4: A TNFR-like receptor kinase involved in maize epidermal differentiation.* Science, 1996. **273**(5280): p. 1406-9.
2. Jin, P., T. Guo, and P.W. Becraft, *The maize CR4 receptor-like kinase mediates a growth factor-like differentiation response.* Genesis, 2000. **27**(3): p. 104-16.
3. Becraft, P.W., S.H. Kang, and S.G. Suh, *The maize CRINKLY4 receptor kinase controls a cell-autonomous differentiation response.* Plant Physiol, 2001. **127**(2): p. 486-96.
4. Tanaka, H., M. Watanabe, D. Watanabe, T. Tanaka, C. Machida, and Y. Machida, *ACR4, a putative receptor kinase gene of Arabidopsis thaliana, that is expressed in the outer cell layers of embryos and plants, is involved in proper embryogenesis.* Plant and Cell Physiology, 2002. **43**(4): p. 419-428.
5. Gifford, M.L., S. Dean, and G.C. Ingram, *The Arabidopsis ACR4 gene plays a role in cell layer organisation during ovule integument and sepal margin development.* Development, 2003. **130**(18): p. 4249-58.
6. Watanabe, M., H. Tanaka, D. Watanabe, C. Machida, and Y. Machida, *The ACR4 receptor-like kinase is required for surface formation of epidermis-related tissues in Arabidopsis thaliana.* Plant Journal, 2004. **39**(3): p. 298-308.
7. De Smet, I., V. Vassileva, B. De Rybel, M.P. Levesque, W. Grunewald, D. Van Damme, G. Van Noorden, M. Naudts, G. Van Isterdael, R. De Clercq, J.Y. Wang, N. Meuli, S. Vanneste, J. Friml, P. Hilson, G. Jurgens, G.C. Ingram, D. Inze, P.N. Benfey, and T. Beeckman, *Receptor-like kinase ACR4 restricts formative cell divisions in the Arabidopsis root.* Science, 2008. **322**(5901): p. 594-7.
8. Stahl, Y., R.H. Wink, G.C. Ingram, and R. Simon, *A signaling module controlling the stem cell niche in Arabidopsis root meristems.* Curr Biol, 2009. **19**(11): p. 909-14.
9. Gifford, M.L., F.C. Robertson, D.C. Soares, and G.C. Ingram, *ARABIDOPSIS CRINKLY4 function, internalization, and turnover are dependent on the extracellular crinkly repeat domain.* Plant Cell, 2005. **17**(4): p. 1154-66.
10. Cao, X., K. Li, S.G. Suh, T. Guo, and P.W. Becraft, *Molecular analysis of the CRINKLY4 gene family in Arabidopsis thaliana.* Planta, 2005. **220**(5): p. 645-57.
11. Stokes, K.D. and A. Gururaj Rao, *Dimerization properties of the transmembrane domains of Arabidopsis CRINKLY4 receptor-like kinase and homologs.* Arch Biochem Biophys, 2008. **477**(2): p. 219-26.
12. Stokes, K.D. and A.G. Rao, *The role of individual amino acids in the dimerization of CR4 and ACR4 transmembrane domains.* Arch Biochem Biophys, 2010. **502**(2): p. 104-11.

13. Meyer, M.R., C.F. Lichti, R.R. Townsend, and A.G. Rao, *Identification of in vitro autophosphorylation sites and effects of phosphorylation on the Arabidopsis CRINKLY4 (ACR4) receptor-like kinase intracellular domain: insights into conformation, oligomerization, and activity.* Biochemistry, 2011. **50**(12): p. 2170-86.
14. Schulze, W.X., L. Deng, and M. Mann, *Phosphotyrosine interactome of the ErbB-receptor kinase family.* Molecular Systems Biology, 2005. **1**.
15. Jones, R.B., A. Gordus, J.A. Krall, and G. MacBeath, *A quantitative protein interaction network for the ErbB receptors using protein microarrays.* Nature, 2006. **439**(7073): p. 168-174.
16. Yaffe, M.B. and A.E.H. Elia, *Phosphoserine/threonine-binding domains.* Current Opinion in Cell Biology, 2001. **13**(2): p. 131-138.
17. Stahl, Y. and R. Simon, *Is the Arabidopsis root niche protected by sequestration of the CLE40 signal by its putative receptor ACR4?* Plant Signal Behav, 2009. **4**(7): p. 634-5.
18. Yi, G., A.M. Lauter, M.P. Scott, and P.W. Becraft, *The thick aleurone1 Mutant Defines a Negative Regulation of Maize Aleurone Cell Fate That Functions Downstream of defective kernel1.* Plant Physiology, 2011. **156**(4): p. 1826-1836.
19. Pimentel, D. and M. Pimentel, *Feeding the world's population.* BioScience, 2000. **50**: p. 387.
20. Meinke, D.W., J.M. Cherry, C. Dean, S.D. Rounsley, and M. Koornneef, *Arabidopsis thaliana: A model plant for genome analysis.* Science, 1998. **282**(5389): p. 662-+.

Figures

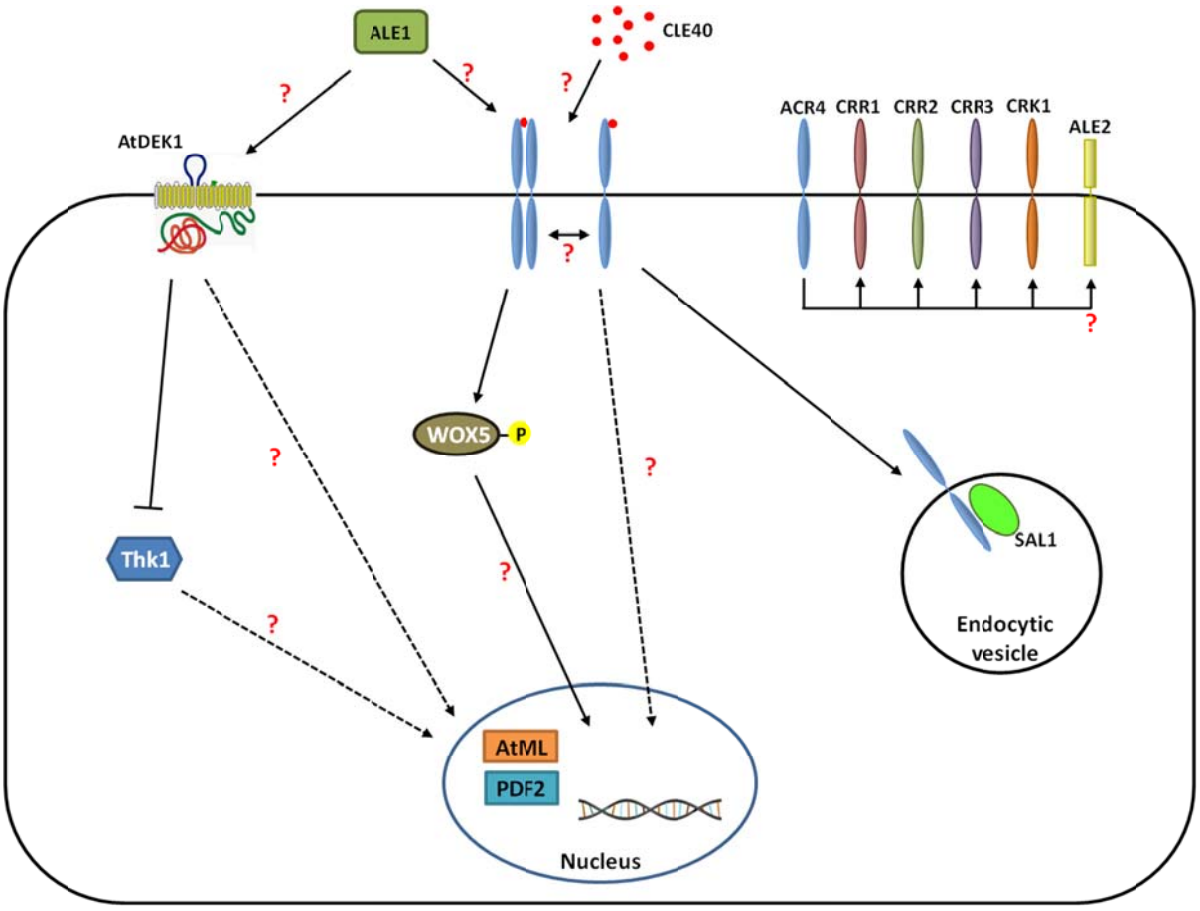

Figure 1. Proteins potentially involved in ACR4 signaling pathway. Diagram of the proteins involved in epidermal cell fate in aerial organs and columella stem cell fate in the root. The first pathway drives epidermal differentiation and maintenance. It involves the secreted protease ALE1, which may produce a peptide ligand for ACR4 or an unknown ligand for the phytocalpain, AtDEK1. Recently, it has been suggested that maize DEK1 can negatively regulate Thk1, a gene that suppresses aluerone differentiation (18). AtDEK1 can potentially modulate expression of the transcriptional regulators, AtML and PDF2. ACR4 expression can be controlled by AtML and PDF2, suggesting a regulatory feedback mechanism. A proteasomal degradation pathway of ACR4 involving SAL1 has been suggested. The second pathway promotes columella stem cell differentiation in the root tip. It involves three central players, a potential peptide ligand, CLE40, the ACR4 RLK, and the WOX5 transcription factor. WOX5 expression is modulated by ACR4 perception of CLE40. Additionally, CLE40 expression is modulated by WOX5, therefore suggesting a regulatory feedback mechanism.